STUDY ON DEEP PERCOLATION FROM SURFACE IRRIGATION

Ph.D. THESIS

by

SAMUEL DAGALO HATIYE

DEPARTMENT OF CIVIL ENGINEERING
INDIAN INSTITUTE OF TECHNOLOGY ROORKEE
ROORKEE-247 667 (INDIA)
APRIL, 2016

STUDY ON DEEP PERCOLATION FROM SURFACE IRRIGATION

A THESIS

Submitted in partial fulfilment of the requirements for the award of the degree of

DOCTOR OF PHYLOSOPHY

in

CIVIL ENGINEERING

by

SAMUEL DAGALO HATIYE

DEPARTMENT OF CIVIL ENGINEERING
INDIAN INSTITUTE OF TECHNOLOGY ROORKEE
ROORKEE-247 667 (INDIA)
APRIL, 2016

INDIAN INSTITUTE OF TECHONLOGY ROORKEE ROORKEE

CANDIDATE'S DECLARATION

I hereby certify that the work which is being presented in thesis entitled "**STUDY ON DEEP PERCOLATION FROM SURFACE IRRIGATION**" in partial fulfilment of the requirements for the award of the degree of Doctor of Philosophy and submitted in the Department of Civil Engineering of the Indian Institute of Technology Roorkee, Roorkee, is an authentic record of my own work carried out during the period from July, 2012 to April, 2016 under the supervision of Dr. K.S. Hari Prasad, Professor, Department of Civil Engineering, Indian Institute of Technology Roorkee, Roorkee.

The matter presented in this thesis has not been submitted by me for the award of any other degree of this or any other institute.

(SAMUEL DAGALO HATIYE)

This is to certify that the above statement made by the candidate is correct to the best of my knowledge.

(K.S. Hari Prasad)
Supervisor

Date .....

The Ph.D. Viva-Voce Examination of **Mr. Samuel Dagalo Hatiye**, Research Scholar, has been held on .....

Chairman, SRC

Signature of External Examiner

This is to certify that the student has made all the corrections in the thesis.

Signature of Supervisor

Head of the Department

Date: .....

ABSTRACT

Deep percolation from an irrigated field has caught less attention in many research works although it contributes to significant loss of water in irrigated fields. Deep percolation is often estimated as a residual in a water balance equation. Several methods are used to estimate deep percolation from a cropped area ranging from empirical relations to physically based models (Willis et al. 1997; Vaccaro 2007; Bethune et al. 2008; Arnold 2011; Ma et al. 2013). However, there are limited studies available concerning deep percolation from water intensive crop fields such as rice and berseem under unpuddled field conditions. The present study is concerned with the prediction and field verification of the deep percolation from water intensive crop fields. Estimation of deep percolation was made using both simple water balance and physically based model. Field observation of deep percolation was carried out using drainage type lysimeters.

Both laboratory and field experiments were conducted to study the performance of the selected models in predicting deep percolation. The laboratory experiments consisted of collection of soil samples from the experimental field and determination of soil bulk density, soil particle density, soil texture, soil water retention and soil hydraulic parameters. The field experiments involved growing rice and berseem crops under varying regimes of irrigation application. Field observations of irrigation, deep percolation, soil moisture content, saturated hydraulic conductivity and crop parameters were conducted. Yield determination of each crop was also conducted to study the water saving and water productivity of each crop season.

Deep percolation has been estimated using the FAO based water balance model after acquiring the necessary data for the components of the water balance. Actual evapotranspiration was computed using the data of reference evapotranspiration, crop and soil moisture stress coefficients in each crop season following FAO procedure (Allen et al. 1998). Penman Monteith approach was used to compute the reference evapotranspiration. The runoff component was only considered when the depth of input water is above the level of field boundary bunds. Groundwater contribution to the root zone has not been considered since the groundwater table in the study area is sufficiently deep. It has been observed that large volume of water is returned as deep percolation loss as physically demonstrated from lysimeter experiments. Nearly 82-87 % of the input water in rice season 1 and 77-80% input water in rice season 2 was accounted for deep percolation from the experimental field. On the other hand, approximately 62-67% of input water in berseem season 1 and 45-52% of input water was lost as deep percolation return flow. The deep percolation computed on daily basis did not agree

with the measured values; however, deep percolation computed based on lumped time steps (weekly basis for rice) and between wetting intervals (for berseem seasons) agreed well with the field observed deep percolation. This could be due to the fact that some time is needed for drainage water to arrive at lysimeter outlets located well below the crop root zone and the model structure which assumes the deep percolation to take place on the day of irrigation or rainfall only. Consequently, it can be concluded that in application of drainage type lysimeter water balance, estimation of deep percolation from a cropped area can be made fairly well on longer time steps than shorter time intervals.

Physically based model predicts deep percolation very well both on daily and lumped time steps unlike the simple water balance model. Model calibrations and validations for soil and crop parameters have been done using field observed data by employing HYDRUS-1D software package. A good agreement between model predicted and field observed deep percolation was obtained. Comparatively, the performance of the model is better in the wet season than the dry season which is attributed to the pronounced development of macropores in the dry season. Although, the physically based model predicts deep percolation well, it could not be able to capture peak deep percolation values which usually result from heavy rainfall storms. Large values of saturated hydraulic conductivity near the soil surface depict the effect of root proliferation, the activities of soil micro organisms, soil cracking which favour the formation of more macropores in the surface layers. The comparison of the two models show that the performance of the models is at par in predicting deep percolation on lumped time steps, although physically based approach showed closer relationship to the field observed deep percolation than the simple water balance model.

Water saving and water productivity of different irrigation schedules have also been investigated. Large saving in irrigation water has been achieved by implementing alternative irrigation schedules when compared with the conventional irrigation practice in both rice and berseem seasons. Nominal yield reduction was observed in both crop periods due to large reduction in irrigation water which has but resulted in comparatively high water productivity.

ACKNOWELDGEMENT

First of all, I praise the Almighty God for His spiritual blessings in heavenly places in Christ and care on this earth. Glory and honour be to God ever and ever in the Name of Jesus Christ who provided me with strength, peace and well being in the course of my life.

I would like to express my deepest sense of gratitude, special thanks and appreciation to my supervisor, Dr. K.S. Hari Prasad, Professor, Department of Civil Engineering, Indian Institute of Technology Roorkee, Roorkee, for his understanding, continuous encouragement, constructive criticism and painstaking efforts in providing valuable suggestions throughout the course of the present study and the long period of my stay in Roorkee. His critical and unreserved support enabled the thesis to be presented in the current shape.

The cooperation and help extended by the head and faculty members, Department of Civil Engineering, Indian Institute of Technology, Roorkee is gratefully acknowledged. I also want to thank my research committee members for providing me insightful and constructive comments.

I would like to acknowledge the support given by the National Institute of Hydrology (NIH) and Department of Hydrology in providing the necessary data for the present work. The cooperation of staff both in the Department of Hydrology and NIH is highly appreciated. I also extend my sincere thanks to Dr. Sentinel, for his kind cooperation during the collection of the required data from NIH. I would like to express my appreciation and thanks to the staff in the Hydraulics laboratory, Department of Civil Engineering. I specially thank Mr. Pramod for his special, technical and continuous assistance during the course of the experimental work. The assistance and cooperation from Mr. Pundir, Lab in-charge, is highly appreciated. I gratefully thank Mr. Ratram, Mr. Vinod, Mr. Arshad, Mr. Ashok, Mr. Bhairav, Mr. Shotelal, Mr. Aslam, Mr. Bitu and Mr. Nadeem for their cooperation and love which made my work in the lab so comfortable. I didn't feel loneliness and homesickness as the staff were so friendly.

I would like to thank Ministry of Education, Ethiopia, for providing me the scholarship. I also extend my thanks to Arba Minch University for allowing me leave of absence for the study period. The cooperation and assistance made by the staff in Ethiopian Embassy, New Delhi, is also highly appreciated.

I express my deep sense of gratitude and reverence to my parents for their blessings and prayer for my peace and to carry out my assignments in due time. The farm experience that my father thought me in my childhood helped me greatly in the field work and I would like to thank him and wish him long life. The prayer that my mother was making has been accepted

and heard in the heavens and it made my day. I thankfully acknowledge the contribution of all my teachers since my school days, for their valuable criticisms, showing me the right path and encouragement.

I would like to extend my appreciation and thanks to fellow African students for being friendly and cooperative to show up pleasing social environment. I also thank all Ethiopian students, my fellow citizens, at Roorkee for providing me courage, inspiration, assistance needed and companionship. It is my pleasure to acknowledge the support extended from research scholars at Department of Civil Engineering. I particularly want to thank Mr. Kaushik, Mr. Hashim, Dr. Nilav and Mr. Umesh who were cooperative and informative during my stay at Roorkee. The cooperation and assistance made by KIH hostel staff is also acknowledged.

Finally, I want to extend my sincere thanks to my spouse, Mrs. Endalech Dea, for her relentless support, encouragement, prayer, love, shouldering all the family issue and bearing all social matters in my absence back at home. She paid off much sacrifice during the course of this study. I reserve my affectionate love to our two sons, Ami Samuel and Esrom Samuel who missed me for so long. I really missed them for the period of the study and appreciate them for their endurance. Thank you my family and God bless you.

Samuel Dagalo

LIST OF CONTENTS

LIST OF FIGURES

LIST OF TABLES

LIST OF NOTATIONS

Symbol	Description	Dimension
C	Specific moisture capacity	(L^{-1})
COV	Coefficient of variation	—
DAP	Diammonium phosphate	—
DAS	Days after sowing	(T)
DAT	Days after transplanting	(T)
D	Soil moisture diffusivity	(L^2T^{-1})
D_i	Soil moisture depletion in time i	(L)
DP	Deep percolation	(L)
E_s	Soil evaporation	(LT^{-1})
ET	Evapotranspiration	(LT^{-1})
ET_c	Crop evapotranspiration	(LT^{-1})
ET_0	Reference evapotranspiration	(LT^{-1})
f	Soil porosity	—
FC	Field capacity	(L^3L^{-3})
GW	Groundwater/Capillary rise from groundwater	(L)
H	well head indicator in Guelph Permeameter	(L)
i	Temporal index	—
I	Irrigation depth	(L)
j	Spatial index	—
K	Unsaturated hydraulic conductivity	(LT^{-1})
K_c	Single crop coefficient	—
K_{cb}	Basal crop coefficient	—
K_e	Soil evaporation coefficient	—
K_r	Relative hydraulic conductivity	—
K_s	Soil moisture stress coefficient	—
K_{sat}	Saturated hydraulic conductivity	(LT^{-1})
L1	Lysimeter 1	—
L2	Lysimeter 2	—
LAI	Leaf area index	(L^3L^{-3})
m	van Genuchten's soil water retention parameter	—
MAD	Management allowable depletion	(L)

n_v	van Genuchten's soil water retention parameter	—
P	Precipitation/rainfall	(L)
p	constant in van Genuchten root water uptake model	
p_r	Depletion fraction for no stress	—
PAR	photosynthetically active radiation	($molL^{-2}T^{-1}$)
PET	Potential evapotranspiration	(LT^{-1})
PWP	Permanent wilting point	(L^3L^{-3})
q	Flux at specified depth below the ground surface	(LT^{-1})
R	Surface runoff	(L)
RAW	Readily available water	(L)
$RMSE$	Root mean square error	varies
RWU	Root water uptake	(LT^{-1})
R^2	Coefficient of determination	—
S	Sink term representing root water uptake	(T^{-1})
SMCC	Soil moisture characteristic curve	—
SP	Seepage	(L)
S_p	Potential root water uptake	(L^{-1})
TAW	Total available water	(L)
t	time coordinate	(T)
TDR	Time domain reflectometry	—
T_p	Plant transpiration	(LT^{-1})
z	vertical coordinate/model domain	(L)
z_r	Root depth	(L)
$\alpha(\psi)$	RWU water stress response function	—
α_v	van Genuchten's soil water retention parameter	(L^{-1})
α^*	microscopic capillary length factor	—
ΔS	Change in soil moisture storage	(L)
$\Delta\theta$	Change in soil moisture content	(L^3L^{-3})
ε	dielectric constant of soil	—
θ	Soil moisture content	(L^3L^{-3})
Θ	Effective saturation	—
θ_{fc}	Soil moisture content at field capacity	(L)
θ_r	Residual soil moisture content	(L^3L^{-3})
θ_{pr}	Soil moisture content at depletion fraction for no stress	(L)

θ_{pwp}	Soil moisture content at permanent wilting point	(L)
θ_s	Saturated soil moisture content	(L^3L^{-3})
λ	Radiation extinction coefficient	—
ρ_b	Bulk density	(ML^{-3})
ρ_d	Particle density	(ML^{-3})
ψ	pressure head	(L)

CHAPTER 1
INTRODUCTION

1.1 GENERAL

Fresh water is mainly consumed for the purposes of agricultural, domestic and industrial water needs. Agriculture is by far the largest consumer of fresh water of the globe; that is, water put to irrigate a cropland to produce crops. In 2000, agriculture accounted for 70 percent of water withdrawals (in developing countries the proportion exceeds 80 percent (FAO 2002) and 93 percent of water consumption worldwide, where consumption refers to withdrawals net of return flows and evaporation. However, industrial sector has accounted for 20 percent of withdrawals and 4 percent of consumption, and household use accounted for 10 percent of withdrawals and 3 percent of consumption worldwide in 2000 (FAO 2004).

Irrigation involves the artificial application of water to the soil, usually for assisting the growth of crops in dry areas or where there is a shortage of rainfall. It can be applied in various forms such as surface irrigation methods (flooding, basin, border or furrow) or through pressurized systems (sprinkler or drip). The scope for further irrigation development to meet food requirements in the coming years is still increasing, however, severely constrained by decreasing water resources and growing competition for clean water. Serious water shortages are developing in many parts of the world as existing water resources reach full exploitation. The situation is exacerbated by the declining quality of water and soil resources. The great challenge for the coming decades will therefore be the task of increasing food production with less water (FAO 2002). Hence, it obliges to look for alternative, efficient and sustainable water management strategies, in the agricultural water sector, now and in the coming generations to meet the demands of all sectoral water users with the limited available supplies.

Due to limitation in resources, surface methods of irrigation are usually practiced in developing countries. In particular, flooding way of water application is implemented in water intensive crop fields such as rice and berseem fodder. Rice is known to be the staple food grain in several countries, especially in Asia. The most intensively irrigated regions of the world, India and China, produce significant metric tonnes (about 240 million) of rice annually which accounts for nearly 50% of annual global rice production (Muthayya et al. 2014). India shares more than 21% of the global rice production. In India, rice is grown over an area of 43 million ha with an annual production of 124 million tons (IRRI, 2004). Berseem, on the other hand, needs frequent irrigation throughout its growing season because of its shallow root zone that dries up quickly (Tyagi et al. 2003). It requires saturated field condition for its germination,

although it can grow under intermittently irrigated farms. As much as 500 kilograms of water is required for every kilogram of berseem plant dry matter produced in a dry climate. There is also a huge demand to grow more fodder crops in general (currently around 8.4 million ha) and berseem fodder (also called king of fodder crops) in particular owing to large demands in dairy products in India (Sunil et al. 2012) which calls for increase in fresh water demand. However, losses such as deep percolation (*DP*) are major drawbacks which lower the efficiency of this type of irrigation. Hence, there is an urgent need for an accelerated increase of agricultural water use efficiency such as reducing deep percolation losses.

1.2 PROBLEM STATEMENT

Deep percolation, the water that goes below crop root zones, from frequently irrigated fields seriously diminishes irrigation efficiency, jeopardises proper water management and minimizes water productivity. Deep percolation also causes environmental problems such as groundwater pollution, water logging and secondary salinization in irrigated agriculture. In specific cases of water intensive crops, large volume of water is lost on account of deep percolation (Garg et al. 2009). This is quite dominant in coarse textured soils where water holding capacity is relatively less. Significant efforts have been made so far to reduce deep percolation especially from rice fields: alternate wetting and drying (AWD) (Bouman et al. 2007b; de Vries et al. 2010; Tan et al. 2014), aerobic rice (Nie et al. 2012), delayed application of continuous flooding (Dunn and Gaydon 2011) and puddling (Kukal and Aggarwal 2002; Kukal and Sidhu, 2004). Most of the research studies, however, consider the presence of puddled layer (a relatively impermeable hard pan) in the root zones of rice field in reducing deep percolation.

Puddling operation is believed to be a defensive mechanism to reduce deep percolation in rice field. However, hard pan under coarse textured soil conditions is not proved to be efficient (Bouman et al. 2007a). Incidences of large deep percolation under field bunds were also commonly reported in puddled field conditions (Garg et al. 2009; Janssen and Lennarth 2009). Puddling operation is costly and labour intensive besides changing soil structure and requiring more water (Humphreys and Gaydon 2015a). Another problem which has been recognized due to puddling practices in rice fields is the interference of the puddled layer with the next crop (Mitchell et al. 2013). Therefore, nowadays rice farmers are shifting from the puddling step, either by transplanting rice seedlings or directly sowing the same on prepared beds, to unpuddled field operations as getting practiced in the study area. However, there are only limited studies conducted so far in such unpuddled transplanted rice environment.

There were also no studies conducted concerning root zone soil water balance and flow dynamics in berseem fodder crop fields. Moreover, no comparative studies were made so far on quantification of deep percolation from different seasons and crops involving field observations using drainage type lysimeters. It is imperative to investigate deep percolation phenomena over different crops and cropping seasons which were not studied so far in the earlier researches.

1.3 HYPOTHESIS OF THE RESEARCH

The following hypothesis is being made to carry out the present study.

Large volume of deep percolation occurs from root zones of water intensive crops such as rice and berseem, particularly under unpuddled field and course textured soil conditions. Large losses of water from root zones of water intensive crops would further pollute groundwater and surface water systems, cause secondary salinzation besides unproductive loss of water in such fields. It is also further hypothesized that deep percolation in such water intensive crops could be reduced by introducing alternative irrigation schedules. Both the water balance and physically based models can predict percolation losses from irrigated fields very well.

1.4 RESEARCH QUESTIONS

The following list of research questions have been designed to conduct the current research work.

i. How much amount of deep percolation occurs from root zones of irrigated rice and berseem crop fields?
ii. Does lowering of water input in rice and berseem crop fields' lowers deep percolation amount?
iii. How deep percolation is being characterized in water intensive crop fields under differing regimes of water application?
iv. How well can simple water balance and physically based single porosity model can predict deep percolation from irrigated fields such as rice and berseem in different seasons and under different regimes of water application?
v. How do locally constructed drainage type lysimeters enable metering DP loss from water intensive crop fields?
vi. How much extent of yield reduction can be occurred due to water reduction in input water while maintaining other conditions same?

1.5 OBJECTIVE OF THE STUDY

The main objective of the present study is to estimate deep percolation from water intensive crops such as rice and berseem fodder fields employing field observations and using both the water balance and physically based modeling approaches. The specific objectives are:

1. Review of deep percolation phenomena under various cropping conditions, the physics of flow in crop root zone, methods of deep percolation estimations, methods of acquiring data on soil and crop parameters for root zone flow simulation.
2. Investigation of the performance of the selected models in estimating deep percolation in different time steps by comparing with field observations.
3. Comparative study of the deep percolation from the lysimeters and field plots using the water balance approach.
4. Estimation of actual evapotranspiration using the FAO procedure considering crop growth stage and soil moisture content.
5. Calibration and validation of the soil hydraulic and root water uptake parameters using the field observed deep percolation data.
6. Determination of crop yield, evaluation of water productivity and assessment of reduced irrigation application on overall water saving and deep percolation response under unpuddled field conditions.

1.6 SIGNIFICANCE OF THE STUDY

Pressure on water resources will increase with the rising demand from agricultural, municipal, industrial and environmental water uses besides the changing climate conditions of the globe and regions. Because of large demand in food production, irrigated agriculture is becoming a way out to increase production and thus irrigation water demand will increase. However, agriculture will be challenged by shortage and lack of fresh water due to the competing sectoral demands, climate change and irrigation inefficiency.

In spite of changes in water demand, agricultural water use trend has not been changed significantly through times and efficiencies of irrigation have not been improved as expected. Hence, most valuable water is being lost as deep percolation/irrigation return flow/, runoff etc. from agricultural areas and further creates environmental problems. This compels for efficient utilization mechanisms; such as reduction in losses, optimum irrigation scheduling, reuse of irrigation return flows, employment of reduced irrigation etc. to better utilize and manage fresh water resources. Therefore, thorough understanding and investigation of deep percolation

losses is important particularly from water intensive crop fields for effective water resources management in an area.

1.7 ORGANIZATION OF THE THESIS

The organization of the thesis is presented in the following paragraphs.

In chapter one, a brief introduction regarding background information related to irrigated agriculture, agricultural water management and utilization with due concern to increasing demand for fresh water is being discussed. The chapter highlights the unproductive water losses which made agricultural water management at its lower gauge. The main problem which triggered this research study is also presented in this chapter while framing strategies to measure and estimate deep percolation from water intensive crop fields.

A comprehensive literature review on deep percolation and flow through the crop root zone is presented in chapter two. This chapter is devoted to extract findings from earlier research works and outputs related to the phenomena of deep percolation and the key models usually employed in estimating deep percolation. Detailed reviews and discussions are made on the water balance and physically based models, the components of the models and inputs related to the model parameters.

Chapter three deals with the experimental program which has been conducted in the laboratory and field to acquire important data for evaluating the performance of the proposed models in estimating deep percolation from water intensive crop fields such as rice and berseem. Thorough explanation and discussion of the procedures undertaken and methods utilized in conducting the experimental session is made in the particular chapter. The laboratory experiments consisted of collection of soil samples from the experimental field and determination of soil bulk density, soil particle density, soil texture and soil hydraulic parameters are presented in this chapter. Most important inputs to the models such as irrigation, rainfall and evapotranspiration are discussed and the way how these were obtained is presented. Drainage outflow well below the crop root zone was routinely observed and the way how the data was collected and the setup of lysimeters is briefly discussed. The working principles and operations of the soil moisture monitoring instrument (profile probe-PR2/6), the leaf area index determination ceptometer (LP 80 AccuPAR) and the Guelph Permeameter are presented in this chapter among others.

The results of experimental measurements in the field and application of the water balance model to estimate deep percolation is presented in chapter four. The domain for the model is the 1.35 m depth below the ground surface which includes the crop root zone

environment. In fact, the dynamics of water, solute and heat flow in this range of the vadose environment is quite complex. Owing to this, the computed deep percolation using simple water balance model poorly agrees with the measured deep percolation when the time step considered is short; although it works better when the time step size is longer.

In chapter five, physically based model is employed to estimate deep percolation from a cropped area by using the HYDRUS-1D software which solves the Richards (1931) equation coupled with the root water uptake term. The performance of the model is evaluated using field measured data for each crop season.

In chapter six, the importance of reduced water application in enhancing the water productivity is presented briefly. The chapter shows the possibility of large water saving, increased water productivity and reduction in deep percolation in rice and berseem fields without the effort of field puddling.

Finally, in chapter seven, major conclusions and scope for further research on deep percolation from water intensive crops is indicated.

CHAPTER 2
LITERATURE REVIEW

2.1 GENERAL

Irrigated agriculture increases yield of agricultural production and allows stability in the supply of food and other agricultural products. Only 20% of the world's land generates 40% of agricultural production, consuming nearly 70% of the global fresh water resources (FAO 2003). Although the water withdrawn to be used in agriculture is elevated, FAO (2003) estimates that only half of the water applied is consumed by plants, and considerable part of it ends up in aquifers and rivers (García-Garizábal and Causapé 2010).

Irrigated agriculture is required to release more water to the other demanding sectors while required to produce more food at the same time (Madramoottoo and Fyles 2010). This is to mean that irrigated agriculture should be improved ever than conceived to meet these requirements. However, irrigation is usually criticized as a profligate and wasteful user of fresh water to date (Perry et al. 2009). This may be due to the fact that irrigation is linked with complex processes such as infiltration, soil water storage, evaporation/transpiration, seepage and deep percolation, which are spatially and temporally dynamic and difficult to handle in the practical conditions (Hillel 2004).

Unproductive losses of water in agriculture such as deep percolation and runoff shall be limited to enhance irrigation efficiency and the productivity of water. Therefore, thorough understanding of such processes in an irrigated area is important not only to reduce losses but also to take effective measures to reduce these losses.

2.2 DEEP PERCOLATION FROM A CROPPED AREA

Deep percolation from a cropped area refers to the vertical movement of water below the crop root zone (Huntington and Allen 2009; Vaccaro 2007; Ochoa et al. 2007). Percolated water can either recharge groundwater aquifer or further flow laterally to join surface water body (Kim et al. 2009). Sometimes, it becomes difficult to differentiate between deep percolation and seepage since both processes take place in the subsurface environment. Water which is percolating can change direction at some point and start seeping at the other place and vice versa. The deep percolating water may be held up above confining layers and flow laterally if such restricting layers are sloping (Bouwer 1987).

Deep percolation can be expressed using terms such as downward drainage (Allen et al. 1998), groundwater recharge (Xu et al. 2015) or return flow (Oad et al. 1997). Deep percolation

can ultimately supplement the groundwater reserve and hence can be referred as groundwater recharge (Xu et al. 2015; Sobowale et al. 2015; Ochoa et al. 2007; Vaccaro 2007). Some other authors specify deep percolation as a "potential recharge" to indicate deep percolation from crop root zones could potentially recharge groundwater reserve (Anuraga et al. 2006). Sometimes deep percolation can also be termed as return flow from an irrigated area (Oad et al. 1997). However, irrigation return flow is a broader concept which incorporates deep percolation, seepage and runoff from an irrigated area (Kim, et al. 2009; Arnold 2011; Lin and Garcia, 2012). Some other authors also indicated percolation as bottom flux or leaching water (Li et al. 2014; Ma et al. 2013; Sutanto et al. 2012).

2.2.1 Factors Affecting Deep Percolation

Many factors could influence percolation phenomena through and below the bottom of a crop root zone. These factors include ponding size, water table depth, evapotranspiration, antecedent soil moisture condition, soil texture and structure, shrinkage behaviour of soil, biotic activities in root zone, irrigation size and time, climatic condition, crop type and characteristics, water management and agronomic practices, puddling intensity and depth (Kukal and Aggarwal 2002; Bouman et al. 2007a; Bethune et al. 2008; Selle et al. 2011). Ponding size or input water depth, in general, directly affects deep percolation irrespective of the other factors (Kukal and Aggarwal 2002; Smith et al. 2005; Bethune et al. 2008). Proper irrigation schedules could reduce input water depth and thus deep percolation (Ji et al. 2007). Deep percolation basically raises the groundwater table. When the groundwater table is shallow, capillary rise can also to take place in response to evapotranspiration while deep water table conditions usually call for more deep percolation (Xu et al. 2015; Bethune et al. 2008; Liu et al. 2006). Evapotranspiration and percolation are non-linearly related in root zone water balance. Both of the processes lie on the outflow side of the balance equation, although percolation occurs with certain time lag for considered depth of interest below crop root zone than evapotranspiration (Loos et al. 2007).

Antecedent soil moisture conditions could also affect the deep percolation quantity and characteristics in that whenever the soil is above field capacity, it drives more percolation since the micro and macropores are previously occupied by water given that the groundwater table is deep. On the other hand, when the initial water content before anticipated rainfall or irrigation is very low, there exists large room to occupy the input water which results in less or no percolation (Dorrenbos and Pruitt 1977; Liu et al. 2006; Ma et al. 2013). However, such condition of flow in the soil root zone could be violated due to the effect of preferential flow

(Garg et al. 2009; Hardie et al. 2011; Selle et al. 2011; Baram et al. 2012). Evidently, coarse textured soils favour more deep percolation than fine textured soils and vice versa in response to the water holding capacity and hydraulic characteristics of such soils. Soils which undergo shrinkage and cracking can facilitate deep percolation even at soil moisture contents below field capacity since water flows through larger desiccated openings very easily (Liu et al. 2004; Hardie et al. 2011; Baram et al. 2012). On the other hand the biotic activities in crop root zone including the root penetration provide further channels for deep percolating water (Garg et al. 2009; Sutanto et al. 2012; Li et al. 2014).

Irrigation scheduling and method clearly affect deep percolation phenomena. Surface methods of irrigation are usually accompanied with large percolation depth and hence lower irrigation efficiencies (Home et al. 2002; Wang et al. 2012; Ji et al. 2007, Smith et al. 2005). With regard to climate, generally, wet climates are suitable for aggravated deep percolation than dry climates. Crops differ in their water consumption behaviour as well as tolerance of extreme climatic conditions such as water logging or drought. Some crops such as rice for example, thriving in aquatic environment while others could sustain under arid climatic conditions. Crops can also vary in their anatomical structure in which those with deep roots could extract water from deeper layers (Ruiz et al. 2010) and reduce deep percolation whereas those with shallow roots could extract water mainly from the top layers and hence may contribute to large percolation. Further, water management and agronomic practices could play important role in regulating deep percolation. Tillage practices (Kukal and Aggarwal 2003), puddling (Kukal and Aggarwal 2002; Bouman et al. 2007a), delaying continuous flooding application (Dunn and Gaydon 2011) are some of the methods which could be mentioned specific to water intensive rice fields in reducing the deep percolation. Li and Shao (2014) also described that timing of sowing periods has an influence on deep percolation and thus on water balance components which may be attributable to the seasonal variations of climatic parameters.

2.2.2 Merits and Demerits of Deep Percolation

Groundwater replenishment is by far the most important aspect of deep percolation phenomena (Ochoa et al. 2007; Kendy et al. 2004; Chen and Wuing 2002). Sustainable water management can be achieved by making reuse of the drainage water at downstream by extracting groundwater (Ahmad et al. 2014) when considered in the context of basin water management. Therefore, deep percolation is not taken as loss, in certain cases, considering the reuse of percolation water from groundwater aquifers or effluent streams (Ahmad et al. 2014;

Gardner 1992). However, this needs accurate determination of return flow volume so that proper management and use of drainage water is achieved. Certain volume of drainage water is also needed to leach out salt accumulation in the root zone so that salt balance is maintained in the crop root zone. Therefore, irrigation system designs and operations usually consider additional water requirement besides the crop consumptive demand (Bouwer 1987).

However, the demerits of deep percolation from irrigated areas seemed to outweigh the advantages since percolation phenomena from frequently irrigated fields seriously diminish irrigation efficiency, jeopardize proper water management and minimize water productivity. This is quite sound in coarse textured soils where water holding capacity is relatively low. Percolation loss of water from irrigated field is not only reducing irrigation efficiency but also becoming a haphazard to an environment by carrying agriculture based chemicals to the surrounding water bodies, especially to the groundwater aquifer systems (Bouman et al. 2002; Asadi and Clemente 2003; Vereecken 2005; Shrestha et al. 2008; Antonopoulos 2010). Seepage and percolation losses of water are major reasons behind the poor water productivity in wetland rice (Patil et al. 2011). The problem gets worse with water intensive crops such as rice or berseem fodder since large volume of water is applied to the field. It has been indicated that large volume of nitrogen leaching can take place in rice fields (Bouman et al. 2002). Nitrogen leaching from agricultural areas joining groundwater could pollute freshwater aquifers (Bouman et al. 2002; Antonopoulos 2010; Ji et al. 2007; Tafteh and Sepaskhah 2012; Qin et al. 2011; Wallis et al. 2011). Additionally, other chemical residues (for example pesticides) leaching from agricultural areas could also contaminate a groundwater system (Vanderborght et al. 2011).

Surface streams and water bodies can also be affected by return flow which also includes deep percolation from irrigated areas (Kim et al. 2009; Lin and Garcia 2012). Kim et al. (2009) have showed that substantial amount of water is returned as irrigation return flow from rice fields joining adjacent streams as quick return flow. Lin and Garcia (2012) assessed the impact of irrigation return flow on river salinity in Arkansas River valley by constructing a response function for the tail water. Return flow in their case refers to the in-field deep percolation, canal seepage and tail water (runoff).

Agricultural areas irrigated with surface methods of irrigation are largely prone to rising groundwater levels, water logging and salinity mainly due to the deep percolation contribution (Singh et al. 2010; White 2006; Willis et al. 1997). Water logging problems are crucial in some irrigated areas of rice cultivation due to rising water levels. For instance, the sustainability of the rice-wheat cropping system in an irrigated semi-arid area of Haryana State (India) reported

to be under threat due to the continuous rise in the poor quality of groundwater table, which is caused by the geo-hydrological condition and poor irrigation water management (Singh et al. 2010; Singh 2011). In particular case of rice environments, high methane (CH_4) emissions can strongly contribute to the accumulation of greenhouse gases into the atmosphere, contradicting with the eco-compatibility and production of rice. Since high water table conditions are linked with infiltration and deep percolation processes, there exists strong relation between methane emission and percolation processes from rice fields as more percolation favours high water table conditions through time (Rizzo et al. 2015). Proper management of percolation and provision of drainage facility in irrigated rice systems may alleviate the problem.

In extreme cases, the negative effects from deep percolation may lead to loss of cropping land, serious reduction in crop yields, acute environmental pollution and create huge costs for management.

2.3 CHARACTERISTICS OF DEEP PERCOLATION

Deep percolation at specified depth below crop root zones reveals delayed response to input water occurred at soil surface in a given area. Some model studies indicated that the long-term pattern of groundwater recharge/deep percolation has closely followed that of irrigation. After crop-water requirements are met, excess water applied to the land surface simply drains through the soil profile to recharge the aquifer. Short-term perturbations in the recharge pattern are responses to precipitation, which varies greatly from year to year, and periodically generates significant pulses of groundwater recharge (Kendy et al. 2004). In an irrigated area, large magnitude of deep percolation occurs at head end than the tail end of irrigation borders or furrows. This is mainly due to the non-uniformity of infiltration which depends on particular soil properties (Sharma and Singh 2009).

With reference to specific location in an agricultural field, how deep percolation phenomena takes place was a concern for many researchers. In many instances, percolation from root zone is assumed as a cumulative pulse occurring on a day (Doorenbos and Pruitt 1977; Ochoa et al. 2007) when there is irrigation or rainfall. Walker et al. (1995), on the other hand, showed that deep percolation becomes maximum on the first day after irrigation or rainfall and linearly decreasing until it ceases when soil moisture storage in the root zone is less than field capacity. Danuso et al. (1995) and Parkes et al. (1995) adopted the non linear decay curve or a power law function which depends on the hydraulic conductivity to characterize deep percolation. Liu et al. (2006) established parametric functions which are used to estimate and characterize deep percolation in which the parametric functions follow a power law or a

decay curve. Wang et al. (2012) also showed that deep percolation becomes maximum on the first day after irrigation and decreases then after until it ceases in both cases of sprinkler and flood irrigation methods. Hence, in many cases, deep percolation under irrigated area is characterized by maximum rate at certain time after irrigation and rainfall occurrence and then continues with a decreasing trend until it ceases. This might be due to the characteristics of flow in a porous media.

Deep percolation can also take place in unsaturated flow conditions below a crop root zone. Preferential flow phenomena due to macropores (formed as a result of soil shrinkage, root growth, chemical weathering, etc (Beven and Germann 1982), finger flow phenomena (caused either by water repellency or air entrapment (Glass et al. 1988; Wessolek et al. 2008) or funnel flow (due to lateral redirection of percolating water resulting from changes in soil layer texture (Kung 1990)) could facilitate more deep percolation, even in unsaturated conditions. As a matter of fact, these flow phenomenon are not obeyed by the classical Richards (1931) equation (Hendrickx and Flury 2001; Šimůnek and van Genuchten 2007; Bethune et al. 2008; Selle et al. 2011; Hardie et al. 2011; Mohanasundaram et al. 2013). In such cases, in general, percolation is taking place without satisfying the water storage requirements and redistribution processes in the root zone (Liu et al. 2004). On the other hand, the lateral dimensions of flow paths in the soil zone can be increased due to removal of finer particles with the flowing water resulting in an increase of porosity and hydraulic conductivity (Govindaraju et al. 1995) which may further yield more deep percolation.

Evapotranspiration takes place during the daylight hours when the energy is sufficiently available to facilitate evaporation from soil and plant surfaces which further necessities crops to transpire to meet the evaporative demand of the atmosphere. In contrast, nocturnal evapotranspiration is very small or negligible. This phenomenon could lead to more percolation during the night periods. Paltineanu et al. (2013) have noted that daylight soil water discharge (SWD) in response to evapotranspiration is higher than night time SWD mainly due to solar radiation, higher vapour pressure deficit, and wind speed, with crop transpiration and crop water uptake being higher during daylight than night-time. Hatiye et al. (2014) have also shown that deep percolation from cropped rice and berseem fields have less percolation during day time than night times which is attributable to the effect of evapotranspiration during the day time.

2.4 MEASUREMENT OF DEEP PERCOLATION

Lysimeters are often used to measure deep percolation or to determine the quality of percolating water (Qureshi and Madramootoo 2001; Hillel 2004; Loos et al. 2007; Evett et al. 2012). Lysimeters are generally large containers of soil, set in the field to represent the prevailing soil and climatic conditions and allowing more accurate measurement of physical processes than can be carried out in the open field. The use of lysimeters was first reported in the Netherlands and France mainly to study crop water use (Hillel 2004). Field studies using lysimeters represent an accurate tool in the determination of the water balance components in the soil-plant-atmosphere system, representing the real field conditions (Loos et al. 2007). Gee and Hillel (1988) also showed that lysimeters are usually better for evaluating the water balance compared to other methods.

Lysimeters can be broadly classified as percolation lysimeters (drainage type lysimeters) and weighing type lysimeters. Percolation and weighing type lysimeters differ in their measurement methods to determine the crop consumptive water use and/or soil-water evaporation. Percolation lysimeters are suggested to be used with a soil-water profile measurement tools (such as for example, neutron scattering; tensiometry; time domain reflectometry (TDR)) to estimate 'indirectly' the water use in evaporative processes. Weighing type lysimeters permit the mass or volumetric soil-water content change to be determined by weighing the lysimeter and determining its mass change over time. Weighing lysimeters, thus, can determine the 'net' infiltration from rainfall or irrigation and the amount of evaporation between wetting events. If properly designed, weighing type lysimeters can concurrently measure the drainage rate as well as the evaporation rate. Percolation lysimeter accuracy of the evaporative water balance is directly related to the precision of the soil water measurement and its integration through the vegetation root zone. The precision of weighing type lysimeters depends on many factors such as scale resolution, counterbalancing, and area-to-volume ratio (Hillel 2004). In general, weighing type lysimeters are more accurate than drainage type lysimeters. However, weighing type lysimeters are criticized to be costly to install, maintain and operate; and as such they often are used singly such that adequate replication of measurements is not possible (Hillel 2004; Bethune et al. 2008; Evett et al. 2012).

Many factors need to be considered in the design of lysimeters including the experimental purpose, shape and area of the lysimeter, lysimeter depth, lysimeter tanks and drainage systems as described by Hillel (2004). If the lysimeter facility is required to replicate the surrounding environment, an adequate fetch shall be available in the surrounding of the site selected for lysimeter installation. Preferably, rectangular or square configuration with areas

ranging from 1 to 30 m^2 is suited for most conditions of a cropped environment. Obviously, larger sizes are desired, but they are restricted by capital resources as well as operational and construction difficulties. The basic consideration in fixing lysimeter depth is to duplicate adequately the field rooting depth for the species being studied. Additionally, lysimeter depth has been shown to affect the lysimeter water holding capacity and the soil water flux through the profile (Hillel 2004).

Drainage type lysimeters are considered to be the most important facilities, at field level, to measure percolation. Oad et al. (1997) presented a study on how small lysimeters were able to estimate deep percolation from lawn grass. Qureshi and Madramootoo (2001) employed drainage type lysimeters to monitor bottom flux under varying water table conditions. Bethune et al. (2008) conducted a lysimeter experiment to understand and quantify deep percolation response under irrigated pasture to different soil types, water table depths, and ponding times during surface irrigation. Feltrin et al. (2011) also used drainage type lysimeters to study the behaviour of water balance components in the Southern Brazilian Atlantic forest region. They have investigated significant amount of deep drainage in the region which cannot be neglected.

Loos et al. (2007) have used an extensive set of weighing type lysimeters in south Germany with rotative crop vegetations over 5 years to evaluate different modeling approaches for the estimation of soil hydraulic characteristics and evapotranspiration (*ET*). Weighing type lysimeters are usually employed as a bench mark devices for estimating evapotranspiration component of the water balance (Pruitt and Angus 1960; Holmes 1984; Young et al. 1996; Vaughan et al. 2007; Lo´pez-Urrea et al. 2006). Drainage type lysimeters were also involved in estimating evapotranspiration from a cropped area. Benes et al. (2012) have used drainage type lysimeters to measure evapotranspiration and compared it with evapotranspiration from surface renewal methods. Evett et al. (2012) investigated the ability of large weighing lysimeters in reproducing the surrounding field evapotranspiration measured by flux stations (Bowen ratio and eddy covariance measurements). They concluded that if supported by a sufficiently dense and widespread network of deep soil water balance based estimates of *ET* in the surrounding patch and by ancillary measurements of crop stand and growth within the lysimeter and in the surrounding patch, a weighing lysimeter can provide accurate *ET* ground truth for comparisons with *ET* estimated using flux stations or *ET* calculated using satellite imagery.

Recently, many modifications on lysimeter configuration and setup have been evolved owing to the different field conditions, purpose, operation principles etc. Abdulkareem et al. (2015) conducted a review on common types of lysimeters used in solute transport studies. They reviewed the features, setup, working principles, advantages and disadvantages of pan or

zero tension, free drainage, passive wick type, suction cup and suction plate type lysimeters. Free drainage lysimeters are lysimeters where water is allowed to drain freely through the soil under gravity whereas suction controlled drainage systems consist of suction cups, wick samplers, or porous plates at the lower boundary to collect the percolating water. The detailed description and working principles of such types are provided in (Abdulkareem et al. 2015). Zhu et al. (2002) have also showed the construction procedures and efficiency of both the pan and wick type lysimeters in capturing the leacheate or drainage. Nowadays, very high precision lysimeters have been made possible at natural field conditions which can account for inputs such as dew and fog besides accurate measurement of seepage, rainfall and evapotranspiration (Meiβner et al.2010). Although water can move upward, most lysimeters are not equipped to measure or add water to simulate upward water fluxes. In some cases, lysimeters are required to maintain dynamic water table conditions to mimic field conditions besides drainage monitoring. These lysimeters are equipped with facilities to add or withdraw water from lysimeters to maintain the water table depth in the lysimeters similar to the surrounding fields (Qureshi and Madramootoo 2001; Kowalik 2006). However, these types of lysimeters are expensive to install and operate under actual field conditions (Abdulkareem et al. 2015).

'Lockup bay tests' as proposed by Humphreys (1992) together with a modified lysimeter experiment (Bethune et al. 2001) can also be used to measure deep percolation particularly in rice fields. In this case, a series of three lysimeters are installed to measure transpiration, evaporation and deep percolation. Two lysimeters are provided with an open ended bottom in which one is located inside a cropped area (to measure water loss due to transpiration, evaporation and deep percolation) and the other is outside the cropped area (to measure loss due to evaporation and deep percolation). The third lysimeter is located outside the area with a sealed bottom to measure evaporation only. In this way, one can measure transpiration, evaporation and deep percolation from a cropped area.

Micro lysimeters (ML) are small tubes filled with soil of intact structure, installed at ground level and weighed regularly to measure the difference in mass due to evaporation during a given period. They can be constructed of different materials and specifications to monitor soil evaporation. A number of successful studies were conducted employing micro lysimeters (Daamen et al. 1993; Evett et al. 1995; Flumignan et al. 2012). However, the implementation of ML is limited to near soil surface and often labour intensive due its nature of data acquisition. Further, lysimeters can be constructed at laboratory and can be used in the study of water or solute transport (Sutanto et al. 2012).

Percolation from crop root zone might also be estimated using infiltrometer tests (Kukal and Agarwal 2002; Kukal and Sidhu 2004), however, such tests are good enough in ponded water conditions such as the case of rice fields.

2.5 ESTIMATION OF DEEP PERCOLATION

Different methods can be used to estimate deep percolation from a cropped area ranging from empirical relations to process based mechanistic models (Doorenbos and Pruitt 1977; Sammis et al. 1982; Willis et al. 1997; Allen et al. 1998; Weaver et al. 2005; Vaccaro 2007; Ochoa et al. 2007; Bethune et al. 2008; Arnold 2011; Ma et al. 2013). However, the most commonly used methods comprise of the unsaturated zone soil water balance (simple water balance) and physically based models. Other methods which were utilized in estimating percolation loss include chloride mass balance, tritium mass balance, water table fluctuation methods and empirical approaches although these are infrequently employed to estimate deep percolation phenomena. Since the present study is concerned with the application of water balance and physically based models for estimation of deep percolation, mainly literature with regard to these two approaches are discussed in detail.

Doorenbos and Pruitt (1977) considered a simple water balance concept to compute deep percolation. Computations of *DP* were carried out assuming that the fluxes occur on the day when excess water is applied, which may not be true for soils where water moves slowly (Liu et. al. 2006) or in lysimeters where there may be a storage effect which could be significantly affect flow phenomena. The basic principle of this model is that whenever soil water content at a given depth below ground surface is above field capacity, it will yield percolation and no percolation would exist if the water content in the root zone is below the soil's field capacity threshold. Sammis et al. (1982) presented three alternative methods to estimate *DP* in the absence of data on input water and evapotranspiration. The methods were 1) Darcy's equation, 2) measurement of the soil temperature profile variation along the vertical depth and 3) measurement of the tritium concentration in the soil water and its relationship to the history of the tritium concentration in the rainfall. The estimation was made for annual deep percolation amount assuming steady state flow condition in a given site. The Darcy equation yields that *DP* is equal to hydraulic conductivity for unit hydraulic gradient under steady flow conditions. The tritium approach is based on the fact that tritium levels in rain water have increased since the advent of nuclear devices and testing since 1950's. If there is appreciable increase in the tritium levels (more than 10 tritium units) in deep soil water, it could probably indicate that there was deep drainage from precipitation. However, this approach is more

qualitative and thus only provides rough estimation of deep drainage. Willis et al. (1997) also employed three different approaches to estimate *DP* from the bottom of irrigated cotton root zone: the water balance, Darcian flux and chloride mass balance approaches. They have analyzed that the chloride mass balance method provides reliable cumulative deep percolation for the growing season while the water balance approach yields fair *DP* estimate for event irrigation/ rainfalls. Walker (1999) also emphasised that large losses of water from wetland rice fields occurs through non puddled under bund percolation.

Allen et al. (1998) described the well known water balance equation in attempt to estimate daily evapotranspiration considering the water balance components in the root zone. Deep percolation is one of the components taken into account in the FAO-56 procedure (Allen et al. 1998) of the water balance technique. However, deep percolation is assumed to occur only on the day when there is heavy rainfall or irrigation and/or the soil water zone is above field capacity water content. Vaccaro (2007) has developed a deep percolation model (DPM) to estimate groundwater recharge and for inclusion into the United States Geological Survey (USGS) modular modelling system. The scope of this model ranges from field level to regional landscapes to estimate *DP* consisting of a layer of modules which include a large range of climatic, landscape, and land-use and land-cover conditions. Ochoa et al. (2007) estimated *DP* below the depth of 1m in alfalfa-grass field using water balance and root zone water quality model (RZWQM) and studied its effect on the rise of shallow groundwater level due to flood irrigation in northern New Mexico. They have showed that the results of *DP* estimated using the two methods is consistent and concluded that flood irrigation is a significant source of shallow groundwater recharge.

Arnold (2011) employed the water balance and ground water level fluctuation approaches to estimate deep percolation from flood and sprinkler irrigated farms. The water balance method equates deep percolation to increase in soil water storage from crop root zone below the ground surface while the water table fluctuation is based on the assumption that rises in unconfined aquifer levels are caused by recharge from downward percolating water and that no other sources or sinks affect groundwater levels during the recharge event. However, lateral subsurface flow into the aquifer of interest may violate the assumption and yield erroneous results.

Kim et al. (2009) estimated irrigation return flow in rice fields considering the soil moisture. The particular study considered deep percolation as one of the components of irrigation return flow; as a vertical percolation taking place through saturated and unsaturated portion of the rice fields. Although not explicitly indicated in this study, quite large volume of

vertical percolation (nearly 50% of the overall input water) has occurred through the bottom of the rice field. Chien and Fang (2012) applied similar water balance model to estimate irrigation return flow considering deep percolation. This study specified the presence of hardpan below an irrigated rice field which could limit deep percolation flow but facilitate lateral irrigation return flow. Wang et al. (2012) used both the water balance and isotope mass balance methods to estimate evaporation, transpiration and deep percolation fluxes from flood and sprinkler irrigated field. They used oxygen-18 isotope mass balance technique to determine the three fluxes in the summer corn and winter wheat fields under existing irrigation pattern in Shanxi Province, China. Several other models were also developed to analyze the root zone soil water balance and its dynamics which also constitute the deep percolation component of the water balance (Li and Shao 2014; Singh et al. 2014; Ma et al. 2013; Eilers et al. 2007; Chen and Liu 2002).

Physically based models, based on the solution of classical Richards (1931) equation, are also often used in estimating deep percolation (Clemente et al. 1994; Bethune et al. 2008; Ji et al. 2007; Selle et al. 2011; Sutanto et al. 2012; Li et al. 2014; Tan et al. 2015). Various models have been developed based on the solution of the Richards (1931) equation in the last few decades; for example, the models Soil WAter and CROP production model (SWACROP) (Kabat et al. 1992), Water and Agrochemicals in soil and Vadose Environment (WAVE) (Vanclooster et al. 1994), Soil-Water-Atmosphere-Plant (SWAP) (Ahmad et al. 2002), HYDRUS-1D (Šimůnek et al. 1998) and MACRO (Jarvis 1994). These models provide accurate computations of deep percolation (Liu et al. 2006) when compared with soil water balance models. However, deterministic approaches require more complete description of the soil water retention and hydraulic properties which limits their wide use under most field conditions since it is often difficult to obtain the relevant data. In addition, large numbers of models addressing problems of unsaturated flow and solute transport have also been developed. Köhne et al. (2009), for example, reviewed different models developed to simulate water flow and pesticide transport in structured soils. Clement et al. (1994) used three different models which were developed based on Richards (1931) to predict soil water content profiles during the growing seasons in field. Further, the Darcy based one dimensional soil water balance model (SAWAH) (ten Berge et al. (1992)), IRRIMOD (Angus and Zandstra 1980) and PADDYWATER (Bolton and Zandstra 1981), ORYZA2000 (Bouman et al. 2001) are also some of the models employed to simulate soil water flow in the rice field and deep percolation among others.

2.5.1 Water Balance Method

The soil water balance, the concept derived from the law of conservation of mass, is used in a large number of studies which are dealing with water flow in the crop root zone, solute transport, groundwater flow and recharge, evapotranspiration, etc. Generally, soil water balance deals with quantification and analysis of each inflow and outflow variables while accounting for storage in the system environment. It is usually described in the form of the following mass balance equation.

$$I_n - O_o = \frac{dS}{dt} \tag{2.1}$$

where I_n[LT^{-1}]= Input, O_o [LT^{-1}]= output, S =Storage[L] and t =Time[T]

When the above equation is further defined for the crop root zone in an irrigated area, without considering snow melt contribution can be written as (Willis et al. 1997; Allen et al. 1998; Eilers et al. 2007; Chen and Liu 2002; Ma et al. 2013; Li and Shao 2014; Singh et al. 2014):

$$(P + I + SP_{in} + GW) - (R + DP + ET + SP_{ot}) = \Delta S \tag{2.2}$$

where P[L] is precipitation, I[L] is irrigation, SP_{in}[L]and SP_{ot} [L] are seepage/lateral inflow and outflow respectively from the root zone, GW[L] is the capillary rise from groundwater, R[L] is surface runoff, DP[L] is deep percolation, ET[L] is evapotranspiration and ΔS[L]is change in soil moisture storage. Some studies have also included snow melt contribution to the water balance (Vaccaro, 2007).

Precipitation and irrigation are inputs to the model and often measured for a given field condition. The seepage inflow and outflow components are usually neglected due to the difficulty in estimation and the concept of equilibrium. The runoff volume out of a given area could be measured using open channel flow measurement techniques (Chien and Fang 2012), estimated using such methods as Soil Conservation Service (SCS) curve number method (Jung et al. 2012) or neglected sometimes in cases like infrequent rainfall coupled with provision of field bunds which stop runoff (Kim et al. 2009). The soil moisture storage, ΔS, can be determined from consecutive measurements of the soil moisture content or determined from the weight differences of weighing type lysimeters. However, GR, ET, and DP are difficult variables to accurately measure in a field (Rashton and Ward 1979; Liu et al. 2006).

The capillary rise, the upward flow of water from the groundwater zone, is mainly considered when the water table is shallow (Raes and Deproost 2003; Tan et al. 2014). Liu et al. (2006) have given an extensive set of literature on the study of capillary rise to the soil water zone. Evapotranspiration, water loss from soil (evaporation) and loss of water through plant leaves (transpiration), could be determined using various approaches which will be dealt in the

next sections. Therefore, deep percolation can be obtained from the above equation having the rest of the components estimated or measured.

2.5.1.1 Crop evapotranspiration

Evapotranspiration is the rate at which water is transferred from land and plant surfaces to the atmosphere. *ET* is a function of the surface radiative and advective energy, and varies in time and space depending on crop/vegetation type and density, soil type and moisture, and local-to-regional meteorological factors such as humidity and precipitation (Beamer et al. 2013). Crop evapotranspiration, ET_c, under standard conditions, also called potential evapotranspiration, is the evapotranspiration from disease-free, well-fertilized crops, grown in large fields, under optimum soil water conditions and achieving full production under given climatic conditions (Allen et al. 1998). The amount of water required to compensate the evapotranspiration loss is the crop water requirement. Crop water requirement refers to the amount of water that needs to be supplied either through irrigation, effective rainfall or contribution of groundwater through capillary rise. The water supplied through irrigation after net precipitation and other input considerations is defined as the irrigation water requirement. ET_c is related to reference evapotranspiration (ET_0) using a crop coefficient (K_c). Generally, ET_c is computed as a product of K_c and ET_0 although there are different methods to determine crop evapotranspiration exist.

2.5.1.1.1 Direct measurement of crop evapotranspiration

Crop evapotranspiration is not easy to measure. Specific devices and accurate measurements of various physical parameters or the soil water balance in lysimeters are required to determine ET_c. Several methods are available to measure and estimate crop evapotranspiration including hydrological, micrometeorological and plant physiology approaches (Rana and Katerji 2000). The hydrological methods include soil water balances and lysimeter measurements. Micrometeorological techniques comprise of eddy covariance and Bowen ratio energy balance methods. Plant physiological techniques usually consist of chamber systems and sap flow measurements. Detailed advantages and limitations of these methods along with their applications to specific conditions are discussed in Nouri et al. (2013). However, frequent applications of these methods for a given field condition remains limited since monitoring devices are often expensive and require skilled personnel to operate the devices.

2.5.1.1.2 Crop coefficient approach

In the crop coefficient approach, ET_c is computed by multiplying the reference evapotranspiration, ET_0, by the corresponding value of crop coefficient for a given cropped area (Allen et al. 1998).

$$ET_c = K_c \times ET_o \tag{2.3}$$

The crop coefficient depends on crop type and its growth stages which also incorporate factors such as crop height, soil-crop surface resistance and albedo (reflectance) of the potential evaporative surface which are distinguishing a crop from the reference crop. Thus, in this way, crop evapotranspiration is differentiated from the reference evapotranspiration under the same climatic conditions (Allen et al. 1998). Moreover, differences in evaporation and transpiration between field crops and the reference grass surface can be integrated into a single crop coefficient or dual crop coefficient in which the crop coefficient is separated into two coefficients: a basal crop (K_{cb}) and a soil evaporation coefficient (K_e); i.e., $K_c = K_{cb} + K_e$. The approach to follow should be selected as a function of the purpose of the calculation, the accuracy required and the data available. Detail procedures of computing and further adjusting K_c values for a given local climatic and agronomic conditions are documented in FAO paper 56 (Allen et al. 1998).

The reference crop evapotranspiration or reference evapotranspiration, $ET_{0,}$ is the evapotranspiration rate from a reference surface, not short of water. The reference surface refers to a hypothetical green grass reference crop which is actively growing, 8-15 cm tall and disease free, completely shading the ground surface and not short of water (Doorenbos and Kassam 1979). Quite large numbers of models have been evolved to date to compute the reference evapotranspiration, ET_0. Most of the methods were based on climatic variables as ET_0 mainly depends on the climatic conditions of a given area.

ET_0 estimation methods based upon climatological data vary from empirical relationships to complex methods such as Penman combination methods based on physical processes (Shankar 2007; Chow et al. 1980). The different methods of ET_0 estimation can be categorized into combination theory types (Penman–Monteith, FAO-24 corrected Penman, 1982 Kimberly Penman), empirical formulations based on radiation (Turc, Jensen Haise, Priestly Taylor and FAO-24 radiation), temperature based (Thornthwaite, SCS Blaney Criddile, FAO-24, Blanney Criddile Hargreaves) and pan evaporation (Christianson Pan, FAO 24 Pan) methods. Comparison of these methods and other local models is done thoroughly elsewhere besides suggesting a suitable method for a given area (Nandagiri and Kovoor 2006). For most

climatic conditions, the FAO Penman-Monteith method is taken as a standard method and widely accepted in many parts of the world (Allen et al. 1998; Nandagiri and Kovoor 2006) which is stated as:

$$ET_o = \frac{0.408 \times \Delta(R_n - G) + \gamma \frac{900}{273+T} u_2 (e_s - e_a)}{\Delta + \gamma(1 + 0.34u_2)} \quad (2.4)$$

where R_n is net radiation at the crop surface (MJ/m^2/day), G is soil heat flux density (MJ/m^2/day), e_s is saturation vapour pressure (kPa), e_a is actual vapour pressure (kPa), T is air temperature at 2 m height (^{o}C), u_2 is wind speed at 2 m height (m/s), Δ is slope of vapour pressure curve (kPa/^{o}C), and γ is psychometric constant (kPa /^{o}C). Penman-Monteith equation takes into account important physiological variables that affect crop evapotranspiration and provides a comprehensive framework to compute potential *ET* which is used as a reference tool to estimate actual evaporation (Narasimhan et al. 2003). Further, the Penman Monteith approach is recommended to be used with strict adherence to the standardized procedures of parameter estimation (Nandagiri and Kovoor 2004).

However, in actual field conditions, the actual evapotranspiration is less than the potential evapotranspiration since either the soil water is limiting (Liu et al. 1998) or the required energy is reduced to produce the potential ET_c (Allen et al. 1998; Chow et al. 1980). Therefore, the soil water stress coefficient, K_s, is introduced in the calculation of the actual evapotranspiration.

$$ET_c = K_s \times K_c \times ET_o \quad (2.5)$$

The K_s is the factor depending on the soil moisture availability for evapotranspiration and is given by:

$$K_s = \frac{TAW - D_i}{TAW - RAW} \quad (2.6)$$

where *TAW* (mm) = total available water = $10*Z_j*(\theta_{fc} - \theta_{wp})$, θ_{fc} and θ_{wp}, respectively, are the field capacity and wilting point soil moisture contents ((%), R*AW* (mm) = readily available water that can be obtained by multiplying *TAW* to a depletion coefficient, p_r, considering the crop water stress resistance. In particular, when water storage in the root zone is equal to RAW, the reduction coefficient K_s is equal to 1. The depletion fraction for no stress (p_r) is crop specific and depends on evapotranspiration. In fact, irrigation is scheduled when there occurs soil water deficit in the root zone, called management allowed depletion (MAD). The irrigation threshold to avoid water stress is when the actual soil moisture content, θ_i, equals the threshold relative to p_r, $\theta_i = \theta_{pr}$, is given by:

$$\theta_p = (1 - p_r)(\theta_{fc} - \theta_{wp}) + \theta_{wp} \quad (2.7)$$

Thus net irrigation depth then can be computed using:

$$I_{ni} = 10 Z_j (\theta_{f_c} - \theta_{p_r}) \quad (2.8)$$

where I_{ni} is the irrigation depth (mm), θ_{wp} the wilting point soil moisture content (%); Z_j = root zone depth (m). When water stress is not admitted, then MAD = p_r; a MAD < p_r is adopted when there is risk aversion or uncertainty, and MAD > p_r when crop water stress is allowed. However, in actual field conditions, uncertainties in estimating soil water thresholds, soil heterogeneity, irrigation application methods, crop type, etc would result in either excess water application or less volume of water supply.

2.5.2 Physically Based Methods

Soil in the unsaturated zone is characterized by pore spaces which are partly filled with water and partly by air. The water molecules are held by the capillary tension force. Hence the pressure in the unsaturated zone is suction pressure, $\psi < 0$. In the saturated zone the pressure head is positive ($\psi > 0$) owing to the hydrostatic pressure at water table, $\psi = 0$. It follows that in the unsaturated zone, the pressure head, ψ, the water content, θ, and the hydraulic conductivity, *K*, are changing both spatially and temporally unlike in the saturated zone where the hydraulic conductivity and water content are constant for a given soil. Hydraulic conductivity, *K*, and water content, θ are functions of the pressure head in the unsaturated zone. The relationship between hydraulic conductivity and water content or pressure head and water content can be expressed by the soil moisture characteristic curve (SMCC). The variation of water content and the pressure head in the unsaturated zone applies to all conditions of wetting and drying of the soil/soil surface, although the path followed by the SMCC curve often do not follow the same route during wetting and drying due to the effect of hysteresis.

The physically based approach for solving problems of water flow in unsaturated zone involves Darcy or Richards equation. The vertical flow in an unsaturated porous media can be expressed by Darcy equation as follows (Chow 1980).

$$q = -K(\psi) \frac{\partial(\psi + z)}{\partial z} \quad (2.9)$$

Where *q* is the Darcy flux [L/T], *K* is the hydraulic conductivity [L/T] and *z* is the vertical depth [L] along the flow path. Further, the flux can be expressed in terms of the soil water content in the soil water zone employing continuity equation.

$$\frac{\partial \theta}{\partial t} = -\frac{\partial q}{\partial z} \quad (2.10)$$

Substitution of equation (2.9) into equation (2.10) yields the classical Richards equation. Flow in the unsaturated zone is usually simulated by solving Richards equation (1931). The Richards equation can be derived from mass balance and Darcy's equation (momentum equation) considering the unsaturated zone as isothermal, homogenous, isotropic and water as an incompressible fluid (Guymon 1994).

2.5.2.1 Richards equation

The Richards equation may be expressed in several forms using either pressure head (ψ) or moisture content (θ) as the dependent variable. The constitutive relationship between θ and ψ allows for conversion of one form of the equation to another (Celia et al., 1990). Three standard forms of the Richards equation have been identified: The θ based form, the ψ based form and the mixed (θ-ψ) forms.

θ based form:

$$\frac{\partial \theta}{\partial t} - \nabla \bullet D(\theta) \nabla \theta - \frac{\partial K(\theta)}{\partial z} = 0 \qquad (2.11)$$

ψ based form:

$$C(\psi)\frac{\partial \psi}{\partial t} - \nabla \bullet K(\psi) \nabla \psi - \frac{\partial K(\psi)}{\partial z} = 0 \qquad (2.12)$$

mixed form:

$$\frac{\partial \theta}{\partial t} - \nabla \bullet K(\psi) \nabla \psi - \frac{\partial K(\psi)}{\partial z} = 0 \qquad (2.13)$$

where in equations 2.11-2.13, θ is the moisture content [L^3L^{-3}], ψ is the pressure head [L], z is the vertical coordinate taken positive upwards [L], *t* is the time coordinate[T], $C = d\theta/d\psi$ the specific moisture capacity of a given soil [L^{-1}], *K* is the hydraulic conductivity of the soil [LT^{-1}] and $D = K/C$ is the soil moisture diffusivity [L^2T].

Analytical solution of the above forms is seldom available due to the non-linear behaviour of the equations. Therefore, numerical approaches are usually employed. The numerical approaches often used are the finite difference and finite element solution techniques. The detail development, merits and limitations of these methods have been dealt in Celia et al. (1990) and Clement et al. (1994) making use of measured field data.

The θ based formulation provides improved performance due to small variations of the magnitude in comparison to the head based formulation when, for example, modeling infiltration into very dry soil (Hills et al. 1989). However, θ based forms could not be used for problems involving saturated regions since soil moisture diffusivity becomes undefined in such

regions. In contrast, the ψ based formulation can be applied for both saturated and unsaturated soils. Nonetheless, ψ based formulation requires small time steps to maintain numerical stability and minimize truncation errors, particularly while solving problems with steep wetting fronts. Further, the solution of ψ based form suffers from inaccuracies and poor mass conservation (Celia et al. 1990; Clement et al. 1994).

A mixed form of Richards equation, which inherits the advantages of the earlier forms and removes their limitation, is used in many studies (Celia et al. 1990; Clement et al. 1994; Shahraiyni and Ataie-Ashtiani 2012). The mixed form includes both moisture content and pressure head as unknowns. It conserves mass better than the ψ based form as well as fairly applied for problems in saturated and unsaturated soils.

2.5.2.2 Soil moisture movement in the crop root zone

The soil moisture movement in the crop root zone is the response mainly due to soil evaporation, crop transpiration and deep drainage. Soil evaporation mainly occurs on or near the soil surface while root water uptake takes place in the entire crop root zone. Crop roots extract water through their microscopic openings and water is conveyed through the crop stems to satisfy the climatic demand by releasing water in the form of vapour to the ambient atmosphere. This phenomenon which occurs through crop stomatal opening is referred to as crop transpiration.

After water infiltrates into the root zone it undergoes redistribution which could be explained by the Richards equation. To examine the water flow in cropped soils, a sink term is usually added to the Richards equation to account for vertical accretion of the root water uptake (Govindaraju and Kavvas 1993). The sink term accompanying the Richards equation has been considered quite in numerous studies elsewhere (Ji et al. 2007; Sutanto et al. 2012; Shankar et al. 2012; Li et al. 2014). The mixed form of Richards equation with sink term accounting for root water uptake and neglecting non-hysteretic flow condition is given as:

$$\frac{\partial \theta}{\partial t} = \frac{\partial}{\partial z}\left[K(\psi)\left(\frac{\partial \psi}{\partial z} + 1 \right) \right] - S(z,t) \qquad (2.14)$$

where *S(z,t)* is the sink term in the flow equation accounting for root water uptake. The solution of equation (2.14) yields the pressure head or soil moisture content in space and time domain which will be used to evaluate the soil water movement in the crop root zone such as the phenomena of infiltration, evapotranspiration, plant moisture uptake, deep percolation, etc. (Shankar 2007).

In particular, the deep percolation below crop root zone at a given depth can be computed as a flux passing through the particular point after all sink and source terms are accounted. The percolation at specified depth can be obtained from Darcy equation (2.9) after pressure head and water content values are computed. Components of the Darcian flux are computed at each time level during the simulation period when the flow equations are solved.

2.5.2.3 Constitutive relationships

The Richards equation is highly non-linear due to the fact that the independent variable (soil moisture content, θ) and storage properties (*K*, *C* and *D*) are functions of dependent variable (pressure head, ψ). Thus, the solution needs constitutive relationships which are also described as soil hydraulic models. The relationship between ψ and θ yields soil-water characteristic curve (SWCC) or retention curve (RC) (Nandagiri and Prasad 1997). On the other hand, the relationship between ψ and *K* or θ and *K* refers to the conductivity curve. The SWCC is an essential input data for modelling and understanding the behaviour of flow in unsaturated soils and employed in problems related to road and railway embankments, irrigation water management, waste containment and solute transport in the vadose zone (Malaya and Sreedeep 2012). The SWCC is influenced by many factors. A critical review on factors influencing the SWCC has been provided by Malaya and Sreedeep (2012).

$\psi - \theta$ Relationship

Many researchers used empirical and semi empirical relations to describe the SWCC. The contributions from Brooks and Corey (1964), Campbell (1974) and van Genuchten (1980) offer a piece wise continuous relation for the $\theta - \psi$ characteristics. Other forms of models which include regression analysis and pedo-transfer functions have also been designed to describe SWCC (Loos et al., 2007; Ghosh 1980; Gupta and Larsen, 1979). Fredlund and Xing (1994) provided a large listing of different mathematical forms for defining SWCC.

However, of many empirical functional forms available in the literature, the models by Brooks and Corey (1964), Campbell (1974) and the van Genuchten (1980) are popular and widely used.

Brooks and Corey's relationship:

$$\Theta = \left(\frac{\psi_b}{\psi}\right)^{\lambda_b} \quad \text{for } \psi \le \psi_b$$

$$= 1 \quad \text{for } \psi > \psi_b \qquad (2.15)$$

where ψ_b is the bubbling pressure, λ_b is the pore size index and Θ is the effective saturation which is defined as:

$$\Theta = \frac{\theta - \theta_r}{\theta_s - \theta_r} \tag{2.16}$$

where θ_s is the saturated soil moisture content, θ_r is the residual soil moisture content.

Campell's Relationship:

$$\frac{\theta}{\theta_s} = \left(\frac{H_b}{\psi}\right)^{1/b} \quad \text{for } \psi \le H_b$$

$$= 1 \quad \text{for } \psi > H_b \tag{2.17}$$

where H_b is the scaling parameter with dimensions of length and b is a constant.

van Genuchten's relationship:

$$\Theta = \left[\frac{1}{1+\left|\alpha_v \psi\right|^{n_v}}\right]^m \quad \text{for } \psi \le 0$$

$$= 1 \quad \text{for } \psi > 0 \tag{2.18}$$

where α_v and n_v are unsaturated soil parameters with $m = (1-(1/n_v)$.

The SWCC should present continuity in the slope of the curve and yield a closed form equation for the representation of the total SWCC. The relationship according to van Genuchten (1980) satisfies a closed form representation while the models presented by Brooks and Corey (1964) and Campbell (1974) exhibit discontinuity near zero or bubbling pressure.

Soil moisture content can be determined using various methods including the ground based sensor measurements, gravimetric method and remote sensing approaches. However, each of these have their own advantages and limitations to hydrologic studies (Ojha and Govindarju 2015; Vereecken et al. 2008). The point scale measurements enable determination of soil moisture content in the soil depth profile and limited to spatial extent. The remote sensing approach provides information on soil moisture content on large spatial extent but limited to surface soil layers only (Ojha and Govindaraju 2015). Both field and laboratory methods have been developed to furnish SWCC for a given soil (Rao and Singh, 2012). Laboratory determination of SWCC involves desorption/drying of initially saturated soil sample to specific pressure value at which water content of the sample is evaluated. Such methods range from thermocouple psychrometry, heat dissipation sensors, dew point potential meters, hanging water columns, pressure plate apparatus, suction tables and vapour pressure methods (Bittelli 2010). Field level soil water content measurement tools may include

tensiometers, heat dissipation sensors, dielectric sensors (such as time domain reflectometry (TDR)) and thermocouple psychrometry (Bittelli 2010). The working principles and field operations of these instruments is well documented. These methods determine the soil water status (on water content base or pressure base) at a given depth of interest and either pressure or soil water content is determined by coupling another method to determine SWCC, i.e., usually two sets of methods are employed to determine SWCC.

Further, SWCC may exhibit hysteresis, the condition in which the moisture characteristic curves do not follow the same path during wetting and drying (Witkowska-Walczak 2006; Hillel 1980). The effect of hysteresis is dependent upon the soil porosity; for coarser soils where the size of voids is large, its effect is minimal and vice versa. The phenomena of hysteresis added extra complication in further understanding of the unsaturated flow behaviour and usually neglected in practical considerations (Hillel 2004).

$K-\theta$ Relationship

The hydraulic conductivity, *K*, is the measure of the ability of soil to transmit water. The hydraulic conductivity depends both on the porous media property and the flowing fluid (Todd 1980). The hydraulic conductivity in partially saturated zone is known as unsaturated hydraulic conductivity whereas the hydraulic conductivity in the saturated zone or conditions is referred as saturated hydraulic conductivity. The unsaturated hydraulic conductivity is a non linear function of the soil moisture content in the unsaturated zone.

The fact that unsaturated hydraulic conductivity could not be easily measurable under field conditions led to development of functions which depend on saturated hydraulic conductivity, effective saturation and soil moisture content. Several equations have been developed to determine unsaturated hydraulic conductivity. However, the pioneering methods involve those of Burdine (1953), Childs and Collis-George (1950), Mualem (1976) and van Genuchten (1980) methods. The Mualem (1976) and van Genuchten (1980) methods are given as:

The Mualem equation:

$$K_r(\theta) = \Theta^{1/2}\left[\frac{\int_{\theta=0}^{\theta} d\theta/\psi}{\int_{\theta=0}^{\theta_{sat}} d\theta/\psi}\right]^2 \tag{2.19}$$

where K_r is the relative hydraulic conductivity in which $K_r = K/K_{sat}$.

The van Genuchten equation:

$$K_r = \Theta^{1/2}\left[1-\left(1-\Theta^{1/m}\right)^m\right]^2 \quad (2.20)$$

The van Genuchten equation has been derived based on equation (2.18) and (2.19) given earlier.

2.5.2.4 Initial and boundary conditions

The numerical solution of the Richards (1931) equation requires a specified initial and boundary conditions. The initial and boundary conditions are important criteria to solve the water balance and physically based models under practical field conditions. Initial conditions are required to start simulation while boundary conditions facilitate for the formation of a system of linear equations.

2.5.2.4.1 Initial conditions

Initial conditions characterize the initial state of the crop root zone either in terms of the water content or pressure head. These conditions can be made available from field observations or assumed conditionally depending on the antecedent field conditions. For numerical models it is generally best to specify initial conditions in terms of the pressure head, since this variable is the driving force for water flow. On the other hand, specifying initial condition in terms of water content may lead to unrealistically large pressure head gradients and consequently water fluxes (Huang et al. 2012). However, either the water content or pressure head can be used to define the initial conditions.

Initial condition based on pressure head:

$$\psi(z,t) = \psi_i(z,0) \quad (2.21)$$

Initial condition based on water content:

$$\theta(z,t) = \theta_i(z,0) \quad (2.22)$$

where ψ_i and θ_i are the initial values of pressure head and water content, respectively.

2.5.2.4.2 Boundary conditions

For one dimensional vertical flow, the boundary conditions can be either top or bottom boundary conditions. The top boundary condition takes into account processes such as evaporation (bare soil), evapotranspiration (cropped soil) or infiltration (rainfall or irrigation). These processes, however, are limited by soil water transport, vegetation cover and infiltration characteristics of the soil. Two types of conditions are being explained: system dependent and system independent boundary conditions. The former case refers to the boundary conditions for which the actual boundary conditions depend on the status of the system and computed by the

model itself. In the later case, the specified boundary values (pressure head, water content, water flux or gradient) do not depend on the status of the soil system.

Several system independent boundary conditions may apply to transport domain boundaries. When the pressure head at the boundary is known, Drichilet type boundary condition could be used. For example, at the water table, $\psi = 0$ provides Drichilet boundary condition. This boundary condition must be used when simulating ponded infiltration, the position of groundwater table or describing the hydrostatic pressure between soil and flowing or standing water (Huang et al. 2012). When the water flux across the boundary is known, Neumann type boundary condition is suggested. The Neumann type boundary condition is often referred as flux type boundary condition. This boundary condition is used only along boundaries where flux is known, provided the flux does not depend on the soil system. Hence Neumann boundary condition cannot be used to model precipitation or irrigation since precipitation or irrigation rate may exceed the infiltration capacity of the soil, in which case ponding will occur and the actual boundary flux will decrease. The Cauchy boundary condition is the case which comprises both Drichilet and Neumann type boundary conditions and mostly used in regional subsurface flow problems.

Drichilet or type-1 boundary condition:

$$\psi(z,t) = \psi_0(z,t) \tag{2.23}$$

where ψ_0 is the prescribed pressure head at the boundary.

Neumann type (type-2) boundary condition:

$$-K(\psi)\left(\frac{\partial \psi}{\partial z} + 1\right) = q_z(z,t) \tag{2.24}$$

where q_z is the specified flux at the given boundary.

Top Boundary Conditions

Either flux dependent (Neumann type) or head dependent (Drichilet) boundary condition can be prescribed at top. However, in many applications, neither the flux nor the pressure head is known at the soil surface apriori and follows from interactions between the soil and its surrounding (Huang et al. 2012). The processes that take place at the soil surface determine the top boundary conditions. These processes include evaporation (in case of bare

soil), evapotranspiration (in case of cropped soil) and infiltration (due to rainfall or irrigation). These processes depend on the soil condition to transport water, vegetation cover and infiltration capacity of the soil.

Feddes et al. (1974) provided a generalized boundary condition at top which is given as:

$$\left.\begin{aligned} &\left| -K(\psi)\left(\frac{\partial \psi}{\partial z}+1\right)\right| \le |q| \\ &\psi_{\min}(0,t) \le \psi(0,t) \le 0 \end{aligned}\right\} \quad z=0, t>0 \qquad (2.25)$$

where q is the prescribed maximum possible flux at soil surface governed by meteorological and external conditions such as rainfall/irrigation and evapotranspiration. $K(\psi)$ is the hydraulic conductivity; ψ is the pressure head; z refers to the vertical direction; $\psi(0,t)$ is the pressure head at the soil surface; $\psi_{min}(0,t)$ refers to the minimum pressure head at soil surface (dry condition) and $\psi(0,t) = 0$ refers to saturated conditions on the day of irrigation or rainfall.

In equation (2.25) q provides the upper limit of flux at the soil surface. However, this limit is controlled by soil properties and the soil water status at the soil surface. When soil moisture is not limiting, evaporation/evapotranspiration can take place at potential rate. Evaporation/ evapotranspiration go on reducing as the soil moisture availability is falling until soil water content is near permanent wilting point after which evaporation/evapotranspiration becomes negligibly small (Hillel 1977). Infiltration, from applied irrigation/rainfall, continues until it reaches the final infiltration rate after which ponding occurs since the soil gets saturated. Thus on the day of irrigation or rainfall, the boundary condition can be changed from Neumann type to Drichilet type after water starts ponding on the ground surface. However, whether the Drichilet type boundary condition maintains depends on the infiltration characteristics of a particular soil types.

Bottom Boundary Conditions

Different types of boundary conditions can be specified at the bottom of model domain. The bottom boundary condition is related with the knowledge of groundwater table, flux or pressure head at specific depths. When groundwater table is shallow and specified, it can serve as either variable or constant pressure head boundary (Drichilet type) condition. Otherwise, pressure head values may be obtained from field observations to serve as boundary conditions. On the other hand, when flux is specified at a given depth (model boundary), then the flux can be used as bottom boundary condition (Neumann type boundary conditions). However, flux is usually obtained from considerations of the position of groundwater table. When the

groundwater table is sufficiently deep, free drainage boundary condition is considered. The free drainage condition offers determination of the boundary flux considering zero gradient assuming negligible variation of pressure head at the bottom boundary (Shankar et al. 2012).

$$-K(\psi)\left(\frac{\partial \psi}{\partial z}+1\right)=-K(\psi)\Big\} \qquad z=L,\ t>0 \tag{2.26}$$

A deep drainage condition as described by Hopmans and Stricker (1989) can also be implemented as a bottom boundary condition. In this case, a lower boundary condition which is governed partly by the physical properties of the deeper layers is considered. A relationship between a local value of pressure head (*h*), the reference position of groundwater level (GWL) and bottom flux, *q(h),* is established to account for bottom boundary conditions:

$$q(h) = -Ae^{(B(h-GWL))} \tag{2.27}$$

where *A* and *B* are empirical parameters obtained from field measurements of *h* and *q(h).*

2.6 ROOT WATER UPTAKE

The sink term in equation (2.14) refers to the root water extraction from a crop root zone. Basically, two approaches prevail in literature to express root water uptake: the microscopic and macroscopic approaches. A number of microscopic and macroscopic approaches to modeling root water uptake have been proposed over the years (Skaggs et al. 2006). The microscopic approach involves descriptions of radial flow to, and uptake by, individual roots (Hillel et al. 1975; Raats 2007). In the macroscopic approach the overall root system is assumed to extract moisture from each differential volume of the root zone at some rate. At a given point, the rate depends on space, time, moisture content, water potential or the combinations of these (Shankar 2007). Modelling uptake with a sink term in the Richards equation (Eq. 2.14) uses a typical macroscopic approach that averages uptake over a large number of roots. The approach ignores pore-scale variations in the pressure head or solute concentration in the immediate vicinity of individual roots.

Several linear as well as non linear root water uptake models were developed to date. However, the models by Feddes et al. (1978) and van Genuchten (1987) are commonly used (Skaggs et al. 2006; Li et al. 2014). These models are coupled with root zone modeling tools such as, for example, HYDRUS-1D (Šimůnek et al. 2008), SWAP (Ahmad et al. 2002) and many others to simulate moisture dynamics in the soil root zone. In the following sections two root water uptake functions are being discussed.

2.6.1 Feddes et al. (1978) Model

Feddes et al. (1978) defined the root water uptake term, *S*, as:

$$S(\psi) = \alpha(\psi) S_p \tag{2.28}$$

where α(ψ) is the root-water uptake water stress response function, dimensionless function of the soil water pressure head, ($0 \leq \alpha\ (\psi) \leq 1$) and S_p is the potential root water uptake rate [T^{-1}]. To describe water stress, Feddes et al. (1978) proposed a piece wise linear reduction function parameterized by four critical values of the water pressure head, $\psi_4 < \psi_3 < \psi_2 < \psi_1$. More precisely, $\alpha(\psi)$ can be described by the following expressions (Skaggs, et al. 2006).

$$\alpha(\psi) = \begin{cases} \dfrac{\psi - \psi_4}{\psi_3 - \psi_4}, \psi_3 > \psi > \psi_4 \\ 1, \qquad \psi_2 \geq \psi \geq \psi_3 \\ \dfrac{\psi - \psi_1}{\psi_2 - \psi_1}, \psi_1 > \psi > \psi_2 \\ 0, \qquad \psi \leq \psi_4 \ or \ \psi \geq \psi_1 \end{cases} \tag{2.29}$$

In general, equation (2.26) expresses that water uptake is reduced at high and low water contents. Uptake is at the potential rate when the pressure head is $\psi_3 > \psi > \psi_2$, drops off linearly when $\psi > \psi_2$ or $\psi < \psi_3$, and becomes zero when $\psi > \psi_4$ or $\psi < \psi_1$. The value of ψ_3 is expected to be a function of evaporative demand and can be classified as ψ_{3l} and ψ_{3h} to account for, respectively, low and high rates of transpiration. For higher transpiration, reduction in water uptake occurs at relatively wetter conditions than that for lower transpiration (Fig. 2.1).

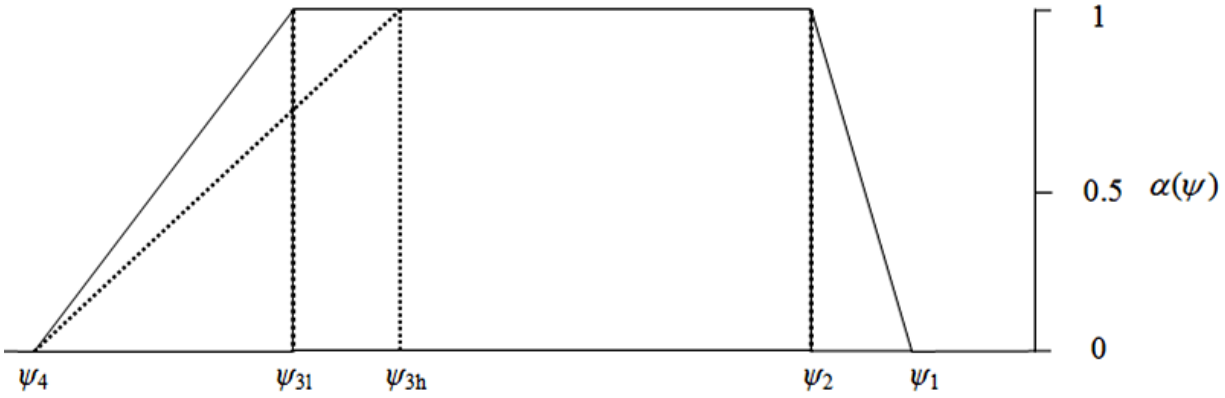

Fig 2.1 Schematic diagram of plant water stress response function as used by Feddes et al. (1978)

2.6.2 van Genuchten (1987) Model

van Genuchten (1987) further expanded the Feddes et al. (1978) function by introducing osmotic stress in the root water uptake stress response function as follows:

$$S(\psi) = \alpha(\psi, \psi_\phi) S_p \tag{2.30}$$

where ψ_ϕ is the osmotic head (L)

Van Genuchten (1987) proposed an alternative S-shaped function to describe the water uptake stress response function (Fig. 2.2), and suggested that the influence of the osmotic head reduction can be either additive (equation 2.31) or multiplicative (equation 2.32) as follows:

$$\alpha(\psi, \psi_\phi) = \frac{1}{1 + \left(\frac{\psi + \psi_\phi}{\psi_{50}} \right)^p} \tag{2.31}$$

$$\alpha(\psi, \psi_\phi) = \frac{1}{1 + \left(\psi / \psi_{50} \right)^{p_1}} \frac{1}{1 + \left(\psi_\phi / \psi_{50} \right)^{p_2}} \tag{2.32}$$

where p, p_1, and p_2 are experimental constants. The exponent p was found to be approximately 3 when applied to salinity stress data only (van Genuchten 1987). ψ_{50} and p are adjustable parameters. ψ_{50} is the pressure head at which the water extraction rate is reduced by 50% during conditions of negligible osmotic stress. Equation (2.31) is describing additive approach which is commonly utilized. In the absence salinity stress, only water stress is considered. Fig. 2.2 presents the van Genuchten (1987) plant water stress response function (S curve) for root water uptake.

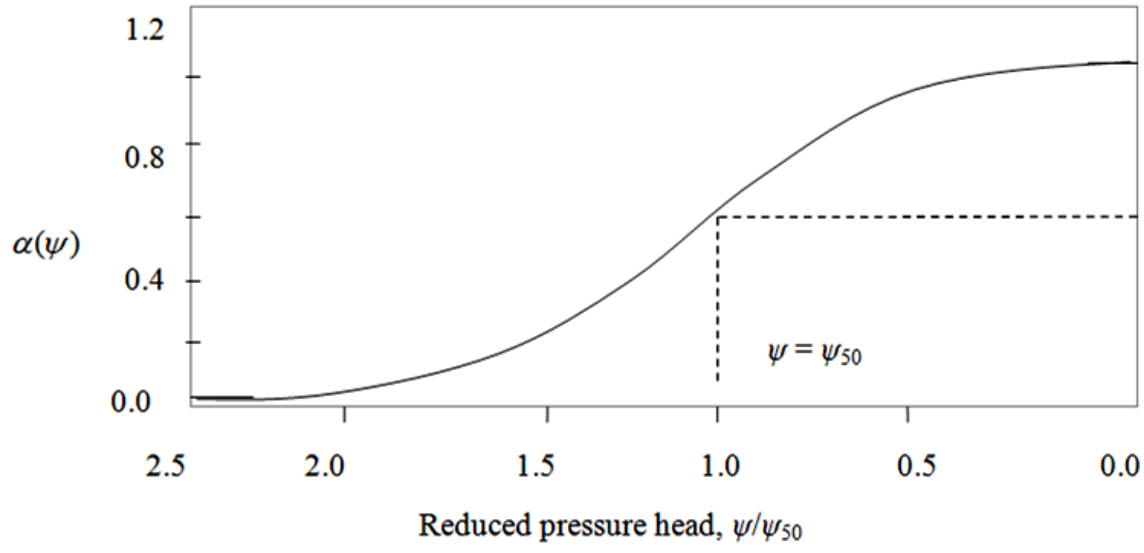

Fig. 2.2 Schematic diagram of plant water stress response function as used by van Genuchten et al. (1987)

2.7 COMPONENTS OF EVAPOTRANSPIRATION

In the preceding sessions it has been indicated that evapotranspiration is one of the key inputs in the physically based model taking place at top boundary (evaporation) and/or prevailing in the crop root zone (transpiration). Evapotranspiration (*ET*) is composed of three important processes: soil evaporation (E_s), interception evaporation (I_c) and plant transpiration (T_p). When a crop is first sown or planted, larger areas are exposed to soil evaporation and transpiration is minimal. As the crop gradually grows, more areas are being covered by the canopies and hence evaporation is reducing till it reaches minimum during when the crop covers full area in the mid stage of the growth period. Transpiration on the other hand increases to its maximum during the full canopy cover and reduces as the crop canopy undergoes senescence in the later stages of crop development. Canopy interception during rainfall or specific irrigation events also gets more during the mid stage growth period, which later on evaporates from the canopy surface. In general, soil evaporation (E_s), plant transpiration (T_p) and canopy interception (I_c) fluxes vary in space as well as time and need due attention in modelling water movement in the crop root zone and should be studied separately for better understanding of flow phenomena and field agricultural water management.

Several studies have been conducted to separate the total evapotranspiration into its sub-components: E_s, T_p and I_c (Sutanto et al. 2012; Wang et l. 2012; Blyth and Harding 2011; Merta et al. 2006; Grelle et al. 1997). Grelle et al. (1997) used a combination of observations and a model to quantify interception, soil surface evaporation and transpiration of boreal forest. Merta et al. (2006) also used a combination of a model and observations to separate soil evaporation and plant transpiration using leaf area index. Sutanto et al. (2012) used a HYDRUS-1D model and isotope measurements for the partitioning of total evaporation. Similarly, Wang et al. (2012) also used the water balance and isotope mass balance methods to estimate transpiration, evaporation and deep percolation. Experimentally, several researchers used micro lysimeters between crop rows to estimate evaporation (Shawcroft and Gardner 1983; Klocke et al. 1985; Ham et al. 1990). However, micro lysimeter measurements are not hydraulically representative to the surrounding soils and also scale effects are harmful to the data obtained from such measurements. Ham et al. (1990) conducted field experiments on cotton crop using the Bowen ratio energy balance and sap flow measurements to make near instantaneous measurements of *ET* and *Tp*, respectively. The soil evaporation is computed from the difference between evapotranspiration and transpiration. Further, they evaluated the accuracy of the method by comparing the computed values of E_s with measured values obtained from micro lysimeters. Better results were obtained.

Measurements and estimation of interception are difficult and bear large uncertainties since intercepted water could vanish within 10 minutes after rainfall (Blyth and Harding 2011). Further, the magnitude of interception compared to transpiration and evaporation is quite less. Therefore, usually evaporation and transpiration components of the total evaporation are considered (Shankar 2007).

2.7.1 Soil Evaporation

Various approaches of estimating soil water evaporation have been identified. The usual way to measure soil surface evaporation is using micro lysimeters (Shawcroft and Gardner 1983; Klocke et al. 1985; Ham et al. 1990). Daamen et al. (1993) gave an overview of micro lysimeters. Like the principle of measurement in weighing type lysimeters, the assumption made is that evaporation can be measured by weighing the soil above. These have been used for studies ranging from agricultural area (Leuning et al. 1994; Villalobos and Fereres 1990) to studies of agro-forestry (Jackson and Wallace 1999). Contrary to several successful applications of the system, Allen (1990) found that micro lysimeters were unreliable with heavy rain in his study in northern Syria. In fact, micro lysimeters are labour intensive and thus inapplicable during periods of rainfall. Grelle et al. (1997), on the other hand, used chambers to measure evaporation over bare soil areas although the method did not provide good temporal resolution and had not been widely used. Therefore, they have employed other alternative approaches comprising empirical, analytical or modelling approaches.

The relation between transpiration and soil evaporation depends strongly on the density of the plant cover, expressed by the leaf area index (*LAI*). During the vegetation period, transpiration achieved is the highest portion of the total evapotranspiration (dense agricultural crops covering nearly 100% of the soil surface). In the study by Merta et al. (2006) soil evaporation decreased rapidly with increasing *LAI* and at a *LAI* value of 2, soil evaporation contributed less than 10%). Marta et al. (2006) proposed a function for evaporation to evapotranspiration ratio based on results from wheat and maize crop fields given as follows:

$$\frac{E_s}{ET_c} = 0.23 \cdot LAI^{-1.8} \tag{2.33}$$

For a crop partly covering the soil surface, ET_c is divided into potential evaporation, E_s, and potential transpiration, T_p. Belmans et al. (1983) provided the following relationship to compute soil evaporation and crop transpiration by using data on crop leaf area index:

$$E_s = ETc \times e^{-\lambda \times LAI} \tag{2.34}$$

$$T_p = ET_c - ET_c \times e^{-\lambda \times LAI} \quad (2.35)$$

where λ is an extinction coefficient for global solar radiation; *LAI* is leaf area index. The value of extinction coefficient for different crops can be obtained from experiments or model calibration. Similar way of partitioning evaporation and plant transpiration has also been used by Allen (1990) and Vanclooster et al. (1995).

2.7.2 Plant Transpiration

The pant transpiration rate is influenced by crop characteristics, environmental aspects and agronomic conditions. Under non limiting water conditions, crops transpire as if water evaporates from open water bodies.

Several methods are available for measuring and estimating transpiration. Potometers are usually described for measurement of transpiration of a given plant, but they are often limited to laboratory conditions. In order to measure transpiration and calculate conductance, accurate determinations of vapour pressure, air flow and leaf temperature are necessary. Among the large variety of humidity sensors, only few are accurate enough to monitor transpiration and leaf conductance at field level which include infrared gas analyzers, dew point mirrors and thin-film capacitance-type sensors. However, these sensors have been developed for industrial applications of sensing humidity levels and not used for flux rate measurements. Detailed account of the principles, procedures of measurement and estimation procedures of transpiration using such sensors is given in Pearcy et al. (2000). Sasaki and Amano (2010) have also shown an alternative approach for measuring transpiration from mangrove plant using miniature temperature/humidity sensors attached onto the leaf surface of the plant.

Other authors considered observation of root zone water depiltion to measure transpirtion (Ferrara and Flore 2003, Vadez et al. 2014). Ferrara and Flore (2003) compared five different methods of measuring and estimating transpiration consisting of gravimeteric analysis, heat pulse velocity (HPV), time domain reflectometery (TDR), single leaf and whole plant infrared gas exchange measuremts by conducting tests on two varieties of apple trees. They found that the TDR method provided an accurate result compared to the control (gravimetric method) followed by the HPV method. Vadez et al. (2014) also conducted lysimetric method for assessing transpiration efficiency (TE) and concluded absence of relationship between TE and the total crop water use.

The most widely used method of measuring transpiration directly is the sap-flow method. In this method, observation of heat transfer is made between a heat source and a thermometer probe inserted above it in the stem of a plant. The speed of the flow of water up

through a plant can be inferred from the speed of the transfer of heat from the source to the thermometer (Blyth and Harding 1995). Similarly, Ansley et al. (1994) have compard stem (sap) flow and porometer measurements of transpiration from honey mesquite (*Prosopis glandulosa*) trees. They observed comparable results from the two methods although significant variations prevail during high transpiration rates. In this case, the porometres were observed to suffer from limitations in capturing the transpiration rate due to scale effects.

Further, determination of soil water evaporation enabled computation of plant transpiration from the total evapotranspiration making use of leaf area index and extinction coefficients as shown in equation (2.35) above. This method is receiving wide acceptance since obtaining information on leaf area index is easier than acquiring data on transpiration measurements.

2.7.3 Plant Parameters

In an attempt to estimate transpiration and evapotranspiration, crop parameters such as root depth (z), leaf area index (LAI) and crop coefficient (K_c) are widely utilized. Therefore, it is important to study and understand the procedures of measurement and characteristics of such crop parameters.

2.7.3.1 Root depth

Plant roots serve to connect the soil environment to the atmosphere since they link the pathway between soil-plant and the atmosphere. Fluxes along the soil–plant–atmosphere continuum are regulated by above-ground plant properties like the leaf stomata, which can regulate plant transpiration when interacting with the atmosphere, and plant root-system properties like depth, distribution and activity of roots (Feddes et al. 2004). The amount of water available to plants is determined by the available soil water, root depth and root density at a given soil water zone of the subsurface. The effective depth of root zone is more significant in water uptake from crop root zone than the maximum root depth. The effective root zone can be expressed as the depth from which, the roots of average mature plant are capable of extracting soil moisture to the extent that it should be replaced by irrigation application. Yu et al. (2007) explain that depth of the most densely rooted soil layer is more important than the maximum rooting depth for increasing the ability of plants to cope with the shortage of water. Plant root systems show a remarkable ability to adapt to soil depth and to changes in the availability of water and nutrients and the chemical properties (e.g. salinity) in soils (Feddes et al. 2004). Occurrence of the highest length-density roots at deeper soil profiles can enhance the ability of crops to cope with water shortage because of less soil drying by climate in deeper

soils. However, if the most densely rooted layer occurs too shallow, plants might become very vulnerable to the adverse effect of water deficiency (Yu et al. 2007). Therefore, obtaining root depth, distribution and density data in field provides valuable information for water balance and water dynamics study in a crop root zone.

Several methods are available to study crop rooting system such as excavation method, trench profile wall method, auger method, monolith core method and soil moisture profile methods. Kücke et al. (1995) compared four methods of rooting measurements including (i) the core method where roots are extracted and root length is directly measured, (ii) the core-break method where the visible roots are counted on the faces of a broken soil column, (iii) the trench profile wall method where the number of visible roots were counted and the root length density is estimated on a profile wall and (iv) the monolith methods where the roots are extracted from monoliths dug out from a profile wall. The particular study showed that the different methods of measurement did not provide similar results and need calibration in the face of extraction methods. Most excavation and trenching approaches are used to measure root depth to the first meter and reach only occasionally to soil depths of two meters and below (Dauer et al. 2009; de Azevedo et al. 2011). Therefore, these methods can suitably apply for field crops. All direct methods of root system studies are labour intensive and hence indirect approaches are preferably implemented. Indirect methods are usually based on soil moisture depletion patterns from which inferences can be made assuming correlation between soil moisture depletion and root depth and density at specific depth of soil (Davis et al. 1965).

No single method of rooting system studies is successful in its own. A combination of two or three methods is suggested to provide reliable results. To adequately interpret the data, information on the factors affecting root growth such as soil water availability, soil properties and depletion pattern are important (Boehm 1977; Feddes et al. 2004) which could be acquired together with the rooting information.

2.7.3.2 Leaf area index

Leaf area index (*LAI*) is a dimensionless quantity that characterizes plant canopies. Various definitions were given so far depending on orientation of leaves and its geometry. Watson (1947) defined *LAI* as the one-sided green leaf area per unit ground surface area. Despite this definition applies for broadleaf canopies, it could not fit for the case of foliage elements having non-flat and needle shaped, wrinkled, bent or rolled orientations. Some authors therefore proposed a projected leaf area to take into account the irregular form of needles and leaves (Smith 1991; Bolstad and Gower 1990). However, in this case the choice of projection angle is decisive, and a vertical projection does not necessarily result in the highest

values. Myneni et al. (1997) consequently defined *LAI* as the maximum projected leaf area per unit ground surface area. Contrarily, Chen and Black (1992) suggested that half the total interception area per unit ground surface area would be a more suitable definition of *LAI* for non-flat leaves than projected leaf area. Still other definitions and interpretations of *LAI* have been proposed based on the technique used to measure *LAI*. Some brief explanations on the various definitions of *LAI* has been presented by Weiss et al. (2004).

The leaf area index is the main variable used to model many processes, such as canopy photosynthesis and evapotranspiration. However, it is one of the difficult parameters to quantify properly, owing to large spatial and temporal variability (Breda, 2003) in species composition, developmental stage, prevailing site conditions, seasonality, and the management practices (Jonckheere et al. 2004). Various methods have been developed to quantify *LAI* from the ground. Breda (2003) discusses the different methods, instruments, the advantages and disadvantages of the methods. In general, two methods have been identified to measure the leaf area index: The direct and indirect methods.

The direct methods constitute destructive sampling of green foliage vegetation which is used in crops and pastures by harvesting the vegetation and measuring leaf area within a certain ground surface area. However, that would be difficult to apply and unethical in natural ecosystems. After leaf collection, leaf area can be calculated by means of either planimetric or gravimetric techniques (Daughtry 1990). The planimetric approach is based on the principle of the correlation between the individual leaf area and the number of area units covered by that leaf in a horizontal plane. The other direct method involves collecting leaves during leaf fall in traps of certain area distributed below the canopy as can be applied in deciduous species. The area of the collected leaves can be measured using leaf area meter or image scanner and image analysis software. The measured leaf area can then be divided by the area of the traps to obtain *LAI*. Alternatively, leaf dry mass to specific leaf area ratio approach involves measuring the dried mass of collected leaves from a sampled area under the canopy. Collected leaves are dried at 60–80 °C for 48 hours and weighed. The leaf area index is obtained by multiplying specific leaf area and dry mass. However, direct methods of *LAI* are criticized for extreme time-consumption, labour intensiveness and difficulty in large scale implementation (Jonckheere et al. 2004).

Due to the inherent nature of the direct methods, indirect measurements are typically preferred and becoming more and more important. Indirect methods, in which leaf area is inferred from observations of another variable, are generally faster, amendable to automation, and thereby allow for a larger spatial sample to be obtained. Indirect methods of estimating *LAI*

in situ can be divided into two categories: (1) indirect contact *LAI* measurements; and (2) indirect non-contact measurements. Detailed account of these methods and explanations is provided in Jonckheere et al. (2004). The methods such as the hemispherical photography, Hemiview Plant Canopy Analyser (Delta-T devices, Cambridge, UK), the CI-110 Plant Canopy Analyzer (CID Bio-Science, inc), *LAI*-2200 Plant Canopy Analyzer (LI-COR Biosciences inc) and the LP-80 *LAI* ceptometer (Decagon Devices Inc., Pullman, WA, USA) are the non-contact tools usually employed to measure LAI in a non-destructive way in recent days. The LP-80 calculates *LAI* by means of measuring the difference between light levels above the canopy and at ground level, and factoring in the leaf angle distribution, solar zenith angle, and plant extinction coefficient.

2.7.3.3 Crop coefficient

Crop coefficient, K_c, is an important parameter in the estimation of water consumption of a given crop. It refers to the ratio of the potential crop evapotranspiration, ET_c, to reference evapotranspiration, ET_0 as given in equation (2.3). K_c represents an integration of the effects of three primary characteristics that distinguish a crop from the reference crop such as crop height, crop-soil surface resistance and albedo. A comprehensive set of K_c values for various crops originally has been provided by FAO (Doorenbos and Pruitt 1977; Allen et al. 1998). However, these values apply for a specific humid climate and need adjustment for other areas accordingly taking into account climatic, agronomic and crop specific conditions. FAO also documented the detail of procedures for adjusting the K_c values. Doorenbos and Prutt (1977) suggest that the K_c values for a given crop should be derived from lysimeter data and local climatic conditions.

Two approaches are available to determine crop coefficient: the single and the dual crop coefficient approaches. In the single crop coefficient approach, the difference in evapotranspiration between the cropped and reference grass is combined into one single coefficient. In the dual crop coefficient approach, the crop coefficient is split into two factors describing separately the differences in evaporation and transpiration between the crop and reference surface. More accurate values of crop coefficients can be obtained using the dual crop coefficient approach than the single crop coefficient approach. However, dual crop coefficient approach is more complicated and more computationally intensive than the single crop coefficient approach (Allen et al. 1998).

2.8 FEW OTHER METHODS FOR ESTIMTION OF DEEP PERCOLATION

Different models have been formulated so far to estimate deep percolation apart from the water balance (section 2.5.1) and physically based approaches (section 2.5.2). In this section, a listing of such models is presented.

Bethune et al.(2008) (Conceptual model)

$$DP = (SSP + NSSP)\, f\,(GWD) \tag{2.36a}$$

$$SSP = i_f t_0 \tag{2.36b}$$

$$NSSP = \zeta \frac{DW}{ET} i_f \tag{2.36c}$$

$$f\left(GWD\right) = \tanh\left(0.55 \frac{GWD}{GWD_0}\right) \tag{2.36d}$$

where *SSP* is steady state percolation and *NSSP* is non steady state percolation, i_f is the final infiltration rate of the subsoil, t_0 is the period of ponding, ζ is empirical coefficient (0.2 – 0.25); *DW* is the amount of water stored in the root zone between saturation and field capacity; *ET* is evapotranspiration. GWD_0 is defined as the half depth of water table influence (analogous to the half-life concept in radioactive decay), i.e., when $GWD = GWD_0$, the reduction factor *f* is 0.5. The reduction factor becomes zero for water tables at the soil surface (no deep percolation) and approaches unity for deep water tables (free draining conditions or no capillary rise).

Doorenbos and Pruitt (1977):

$$DP = \begin{cases} 0 & if\ W < W_{fc} \\ W - W_{fc} & if\ W > W_{fc} \end{cases} \tag{2.37}$$

where *DP* is the deep percolation; *W* is the actual soil water storage in the root zone; W_{fc} is the soil water storage for the same depth at field capacity.

Liu et al. (2006) (Parametric approach):

$$DP_{i+1} = W_i - W_{i+1} \tag{2.38a}$$

$$W_i = W_{i-1} - ET_{mi} + P_{ei} + I_{ri} \tag{2.38b}$$

$$W_{i+1} = a\left[1 + \left(\frac{W_i}{a}\right)^{1/b}\right]^b - ET_{mi+1} \tag{2.38c}$$

where DP_{i+1} is deep percolation at current date, W_i is the storage at the initial/previous date, W_{i-1} is the carry over moisture storage the date before the initial date, W_{i+1} is the soil water storage at current date. ET_{mi} is potential crop evapotranspiration, P_{ei} is rainfall and I_{ri} is over irrigation all refer to the initial/previous date, *a* and *b* are site-specific constants which can be determined from experimental data and ET_{mi+1} refers to the potential crop evapotranspiration for the current date.

Ma et al. (2013):

$$D = k\theta_{t-1}\left(\frac{\theta_c - \theta_{t-1}}{z/2}\right)\Delta t \tag{2.39}$$

where *D* is deep percolation (mm), θ is volumetric water content at the bottom of the root zone (cm^3/cm^3), z is the root zone depth (cm), θ_c is the critical water content corresponding to average soil water content of the deep soil zone (= 0.75 x field capacity), Δt is daily time step (days), *k* is an introduced coefficient. θ_{t-1} is the soil water content corresponding to previous time step.

Weaver et al. (2005); Willis et al. (1997) Chloride mass balance method:

$$DP = t(I + R)\left(\frac{C_i}{C_z}\right) \tag{2.40}$$

where *t* is time, *I* is the infiltration of irrigation water, *R* is infiltration of rainfall water, C_i is the average chloride concentration of irrigation water and C_z is the average chloride concentration of drainage water. The time can be taken as any interval based on the measurements of infiltration and concentration measurements. Volumetric soil water contents measured at each depth increment immediately before and after each irrigation event are summed to give the total water content of the profile above the required depth where DP is going to be estimated. The amount of irrigation/rainfall water that infiltrated is calculated as the difference in volumetric soil water content immediately before ($\theta(0-z)_{pre\_irrigation}$) and after ($\theta(0-z)_{post\_irrigation}$) irrigation plus any evapotranspiration between irrigation onset and cut-off (Willis et al. 1997).

$$I = \theta(0-z)_{post\_irrigation} - \theta(0-z)_{pre\_irrigation} + ET \tag{2.41}$$

The procedures of determining chloride concentrations and measurement procedures are documented in Wills et al. (1997) and Weaver et al. (2005). The above equation pertains to the steady rate of chloride mass balance model, whereas transient state of chloride mass balance

model can also be considered. However, the steady state chloride mass balance model is frequently used due to its easiness and prevailing field conditions (Weaver et al. 2005).

2.9 DEEP PERCOLATION FROM RICE AND BERSEEM CROP FIELDS

Naturally, some crops are stress tolerant while others are water intensive (most thirsty). More percolation can take place from the root zones of water intensive crops than stress tolerant crops since more water is being supplied for water intensive crop fields. Both rice and berseem fodder are considered to be water intensive crops. Many authors have described rice as a water intensive crop (Chen and Liu 2002; Naftchali et al. 2013; Tan et al. 2014).

Irrigated area under water intensive crops such as lowland rice (*Oryza sativa L.)* and berseem fodder (*Trifolium alexandrinum L)* consume large volume of water due to the conventional flooding method of water application. In rice fields water is applied to retain submerged field conditions (Bouman et al. 2007a; Garg et al. 2009; Patil et al. 2011). In India, rice is grown over an area of 43 million ha with an annual production of 124 million tons (IRRI, 2004) and average productivity is only 2-3.5 tons/ha (Ladha et al. 2000). The need for increasing rice production is growing due to increasing number of population in the region and over the world. Increasing the production could be achieved through increases in inputs such as fertilizer, selection of high yielding short duration varieties, proper control of weeds and crop diseases, water management and implementation of recommended agronomic practices. However, adequate management of water in rice fields is sought to be hectic due to the nature of water application in which rice is criticized to be an inefficient water user (Bhuiyan et al. 1995; Garg et al. 2009). To produce 1 kg of grain, farmers put 2 to 3 times more water in rice fields than other cereals (Tuong et al. 2005).

Berseem, on the other hand, needs frequent irrigation throughout its growing season because of its shallow root zone that dries quickly (Tyagi et al. 2003). It requires saturated field condition for its germination, although it can grow under intermittently irrigated farms. As much as 500 kilograms of more water is required for every kilogram of berseem plant dry matter produced in a dry climate. There is also a huge demand to grow more fodder crops in general (currently around 8.4 million ha) and berseem fodder owing to large demands in dairy products in India (Sunil et al. 2012) which calls for increased demand for fresh water. Therefore, there is an urgent need for an accelerated increase of agricultural water use efficiency such as reducing deep percolation losses.

However, deep percolation phenomena from frequently irrigated fields seriously diminish surface irrigation efficiency, jeopardize proper water management and minimize

water productivity. This problem is quite important in coarse textured soils where water holding capacity is relatively less. Percolation loss of water from irrigated field is not only reducing irrigation efficiency but also becoming a haphazard to an environment by carrying agriculture based chemicals to the surrounding water bodies, especially to the groundwater aquifer systems (Bouman et al. 2002; Antonopoulos 2010). Seepage and percolation losses of water are major reasons behind the poor water productivity in wetland rice (Patil et al. 2011). The problem gets worse with water intensive crops such as rice or berseem fodder since large volume of water is applied to the field. Large volume of deep percolation loss could exist during the continuous flooding operation of rice, even in puddled conditions (Kukal and Aggarwal 2002; Bouman et al. 2007b; Sudhir-Yadav et al. 2011). Bouman et al. (2007b) reported that around 70% of input water could go for percolation loss when groundwater depth is equal to or more than 2 m. Sudhir-Yadav et al. (2011) observed that about 81% of water added was drained beyond the root zone (0–60 cm) with continuously flooded rice. Dewandel et al. (2008) explained that the flooded type of irrigation in rice fields can yield up to 50% of the applied irrigation water as deep percolation return flow while irrigation using micro-systems/drip/ can lower down DP up to 0 %. Water losses by seepage and percolation account for about 50–85% of the overall water input in coarse-textured soils with deep groundwater tables (Sharma et al., 2002, Singh et al., 2002). Although several estimates of deep percolation from rice fields were reported, no significant quantification of percolation loss from berseem fodder crop was documented.

Considerable efforts have been made so far to reduce deep percolation especially from rice fields: alternate wetting and drying (AWD) (Bouman et al. 2007b; de Vries et al. 2010; Tan et al. 2014), aerobic rice (Nie et al. 2012), delayed application of continuous flooding (Dunn and Gaydon 2011), puddling (Kuakal and Aggarwal 2002; Kukal and Sidhu 2004). Most research studies consider presence of an impermeable layer (hard pan) below the bottom of rice in reducing deep percolation. However, the efficiency of hard pan under farmer operated field conditions, apart from experimental set-ups, is not proved to serve the purpose. Incidences of large deep percolation under bunds and cracks in the field were commonly reported in puddled field conditions (Garg et al. 2009; Janssen and Lennarth 2009). Another problem which has been noticed against puddling practices in rice fields is the interference of the puddled layer with the next crop (Mitchell et al. 2013). Puddling operation is a costly task as it needs extra labour and effort with regard to small farm holdings where farm machinery could not be affordable. Above all, the practice itself consumes large volume of water. Currently, rice farmers are escaping the puddling step, either transplanting rice seedlings on un-paddled soils

or directly sowing the same on prepared beds. Further, there is also no considerable attempt made to reduce deep percolation from crops like berseem fodder. Hence, in this study, the presence of hard pan below the crop root zone is not considered. The particular study could provide more understanding of deep percolation process in water intensive crops and shed light to the proper water resources management of such fields in a given area.

2.10 CLOSURE

Deep percolation from water intensive crops is thought to be seriously lowering irrigation efficiency and thereby the water productivity. So far considerable efforts have been made to reduce deep percolation from rice field particularly by employing puddling practice. However, literature indicates that there is quite large volume of water goes on account of deep percolation even under puddled conditions, the process which is practiced to reduce deep percolation from rice fields. The puddling practice is criticized for its side effects besides its extra labour and water requirements. Therefore, farmers are, nowadays, escaping this practice and adopting either direct transplanting or dry seeding of the rice crop.

Although there are several studies conducted to estimate deep percolation loss, deep percolation under unpuddled rice field conditions using lysimeter measurements was scarcely studied and need due attention. The reason may be due to the fact that drainage volume through the bottom of water intensive crops is large which is difficult for continuous monitoring. Further, although the demand and consumption of crops like berseem fodder is increasing, there is dearth of research work addressing the problem of deep percolation and its quantification.

Deep percolation can be estimated using either the root zone soil water balance or physically based models. However, there is paucity of studies concerning deep percolation from rice and berseem field conditions under varying regimes of water application. Comparative advantages and disadvantages of these models have not been well dealt in earlier studies. Previous studies concerning deep percolation from water intensive crops mostly lack through field observations and mainly depend on mathematical models only. Therefore, this study is aimed at estimating deep percolation using both the simple water balance and the physically based models by employing field observations to verify the ability/discrepancy of these models.

CHAPTER 3
EXPERIMENTAL PROGRAM

3.1 PREAMBLE

The complexity of governing processes affecting variably saturated flow in crop root zone demands mathematical modelling studies. The mathematical models predict state variables depending up on enforcing variables and parameters. However, the modelling studies are required to be evaluated based on measured data points from laboratory and/or field experiments. Deep percolation from irrigated fields is one of the processes often determined using mathematical modelling without field measured data sets. In the present chapter, field and laboratory measurements conducted to determine the various flow variables and parameters in crop root zone are described.

Field observations including irrigation application, deep percolation, crop management and soil moisture monitoring have been conducted. Meteorological data needed for estimating evapotranspiration of the experimental field has been acquired from the nearby meteorological station. Laboratory experiments for determining soil and crop parameters were also carried out. Overall, four crop seasons of experimental run in rice and berseem crops was conducted for varying regimes of water application to analyse deep percolation and water productivity. The measured data sets are used to evaluate the models used to predict deep percolation which are presented in chapter four (simple water balance model) and chapter five (physically based model), respectively.

3.2 THE EXPERIMENTAL SITE

The experimental site is located at the Department of Civil Engineering, Indian Institute of Technology, Roorkee, in the State of Uttarakhand, India. The site is located near the Ganges River in the geometric grid of 77°53’52” east longitude and 29°52’00’’ north latitude at an average altitude of 274 m above mean sea level. The climate of Roorkee is typical of north western India with hot humid summer and very cold dry winter (Shankar 2007). According to Thornthwaite climate classification (Thornthwaite 1948), which is based on average annual temperature, Roorkee is semi-arid. However, according to Köppen climate classification, which is based on average annual and monthly temperature and precipitation, the seasonality of precipitation and type of native vegetation, the study area falls under humid subtropical class (Kottek et al. 2006). The monthly average maximum temperature of the study area is recorded in the range of 19 °C (January) to 38 °C (May) and monthly average minimum temperature falls in the range of 7 °C (January) to 26 °C (July) according to long years of data record at National

Institute of Hydrology (NIH), Roorkee. The average relative humidity ranges from 52% (May) to 90 % (January). The average annual sunshine duration is 2800 hrs. The normal rainfall of Roorkee is 1051 mm per annum of which almost 80% is recorded during the monsoon season (June to September). The soil in the region can be classified as 'soils in old alluvial plains', which are well drained fine loamy soils on nearly level plain with sandy loam surface (Shankar 2007).

3.3 LAND PREPARATION AND CROP MANAGEMENT

The field experiments consisted of growing rice (*Oryza Sativa L.)* (var. basmati) with continuous saturation of the field with irrigation from 23 July, 2013 (date of transplanting) to 02 November, 2013 (date of harvesting), for season 1 and with intermittent irrigation application from 15 July, 2014(date of transplanting) to 22 October, 2014 (date of harvesting), for season 2. Similarly, berseem fodder crop (*Trifolium alexandrinum L.) (*var. JB-1*)* was grown with conventional surface irrigation from 12 December, 2013 (date of sowing) to 08 May, 2014 (date of final harvest) for season 1 and with reduced irrigation application from 17 November, 2014 (date of sowing) to 16 April, 2015 (date of final harvest) for season 2.

Field preparation was carried out manually during the crop seasons. Field instrumentation was also conducted along with field preparation. The experimental site consists of two compartments in which the first compartment was provided with open boundaries to mimic actual field conditions elsewhere in the area while the boundaries of the second compartment were provided with plastic sheets buried at field boundaries to a depth of 60 cm to impede lateral seepage out of the field as shown in Fig. 3.1. Two lysimeters were also installed in compartment 2. The lysimeter setup is explained in detail in section 3.8. Each compartment has been further partitioned into smaller plots to manage experimental runs.

During the rice growing season, 21 days old seedlings were transplanted after thorough field preparation and flooding to saturate the soil (Fig. 3.2). A total of 5 days flooding before transplanting was made, which favoured initial conditions for the crop growth. No puddling was conducted for the experimental field since this needs extra labour and water. A basal dose of diammonium phosphate (DAP) and zinc sulphate were applied during transplanting. Urea was applied in three schedules: during transplanting, three weeks after transplanting and during panicle initiation following agronomic practices in the study area. Weed control was undertaken manually by removing all the weeds from the field two to three times during the growth periods of the crops. The crop was also protected from threatening insects by applying insecticides commonly used in the study area. Finally, irrigation application was ceased a week

before harvest to facilitate field drainage. At maturity, the crop was harvested, air dried and threshed. Grain yield was determined at 14% grain moisture content (de Vries et al. 2010; Chahal et al. 2007). Grain moisture content refers to the amount of moisture present in the grain which is determined by different approaches (Chen 2003).

Similarly, in the winter season berseem fodder crop was sown on prepared beds on the same plot. The soil was soaked with water before sowing the seed to favour easy seed germination. The seed was also first soaked into fresh water for about 12 hours and then dried in a cool shady place before sowing. The seed was then sown on wet beds by broadcasting. Required dose of DAP was applied for the fodder crop and weed control was undertaken in similar way as that of the rice. Being a fodder crop, berseem was harvested at intervals and the yield was recorded regularly. The first harvest was made between 70-85 days after sowing and the consecutive cuttings were made in shorter intervals till final harvest.

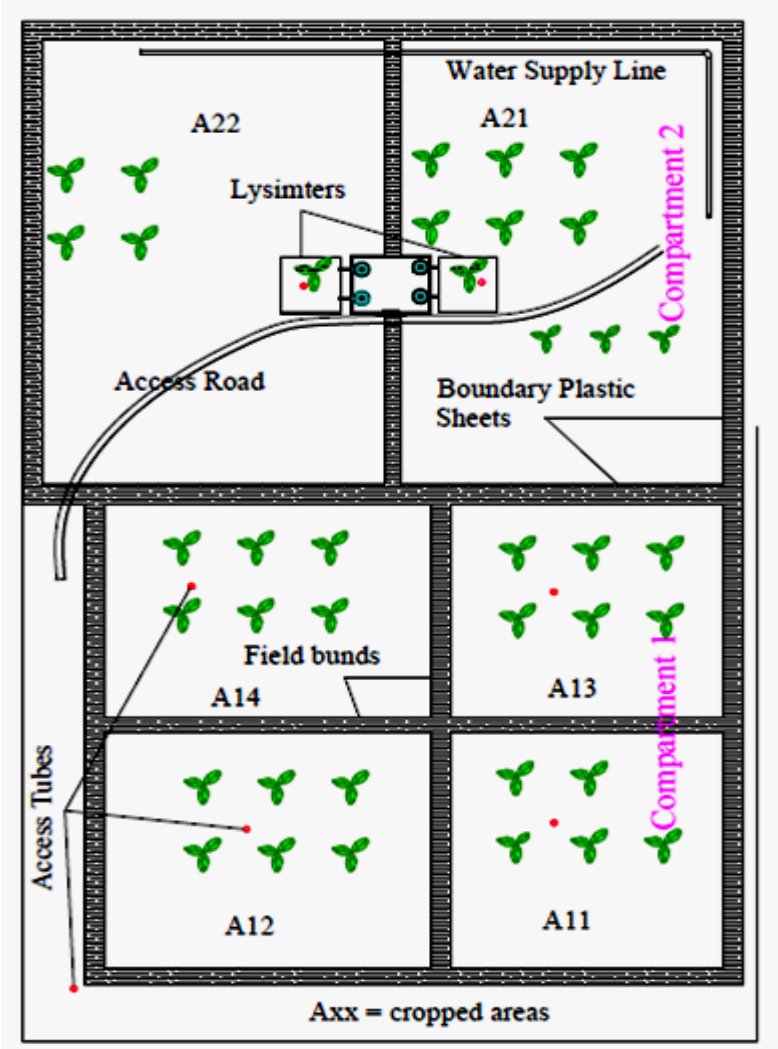

Area	*Size (m^2)*
A11	3x3.5 = 10.5
A12	3x3.5 = 10.5
A13	3x3.5 = 10.5
A14	3x3.5 = 10.5
A21	4x3.5 = 14
A22	4x5 = 20
Lysimeter 1	1x1 = 1
Lysimeter 2	1x1 = 1

Fig. 3.1 Experimental field layout details: line drawing

Fig. 3.2 Experimental field layout and rice transplanting (season 2)

3.4 IRRIGATION APPLICATION

Irrigation water was applied for a specific area by measuring discharge and calculating time required to provide a predetermined depth of water. Areas of specific plots and lysimeters were predetermined. The amount of discharge from water supply pipe at the boundary of the experimental station was measured by using known volume of container and a stop watch. The required depth of water to be applied to a specific plot is determined from required ponding (during rice season) or soil moisture deficit in the root zone during berseem crop period. From known discharge (assumed to be constant for plot irrigation period), area of plot and depth of application, the time required for water flow to spend in a particular plot is determined which is again monitored with the help of stop watch. The water is tapped to specific plot area by plastic pipes. Table 3.1 provides the measured data of typical irrigation application and other salient features as used in the experimental runs.

During rice growing period, irrigation size ranging between 20 mm to 100 mm was applied to all the plots throughout the crop period in the first crop season which is mainly practiced in the study area. However, in the second season imposed irrigation sizes much less than that of season 1 to the plots have been applied ranging between 10 mm to 50 mm in plots A21 and L2(lysimeter 2), 15 mm to 50 mm in plot A13 and 10 mm to 40 mm in plots A11,A12, A14, A22 and L1 (lysimeter 1). On the other hand, during berseem crop season irrigation was scheduled when nearly 40 percent of moisture depletion in the root zone took

place. Similar depths of irrigation were provided for all the plots in season 1. However, during season 2 varying depths of irrigation applications satisfying 100% (Plots A11 and A12), 80% (plots A13 and A14), and 60% (plot A21 and lysimeter 2) and 40% (plot A22 and L1) soil moisture deficits were imposed. Irrigation was also provided during the winter season when the moisture depletion was not significant to ease the soil freezing effect on the crop.

Table 3.1 Typical irrigation application during berseem season 2 growth period

Plot number	Area (m^2)	Discharge (l/sec)	Depth (cm)	Time required for the flow (min:sec)	Remarks
A11	10.5	0.328	3.0	16:02	irrigation depth =100% of root zone deficit
A12	10.5	0.328	3.0	16:02	
A13	10.5	0.328	2.4	12:49	irrigation depth =80% of root zone deficit
A14	10.5	0.328	2.4	12:49	
A21	14.0	0.317	1.8	13:16	irrigation depth =60% of root zone deficit
A22	20.0	0.317	1.2	12:38	irrigation depth =40% of root zone deficit
L1	1.0	0.317	1.2	00:38	
L2	1.0	0.317	1.8	00:57	irrigation depth =60% of root zone deficit

3.5 METEOROLOGICAL DATA

Meteorological data required for the study were obtained from the nearby meteorological stations. Two automatic meteorological stations are available near the experimental site within 800 m areal distance from the experimental station at National Institute of Hydrology and Department of Hydrology, Indian Institute of Technology, Roorkee. Relevant data with respect to air temperature, relative humidity, sunshine hours, pan evaporation, rainfall, and wind speed were collected from these stations. The data from Department of Hydrology is somehow extensive in that it also contains dew point temperature, air pressure and groundwater level data. The availability of meteorological data from such stations enabled for cross checking of the validity of the meteorological data for the area. The data from both stations are consistent. The data obtained from NIH has mainly been used; although any missing data has been refilled from the data from Department of Hydrology. These meteorological data were majorly used in determination of reference evapotranspiration, ET_0.

The rainfall measurements were made at 08:30 hours with standard tipping bucket type recording rain gauge. Pan evaporation is monitored using both class-A pan and Colorado sunken type evaporimetres on daily basis. Mean wind velocity at 2 m height above the ground and sunshine hours during the last 24 hours are measured on daily basis at the stations. Maximum and minimum temperatures (°C) and estimates of relative humidity are available from the stations. Fig. 3.3 presents the salient meteorological data for the experimental period.

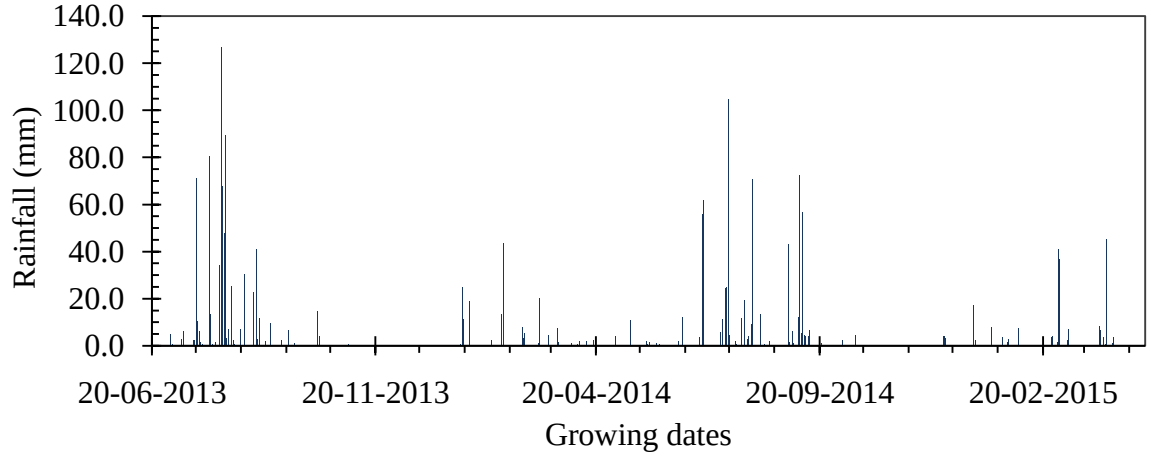

Fig. 3.3(a) Rainfall depth in the growing seasons

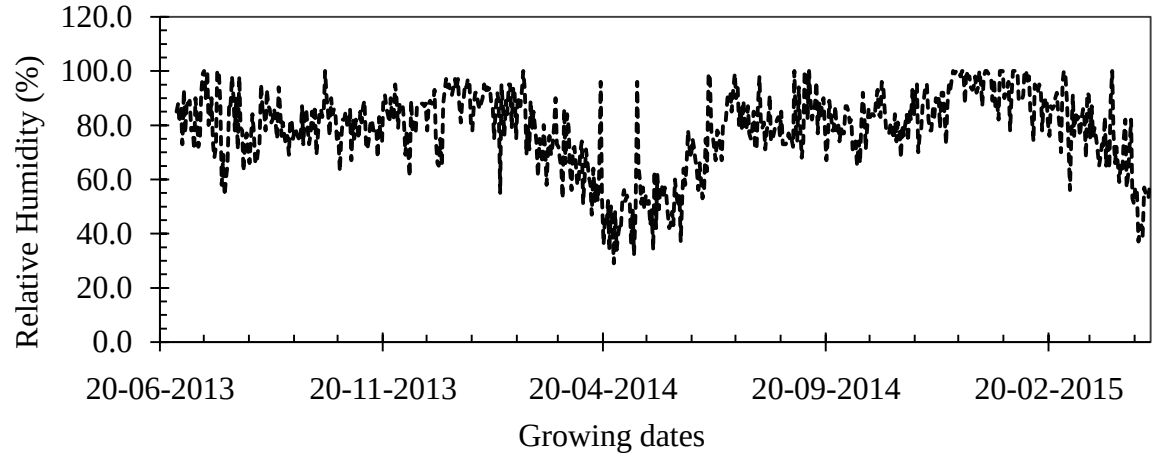

Fig. 3.3(b) Relative humidity in the growing seasons

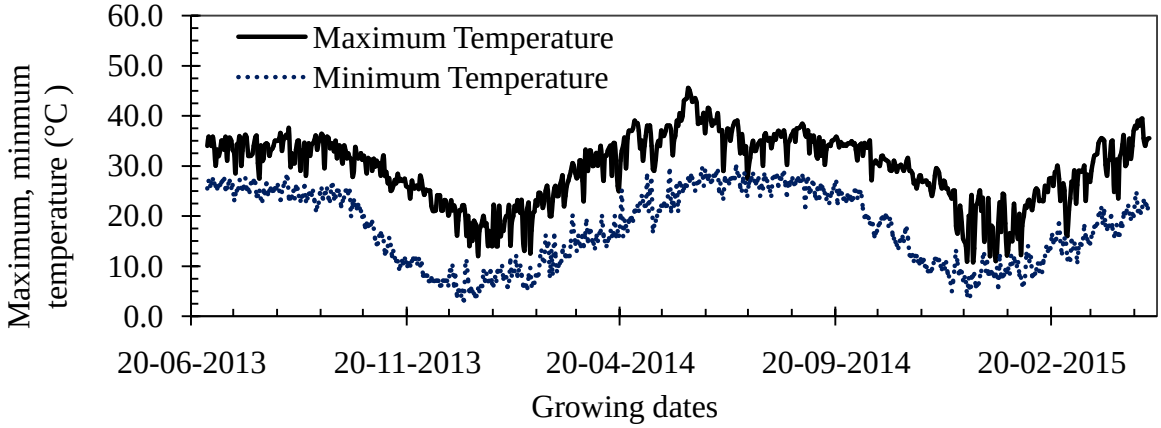

Fig. 3.3(c) Maximum and minimum temperatures in the growing seasons

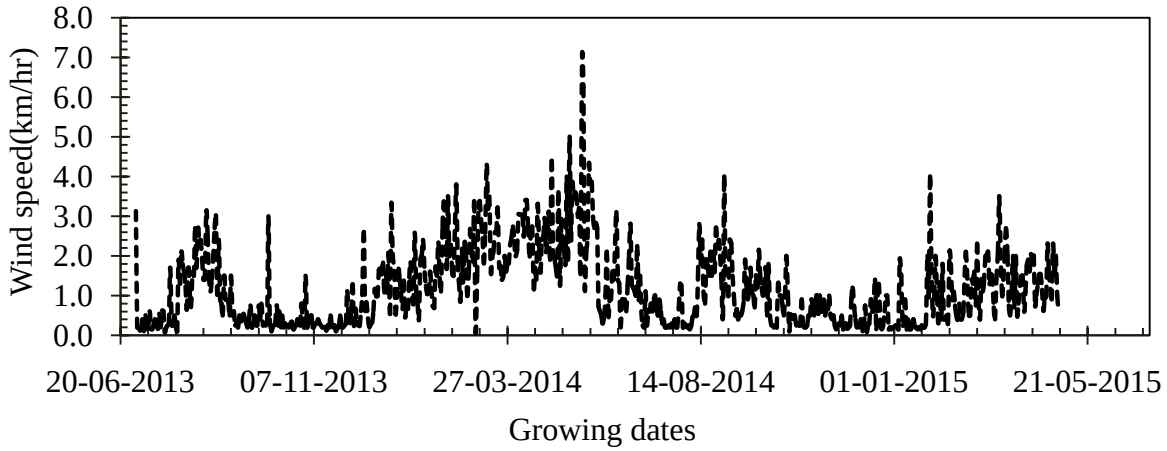

Fig. 3.3(d) Wind speed in the growing seasons

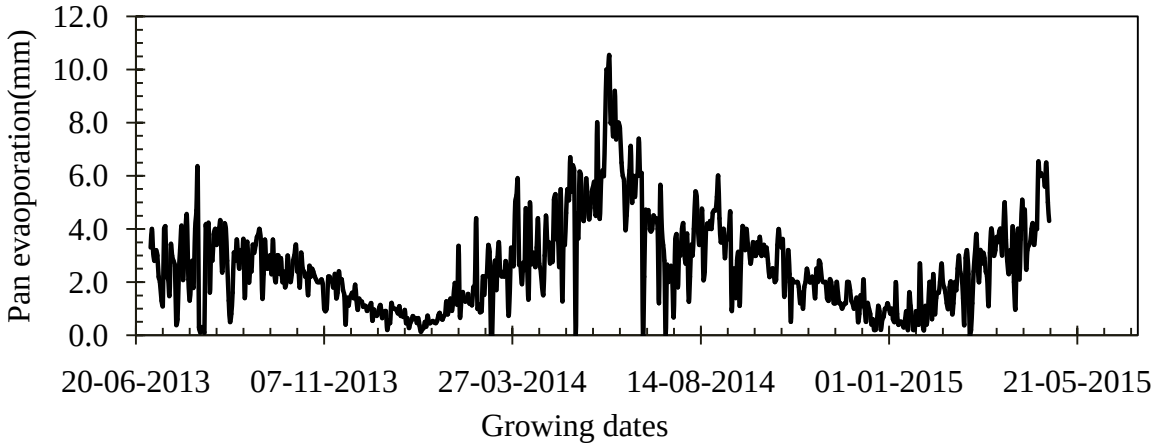

Fig. 3.3(e) Pan evaporation in the growing seasons

3.6 DETAILS OF VARIABLES OBSERVED

Besides the meteorological data obtained from the nearby stations, soil and plant parameters observed either in the field or laboratory along with instruments used and their importance in the study are presented in Table 3.2.

Table 3.2 Summary of variables observed during the experimental program

S. N	Category/ class of data	Variable/ Parameter	Materials or equipment required/procedure followed	Importance in the study
1	Hydro-Met data	Rainfall	Rain gauge/nearby meteorological station	input in the models
		Temperature, humidity, wind speed, sunshine hours	nearby meteorological station	input to reference evapotranspiration determination
2	Irrigation and drainage	Irrigation size	known volume of bucket and stop watch	input in the models
		Drainage size/Deep Percolation	Drainage type lysimeters	output in the models
3	Soil hydraulic Variables	Saturated hydraulic conductivity, K_{sat}	Guelph type Permeameter	to measure the saturated hydraulic conductivity of the field
		Soil moisture content	Profile probe (PR-2/6)	to monitor soil moisture content (for irrigation application in the field
4	Soil property variables	Texture	Mechanical sieve/Hydrometer	soil class/type determination
		Bulk density	Core Samplers	to compute the saturated water content
		Particle density	Pycnometer	to compute the saturated water content
		Soil moisture characteristic curve (SMCC)	Pressure plate apparatus	to obtain model parameters such as "θ_r", "θ_s", "m", "n_v", and "α_v"
5	Plant characteristics	Crop height	Tape meter	requirement in the models
		Root depth	Simple digging tools/tape meter	requirement in the models
		Crop phonological stages	Crop growth stage observation	requirement in the models
		Leaf area index	Planimeter or *LAI* meter	requirement in the models

3.7 SOIL MOISTURE CONTENT

The soil moisture content is defined as the ratio of volume of water present in the soil to the volume of soil (θ) and is required to determine the amount of water available in the crop

root zone. Several methods are available to measure soil moisture content. In this study, the soil moisture content was monitored by using soil water profile probe (PR2/6; Delta T Devices, Cambridge, United Kingdom) inserted through access tubes which were installed both inside and outside the lysimeters. The details of the probe are shown in Fig. 3.4. The profile probe sensor which is connected to a special HH2 moisture meter provides soil water content at 10, 20, 30, 40, 60 and 100 cm depths from a reference mark shown on the tube, i.e., it could provide soil moisture content up to 1 m depth below the ground surface. The probe consists of a sealed polycarbonate rod approximately 25 mm diameter, with electronic sensors arranged at fixed intervals along its length. Each of the sensors comprises a 100 MHz oscillator and transmits an electromagnetic field extending about 100 mm into the soil. The moisture content of the soil surrounding the rings dominates its permittivity, $\sqrt{\varepsilon}$. A relationship between the soil moisture content and permittivity can be established using the following equation (Whalley et al. 2004; Schaap et al. 1997).

$$\sqrt{\varepsilon} = a_0 + a_1 \times \theta \qquad (3.1)$$

where ε is the dielectric constant of soil, a_0 and a_1 are calibration constants between the soil permittivity and θ is the soil moisture content (fraction). The constants a_0 and a_1 are dependent on soil type and enable to convert probe readings into soil moisture content values. The permittivity of a material is a measure of its response to polarisation in an electromagnetic field. Water having a strong permittivity (≈ 81) than soil (≈ 4) and air (≈ 1) can easily be detected in an electromagnetic field. The detectors are sensitive to the different proportions of transmission and refection, and convert them into stable voltage output that acts as a simple, sensitive measure of soil moisture content. When the probe is installed in an access tube constructed from a composite material it can measure the dielectric constant at soil depths of 10, 20, 30, 40, 60 and 100 cm. The probe can either be logged into the access tube for automatic recording or it can be moved from one access tube to another to make manual spot readings. In this particular study, manual spot readings were recorded. The output of the probe is in volts which are converted into dielectric constant, ε, which is useful for describing the microscopic interaction between electromagnetic radiation and matter (Bohren and Huffman 1983). Hence, having the permittivity and calibration constants for specific soil types, the moisture content of a given soil at given intervals along the depth can be measured. The probe enables to measure the soil water content in volumetric basis for different types of soils ranging from clayey to sandy soils with accuracy between $\pm$0.04 (after soil specific calibration) and $\pm$0.06(after generalized soil calibration in normal soils).

The manufacturer (Delta T-devices) suggests that a generalized calibration for most mineral soils is sufficient. Therefore generalised soil calibration, as recommended by the manufacturer, before starting operation of the instrument has been carried out (User Manual-PR-2/6). Field calibration was not conducted due to the absence of other comparative soil moisture sensing devices such as neutron probe and precision soil sampling auger at desired depth near the sensors.

The access tubes were installed in field spots using the access collars provided for installation of the access tubes. The profile probe is sensitive to open spaces and hence care was practiced to install the access tubes. The access tubes were then plugged with the provided capes at the top and left for some days so that any annular opening between the access tube and the wall of soil column would be filled by rain water.

The soil moisture content was measured on daily basis, near noon, and before and after irrigation or rainfall whenever the events took place. Monitoring of the soil water status enabled for irrigation decisions depending up on specific crop water requirements and stress tolerance level, specifically, for berseem crop. Overall, the access tubes were installed at seven different spots to monitor the root zone soil water dynamics including the access tubes in the lysimeters. Figs. 3.5 (a and b) show field soil moisture measurements using profile probe during both crop seasons.

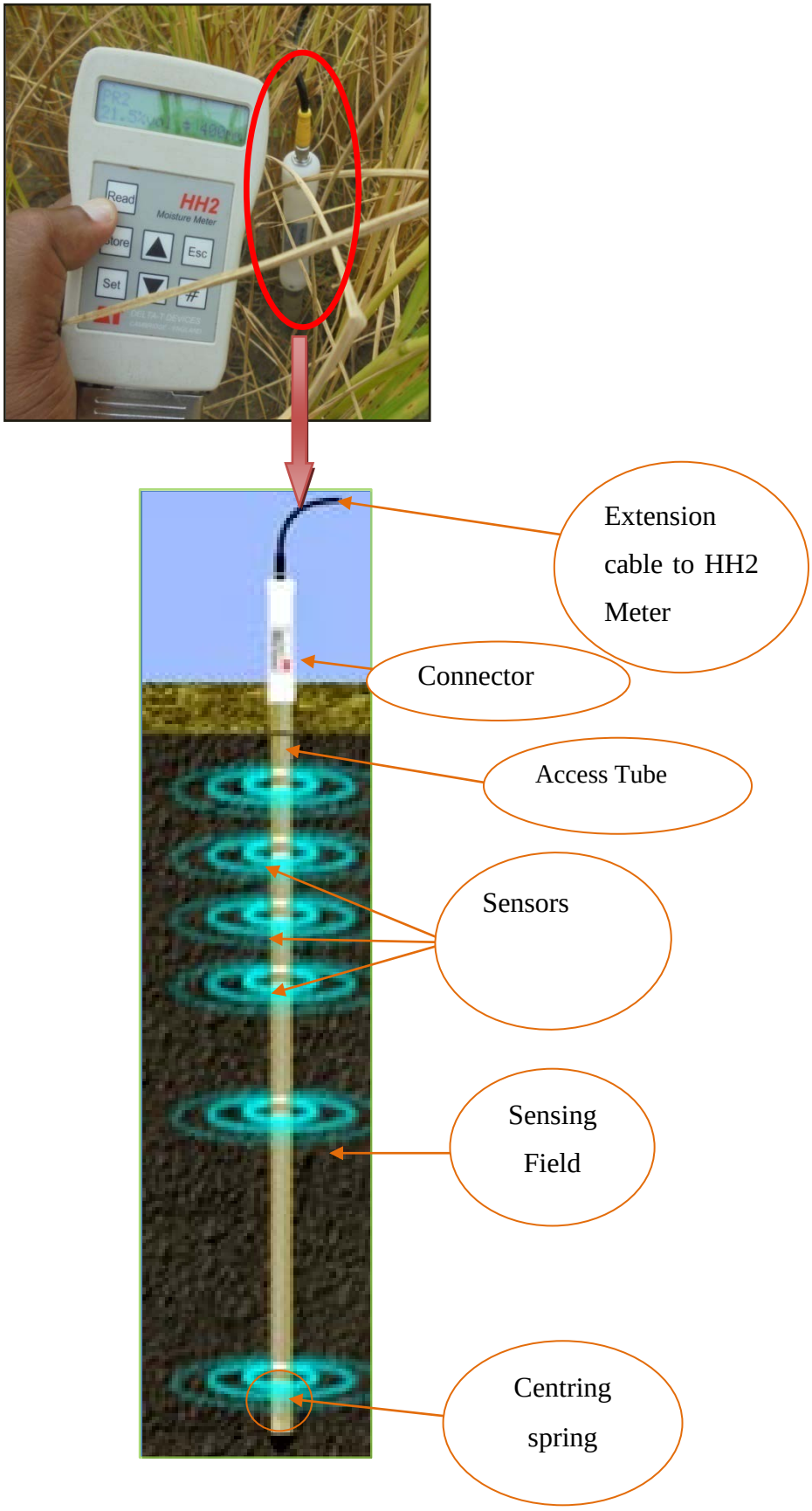

Fig 3.4 Details of profile probe (PR2/6) and HH2 meter (Source: Delta T-devices, UK)

(a) Rice season

(b) Berseem season

Fig 3.5 Monitoring soil moisture using profile probe

3.8 LYSIMETER SETUP AND DRAINAGE OBSERVATION

Lysimeter experiments were conducted at the experimental farm from July 2013 to April 2015. The area of lysimeters was $1m^2$ having a depth of 1.35 m repacked soil similar to that of the experimental field. The construction of the lysimeters took place in 2007 and hence they are considered to replicate the surrounding root zone soil environment (Liu et al. 1998). The lysimeters were constructed of steel metal sheets having a square shape. The soil monolith is a repacked soil material consisting of the upper 1.15 m filled with a sandy loam textured soil, moderately homogeneous throughout the profile, characterized by an organic content of 1.1 to 1.2%. The bottom 0.08m was filled with a coarse gravel of size more than 3 cm diameter overlain by 0.12 m thick gravel of about 2 cm in diameter. This bottom arrangement allows drainage towards outlet pipes which carry percolating water towards collecting buckets (Shankar 2007). The same experimental conditions have been maintained inside and outside the lysimeters throughout the growing period of the crops.

Deep percolation was measured twice in a day at the bottom of lysimeters early in the morning (07:00 a.m.) and evening (07:00 p.m.). However, during rainy days, the collection time could be more frequent so that there would be no overflow from the buckets. The lysimeter rim was kept 10 cm above the ground to avoid run-on or runoff. Collecting buckets in access caisson were used to collect the drainage water. The buckets were securely covered to avoid rainwater inflow besides the plastic sheet shedding provided over the access caisson hall. Fig. 3.6 shows the schematic diagram of the lysimeter setup while Fig. 3.7 shows the actual lysimeters, drainage collection arrangement and access hall.

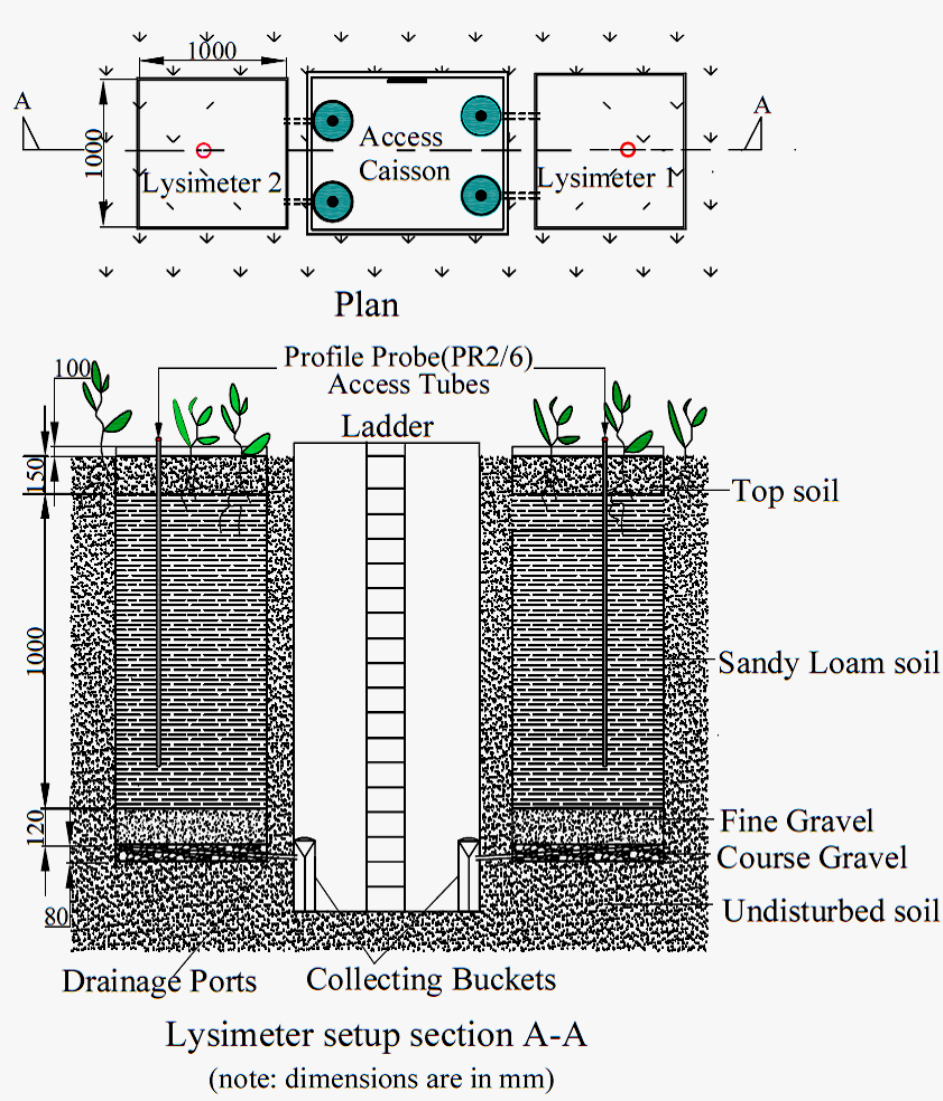

Fig. 3.6 Schematic diagram of lysimeter setup

Fig. 3.7 Lysimeters and drainage collection arrangements

3.9 SOIL FACTORS

The soil physical and hydraulic characteristics were determined in the laboratory for three representative spots of the irrigation plot at different depths from 0 to 140 cm. In this study, laboratory experimental works consisting determination of soil physical properties such as grain size, bulk density, particle density, porosity, hydraulic conductivity and the soil retention parameters were conducted. The following sections describe the experimental program in detail.

3.9.1 Texture

The soil texture refers to the size of aggregates or particles. It is usually determined using mechanical sieve analysis for coarser particles and wet or hydrometer analysis for finer particles. Similarly, in this study, the soil particle size was determined by employing mechanical sieve analysis (for coarser particles) and hydrometer method (for the finer portion of the soil) as recommended by the American Society for Testing and Materials, ASTM.

3.9.1.1 Soil sampling and sieving analysis

Soil samples from representative field spots (3 spots) and five replicate positions along the vertical profile have been extracted for grain size analysis. The extracted samples were transported to laboratory and oven dried for 24 hours at 105 $^{\circ}$C after which required amount of sample was weighed for sieve and hydrometer analysis. Particularly, for the hydrometer analysis 50 gram of oven dried sample that pass through the 200 (75 micron) sieve size was taken. Trout (1982) suggested washing of the coarser particles so that finer particles which are glued over the coarse particles get detached with the flowing water when a sample is washed through the 200 sieve size. Therefore, soil samples were washed before sieve analysis in the current study. The detail of data and analysis for the spots for textural classification is provided in Figs. 3.8 to 3.11 and Appendix A.

The collected samples were first dried and weighed. Then the samples were sieved through 200 sieve size to collect samples for hydrometer analysis and further washed through the 200 sieve size. The washed samples were dried again in oven and well pulverized to avoid any globules. The samples were then placed on standard sieves and mounted on mechanical sieve shaker for at least 10 minutes. Finally, the samples retained on each sieve were weighed and analysed following standard procedures suggested by the American Society for Testing and Materials (ASTM) (ASTM 422) or Trout (Trout, 1982). Fig. 3.8 shows details of sieve analysis in progress.

(a)Washing of samples

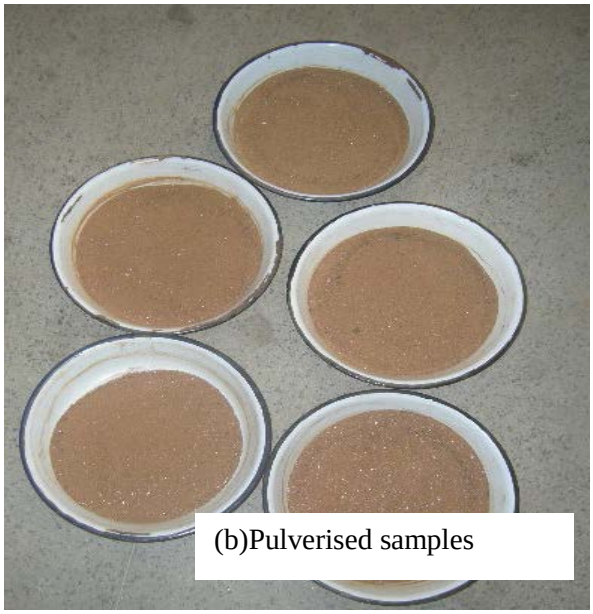

(b)Pulverised samples

(c) Standard sieves on mechanical shaker

Fig. 3.8 Grain size distribution analysis

3.9.1.2 Hydrometer analysis

The Hydrometer analysis is applied to separate finer soil particles (silt and clay) following the principle of Stoke's Law. When soil particles are evenly dispersed in a fluid, the density of the suspension is initially uniform. As time passes, the particles begin to settle out with the larger particles settling out most quickly. Consequently, the density of the suspension varies vertically throughout the suspension and continually changes with time. A hydrometer suspended in the soil-water mixture indicates the density at the elevation of its bulb, which is related to the amount of sediment still suspended at that elevation (Trout 1982). Fig. 3.9 shows hydrometer analysis in progress.

Fig. 3.9 Hydrometer analysis

A total of sixteen sieve and hydrometer analysis were conducted in the experimental plot and different depths along the vertical profile below the field ground level. A grain size distribution curve for both coarse and fine aggregates has been plotted following recommended standard procedures. The grain size distribution curves for samples collected at spot 2 are shown in Fig. 3.10. The United States Department of Agriculture (USDA) method has been employed for classification of soil materials after proper grain size analysis has been conducted.

The grain size analysis curve in all the three spots and the respective depths shows the same trend indicating same textural classification of soil material up to the depth of at least 1.4

m depth. In all cases, the textural classification of the experimental field soil falls in sandy loam portion of the textural triangle.

Fig. 3.11 shows the textural triangle and the location of samples in textural triangle.

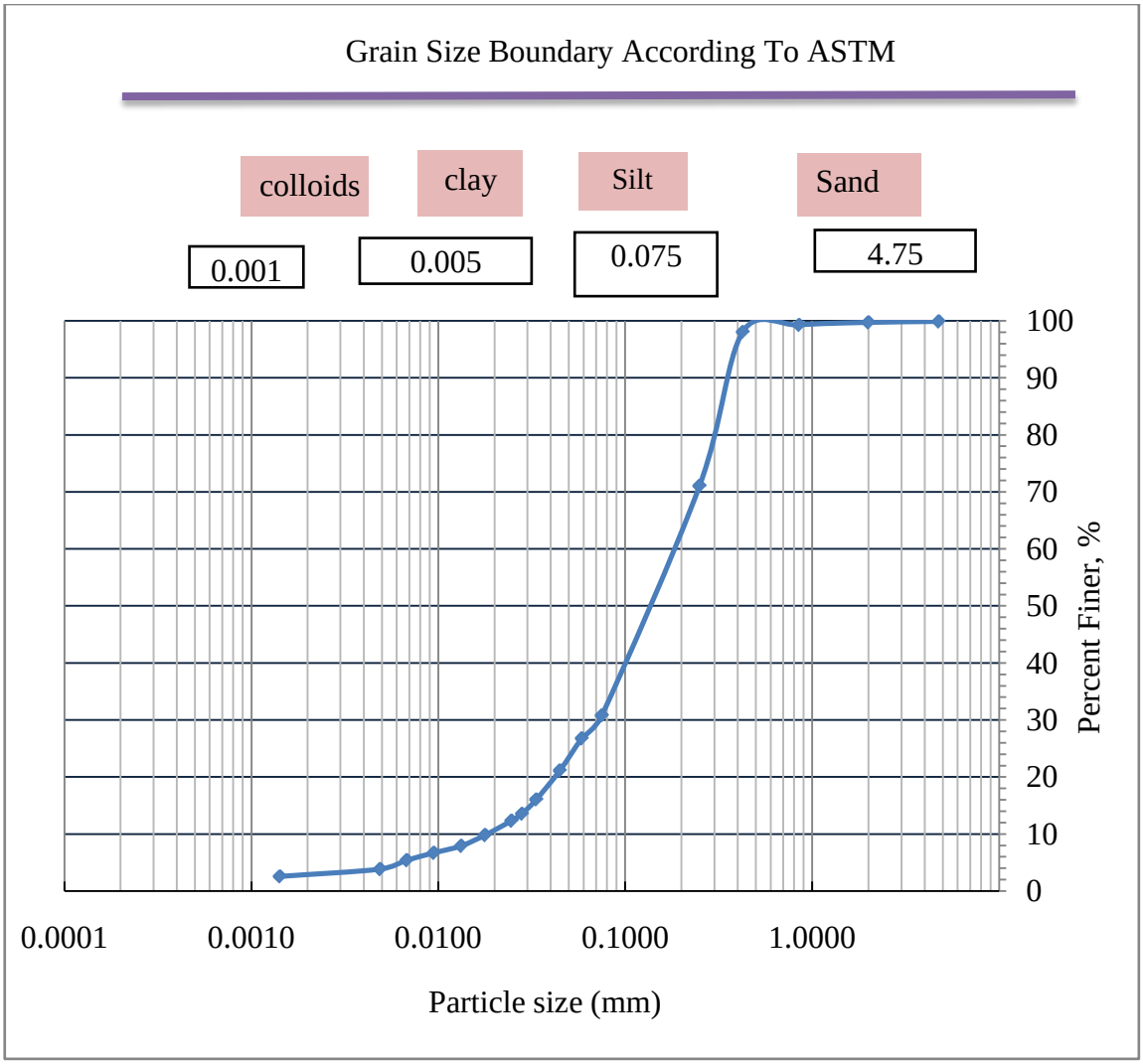

Fig. 3.10 (a) Grain size distribution curve for sample 1(0-30 cm) at spot 2

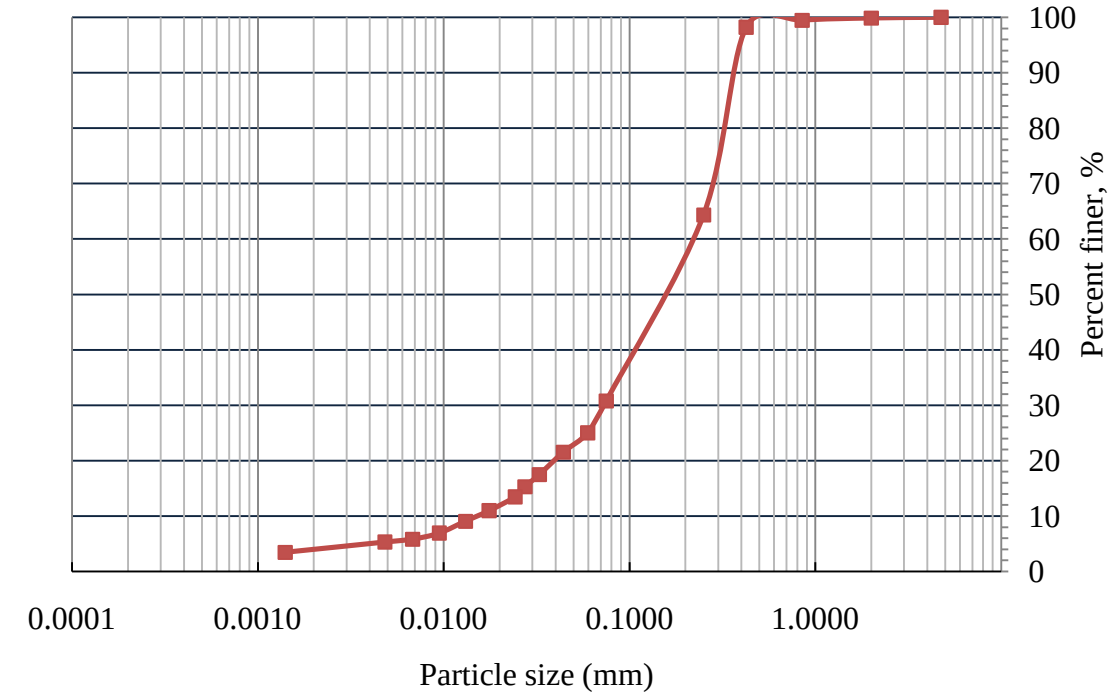

Fig. 3.10 (b) Grain size distribution curve for sample 2(30-60 cm) at spot 2

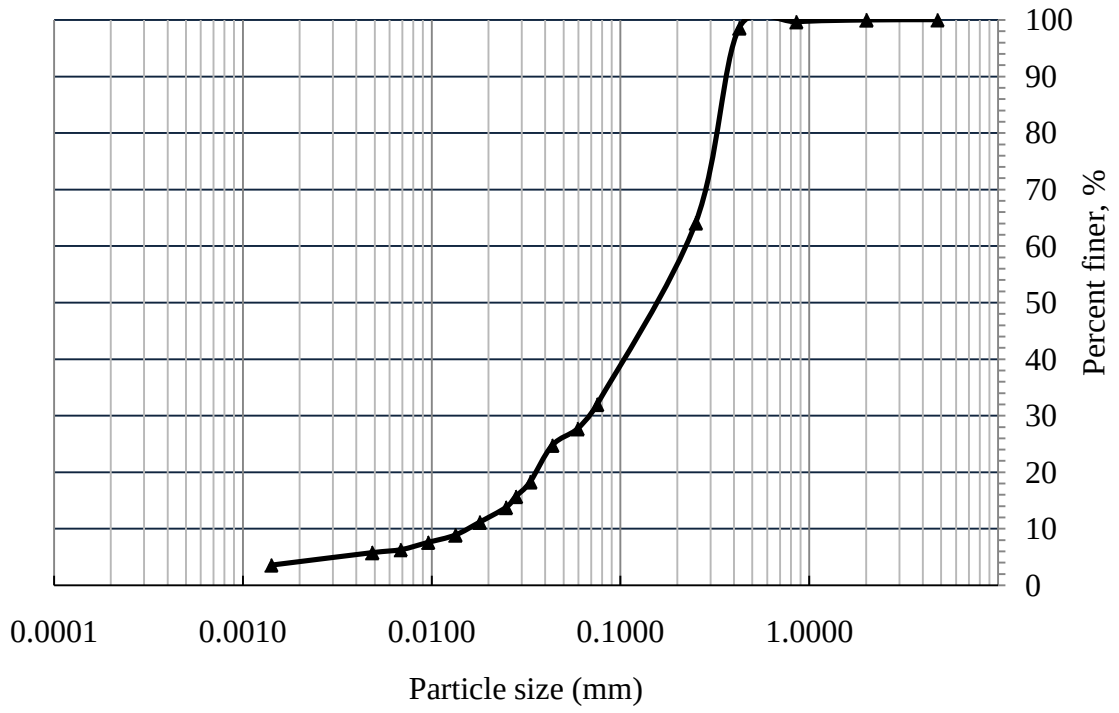

Fig. 3.10 (c) Grain size distribution curve for sample 3(60-80 cm) at spot 2

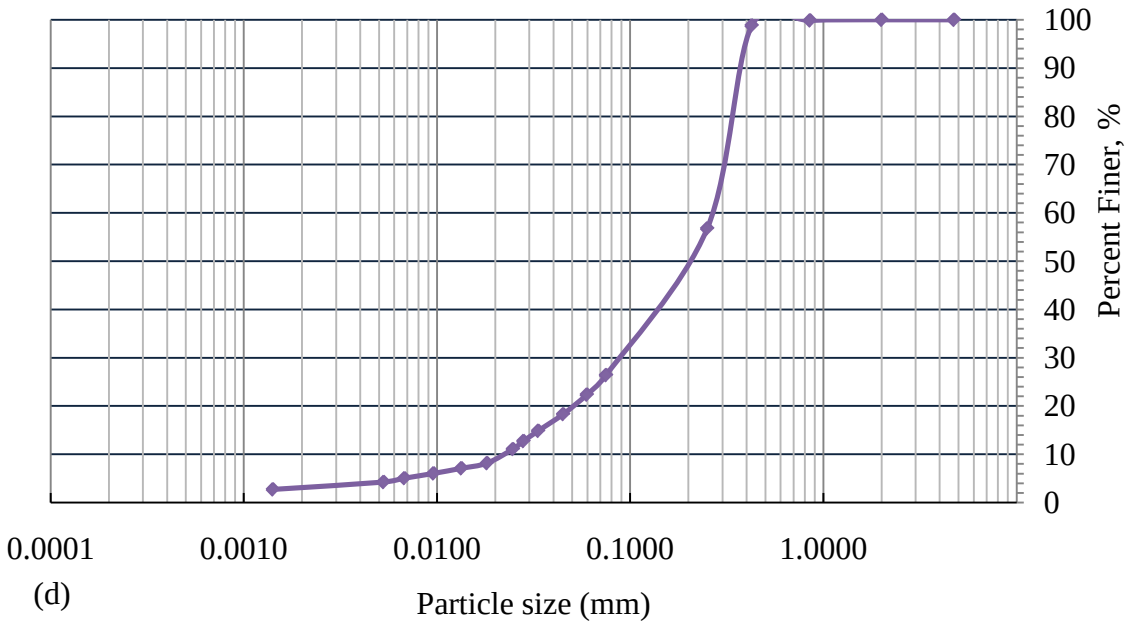

Fig. 3.10 (d) Grain size distribution curve for sample 4(80-100 cm) at spot 2

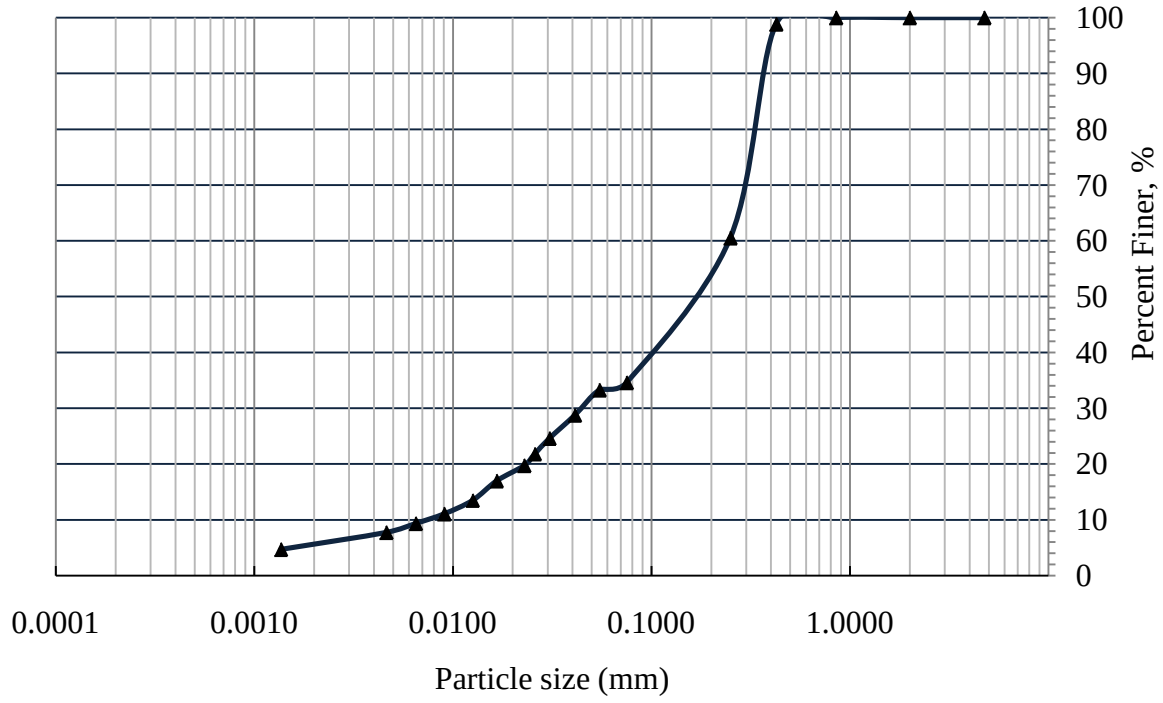

Fig. 3.10 (e) Grain size distribution curve for sample 5(100-140 cm) at spot 2

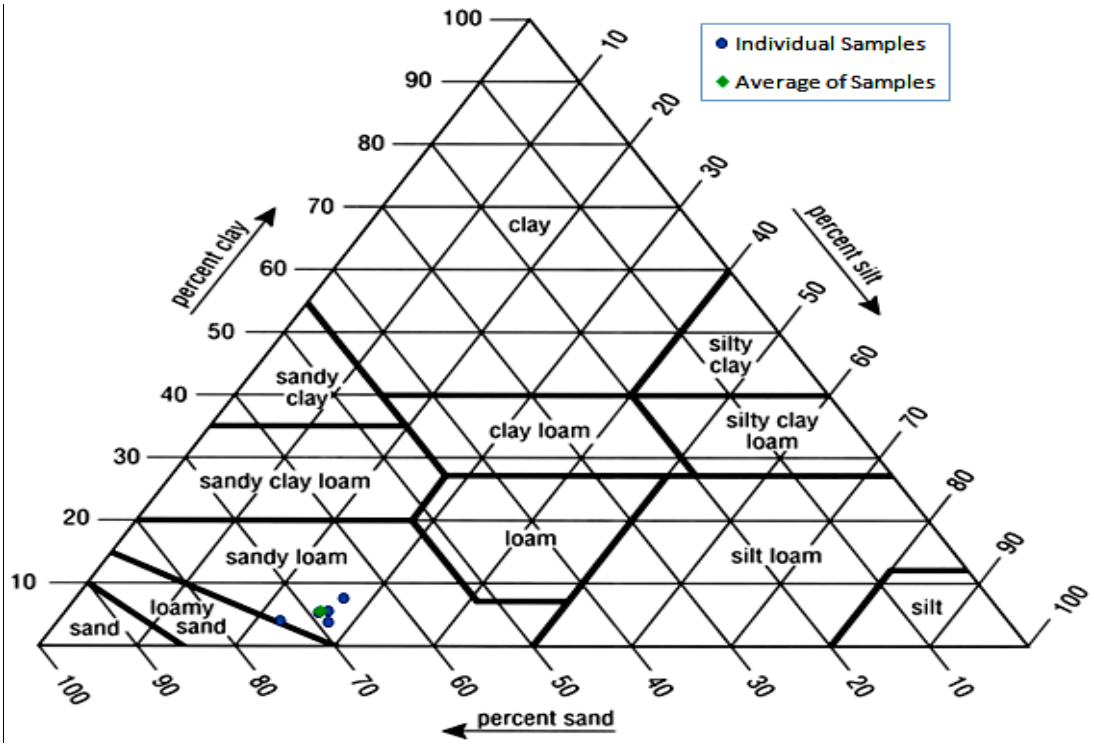

Fig. 3.11 USDA soil textural classification (Cuenca, 1989)

3.9.2 Bulk Density

The soil bulk density is the ratio of the dry mass to the total volume of a given soil sample. Bulk density was determined by using standard core cutter method by extracting undisturbed core samples from spots and corresponding depths where soil samples for grain size analysis were taken. Fig. 3.12 shows field sampling using core cutter method. Thorough caution was taken to avoid disturbance of the samples while collecting the samples. For this purpose, the cores were penetrated into the ground with either gentle blow with hammer on a dolly placed at top of the cutter or pushed with the palm of hand or the sole of foot. The extracted samples were then wrapped in a plastic bag and transported to laboratory for oven drying. The samples were allowed to drying in oven for 24 hours at 105 $^{\circ}$C. The oven dried samples were then measured to determine the dry weight of the soil samples. The total volume of the samples were determined by measuring the inside diameter and height of the core with vernier caliper. The bulk density is determined as:

$$\rho_b = \frac{M_s}{V_t} \tag{3.2}$$

where M_s is the total dry mass of the soil core; V_t is the total volume of the sample referring to the inner volume of the core cutter and ρ_b is the soil bulk density.

3.9.3 Particle Density

The particle density is the ratio of dry mass (oven-dry) of soil sample to the volume of soil particles in the sample. Particle density depends on the densities of the various constituent solids and their relative abundance. Soil samples for this test were also obtained from the same location and respective depths as that for soil bulk density.

$$\rho_d = \frac{M_s}{V_s} \tag{3.3}$$

where M_s is the total dry mass of the soil; V_s is the volume of the soil particles and ρ_d is the soil particle density.

In a given soil sample, the total volume is the sum of voids (liquid and gases) and soil particles. For oven dried sample, the liquid (water) volume is negligible and the total pores are occupied by air. Therefore, air volume is required to be reduced (air has to be expelled) from the sample. This could be achieved by water Pycnometer test which is used in this study. Fig. 3.13 shows the Pycnometer test in progress. The trapped air in the soil sample was removed by frequent shaking and pumping of air from the sample in the Pycnometer. The water Pycnometer test consists of measuring the weight of oven dry soil (W_s), the weight of water and Pycnometer (W_{pw}) and mixture of soil and water in a Pycnometer (W_{spw}). The water Pycnometer test basically enables to determine the volume of water displaced by dry soil sample. The soil particle density is thus determined as:

$$\rho_s = \frac{W_s}{W_s + \left(W_{pw} - W_{spw}\right)} \tag{3.4}$$

Fig 3.12 Field sampling using core cutter

Fig. 3.13 Water Pycnometer in operation

3.9.4 Porosity

Porosity is the ratio of the volume of pores to the total volume of soil sample. It is computed from the knowledge of bulk and particle density values. Soil porosity is used to determine the saturated moisture content in the absence of other reliable methods.

$$f = 1 - \frac{\rho_b}{\rho_s} \tag{3.5}$$

where f is the soil porosity.

The average soil physical properties determined are shown in Table 3.3.

Table 3.3 Soil physical characteristics of the experimental plot

Depth below ground level (cm)	Bulk density (g/cm^3)	Particle density (g/cm^3)	Sand (%)	Silt (%)	Clay (%)	Soil Class (USDA)	Saturated Water content
0-30	1.58	2.55	73.40	22.70	3.90	Sandy Loam	0.38
30-60	1.55	2.57	66.89	28.39	4.72	Sandy Loam	0.40
60-80	1.54	2.56	68.57	26.54	4.89	Sandy Loam	0.40
80-100	1.54	2.58	69.10	26.54	4.36	Sandy Loam	0.40
100-140	1.59	2.62	68.01	27.38	4.61	Sandy Loam	0.39

3.9.5 Soil Moisture Characteristic Curve

Soil moisture characteristic curve (SMCC) is a plot of soil suction pressure against water content of a particular soil. It is an essential parameter in the study of soil water movement, contaminant or solute transport, infiltration and drainage studies in unsaturated

porous media (Malaya and Sreedeep 2012; Freduland and Xing 1994). SMCC reveals how a given soil responds towards the water flow through micro pores and hence play an important role in agricultural water management.

Various methods are available to estimate or measure soil moisture characteristic of a particular soil. The methods include determination of water content in a soil and measuring the corresponding pressure at which the water is maintained at equilibrium. Malaya and Sreedeep (2012) have conducted a critical review on the different methods to determine soil moisture characteristic curve including filter paper, dew point potentiometer, vapour equilibrium, pressure plate, Tempe cell and osmotic methods. In this study, the pressure plate apparatus has been used to determine the soil moisture characteristic curve of the experimental field.

Two pressure plate cells (soil moisture equipment corp., Santa Barbara, California, USA) were used; one for measuring the suction pressure of soil under low range (0-6 bars) and the other for measuring suction pressure under high range (6-15 bars). Fig. 3.14 demonstrates the setup for pressure plate cells and saturating soil samples in progress. In the pressure plate apparatus, disturbed soil samples were placed on a saturated porous ceramic plate, partially saturated and left in the cell for full saturation by imbibition as demonstrated in Fig. 3.14(b). Positive pressure from gas pressure source was applied over the samples to regulate and maintain the required pressure as shown in Fig. 3.14(c). When pressure is applied from the top of a sample, water starts draining through the soil samples since suction pressure is being developed at the bottom of porous ceramic plate. When equilibrium between the suction pressure and applied pressure is reached, the water stops flowing through the outlet, indicating equilibrium pressure. After equilibrium condition was maintained, the soil samples in the ceramic plate were removed and their water content values were determined gravimetrically. There have been five replicate samples representing depth wise variation of SWCC for each spot (spot 1 to spot 3) of the experimental field. Soil samples collected from respective depths, as mentioned earlier, were used to obtain SMCC of the particular samples. Several tests were conducted for each sample and varying magnitudes of equilibrium pressure to obtain a range of pressure-water content data. Tables 3.4-3.6 provide measured pressure and soil moisture content data for different spots and respective samples. The data were then fitted to the Retention Curve (RETC) model (van Genuchten 1980) to determine the SWCC and soil hydraulic parameters. Particularly, the van Genuchten model with m=1-1/n_v has been used. The soil moisture characteristics of the observed and fitted curves of the field soil for corresponding depths using van Genuchten (1980) model are shown in Fig. 3.15 for spot 2. Similar procedures

were carried out to determine SMCC for other spots. The soil hydraulic parameters determined using the van Genuchten model are given in Tables 3.7 to 3.9.

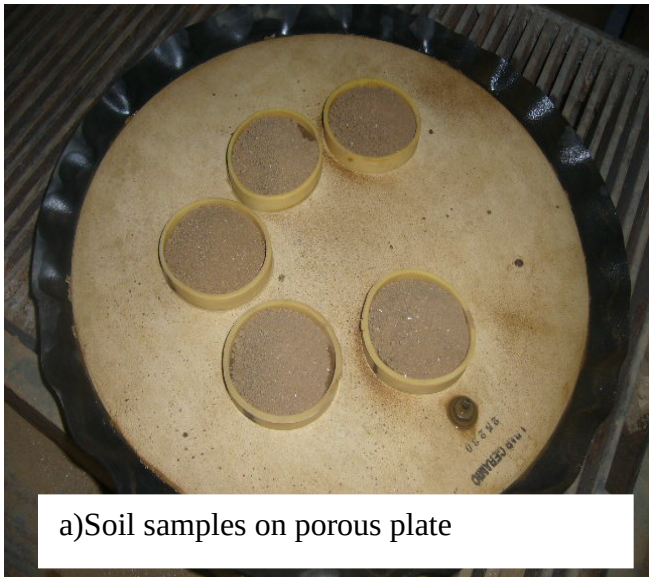

a)Soil samples on porous plate

b) Saturated soil samples ready for operation

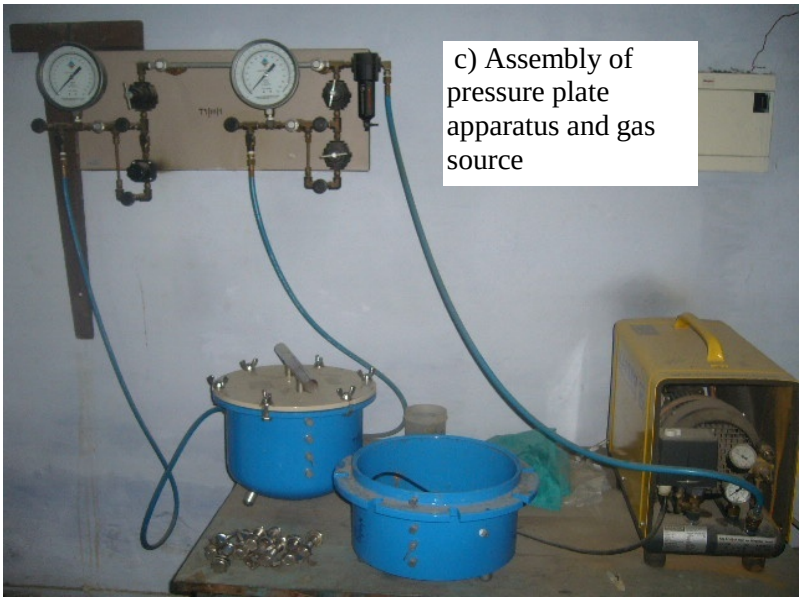

c) Assembly of pressure plate apparatus and gas source

Fig.3.14 SMCC determination using pressure plate apparatus

Table 3.4 Suction head - water content data from pressure plate apparatus for spot 1

Suction pressure(cm)	Water content (%)				
	Sample 1	Sample 2	Sample 3	Sample 4	Sample 5
0	35.70	39.97	38.13	38.97	39.10
300	17.90	24.43	19.20	19.94	19.41
375	17.50	21.71	18.87	18.84	19.35
850	13.80	16.72	13.56	14.78	14.00
1900	7.90	8.56	7.55	8.92	10.68
5000	6.80	6.70	6.12	6.86	7.71
7000	7.00	7.13	6.07	7.11	7.84
9000	6.90	5.86	5.61	5.97	6.49
12000	6.90	7.15	6.56	6.58	7.95

Table 3.5 Suction head - water content data from pressure plate apparatus for spot 2

Suction pressure(cm)	Water content (%)				
	Sample 1	Sample 2	Sample 3	Sample 4	Sample 5
0	35.69	39.96	38.10	38.99	39.1
300.0	17.94	24.43	19.20	19.94	19.41
375.0	17.48	21.71	18.87	18.84	19.35
850.0	13.83	16.72	13.56	14.78	14.00
1500.0	13.22	13.54	13.81	15.19	14.19
1900.0	7.88	8.56	7.55	8.92	10.68
5000.0	6.77	6.70	6.12	6.86	7.71
7000.0	7.01	7.13	6.07	7.11	7.84
9000.0	9.17	9.39	8.79	9.21	10.11
12000.0	6.90	7.15	6.56	6.58	7.95

Table 3.6 Suction head - water content data from pressure plate apparatus for spot 3

Suction pressure(cm)	Water content (%)				
	Sample 1	Sample 2	Sample 3	Sample 4	Sample 5
0	42.00	38.00	41.00	42.00	41.00
80	16.22	21.03	22.42	23.16	20.17
120	12.80	14.66	16.41	16.39	14.91
500	6.69	8.15	7.91	7.55	7.19
850	6.10	7.29	6.48	6.38	6.39
1000	5.82	7.62	6.88	6.58	7.07
2000	5.09	5.26	5.52	5.21	6.54
3000	4.99	5.23	5.02	4.99	4.79
5000	5.03	4.90	4.49	4.54	4.13
7000	3.40	5.04	4.04	3.88	3.83
9000	3.21	4.12	2.34	3.78	2.98
11000	2.53	3.08	2.29	3.34	2.12
12000	2.30	2.45	1.96	2.02	2.11

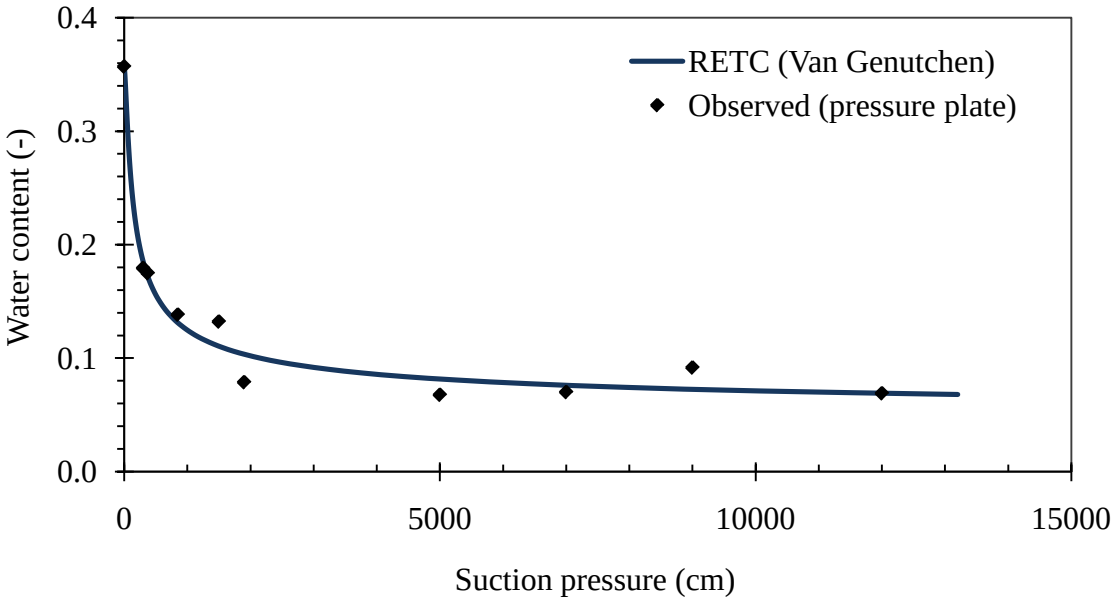

Fig. 3.15 (a) Soil moisture characteristic curve for sample 1 (0-30 cm) at spot 2

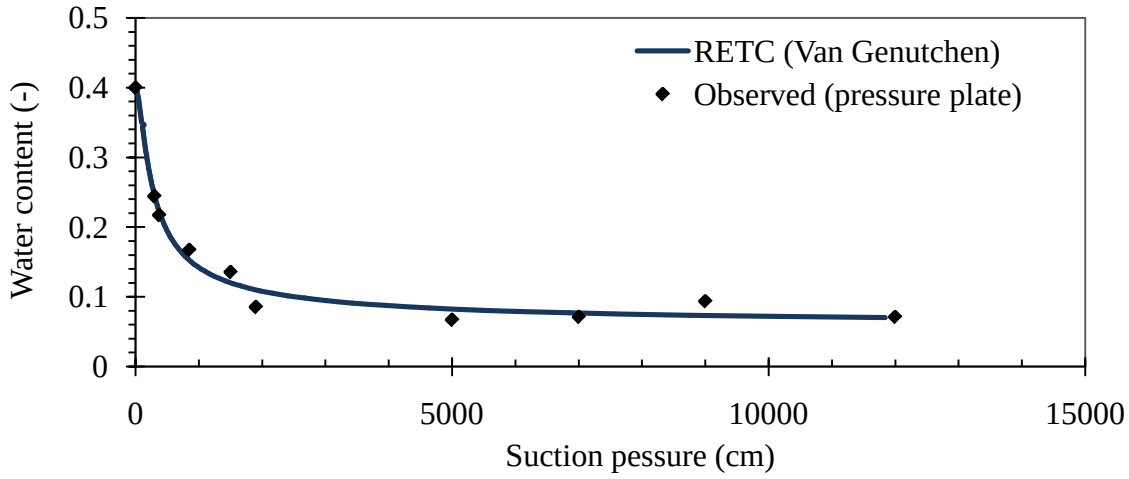

Fig. 3.15 (b) Soil moisture characteristic curve for sample 2 (30-60 cm) at spot 2

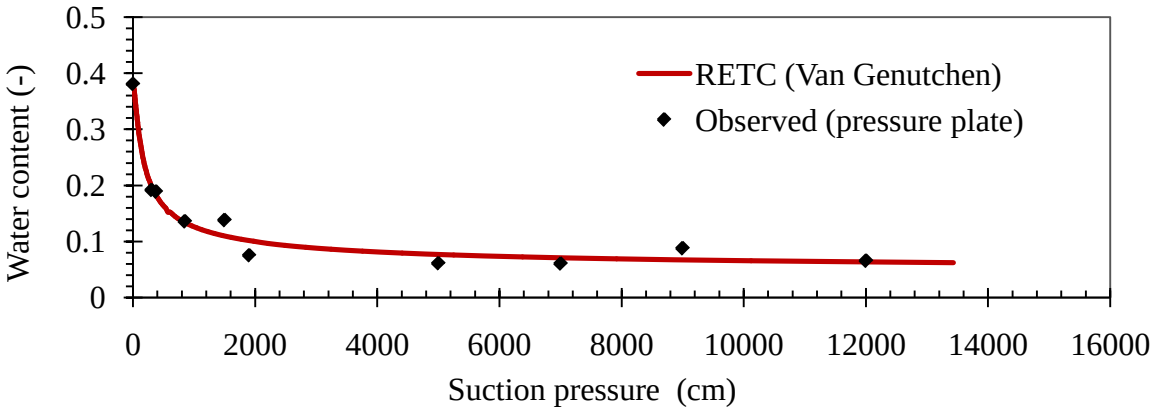

Fig. 3.15 (c) Soil moisture characteristic curve for sample 3 (60-80 cm) at spot 2

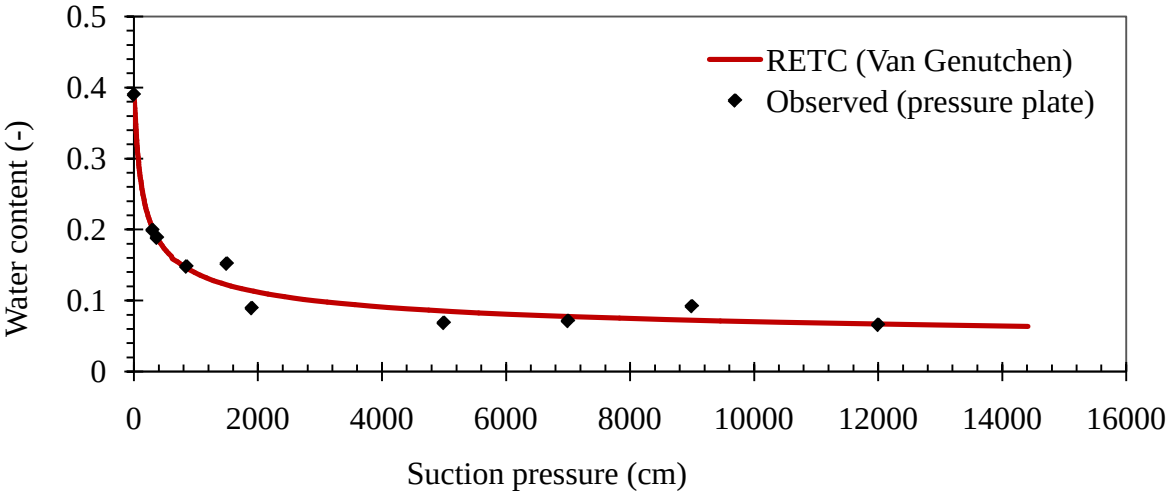

Fig. 3.15 (d) Soil moisture characteristic curve for sample 4 (80-100 cm) at spot 2

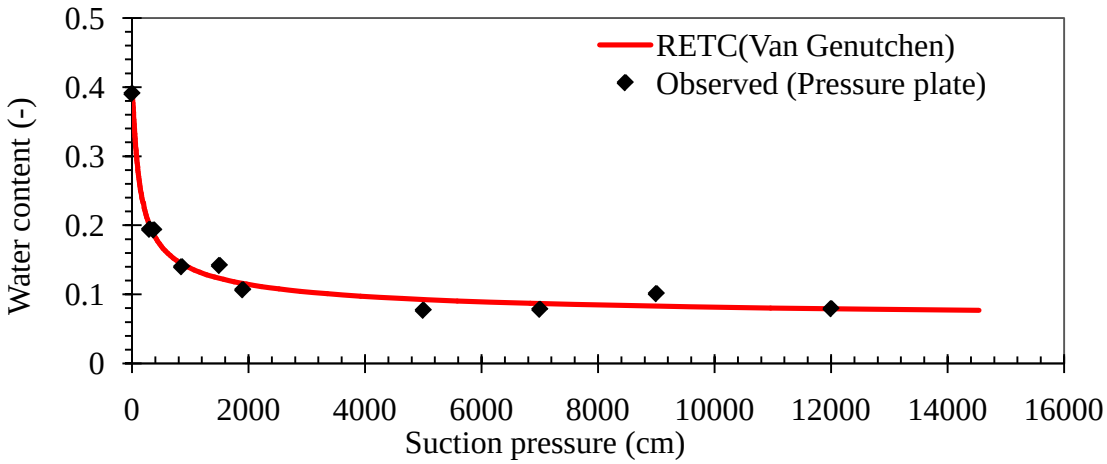

Fig. 3.15 (e) Soil moisture characteristic curve for sample 5 (100-140 cm) at spot 2

Table 3.7 Soil hydraulic parameters based on van Genuchten model for spot 1

Depth (cm)	θ_r	θ_s	α_v (1/cm)	n_v	R^2
0-30	0.046	0.357	0.011	1.630	0.9917
30-60	0.056	0.399	0.006	1.750	0.9916
60-80	0.041	0.381	0.009	1.700	0.9934
80-100	0.018	0.390	0.012	1.532	0.9956
100-140	0.053	0.391	0.014	1.522	0.9962
Average	0.043	0.384	0.011	1.627	0.9940
Standard deviation	0.015	0.016	0.003	0.101	0.0019

Table 3.8 Soil hydraulic parameters based on van Genuchten model for spot 2

Depth (cm)	θ_r	θ_s	α_v (1/cm)	n_v	R^2
0-30	0.049	0.357	0.016	1.493	0.9751
30-60	0.046	0.399	0.006	1.741	0.9827
60-80	0.042	0.381	0.013	1.545	0.9732
80-100	0.034	0.390	0.022	1.366	0.9750
100-140	0.046	0.391	0.018	1.473	0.9855
Average	0.043	0.384	0.015	1.523	0.9783
Standard deviation	0.006	0.016	0.006	0.138	0.00544

Table 3.9 Soil hydraulic parameters based on van Genuchten model for spot 3

Depth (cm)	θ_r	θ_s	α_v (1/cm)	n_v	R^2
0-30	0.022	0.420	0.090	1.540	0.9967
30-60	0.031	0.380	0.037	1.632	0.9919
60-80	0.021	0.410	0.034	1.630	0.9947
80-100	0.033	0.420	0.026	1.820	0.9958
100-140	0.020	0.410	0.050	1.560	0.9935
Average	0.025	0.408	0.047	1.636	0.9945
Standard deviation	0.006	0.016	0.025	0.111	0.0019

3.10 SATURATED HYDRAULIC CONDUCTIVITY

Saturated hydraulic conductivity (K_{sat}) is the key hydraulic parameter to determine flow of water through soils. Determination of hydraulic conductivity enables one to know how easily a liquid flows through a given soil. Various methods are available to determine K_{sat}, viz; the laboratory methods, field in-situ (borehole, tracer, pumping etc.) tests, analytical and theoretical models.

In the present study, field tests were conducted to determine the saturated hydraulic conductivity. In the field, Guelph Permeameter (soil moisture equipment corp., Santa Barbara, California, USA) test was conducted at different sites to determine the saturated hydraulic conductivity at auger hall depths of 30 and 60 cm. Fig. 3.16 demonstrates the Guelph Permeameter (GP) setup and its operation in the locations A21 and A14. The Guelph Permeameter is an in-hole constant-head Permeameter employing the Marriott Principle. The method involves measuring the steady-state rate of water recharge into unsaturated soil from a cylindrical well hole, in which a constant depth (head) of water is maintained.

When a constant well height of water is established in a cored hole in the soil, a “bulb” of saturated soil with specific dimensions is rather quickly established. This “bulb” is very stable and its shape depends on the type of soil, the radius of the well and head of water in the well. The shape of the “bulb” is included in the value of the factor C (Reynolds and Elrick 1986) which is used in the calculations. The factor C is a numerically derived factor which also takes care of variations in well radius and head of water in the well. In this study, a standard C value was used as there was no change of well diameter and head of water in the well from the standard setup. Once the unique “bulb” shape is established, the outflow of water from the well

reaches a steady-state flow rate, which can be measured. The rate of steady outflow of water, together with the diameter of the well, and height of water in the well can be used to accurately determine the field saturated hydraulic conductivity, K_{sat}.

Normally, there are two methods suggested to conduct field experiment with the Guelph Permeameter: one head (height of water level in the well) and two head methods each of which can be executed with combined (inner and outer reservoirs), inner reservoir only or a combination of the two. In this study, two head method (H_1=5 cm and H_2= 10 cm) with the suggested combined reservoir procedure was conducted for determining the saturated hydraulic conductivity at a given depth. Monitoring of the rate of fall of water in the reservoirs continues until the rate of fall does not significantly change in three consecutive time intervals while operating at H_1=5 cm and H_2= 10 cm. Whenever, the three consecutive readings are similar, it shows steady state rate of fall of water in the reservoir which is given as R_1 and R_2 respectively for H_1 and H_2. Table 3.10 provides typical GP readings taken at location A21 with combined reservoir procedure for auger hall depth equal to 30 cm. The GP data for other locations is also provided in Appendix B.

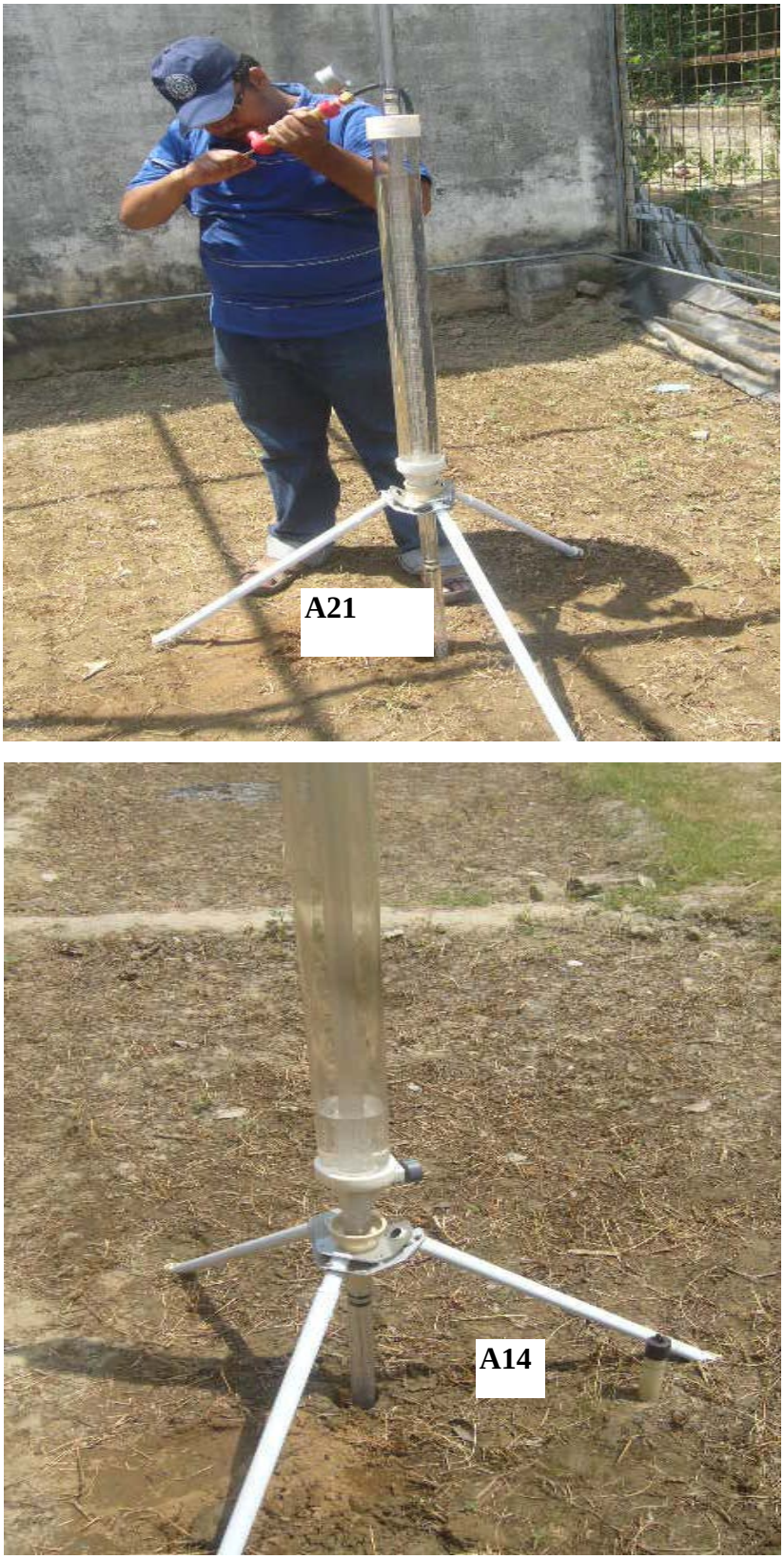

Fig. 3.16 Guelph Permeameter in operation in test spots A21 and A14

Table 3.10 Guelph Permeameter (GP) readings taken at location A21

Well head	Time (min)	Time interval (min)	Water level in the reservoir (cm)	Water level change (cm)	Rate of water level change, R (cm/min),
H_1= 5 cm	0	-	2.0	-	-
	2	2	5.4	3.4	1.7
	4	2	9.0	3.6	1.8
	6	2	13.4	4.4	2.2
	8	2	18.4	5.0	2.5
	10	2	23.6	5.2	2.6
	12	2	29.1	5.5	2.75
	14	2	34.6	5.5	2.75
	16	2	40.0	5.4	2.7
	18	2	45.5	5.5	2.75
	20	2	51.0	5.5	2.75
	22	2	56.5	5.5	2.75
	R_1=				2.75
H_2= 10 cm	0	-	6.50	-	-
	2	2	13.0	6.5	3.25
	4	2	19.0	6.0	3.0
	6	2	25.0	6.0	3.0
	8	2	30.7	5.7	2.85
	10	2	36.5	5.8	2.9
	12	2	42.3	5.8	2.9
	14	2	48.3	6.0	3.0
	16	2	54.3	6.0	3.0
	18	2	60.3	6.0	3.0
	20	2	66.3	6.0	3.0
	R_2=				3.0

For homogeneous soil condition, the following standard equation can be used to compute the saturated hydraulic conductivity from the measurements of the rate of fall of water level in the Guelph Permeameter.

$$K_{sat} = [0.0041 \times C \times R_1] - [0.0054 \times C \times R_2] \quad (3.6)$$

where K_{sat} is the saturated hydraulic conductivity (cm/sec), C is the reservoir constant or shape factor (=35.39), R_1 is the steady flow rate corresponding to H_1 (cm/sec) and R_2 is the steady flow rate corresponding to H_2 (cm/sec). The shape factor is a function of soil type, water height in borehole (H) and borehole radius (a). In standard conditions, the water level in the well is

equal to 5 cm (known as H_1) and equal to 10 cm (known as H_2). The radius of the borehole for standard conditions is equal to 3 cm.

However, perfect homogeneous conditions as required by the above equation may not be attainable in field actual situations. Field soils exhibit variations in texture and structure besides the existence of macrospores, cracks and other kind of openings which favour soil heterogeneity than homogeneity. Therefore, alternative equation for computing K_{sat}, as suggested by Zhang et al. (1998) has been employed.

For non-homogenous soils, use of the one height procedure is suggested to obtain a reasonable value of saturated hydraulic conductivity. In the case of the one height procedure, the hydraulic conductivity is computed using the single head procedure for each well head (H_1 and H_2) and average of the hydraulic conductivity values is then determined (Zhang et al. 1998). The steady flow rates (Q_1 and Q_2) for each head values are computed using the steady rate of fall (R_1 and R_2) and a constant which again depends on whether single or combined reservoir is used. For single head combined reservoir value of constant equal to 35.22 is suggested while for single head inner reservoir a value of 2.16 is recommended (Zhang et al. 1998). Since combined reservoir is used in this study, value of the constant equal to 35.22 is used to compute the steady flow rate.

$$Q_1 = R_1 \times 35.22 \tag{3.7a}$$

$$Q_2 = R_2 \times 35.22 \tag{3.7b}$$

$$C_1 = \left(\frac{H_1 / a}{2.074 + 0.093\left(H_1 / a\right)} \right)^{0.754} \tag{3.8a}$$

$$C_2 = \left(\frac{H_2 / a}{2.074 + 0.093\left(H_2 / a\right)} \right)^{0.754} \tag{3.8b}$$

where C_1 is the well shape factor corresponding to H_1 (cm) and C_2 is the well shape factor corresponding to H_2 (cm) and a is the well radius (cm). R_1 and R_2 are given in cm/min and Q_1 Q_2 are computed in cm/sec.

The saturated hydraulic conductivity, K_{sat} (cm/sec) for each well is computed using the following equation provided by Zhang et al. (1998) depending on the soil texture-structure category.

$$K_{sat1} = \frac{C_1 Q_1}{2\pi H_1^{\,2} + \pi a^2 C_1 + 2\pi\left(H_1 / \alpha^*\right)} \tag{3.9a}$$

$$K_{sat2} = \frac{C_2 Q_2}{2\pi H_2^{\,2} + \pi a^2 C_2 + 2\pi\left(H_2 / \alpha^*\right)} \tag{3.9b}$$

where α^* refers to microscopic capillary length factor which is decided according to the soil texture-structure category. For agricultural structured soils from clays through loams, unstructured medium and fine sands a value of α^* equal to 0.12 is suggested by Zhang et al. (1998).

Finally, the average hydraulic conductivity is determined from the mean of the individual saturated hydraulic conductivity values.

$$K_{sat} = \frac{K_{sat1} + K_{sat2}}{2} \tag{3.10}$$

For example, the saturated hydraulic conductivity using the method for well head 1 (H_1= 5cm) and well head 2 (H_2= 10cm) for the typical GP readings in Table 3.10 is to equal to 209.19 cm/day (=0.5*(253.584+164.791) cm/day. The values of saturated hydraulic conductivity, for each plot, computed using the method are given in Table 3.11.

Table 3.11 Values of saturated hydraulic conductivity using Guelph Permeameter

Location	Well Depth (cm)	K_{sat} (cm/day)	Average K_{sat}(cm/day)
A11	30	189.220	223.35
	60	257.470	
A12	30	139.104	123.56
	60	108.000	
A13	30	238.464	171.07
	60	103.680	
A14	30	163.300	158.98
	60	154.660	
A21	30	209.190	163.35
	60	117.504	
A22	30	243.710	196.77
	60	149.820	

As can be observed from Table 3.11, comparatively close values of K_{sat} were computed for most of the locations tested except few spots. The K_{sat} values in shallow depth of the first 30 cm depth of soil profile are larger than the respective values in the deeper soil layers down near 60 cm in most of the sampling points. This would be due to the fact that the top layer of such an agricultural field is more porous than the sub layers since it is subject to

various influences such as tillage operations, activity of flora and fauna, remains of crop roots, etc.

3.11 CROP PARAMETERS

Crop parameters play an important role in computations of root zone water balance. Among the various parameters of a given crop; parameters such as crop root depth, crop height and leaf area index (*LAI*) are used quite often in problems regarding root zone soil moisture dynamics, solute transport, evapotranspiration, irrigation scheduling and agricultural water management. These parameters were observed in the experimental field for the growth periods of two crops, rice and berseem fodder, which are commonly growing in the study area. The crop parameters were observed following the procedures and methods suggested in the literature.

The entire crop periods of the crops were divided into four respective growth stages: initial, development, mid and late season stages of crop growth periods according to FAO classifications. The crop growth stages have been determined following FAO recommendation for different growth stages considering ground cover and crop conditions in the field (Allen et al. 1998). The initial stage refers to the date from transplanting or sowing to nearly 10% ground cover by the canopies of crop seedlings. Crop development stage starts from the end of initial stage to full ground cover of 70-80%. The mid season stage starts from the full ground cover to the senescence stages when the crop starts maturity. The late season growth period starts from the end of mid season to the date of final crop harvest. Figs. 3.17 to 3.22 show the development stages of rice and berseem fodder crops on typical dates. In the particular case of berseem crop, however, no full growth was achieved since the crop was harvested green either in the development stage or mid season stages since it is a fodder crop meant for frequent cuttings. A total of four harvests were made during each season of the berseem crop. Therefore, individual cutting intervals are provided rather than crop growth stages for berseem crop. Table 3.12 provides the details of crop duration and growth stages/cutting intervals. Cut No 1 refers to the interval between date of sowing to the day of first cut.

Fig. 3.17 Rice in the initial stage (crop season 1)

Fig. 3.18 Rice in the development stage (crop season 2)

Fig 3.19 Rice in the mid season stage (crop season 1)

Table 3.12 Details of crop duration and growth stages/cutting intervals

Rice (*Oryza Sativa L.)*								
Crop season	Variety	Date of transplanting	Date of harvesting	Total duration (days)	Growth stages (days)			
					Initial	Development	Mid season	Late stage
1	Basmati	23 July,2013	02 November, 2013	103	15	30	30	28
2	Basmati	15 July, 2014	22 October, 2014	100	22	25	31	22
Berseem fodder (*Trifolium alexandrinum L.*)								
Crop season	Variety	Date of sowing	Date of final harvesting	Total duration (days)	Individual cutting intervals (days)			
					Cut No 1	Cut No 2	Cut No 3	Cut No 4
1	JB-1	12 December,2013	08 May, 2014	148	72	26	21	29
2	JB-1	17 November, 2014	16 April, 2015	151	81	32	18	20

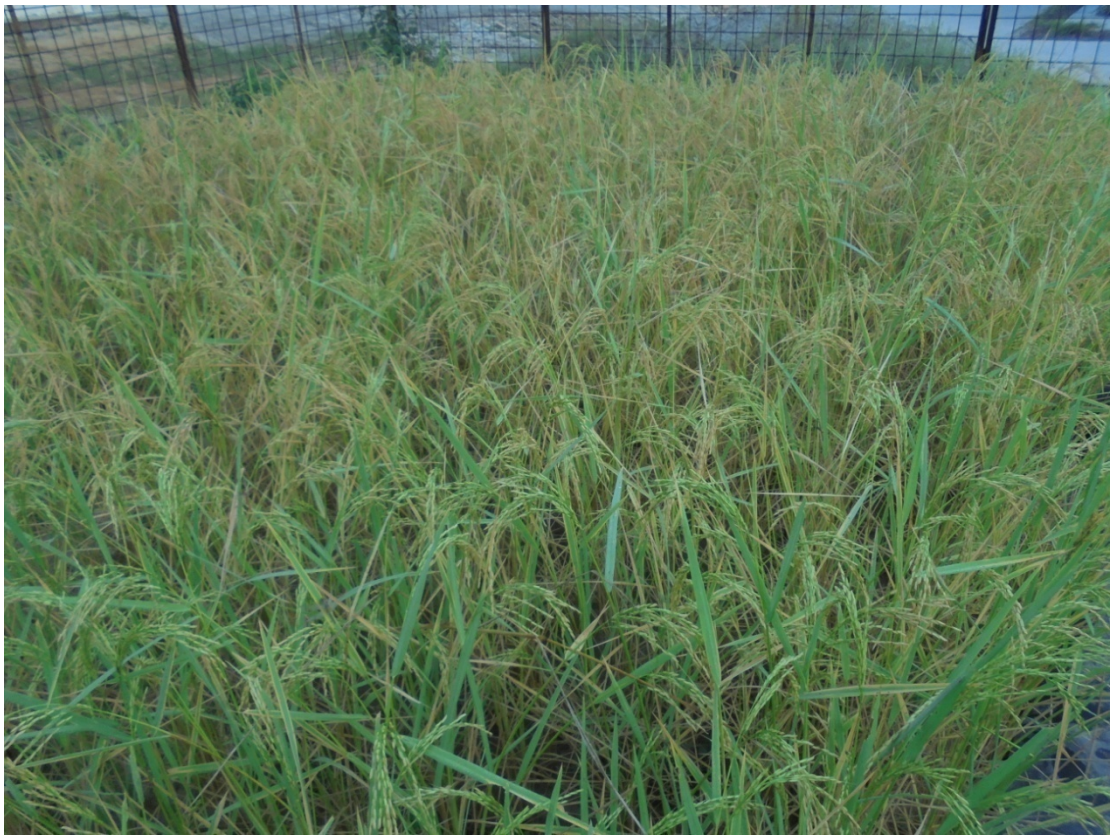

Fig. 3.20 Rice in the late season stage (crop season 2)

Fig. 3.21 Berseem fodder in the initial growth stage (crop season 2)

Fig. 3.22 Berseem fodder in the mid season growth stage (crop season 1)

3.11.1 Crop Height

Average height of crops grown in the experimental field station was recorded on the observation days along with the root depth and leaf area index. Crop height was measured at few randomly selected locations in the field and the average height on the particular day was recorded. Crop growth is rapid during the development and reaches to its maximum height in the mid season stage. The crop height slightly reduces from maximum in the late stage due to the physiological wearing of the crop. During berseem season, the crop height varies due to frequent harvest during its growth season. The crop height is one of the indicators of crop growth used as an input in calculations like adjustment of crop coefficient, K_c (Allen et al. 1998) since it could affect the surface roughness coefficient of the potential evaporative surface.

In rice season 1, the maximum crop height was reached 1.5 m on the 72nd day after transplanting while the maximum crop height on rice season 2 was 1.21 m which was again observed on the 72nd day after transplanting. During the berseem season 1 the maximum crop height was varied from 0.23 to 0.65 m due to periodic cuttings. Similarly, in berseem season 2, the maximum crop height was varied from 0.24 m to 0.57 m. Fig. 3.23 shows the crop height of rice and berseem fodder crops in their respective growing seasons.

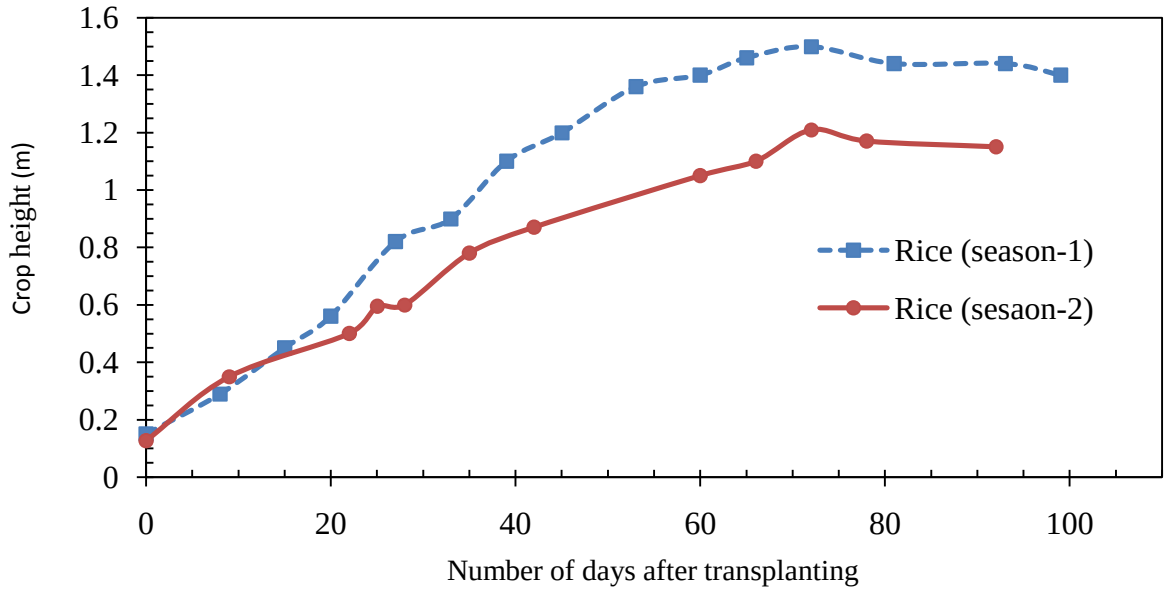

Fig. 3.23(a) Crop height during rice growing seasons 1 and 2

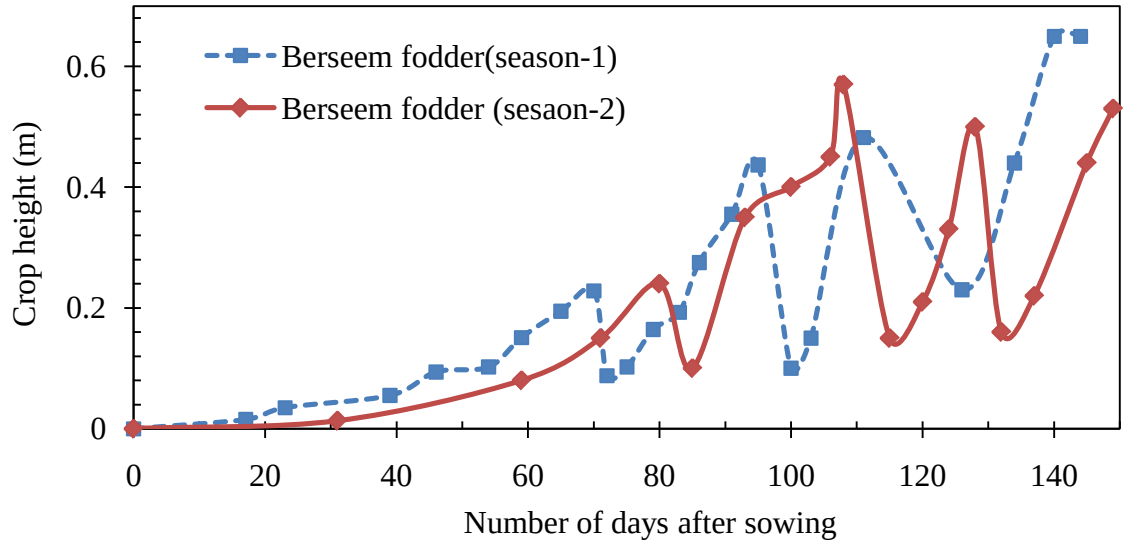

Fig. 3.23(b) Crop height during berseem growing seasons 1 and 2

3.11.2 Root Depth

Rooting depth is one of the important parameters of water balance study and soil moisture dynamics which is also used in the present study. Rooting depth is an essential parameter due to the fact that crops extract water through root openings. Thus, crop roots can affect the whole hydrologic system in a cropped environment. The depth of the root system varies from crop to crop and also throughout the growth stages of a particular plant. Dense and deep roots can extract water from deeper layers while shallow roots extract water from surface layers. Since phenomena like evaporation are taking place on the surface layers and thus shallow rooting would have its own implication on the evaporation and similarly deep rooted

crops on percolation and in this way crop roots can affect the water dynamics. The crop root system can be affected by the available soil water besides the plant physiological factors. Wet soil water regime conditions favour shallow root growth while drier soil conditions call for deep rooting systems for a particular crop. Soil texture, structure and agronomic practices could also affect root growth to a greater extent.

Several methods such as excavation, trench profile wall, auger, monolith core and soil moisture profile are available to measure the root depth. In this study, a method similar to trench profile method was adopted. A trench of nearly 50 cm x 100 cm square area was excavated near the crop roots, exposing the roots carefully with hand tools. The root length was then measured after exposing the longest roots which penetrate deeper than the others. After observation, the trench was backfilled so that the crops shall not fail by wilting due to root exposure. Similar procedure was followed for the next and consecutive observations by trenching at randomly selected locations. The procedure for root observation was explained well in Kücke et al. (1995). Such observations were made nearly on weekly basis until consecutive maximum root lengths were obtained. However, since the observations were made only for sampled spots, it may not represent for the total field condition. Therefore, the soil moisture depletion method was also employed besides the trench profile method.

The soil moisture depletion method is an indirect method in which one observes the soil moisture extraction/depletion by roots (Böhm, 1979). It is based on the fact that water from root zones in a cropped area is extracted by roots and causes soil moisture depletion. It is assumed that between two soil moisture measurements, there is no transfer of moisture from one profile to the other. However, this could not be true particularly on rainy days and after rainfall in which case there could be large transfer of moisture from top layers to bottom layers. Although there are drawbacks with the depletion method, it is possible to observe general trend of soil moisture depletion if soil moisture data is available at different points. In this study, since soil moisture data was measured at different depth intervals, it was possible to find out soil moisture depletion during the crop growth periods and supplement rooting depth data obtained from trench profile method. Soil moisture depletion method can particularly be used in the mid season stage of the growth period since soil moisture extraction by crop roots during this period is remarkable.

The rice roots are fibrous in nature while that of the berseem fodder are leguminous. Fig. 3.24 shows the rooting depth of rice (season 1) and berseem crops (season 1) observed on the 65^{th} days after transplanting and 90^{th} days after sowing, respectively. Fig. 3.25 also depicts the root development pattern of the two crops in the experimental period. The maximum root

depth in rice season 1 was 0.27 m while in rice season 2 the maximum root depth was reached 0.31 m both observed on the 72nd day after transplanting. In berseem season 1, the maximum root depth has reached 0.45 m on the 95th days after sowing while in berseem season 2 the rooting depth has reached 0.47 m after 100th day after sowing.

Fig. 3.24 Root depths of rice (season 1) on the 39th days after transplanting and rooting depth of berseem fodder (season 1) on the 70th days after sowing

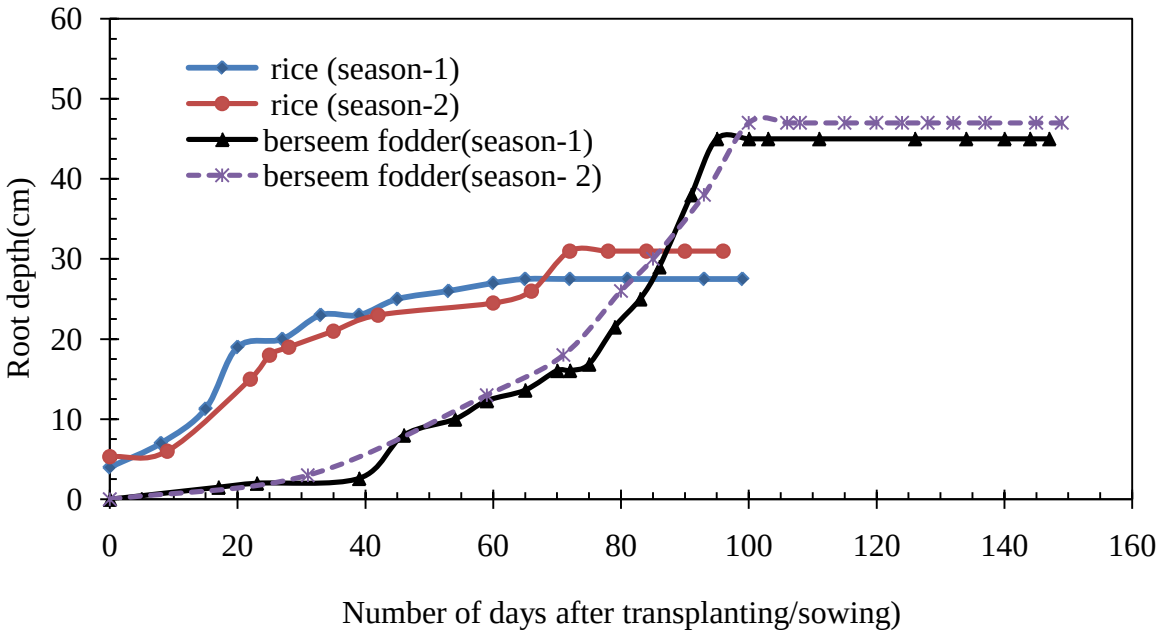

Fig. 3.25 Variation of root growth of rice and berseem during the experimental periods

3.11.3 Leaf Area Index (*LAI*)

Leaf area index (*LAI*) is a factor of primary importance for crop monitoring and in most of the models developed for the simulation of carbon and root zone water dynamics. It is applied in studies regarding ecological monitoring, climate and agriculture (Stroppiana et al. 2006). Particularly in agricultural water management, the role of *LAI* is significant in that it is used to model canopy photosynthesis and evapotranspiration. In many instances, *LAI* is used to partition the crop evapotranspiration into transpiration (productive use of agricultural water) and evaporation. Two major methods are in practice to determine the *LAI*; direct and indirect (Jonckheere et al. 2004; Weiss et al. 2004).

The direct methods involve destructive sampling, measuring the individual leaf area, crop density in a sampled area and optimising sample size. The direct method is tiresome and labour intensive. The indirect methods on the other hand employ other variables which are relatively easy to measure in the field and applied for larger field sizes. Two methods were used in this study: the first was the planimeter direct measurement technique and the second was the use of AccuPAR Ceptometer model LP-80 (Decagon Devices Inc., Pullman, WA, USA). During the first growing season of rice and until the third cutting seasons, the planimeter method was used since the Ceptometer was not available in these times. After the Ceptometer was arrived in the second week of April, 2004, the planimeter technique was abandoned and the Ceptometer was used to acquire *LAI* data.

During the direct (planimeter) method, a representative 2 m x 2 m square area in the cropped field was selected. The density of the crops was determined by direct counting of the active crops in the area. Representative crop leaves were collected by destructive sampling from the quadrat in three classifications as short, medium and long leaves in each time of sampling. The leaves were immediately transported to laboratory and fixed on a flat surface on top of a millimetre paper so that their outlines were traced on. The area traced by the outline of each class of the leaves was then determined using digital planimeter in the laboratory. The total area of the classified leaves was averaged for a sampled crop which was further multiplied by the density of the crops to obtain the leaf area index. Fig. 3.26 shows the operation of planimeter in the laboratory.

AccuPAR Ceptometer, LP-80 consists of an integrated controller and 90 cm long probe. The probe contains 80 photosensors that measure photosynthetically active radiation (PAR) in the 400 to 700 nm waveband and send the data to the controller. The PAR measurements can be used to measure light interception by the plant canopy, or to calculate the leaf area index (*LAI*) of the canopy. The PAR interception and LAI data is automatically calculated and displayed with each measurement. Figs. 3.27 and 3.28 show the field measurements of *LAI* using the Ceptometer. The LP-80 integrates many influencing variables to calculate *LAI* which include PAR, the ratio of below canopy PAR measurements to the most recent above canopy PAR value, zenith angel, fractional beam radiation and leaf distribution parameters. PAR refers to the radiation in the 400 to 700 nanometre waveband. It represents the portion of the spectrum which plants use for photosynthesis. Zenith angle is the angle the sun makes with respect to the zenith which is a function of specific location and time. Since, the zenith angle can be defined for a given place in open daytime hours, *LAI* measurements can be done easily with the Ceptometer. Fractional beam radiation is the ratio of direct beam radiation coming from the sun to radiation coming from all ambient sources like the atmosphere or reflected from other surfaces. Leaf distribution parameter on the other hand refers to the distribution of leaf angles within a canopy which takes care of the variation of leaf configuration/orientation of a particular crop.

Before commencing measurement with the LP-80 Ceptometer, required calibration for the location, altitude, and time zone were made. The external sensor mounted on top of the LP enables simultaneous above and below canopy measurements. Regular measurements of *LAI* from above canopy and below canopy measurements were conducted in the crop periods. The field observed data were then retrieved from the data logger with the R-232 cable and average values of the *LAI* were calculated from several sampled measurements.

Large variations of leaf area index were observed in the two rice growing seasons. The maximum *LAI* in rice season 1 was 7.2 observed on 65th days after transplanting while it was 3.2 in rice season 2 observed on 66th days after transplanting. This might be attributed to water application condition in rice season 1 and 2 which are significantly different. On the other hand, the leaf area index of berseem is fairly similar except few differences. The maximum *LAI* in berseem 1 season was 5.0 just before the 2nd cut while the maximum *LAI* in berseem season 2 was 4.5 just before the first cut. Figs. 3.29 and 3.30 show the variation of observed leaf area index values of the crops in each season.

Fig. 3.26 Digital planimeter for measurement of leaf profile during rice season 1

Fig. 3.27 *LAI* measurement with LP-80 Ceptometer during rice season 2

Fig. 3.28 *LAI* measurement with LP-80 Ceptometer during berseem season 2

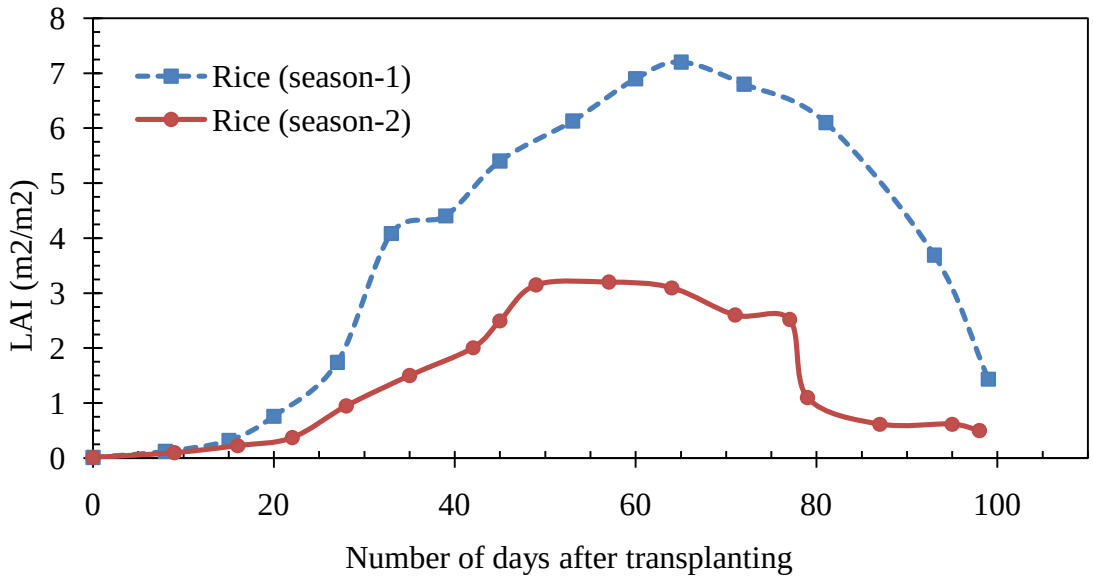

Fig. 3.29 Leaf area index for rice crop for the two growing seasons

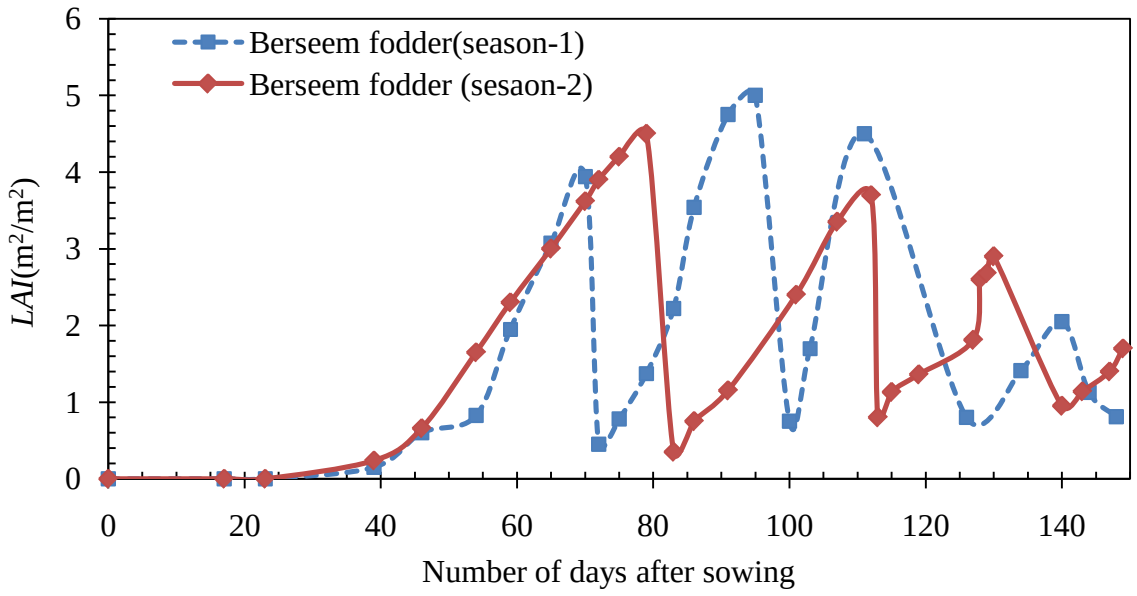

Fig. 3.30 Leaf area index for berseem crop in two growing seasons

3.12 CROP YIELD

The primary purpose of irrigation is to enhance crop production by reducing or eliminating water stress in crops which otherwise could seriously damage crop growth and hence crop yield. Therefore, it is advantageous to investigate water productivity while dealing with water balance of crop root zone or processes attached to it.

Crop yield refers to the weight of a crop that is harvested per unit of land area. Crop yield is the measurement often used for a cereal, grain or legume and is normally measured in kilograms per hectare (metric tons per hectare). In each of the rice crop season, grain yield have been adjusted to have 14% grain moisture content (Chahal et al. 2007). Water productivity can be expressed as the ratio of actual grain yield/green forage harvested to the amount of water consumed by actual evapotranspiration or the ratio of actual grain yield to the water supplied at field level (either irrigation or rainfall). These are the indices which are used to evaluate the performance of a given water application and water use efficiency. Hence, grain yield for rice was determined for each growing season and plots in the experiment. Berseem was harvested green as a fodder when the crop reached full canopy cover. Figs. 3.31 and 3.32 show crop yields and field measurements of harvested yield.

Grain yields ranging from nearly 2.7- 4.9 tones/ha across the plots in rice seasons was observed. In general, there was yield reduction due to reduction in input water in rice season 2. Green forage harvest for berseem fodder crop ranged from approximately 27-56 tones/ha. Similarly, there was yield reduction in the berseem season 2 which might be attributed to input water reduction and date of sowing.

Fig. 3.31 Grain yield for rice season 2

Fig. 3.32 Green fodder harvest in berseem season 2

3.13 CLOSURE

In this chapter, the methodology of field and laboratory observations of important variables and parameters conducted during the growth periods of two crops, rice and berseem

fodder crop is presented. The overall observation includes two seasons for each crop during which time important variables such as water input, drainage outflow and climatic variables were observed. Data on soil and crop parameters important in water balance and physically based models were also collected thoroughly. The values of these observations are going to be an input to the water balance and physically based models and key instruments in evaluating the performance of the deep percolation models in surface irrigated environments, particularly with rice and berseem fodder.

CHAPTER 4
WATER BALANCE MODEL

4.1 PREAMBLE

Soil water balance model is a commonly applied modelling approach to estimate the different components of the soil water balance in an irrigated field. The different components of the soil water balance constitute precipitation, irrigation, seepage/lateral inflow and outflow, capillary rise from shallow aquifer systems, surface runoff, deep percolation, evapotranspiration and change in soil moisture storage. The soil water balance concept is derived from the law of conservation of mass and deals with quantification and analysis of each inflow and outflow variables while accounting for storage in the system. In this case of the model, the spatial model domain is usually lumped while the time domain can be lumped or distributed. The model is commonly applied in studies concerned with agricultural water management, water flow in the soil root zone, solute transport, groundwater flow and recharge, etc. (Kim, et al. 2009; Chien and Fang 2012; Wang et al. 2012).

Several models are developed and used to date to analyse the root zone soil water balance and its dynamics which also constitute the deep percolation component of the water balance. Physically based models based on the classical Richards equation, such as for example, the Soil Water and CROP production model, SWACROP (Kabat et al. 1992), the Water and Agrochemicals in soil and Vadose Environment, WAVE (Vanclooster et al. 1994), Soil-Water-Atmosphere-Plant, SWAP (Ahmad et al. 2002) and HYDRUS-1D (Šimůnek et al. 1998) provide accurate computations of deep percolation (Liu et al. 2006) when compared with soil water balance models. However, physically based approaches require more complete description of soil hydraulic properties which limits their use under most field conditions since it is often difficult to obtain such a comprehensive list of soil hydraulic parameters. Simple water balance model on the other hand is easy, need fewer number of data inputs and can be applied for wider soil and crop environments. In this particular chapter, the water balance model has been employed to quantify the magnitude of deep percolation and investigate its characteristics under water intensive crop fields; in different field scenarios of water application (Willis et al. 1997; Chien and Fang 2012; Wang et al. 2012). The performance of the water balance model will be compared with physically based model which is being dealt in chapter 5.

4.2 MODEL DESCRIPTION

The FAO (Food and Agricultural Organization) based soil water balance model (Allen et al. 1998) which is also applicable for lysimeter water balance is modified and used in this study which is given as:

$$D_i = D_{i-1} - P_i - I_i + ET_{ci} + DP_i + R_i \quad (4.1)$$

where D (mm) = root zone moisture depletion; P (mm) = precipitation; I (mm) = applied irrigation; ET_c (mm) = actual evapotranspiration; DP (mm) = deep percolation of water moving below the root zone; R (mm) = surface runoff, i and i-1 are, respectively, the current and previous time steps. Since the water table was well below the root zone, contribution from groundwater as capillary rise into the root zone has been neglected. Interception loss by crop canopy during rainfall events has also been neglected since the magnitude of interception compared to transpiration and evaporation is quite less (Shankar 2007). Further, measurement and estimation of interception are difficult and bear large uncertainties since intercepted water could vanish within 10 minutes after rainfall (Blyth and Harding 2011).

4.3 SOIL MOISTURE CHANGE

The soil moisture deficit in the root zone is obtained from monitored soil moisture contents at respective depths (intervals of 10 cm). It is usually referenced with the field capacity of a given soil and may be given by:-

$$D_i = 10Z_j \times \left(\theta_{fc} - \theta_i\right) \quad (4.2)$$

where θ_i is the soil volumetric moisture content (%) in the root zone depth, Z_j (m), at the end of day i; θ_{fc} is the soil moisture content at field capacity (%). The deep percolation was computed taking into account the root growth of the crops. The weekly observed rooting depth values have been interpolated for each day of the crop growth periods and used as an input in the computation of the soil water balance model. The temporal variation of rooting depth for each crop season was provided in section 3.11.2.

$$D_i - D_{i-1} = 10\overline{Z_j} \times (\theta_{fc} - \theta_i) - 10\overline{Z_j} \times (\theta_{fc} - \theta_{i-1}) \quad (4.3a)$$

$$D_i - D_{i-1} = 10\overline{Z_j} \times (\theta_{i-1} - \theta_i) \quad (4.3b)$$

where $\overline{Z_j}$ is the average root depth (m) in the time interval between i and i-1 and other terms are as defined earlier. The model has been modified in such a way that the root zone is considered on discrete root depth intervals (layers) for a given time step to compute soil moisture change based on root growth. If the rooting depth is shallow, $\overline{Z_j}$ < 10 cm, as in the

early growth stages of the crops, the soil moisture content on the top layer is considered; when the root depth has grown deeper, water contents measured at deeper depths has been taken into account in computation of soil moisture change besides the soil water content in the surface layer.

Since the root zone is dynamic and changes until the maximum rooting depth is achieved, equation (4.3b) can be generalized as:

$$D_i - D_{i-1} = \sum_{j=1}^{nl} 10\overline{Z_j} \times (\theta_{i-1} - \theta_i) \tag{4.4}$$

More specifically, if the average root zone is taken in intervals of 10 cms then:

$$D_i - D_{i-1} = \sum_{j=1}^{nl} (\theta_{i-1} - \theta_i)_j \tag{4.5}$$

In equation (5) *j* is an index for root zone layer and *nl* is the number of layers. Therefore, the deep percolation from equation (4.1) as unknown can be computed using the following equation.

$$DP_i = \sum_{j=1}^{nl} (\theta_{i-1} - \theta_i)_j + P_i + I_i - ET_{ci} - R_i \tag{4.6}$$

Significant soil moisture change ($\Delta\theta$) is assumed to take place in the dynamic root zone. In non-rooting zone, soil moisture change may be assumed negligible for daily time interval. With such an assumption, one may compare deep percolation measured at lysimeter outlet (situated well below the bottom of a crop root zone) and deep percolation computed using the water balance equation. To start the computation on the first day, measured soil moisture content values prior to date of sowing or transplanting were used.

Figs. 4.1 to 4.4 present the variation of soil moisture change in the crop root zones in the respective growing seasons.

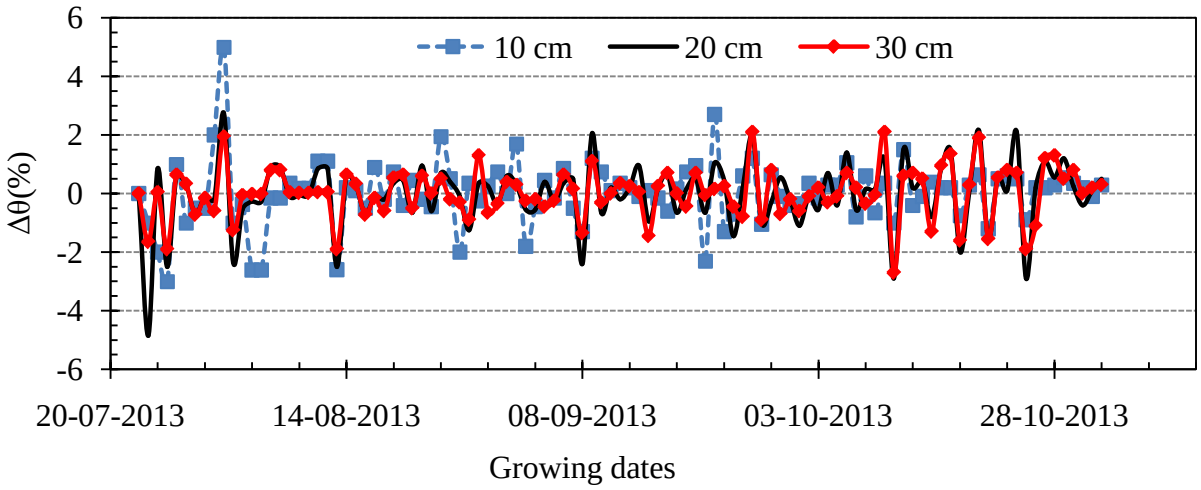

Fig. 4.1 Root zone soil moisture change at different depths in rice season 1

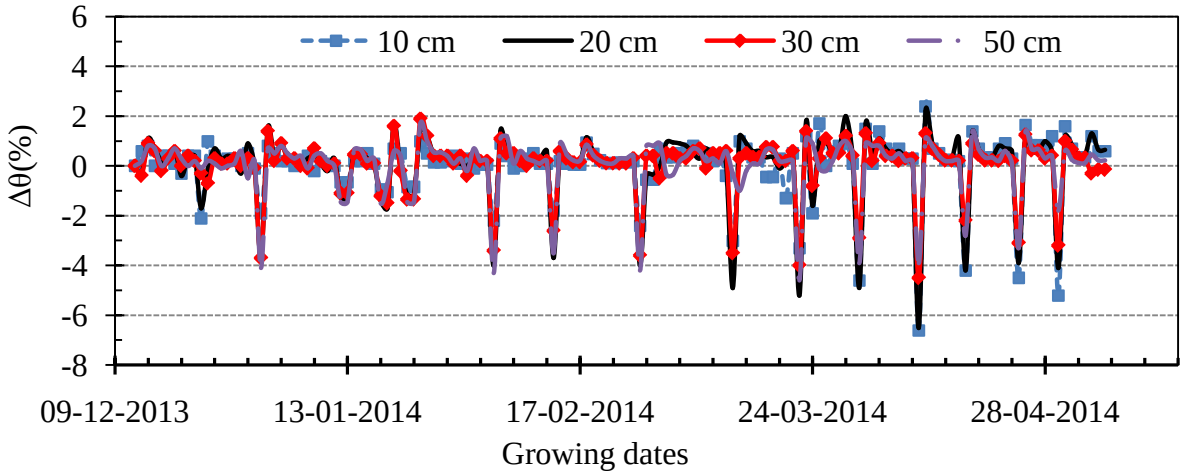

Fig. 4.2 Root zone soil moisture change at different depths in berseem season 1

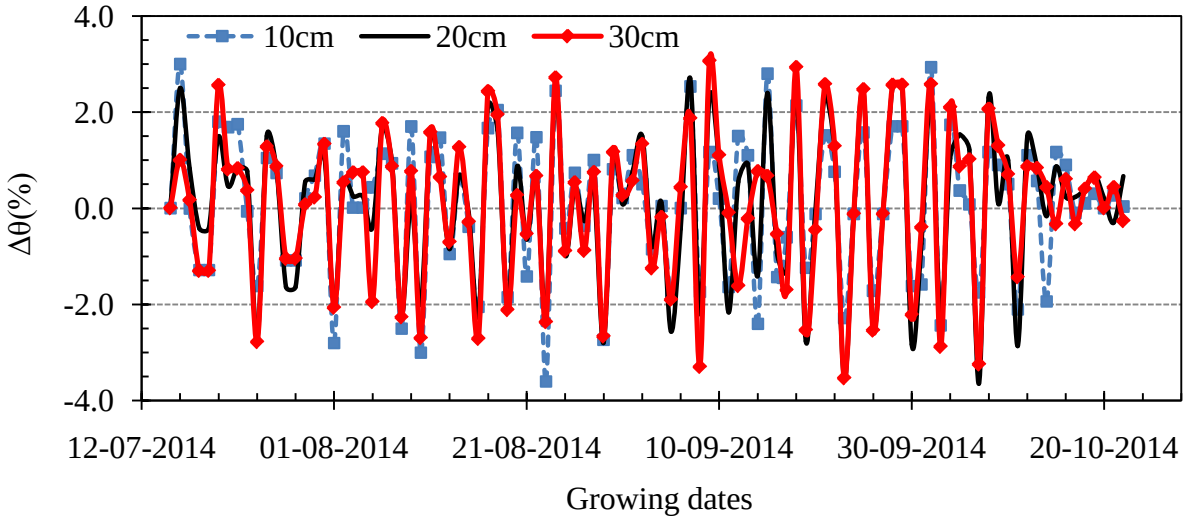

Fig. 4.3 Root zone soil moisture change at different depths in rice season 2

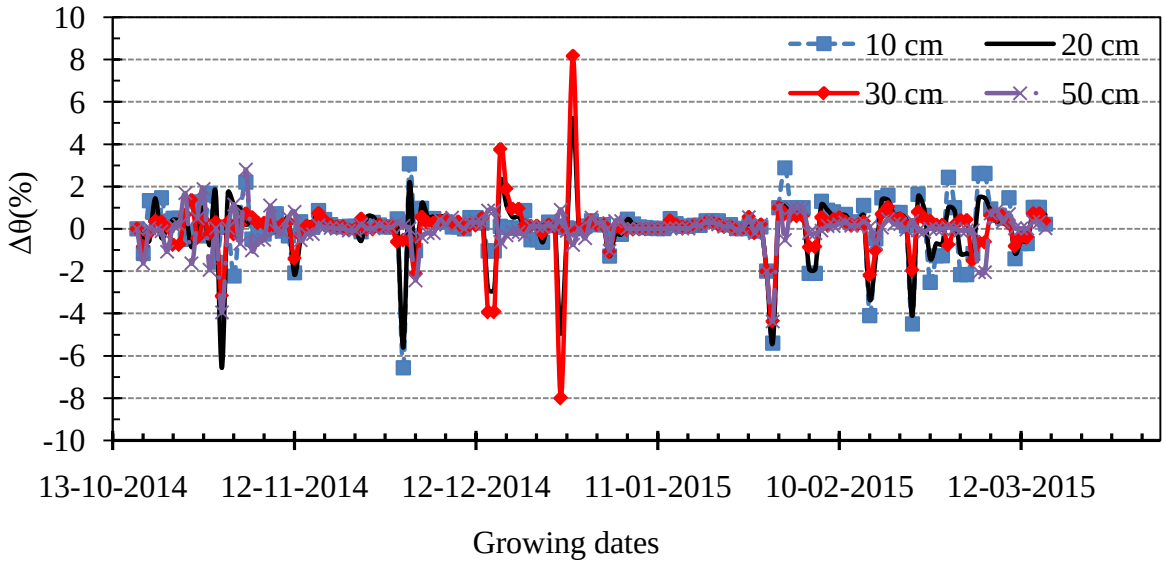

Fig. 4.4 Root zone soil moisture change at different depths in berseem season 2

From Figs. 4.1 to 4.4, it can be seen that the soil moisture content values at different depths are responding to water input, root water extraction and evaporation. In general, maximum variation of soil moisture content occurs in the top layers of the root zone than the bottom layers in response to a coupled effect of soil evaporation and crop transpiration. In the rice season, significant variation of soil moisture change was observed in the first and second layers (10 and 20 cm depths), and more importantly in the top 10 cm layer from initial to mid season growth stages. In the late stages of the crop growth, however, moisture extraction was observed mainly from lower layers (30 cm) of the root zone as shown in Fig. 4.1. For berseem, it took almost two weeks to germinate due to the cold winter and the field beds were bare for the first three weeks. However, soil moisture variation took place since the day of sowing at different depths. This indicates that soil evaporation influences soil moisture variation in the top layer while drainage dominates the lower layer soil moisture variation during this time. Comparatively, larger variation of soil moisture was observed during berseem crop season due to intermittent wetting events as can be inferred from Figs. 4.2 and 4.4. On the other hand, most frequent variation of soil moisture took place in rice season owing to frequency of the wetting events and large evapotranspiration in the season. Horizontal variability of soil moisture across field plots can also be inferred due to unavoidable heterogeneity of field conditions. Specifically, downstream field plots, A12 and A14 near the field boundary and access road exhibit more water holding capacities at the top layer than the other layers.

With reference to equation (4.6), the negative values of change in moisture content in the given root zone depth express the root water uptake and evaporation while the positive change expresses the contribution of soil moisture storage to deep percolation in the given time

interval. The seasonal soil moisture storage is the sum of soil moisture changes during the season. In the other crop seasons, there was soil moisture loss in the field due to the large balance of outflow components than the inflow. The soil moisture change in rice season was generally less. More soil moisture loss was observed in rice season 2 which is mainly attributed to more evapotranspiration and relatively less input water in the particular season. In berseem seasons, more soil moisture loss was observed in the first season than in the second due to higher seasonal evapotranspiration in the first season.

The relation between the net water input (*I+P-ET*) versus soil moisture content in the crop zone has also been seen investigated. There is a clear trend of net water input and SWC in that the SWC responds to the net input water. In general, significant variation of SWC was observed during the berseem season than rice due to the regularity of water application during the rice season. Figs. 4.5-4.8 show the daily variation of net water input and average soil moisture content in the root zone.

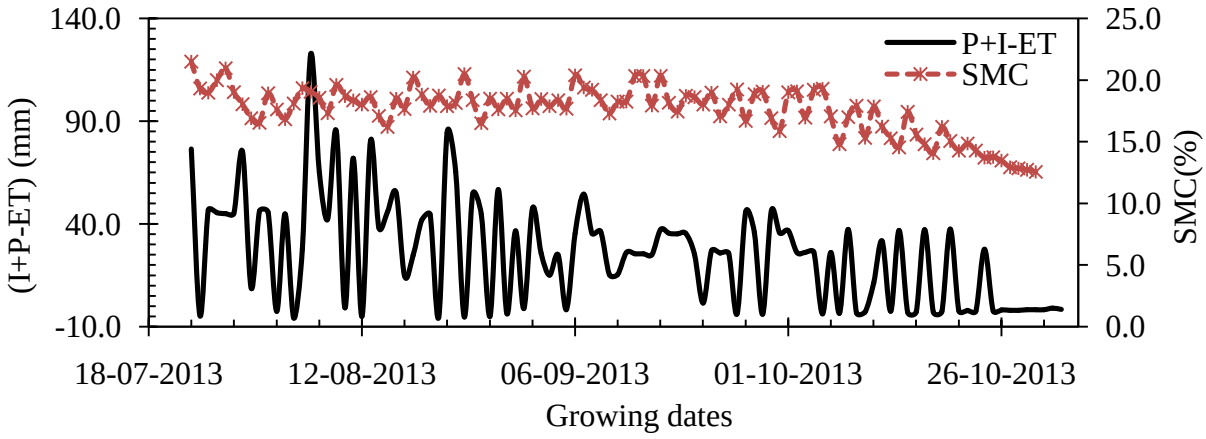

Fig. 4.5 Average soil moisture content and net water input for rice season 1

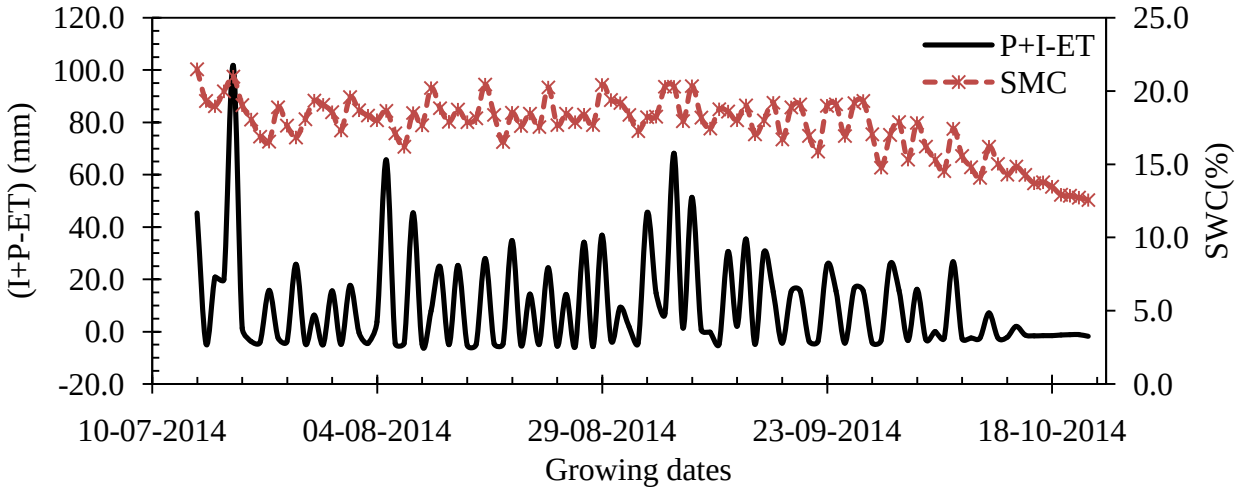

Fig. 4.6 Average soil moisture content and net water input for rice season 2

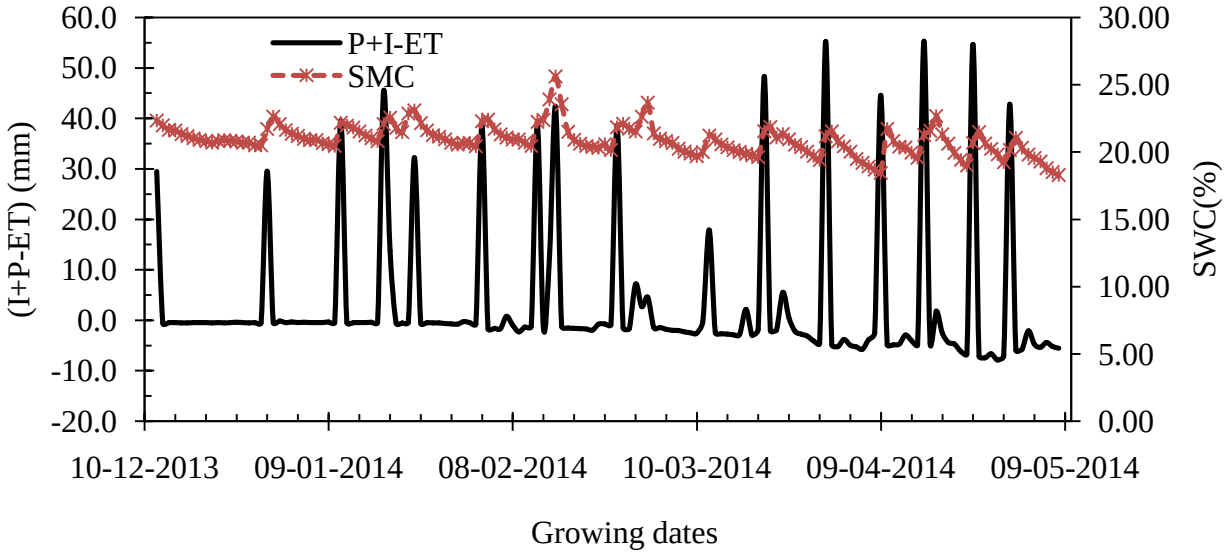

Fig. 4.7 Average soil moisture content and net water input for berseem season 1

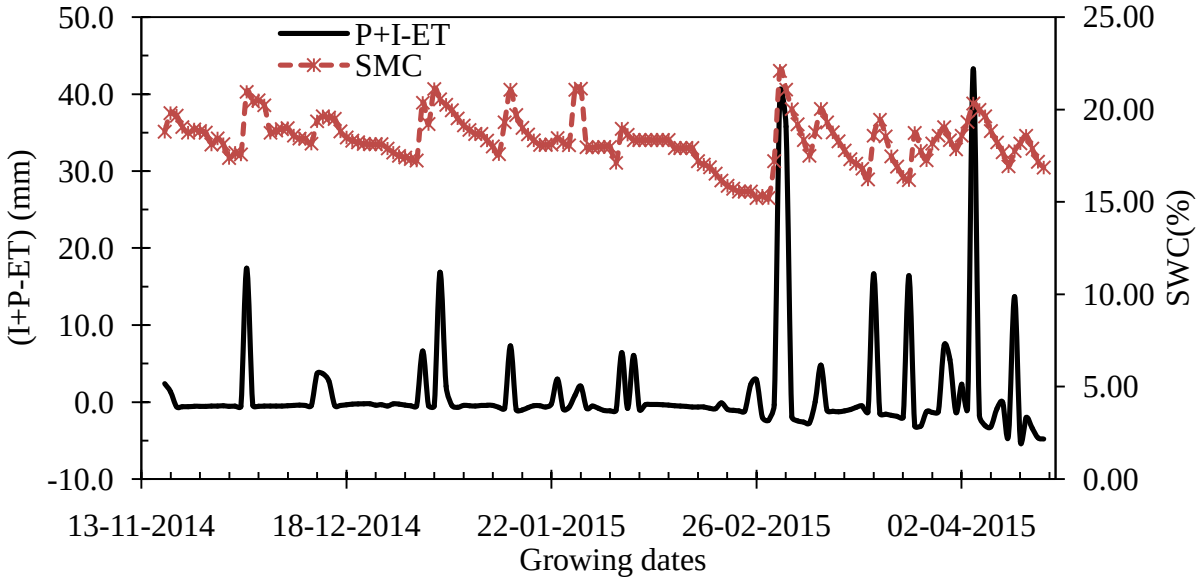

Fig. 4.8 Average soil moisture content and net water input for berseem season 2

Uncertainties and limitations inherent to the soil moisture sensor (profile probe sensor in this study), access tube installation and field measurement in soil moisture data and possible errors thereof are disregarded since change in moisture content than individual moisture content values were used in the calculations.

4.4 WATER INPUT (IRRIGATION AND RAINFALL)

Daily monitored values of irrigation and rainfall depths were provided as an input for the water balance. The total seasonal rainfall that fell during both crop seasons is presented in section 4.10 along with other water balance components. The total numbers of growing days

were almost similar for each season of both crops. Fortunately, the rainfall amount was reduced in the second season of both crops during which time irrigation applications were also reduced for the purpose of this study. However, rainfall was not spread over the entire growing season but concentrated in a small interval of a season in which more water goes away by runoff and/or deep percolation losses. For example, almost half (509 mm) of the annual average rainfall in the year 2013 fell in just 15 days in the month of August in the rice season; five of these 15 day events recorded 365.4 mm. Obviously, the rainfall which occurs during the time when the soil is near field capacity or above could not be utilized by the crops. In the experimental plot where either run-on or run-off was controlled, the excess rainfall goes for augmenting deep percolation. Accordingly, more percentage of rainfall was left unused during the rice seasons than the berseem seasons. This shows that by appropriately reducing irrigation frequency and depth, it is possible to utilize more amount rainfall for crop production.

In the rice growing seasons, intense and continuous downpours for two to three days were not considerably contributed for crop water utilizations. Such rains have more of basin water resources importance than field scale water use as they quickly contribute to runoff or deep percolation and thus for surface water storage or groundwater aquifers. During berseem (winter) seasons, rainfall was intermittent and two to three major storms occurred in both years of growing. As these heavy storms occur after long intervals of time, most of these were returned as percolation losses due to formation of cracks and macropores in the root zone in the season (Garg et al. 2009; Tournebize et al. 2006).

The total amount of applied irrigation during the crop seasons is also shown in section 4.10 along with other water balance components. Figs. 4.9 and 4.10 present irrigation schedules conducted in the two crop seasons. In each of the crop seasons, the first season was used as a reference and resembles typical irrigation applications in the region at farmers' field while the second season presents scenario of reduced water application.

Average depth of applied irrigation per irrigation event for rice season 1 was 40 mm. In this season, irrigation was applied every day, except the rainy days, in the development and mid season growth stages while in the late season stage 2-3 days irrigation interval was imposed. During the initial growth stage, more frequent rainfalls also supplied the water demand of the crop besides irrigation. The schedule in this crop season yielded large volume of irrigation input. Such amount of seasonal irrigation input for rice fields were also reported in literature (Sudhir-Yadav et al. 2011; Boumann et al.2007b), although mainly concerned with puddled field conditions. During rice season 2 average irrigation depths ranging from 20 and 27 mm per irrigation event were imposed. The number of irrigations were halved besides reducing the

depth of irrigation events in the second season of both crop periods. Overall, 59 irrigations during rice season 1 and 31 irrigation events in rice season 2 have been applied. An average irrigation interval of nearly 2 days was practiced in rice season 2 period. Kukal et al. (2005) reported that an interval of 2 days after complete infiltration of ponded water is a recommended procedure in north-western Indian condition irrespective of soil type and irrigation depth under puddled rice fields.

Berseem, on the other hand, needs frequent irrigation throughout its growing season because of its shallow root zone that dries quickly (Tyagi et al. 2003). Average depth of irrigation equal to 47.3 mm per event was applied during berseem season 1 with an average irrigation interval of nearly 9 days. In berseem season 2, the average depth of irrigation application was ranging between 8-11.5 mm per event with an average irrigation interval of nearly 12 days. In berseem season 1 a total of 11 irrigations were applied and only 6 irrigation events were made in berseem season 2. More frequent irrigations were applied near the end of the crop season (April-May) owing to the increased evaporative demand. It has been shown that large saving in irrigation as well as overall input water was achieved by imposing reduced irrigation in both crop seasons.

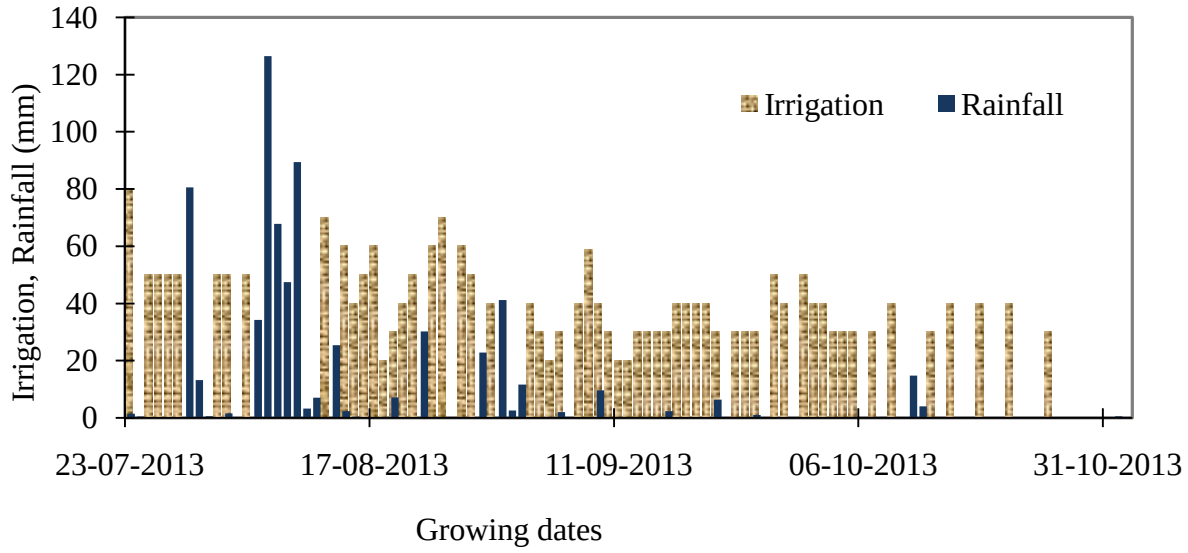

Fig. 4.9 (a) Irrigation schedules and rainfall in rice season 1

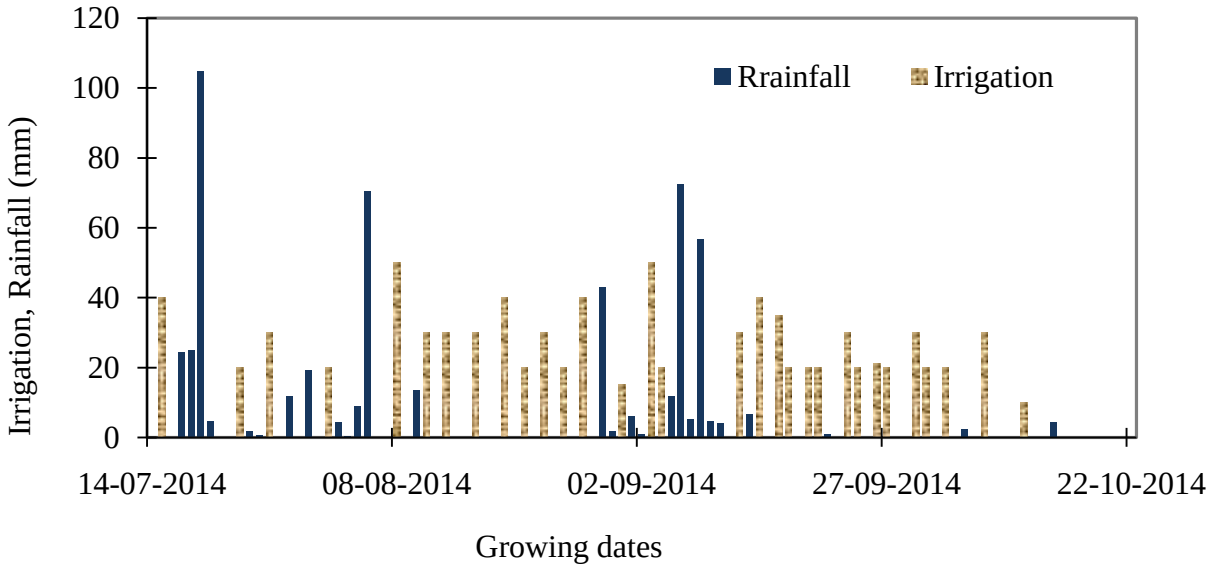

Fig. 4.9 (b) Irrigation schedules and rainfall in rice season 2

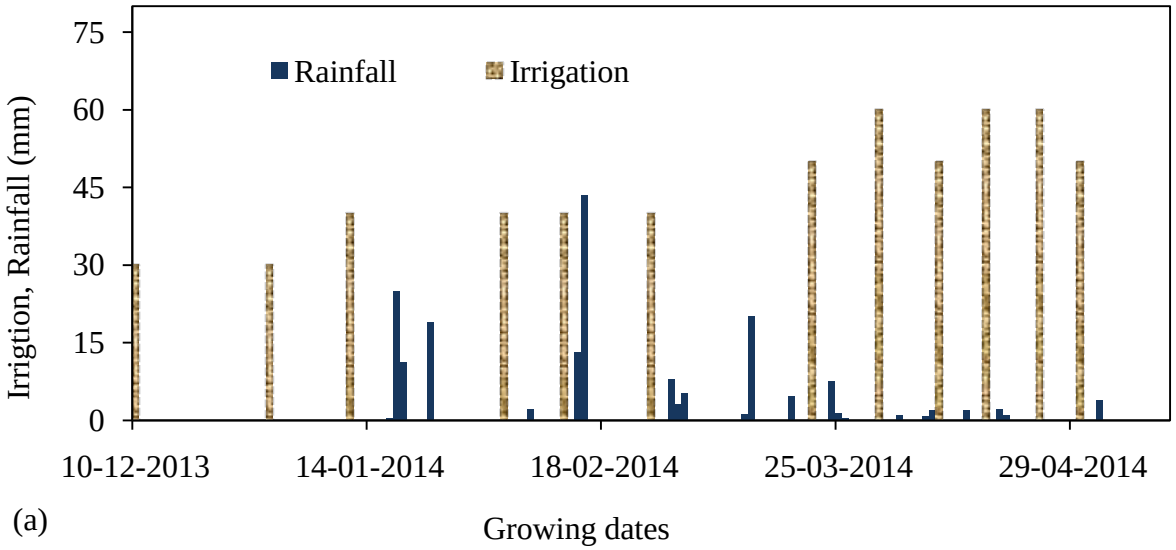

Fig. 4.10 (a) Irrigation schedules and rainfall in berseem season 1

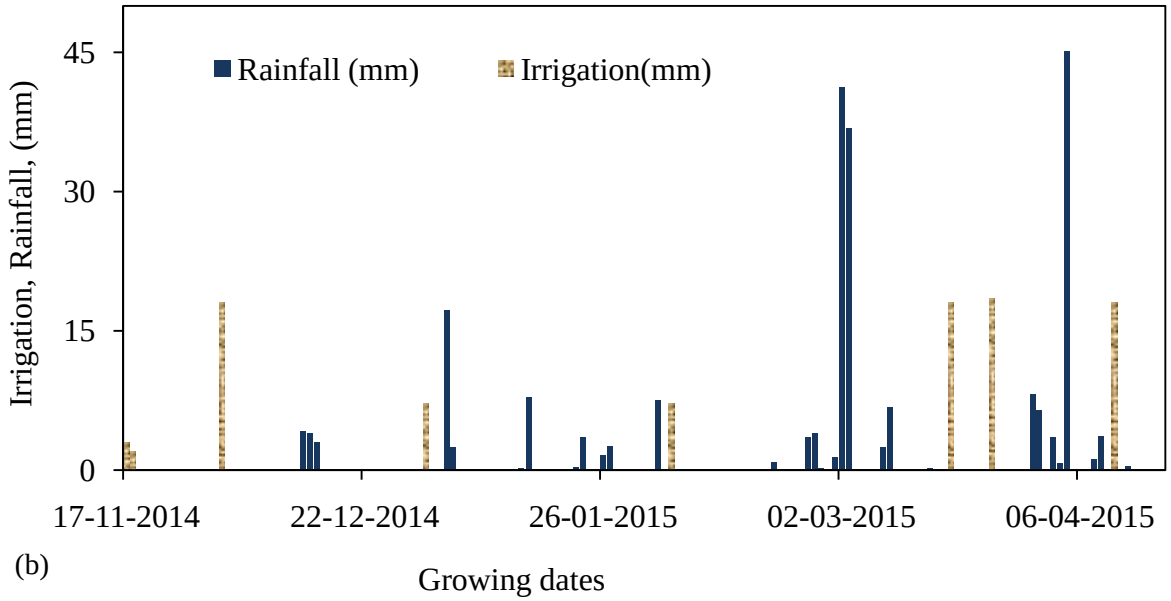

(b)

Fig. 4.10 (b) Irrigation schedules and rainfall in berseem season 2

4.5 EVAPOTRANSPIRATION

The reference evapotranspiration was computed using the Penman-Monteith approach (Allen et al. 1998). This method was also used in the earlier studies (Tyagi et al. 2003; Shankar et al. 2012) and found to be suitable for the region. The reference evapotranspiration, ET_0 (mm/day), according to Penman-Monteith is:-

$$ET_0 = \frac{0.408.\Delta(R_n - G) + \gamma \frac{900}{273+T} u_2 (e_s - e_a)}{\Delta + \gamma(1 + 0.34u_2)} \qquad (4.7)$$

where R_n is net radiation at the crop surface (MJ/m^2/day), G is soil heat flux density (MJ/m^2/day), e_s is saturation vapour pressure (kPa), e_a is actual vapour pressure (kPa), T is air temperature at 2 m height ($^\circ$C) above the ground surface, u_2 is wind speed at 2 m height (m/s) above the ground, Δ is slope of vapour pressure curve (kPa/$^\circ$C), and γ is psychometric constant (kPa /$^\circ$C). Figs. 4.11 and 4.12 show the reference evapotranspiration computed during the crop growing seasons.

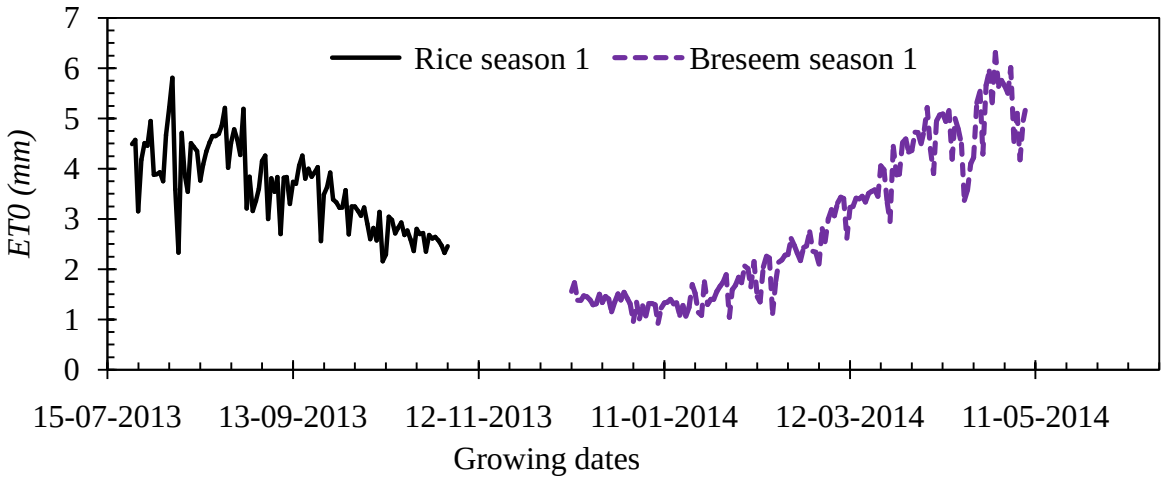

Fig. 4.11 ET_0 for rice season 1 and berseem season 1 periods

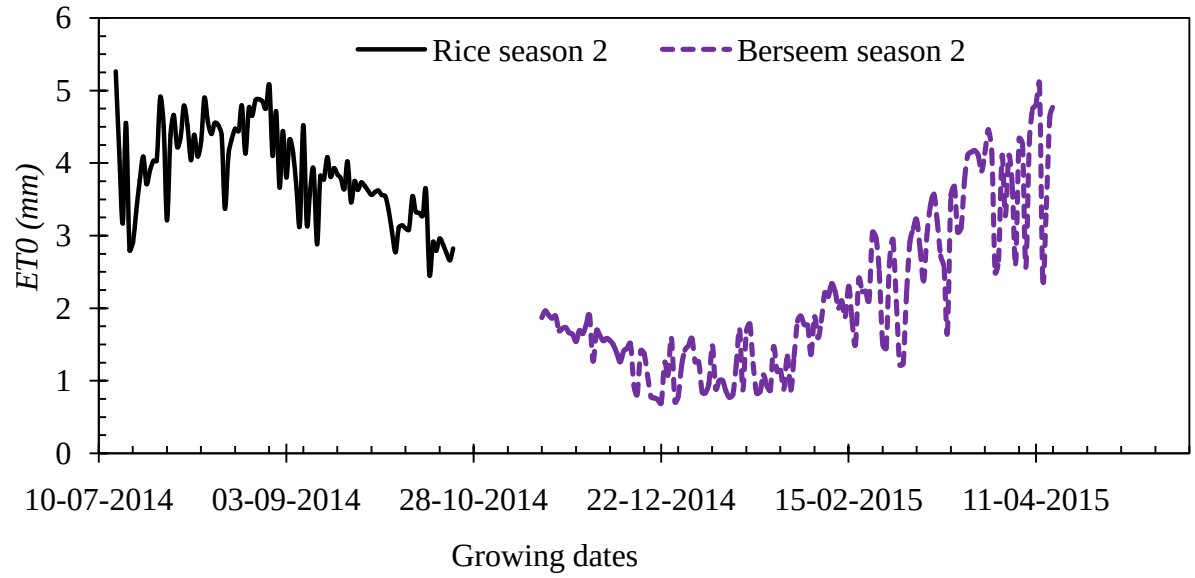

Fig. 4.12 ET_0 for rice season 2 and berseem season 2 periods

The reference evapotranspiration is applied to a hypothetical crop which is assumed disease free, uniformly growing, completely shedding the ground and without shortage of water. Hence, a crop specific coefficient, K_c, is introduced to compute the potential evapotranspiration of a particular crop. The potential evapotranspiration for rice and berseem crops was computed using FAO recommended procedures in the model by incorporating a crop coefficient for a specified crop growth stage. The potential evapotranspiration for non water limiting conditions may be computed using (Rallo et al. 2012).

$$ET_c = K_c \times ET_o \quad (4.8)$$

where ET_c is the potential crop evapotranspiration and K_c is the crop coefficient. It is to be noted that, in actual field conditions, the actual evapotranspiration may be less than the potential evapotranspiration if the soil water is limiting (Liu et al. 1998). In such conditions, the

soil water stress coefficient, K_s, may be introduced in (4.8) to compute actual evapotranspiration.

$$ET_c = K_s \times K_c \times ET_o \tag{4.9}$$

Further, the coefficient K_s is computed as:

$$K_s = \frac{TAW - D_i}{TAW - RAW} \tag{4.10}$$

where TAW (mm) $=1000 Z_j$ (θ_{fc}-θ_{wp}) is the total available water (mm); D_i (mm) is the soil moisture depletion on day i; RAW (mm) is readily available water that can be obtained by multiplying TAW to a depletion coefficient, $p_{r,}$ considering the crop water stress resistance. θ_{fc} is the soil moisture content at field capacity; θ_{wp} is the soil moisture content at permanent wilting point and Z_j is the root zone depth (m).

4.5.1 Crop Coefficient

The crop coefficient for the respective crop development stages of each crop has been modified for Roorkee climatic condition. Single crop coefficient approach has been used in this study. The crop coefficient depends on crop type and its growth stages. The crop coefficient incorporates factors such as crop height, soil-crop surface resistance and albedo (reflectance) of the potential evaporative surface which distinguishes a crop from the reference crop (Allen et al. 1998; Huntington and Allen 2009). First, the crop development stages (initial, development, mid and late seasons) have been distinguished following the recommendations of FAO-56 (Allen et al. 1998). The initial stage runs from planting/sowing date to approximately 10% ground cover. The crop development stage runs from 10% ground cover to effective full ground cover. Effective full cover for many crops occurs at the initiation of flowering. The mid-season stage, on the other hand, ranges from the time of effective full cover to the start of maturity and finally the late season stage runs from the period of full maturity to harvest time or complete dryness of a crop in the field (Allen et al. 1998). Secondly, the crop coefficient values from FAO tables have been retrieved and modified for the particular crop and field conditions. Then the K_c_initial, K_c_mid and K_c_end values of crop coefficients were modified accordingly as suggestion made by FAO 56 (Allen et al. 1998). The K_c values in development and late season stages were computed using linear interpolation as;

$$K_{ci} = K_{c,prev} + \left[\frac{i - \sum\left(L_{prev}\right)}{L_{stage}}\right]\left(K_{c,next} - K_{c,prev}\right) \tag{4.11}$$

where *i* is the day number within the growing season, K_{ci} is the crop coefficient on day *i*, L_{stage} is the length of the stage under consideration (days), L_{prev} is the sum of the lengths of all the previous stages (days), $K_{c,prev}$ is the crop coefficient at the end of the previous stage and $K_{c,next}$ is the K_c at the beginning of the next stage.

Table 4.1 provides the growth stages and crop coefficients recommended by FAO and the present study for individual growth stages of rice and berseem crops. In particular, in berseem growth season, individual cutting dates were considered. Full growth periods of the berseem fodder crops were not allowed, as practiced in the area, since the crop was regularly cut for fodder. Figs. 4.13 and 4.14 depict the daily crop coefficient values of both crops.

Table 4.1 Crop coefficient values in their respective growth periods and cutting cycles

Crop name/K_c values	Crop growth stages			
	Initial	Development	Mid season	Late season
Rice season 1	23/07/13-06/08/13	07/08/13-05/09/13	06/09/13-05/10/13	06/10/13 - 02/11/13
Rice season 2	15/07/14-05/08/14	06/08/14-30/08/14	31/08/14-30/09/14	01/10/14 - 22/10/14
K_c_FAO	1.05	1.05-1.20	1.20	09-0.6
K_c (present study)	1.10	1.10-1.20	1.20	0.67
	Individual cutting dates			
Berseem season 1	21/02/14	19/03/14	09/04/14	08/05/14
Berseem season 2	05/02/15	09/03/15	27/03/15	16/04/15
	Kc initial	Kc before cut	Kc after cut	Kc end
K_c_FAO	0.40	1.15	0.40	1.10
K_c (present study)	0.34	0.99	0.73	0.95

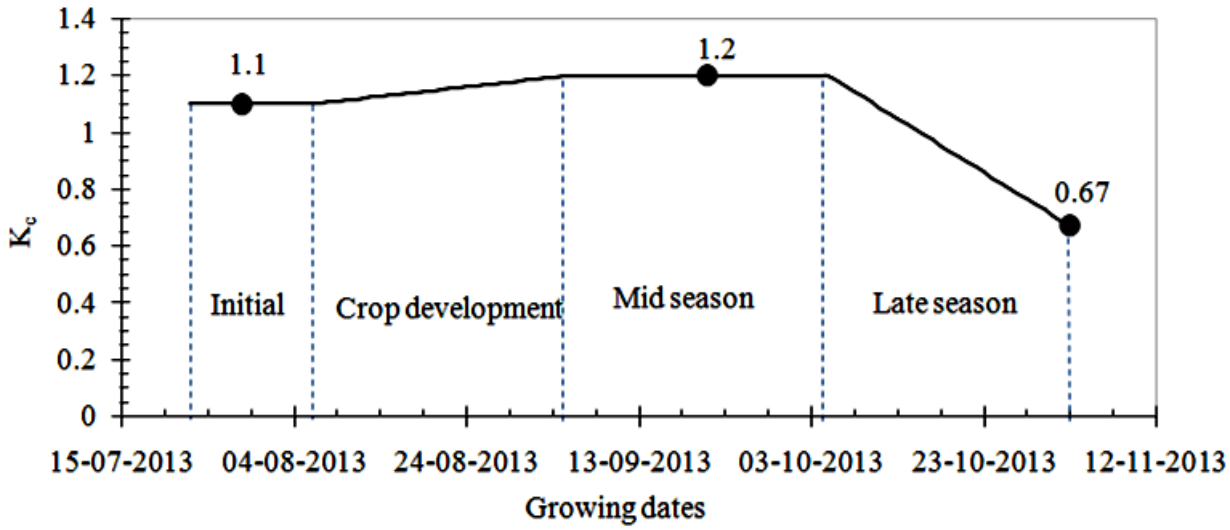

Fig. 4.13 Daily crop coefficient values for rice

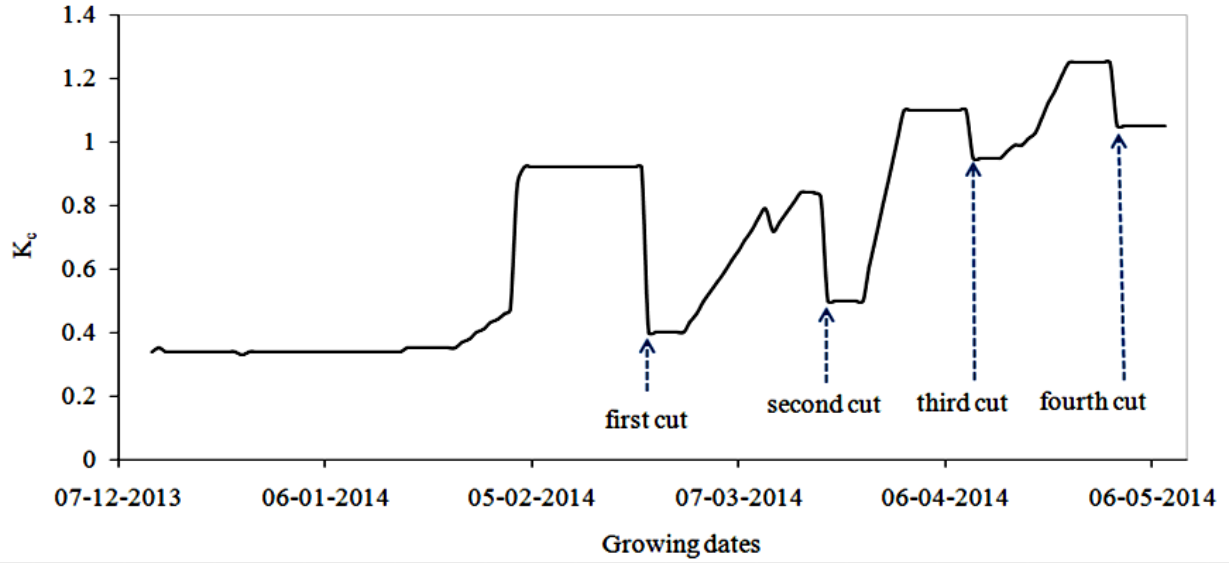

Fig. 4.14 Daily crop coefficient for berseem fodder

It can be seen from Table 4.1 that the crop coefficients obtained for rice in the present study are slightly different from the FAO tabulated values (Allen et al., 1998) owing to local climatic conditions, agronomic practices and specific experimental setup. Various studies on the crop coefficients of rice based systems were undertaken so far in the region (Choudhury et al. 2013; Tyagi et al. 2000). Choudhury et al. (2013) have reported that the K_c values of dry-seeded irrigated bed planted rice ranged from 0.62(initial) to 1.16(mid season) while for dry seeded conventional flat land it varied from 0.61(initial) to 1.42(mid season) in the Indo-Gangetic plains of India. Tyagi et al. (2000) have computed K_c values of 1.15, 1.23, 1.14 and 1.02, respectively for initial, crop development, reproductive and last stages using Penman-Monteith method in the same region grown under submerged conditions. The results at mid stage growth period are fairly at par with the values of K_c in this study although there are

differences in the initial and late season stages owing to differences in the agronomic practices and experimental conditions.

Investigation for berseem K_c was also made in the same region earlier employing weighing type lysimeters (Tyagi et al. 2003). The results reported are significantly different (0.62 -1.27) when compared with the results obtained in the present study. This would be probably due to the differences in agronomic practices, crop variety, consideration of average cutting effects and sowing time which are considerably different from the current condition. In this study, berseem crop coefficients were considered for individual cutting periods which were again conducted sometimes in development stage and other times after full cover (mid season) growth stages. Further, the way the crop has been cut also matters as far as individual cutting events are considered. Individual cuttings with very short stem left behind may reduce the K_c value after cut or cuttings which leave more length of stem and some crop leaves may favour more K_c values. In general, K_c for such crops with frequent cuttings could vary widely based on individual cutting processes, interval between individual cuttings, agronomic and environmental conditions.

4.5.2 Field Capacity and Permanent Wilting Point

The field capacity (*FC*) and permanent wilting point (*PWP*) in the soil water zone refer to the threshold values of the soil moisture content in a crop root zone. They are used to compute the total available water (*TAW*) and readily available water (*RAW*) in the soil for crop growth. The terms *FC* and *PWP* are difficult to determine in the field. In many soils, a nearly constant value of soil moisture content reached after one or two days after cessation of gravity drainage refers to the field capacity. The permanent wilting point soil moisture is the amount of water held so tightly by the soil matrix that roots cannot absorb and at which plants show wilting (Kirkham 2005). In quantitative terms, field capacity water content refers to the soil moisture content at which the soil water is held at matrix suction value of 33 kpa while the permanent wilting point soil water content refers to matrix suction value of approximately 1500 kpa (Cuenca 1989; Hillel 2004). These parameters have been determined from the soil moisture characteristic curve (SMCC) which was developed making use of saturated water content and moisture retention data acquired from pressure plate test discussed in section 3.9.5. Table 4.2 presents the average field capacity and wilting point soil moisture content values for the experimental field soil.

Table 4.2 Field capacity and permanent wilting point values

Depth below ground level (cm)	Field capacity (%)	Permanent wilting point (%)	Saturated water content (%)
0-30	18.5	6.6	38
30-60	24.5	6.6	40
60-80	19.9	6.0	40
80-100	20.2	6.3	40
100-140	20.0	7.6	39

4.5.3 The Soil Moisture Stress Coefficient

The soil moisture stress coefficient, K_s, is a coefficient which modifies the potential evapotranspiration based on soil moisture status. Soil moisture contents observed in the root zone during the crop periods, field capacity and permanent wilting point soil moisture content values were used to compute K_s as shown in equation (4.10). The field capacity and permanent wilting point soil moisture content values were obtained from soil retention curve. The soil moisture depletion, D_i, was computed from field capacity and observed soil moisture contents for a given time step. Readily available water (RAW) was calculated making use of the FAO recommended parameter, p_r (soil moisture depletion fraction for no stress) (Rallo et al. 2012). A value of p_r equal to 0.1 for rice and 0.4 for berseem crops were adopted.

Figs. 4.15 and 4.16 present the K_s value for both seasons of the rice crop. On the other hand, calculations for crop water stress coefficient for berseem crop showed that the crop has not been stressed and K_s remained as 1. In rice season 1, the crop was provided with ample amount of water and hence the value of K_s is almost 1, no stress condition, except the late season by which time no irrigation was applied to drain the field for harvest. However, in the rice crop season 2, when there was intermittent irrigation, the crop was comparatively stressed near the ends of the crop season.

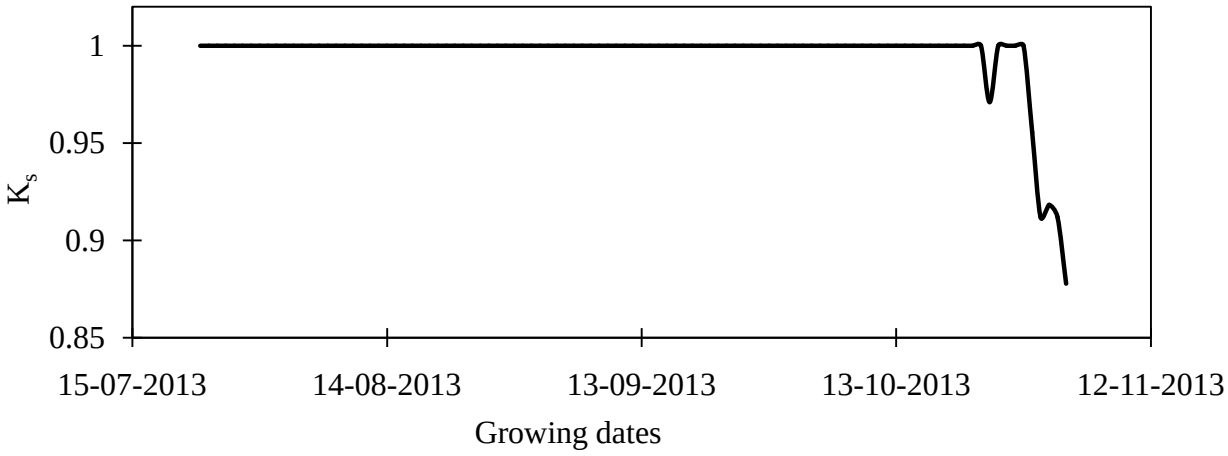

Fig. 4.15 Daily soil water stress coefficient during rice season 1 (2013) (in lysimeter 2)

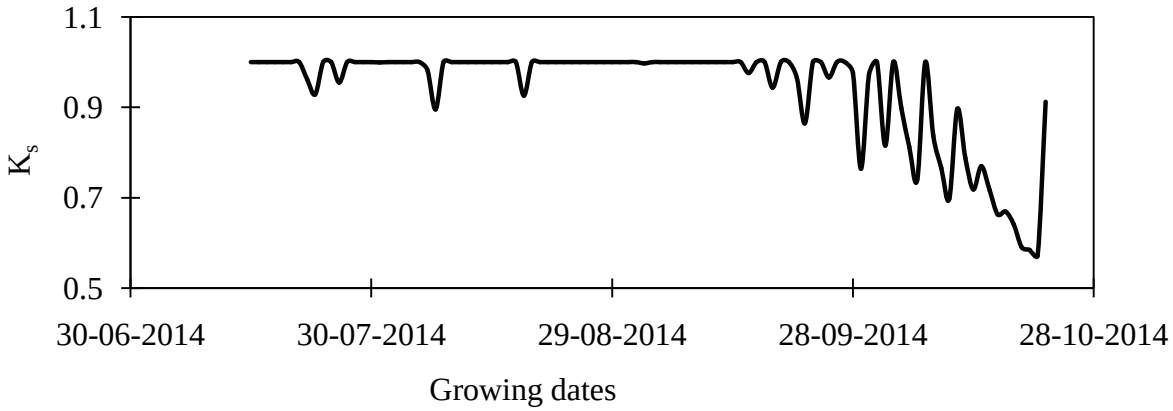

Fig. 4.16 Daily soil water stress coefficient during rice season 2 (2014) (in lysimeter 2)

4.5.4 Potential and Actual Evapotranspiration

The potential evapotranspiration (ET_c) was computed based on equation (4.8). Seasonal ET_c during rice season 1 was 411.72 mm while it was 431.05 mm in rice season 2. The potential evapotranspiration in berseem season 1 was 342.36 mm while it was 162.80 mm in berseem season 2. Actual evapotranspiration (ET_a) has been computed using equation (4.9). In rice season 1, ET_c and ET_a were nearly equal since there was frequent application of water in the particular season. Due to limitations in soil moisture, particularly during the rice season 2 the potential evapotranspiration was slightly reduced. On the other hand, during berseem seasons, ET_c and ET_a were similar as there was no moisture stress in the crop season.

The actual evapotranspiration, on the other hand, varies with each crop season and location owing to variation in the soil moisture content. The computed values of actual evapotranspiration are provided in section 4.10 along with the other water balance components. During the rice seasons, the seasonal actual evapotranspiration is nearly similar in the two seasons while there is large difference between the seasonal actual evapotranspiration in

berseem seasons. This is attributed to variation of the date of sowing in the berseem seasons. In berseem season 2, the date of sowing was nearly one month earlier and thus it had a larger influence on the overall water balance. The maximum ET_a in the 2013/14 growing season was 7.89 mm/day observed near the end of April during berseem season 1 while the maximum ET_a in the 2014/15 season was 6.06 mm/day which was observed during rice season 2 in July. Normally, minimum values of ET_a appear to be occurring in the months of December and January in the area. Therefore, some shifting of cropping periods would result in influence on crop water requirement and consequently the water balance of the crop root zone. However, agronomic requirements often constrain cropping periods. Figs. 4.17 and 4.18 present the potential and actual evapotranspiration during the crop seasons.

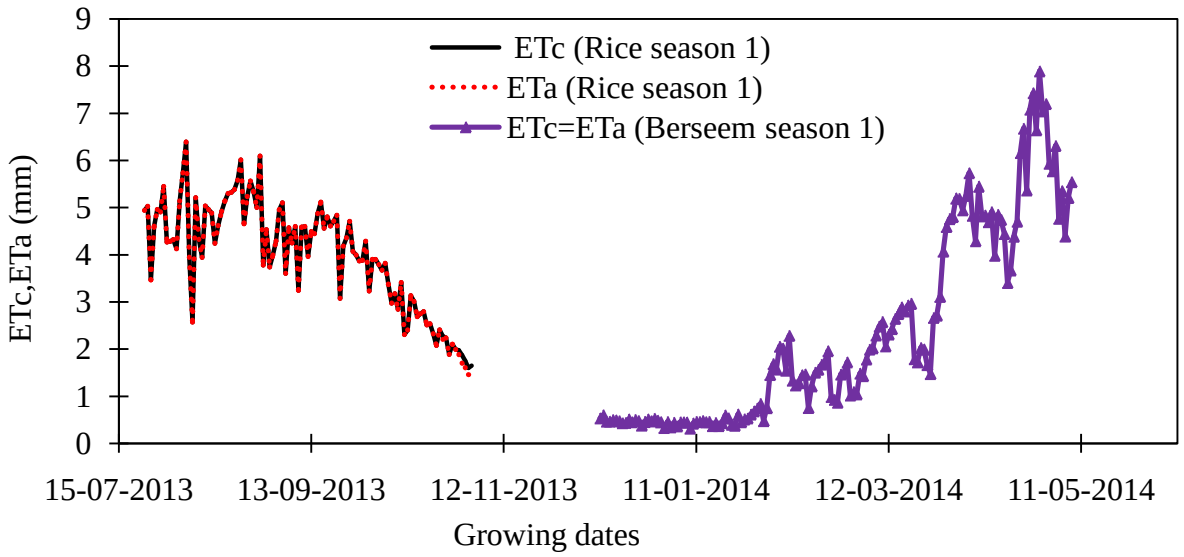

Fig. 4.17 Potential and actual evapotranspiration in rice season 1 and berseem season 1

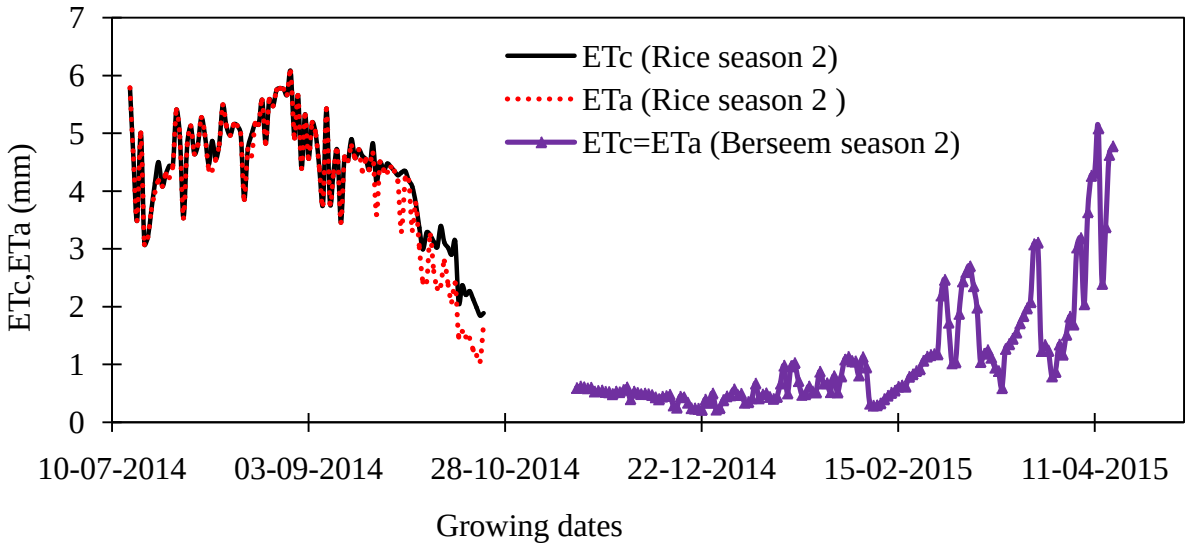

Fig. 4.18 Potential and actual evapotranspiration in rice season 2 and berseem season 2

4.6 RUNOFF

Runoff component of the water balance in lysimeter studies is often neglected since it is either minimal or controlled in such a way that there exists no run-on and run-off (Hillel 2004). If the top level of the lysimeter is constructed slightly above the ground level, surface water inflow or outflow could be eliminated. However, in certain torrential storms, run-on to or runoff from a lysimeter can be considered. Run-on and run-off were controlled in the experimental field by providing field boundaries as practiced in the farmers' field in the study area. Farmers often construct bunds having heights reaching 30 cm around the rice field boundaries aiming to capture rainwater in rice fields. The same has been done in the experimental farm in the present study.

Surface runoff out of the experimental field, for a levelled field area, may be considered only when rainfall of magnitude greater than the height of bund (nearly 20 to 30 cms) occurs according to the following equation:

$$R_i = \begin{cases} P_i - L_{bh} \ \ if \ \ P_i > L_{bh} \\ 0 \ \ if \ \ P_i \le L_{bh} \end{cases} \qquad (4.12)$$

where $R_{i\,=}$ runoff generated (mm); P_i = rainfall (mm) and L_{bh}(mm) = the bund height measured from ground surface at field boundaries. In view of the above concept, runoff generated from field plots was negligible.

4.7 OTHER WATER BALANCE COMPONENTS

Water balance components such as interception, groundwater contribution to the root zone and depression storage were not considered in this study. Interception was neglected since the magnitude of interception compared to transpiration and evaporation is quite less (Shankar 2007). Further, measurement and estimation of interception are difficult and bear large uncertainties since intercepted water could vanish within 10 minutes after rainfall (Blyth and Harding 2011). In actual field conditions, on the rainy days, evapotranspiration decreases due to the cooling effect of the rain. However, computations of *ET* are usually done in the same way as on the non rainy days and hence evapotranspiration estimated on rainy days is on the conservative side than the actual field condition. Hence, this discrepancy may also take care of the loss due to interception to a certain extent. Considering deep water table condition, contribution from groundwater as capillary rise into the root zone has been neglected. Depression storage (surface ponding) was also not considered since such component is indirectly included in input water (irrigation and/or rainfall) for fields provided with boundary bunds where no surface runoff is contributing.

4.8 DEEP PERCOLATION

Deep percolation from cropped area refers to the flow of water beyond the bottom of a given crop. Theoretically, deep percolation occurs when the soil field capacity is satisfied either from irrigation or rainfall (Smith et al. 2005) and the soil moisture content status is at saturated conditions. Gravity drainage below a crop root zone under such conditions entails deep percolation. However, due to the various conditions of subsurface environment, percolation can also take place under unsaturated conditions (Beven and Germann 1982; Kung 1990; Wessolek et al. 2008). Various techniques are available to measure and estimate deep percolation.

The most direct method of deep percolation measurement is undertaken using drainage type lysimeters which is also used in this study. The volume of percolated water at the bottom of lysimeters was measured directly by collecting the drainage water from collecting buckets as specified in chapter three. Deep percolation is computed using water balance model using equation (4.6).

The performance of the water balance model in predicting deep percolation is studied by comparing model predicted deep percolation with field observations. The comparison was done both on daily basis and lumped time steps.

4.8.1 Deep Percolation in Rice Season

4.8.1.1 Estimation of deep percolation in rice season on daily time steps

After obtaining all the daily components of the water balance model, deep percolation was computed using equation (4.6) and compared with field observed daily deep percolation. Figs. 4.19-4.22 illustrate the variation of model predicted and measured deep percolation for the rice crop season on daily time basis.

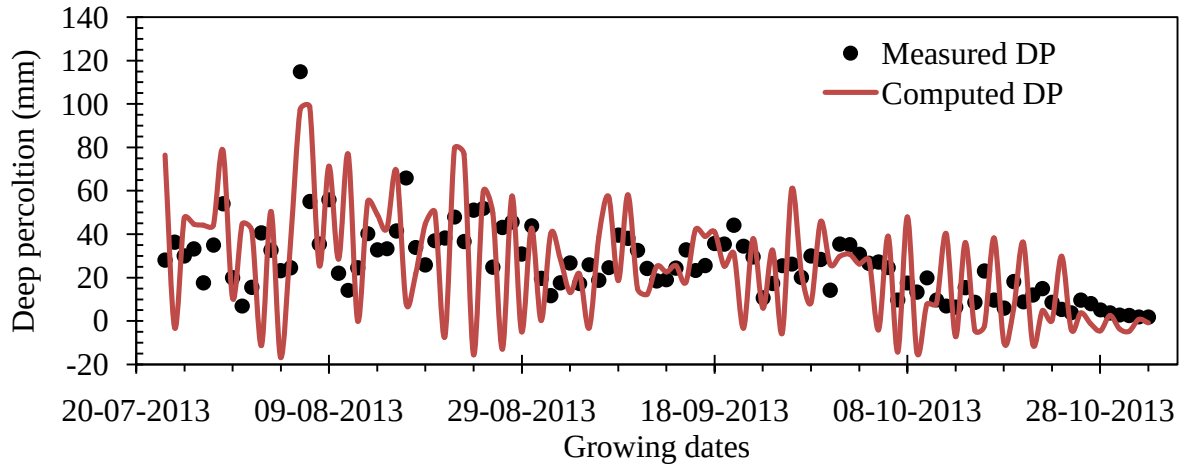

Fig. 4.19 Deep percolation computed and measured on daily time step in lysimeter 1 in rice season 1

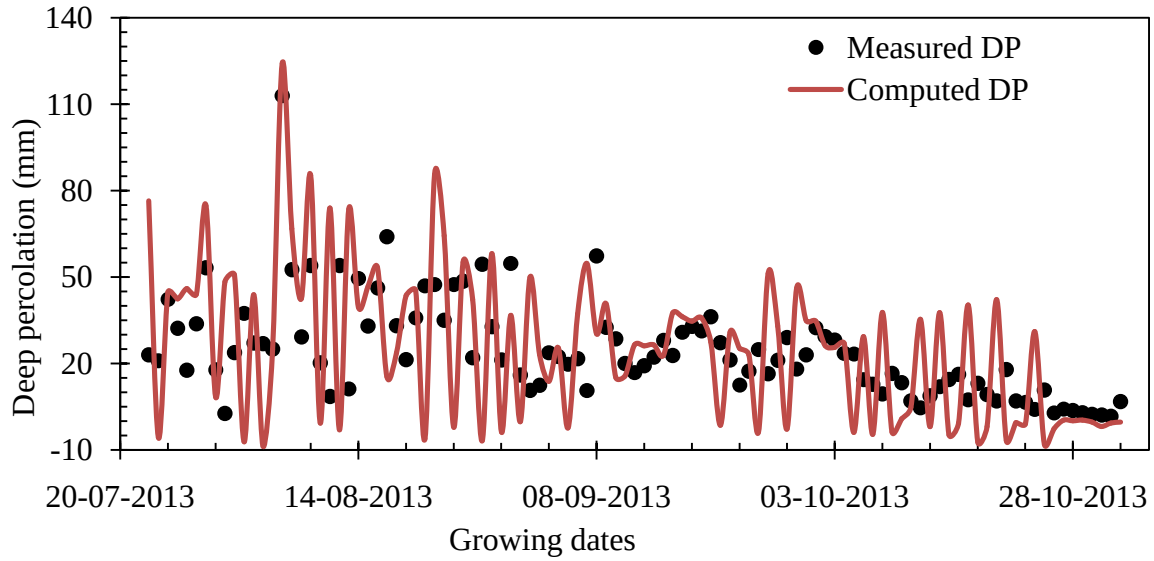

Fig. 4.20 Deep percolation computed and measured on daily time step in lysimeter 2 in rice season 1

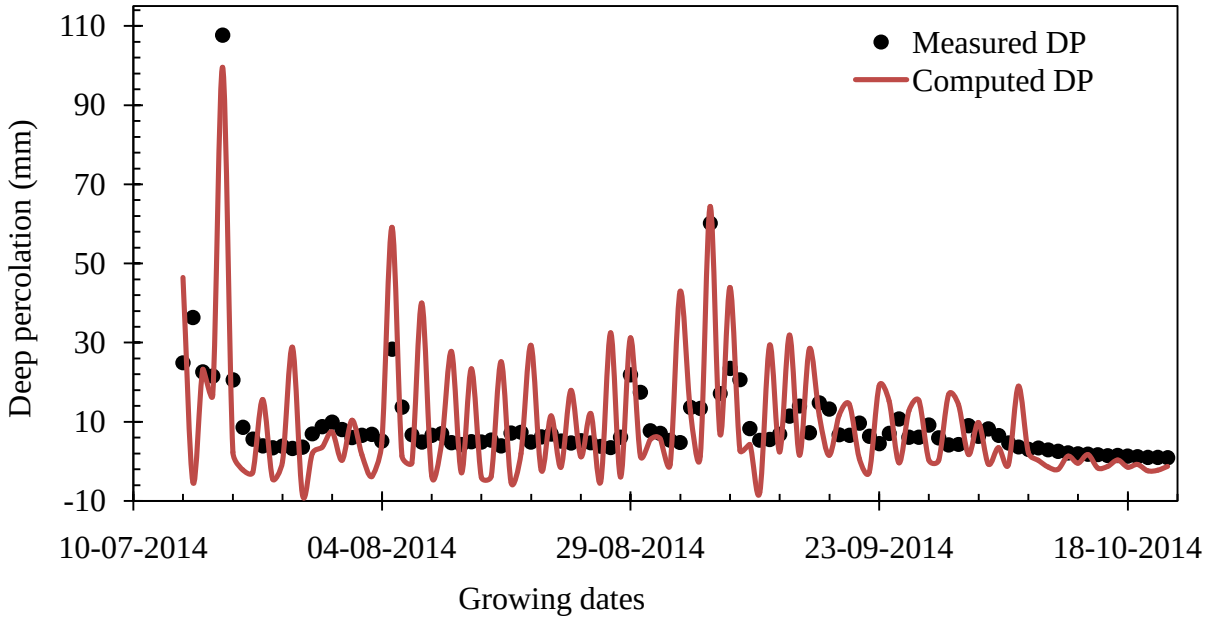

Fig. 4.21 Computed and measured deep percolation on daily time step in lysimeter 1 in rice season 2

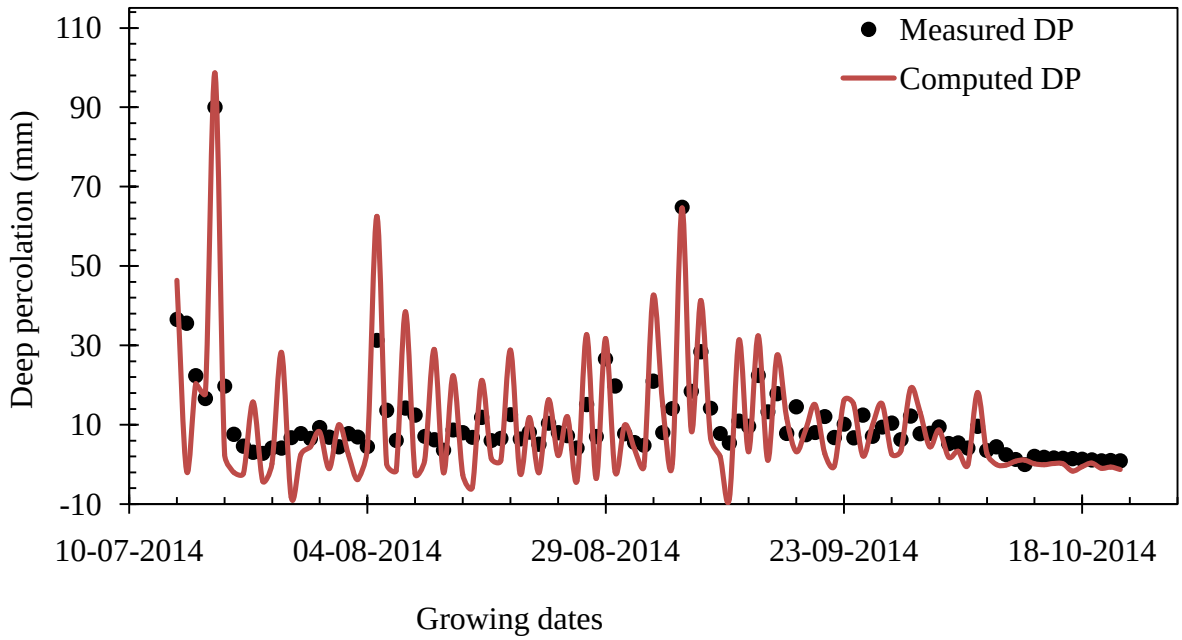

Fig. 4.22 Deep percolation computed and measured on daily time step in lysimeter 2 in rice season 2

4.8.1.2 Estimation of deep percolation in rice season with lumped time steps

Deep percolation was also computed on lumped time steps by cumulating the variables given in equation (4.6). Different time steps were considered for computing deep percolation on lumped time steps. In the rice season, deep percolation computed on weekly time steps agree well with the field observed deep percolation. Although, most computations involving deep percolation in literature are based on lumped time steps (weekly, monthly, seasonal or annual) (Li et al. 2014; Sudhir-Yadav et al. 2011; Willis et al. 1997), it was not explicitly explained why and how these time steps were used. Ochoa et al. (2007) computed daily deep percolation from alfalfa grass crop field in New Mexico using time domain reflectometry (TDR) measurements in the crop root zone. However, their analysis was conducted without measured deep percolation data points and considered average soil moisture content over the entire depth of crop root zone. In this particular case, discrete intervals of root depth have been considered to incorporate the effect of root water extraction in the form of moisture depletion while calculating the deep percolation.

Figs. 4.23 to 4.26 provide the variation of computed and measured deep percolation values on weekly basis for rice growing season.

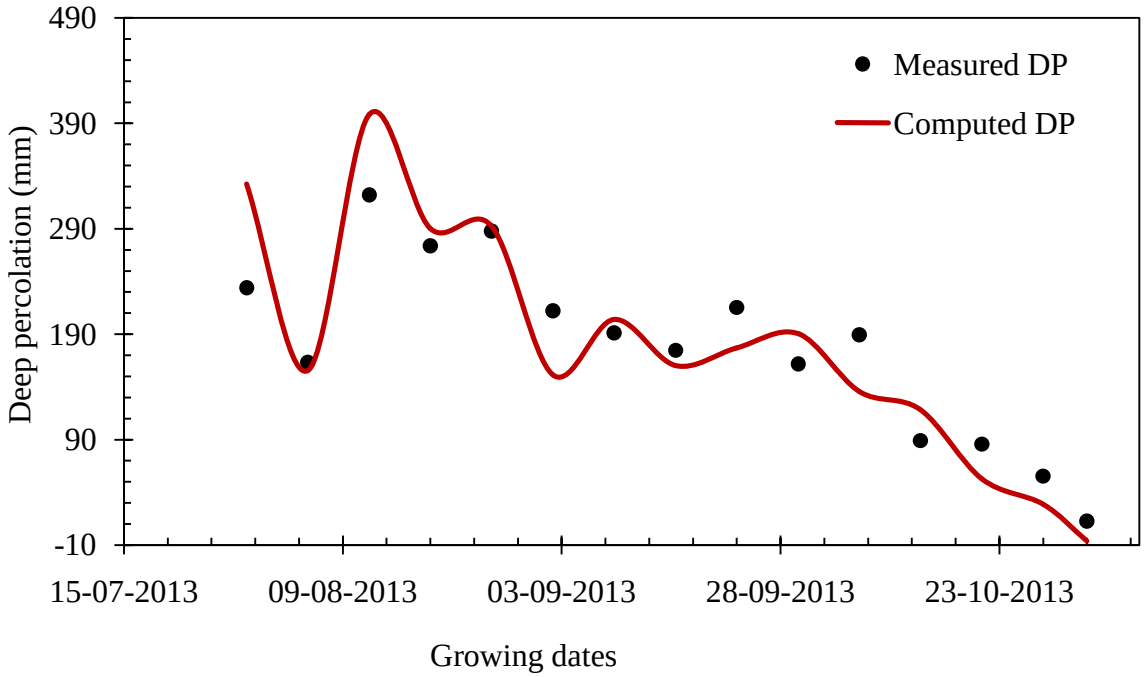

Fig. 4.23 Computed and measured deep percolation with weekly time steps in lysimeter 1 in rice season 1

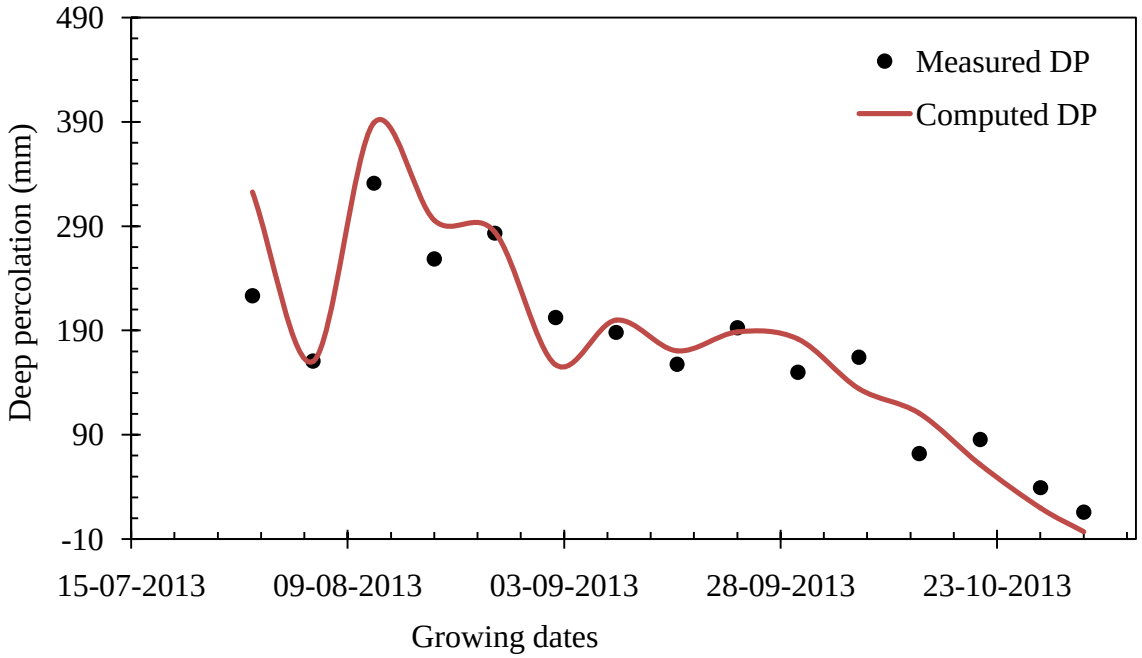

Fig. 4.24 Computed and measured deep percolation with weekly time step in lysimeter 2 in rice season 1

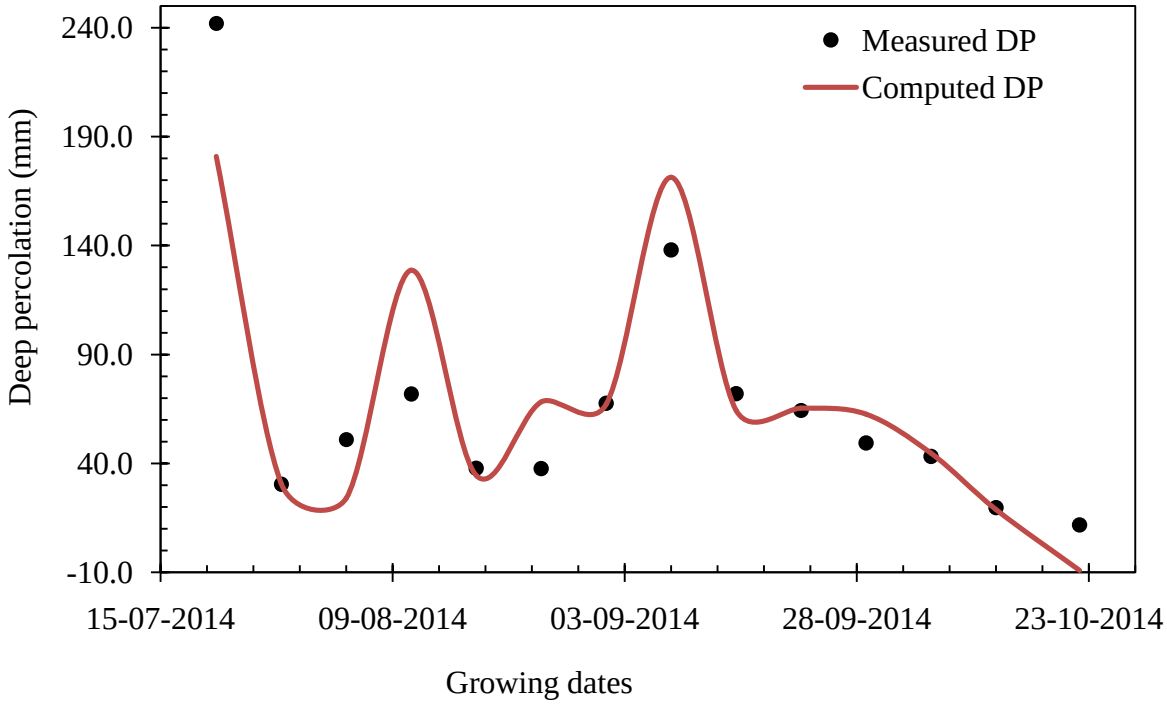

Fig. 4.25 Computed and measured deep percolation with weekly time step in lysimeter 1 in rice season 2

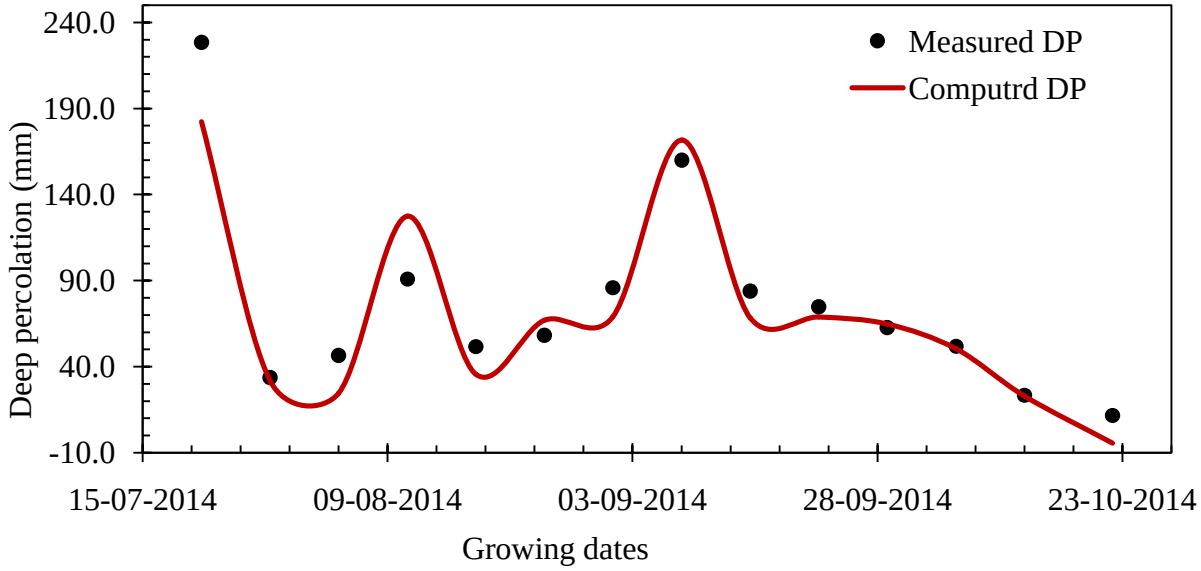

Fig. 4.26 Computed and measured deep percolation with weekly time step in lysimeter 2 in rice season 2

4.8.2 Deep Percolation in Berseem Season

4.8.2.1 Estimation of deep percolation in berseem season on daily time steps

Similarly, for the berseem crop season, deep percolation was also computed on daily basis after acquiring daily data on the other components of the water balance. Figs. 4.27 to 4.30

present the variations of the computed and measured daily deep percolation in the two seasons of berseem crop.

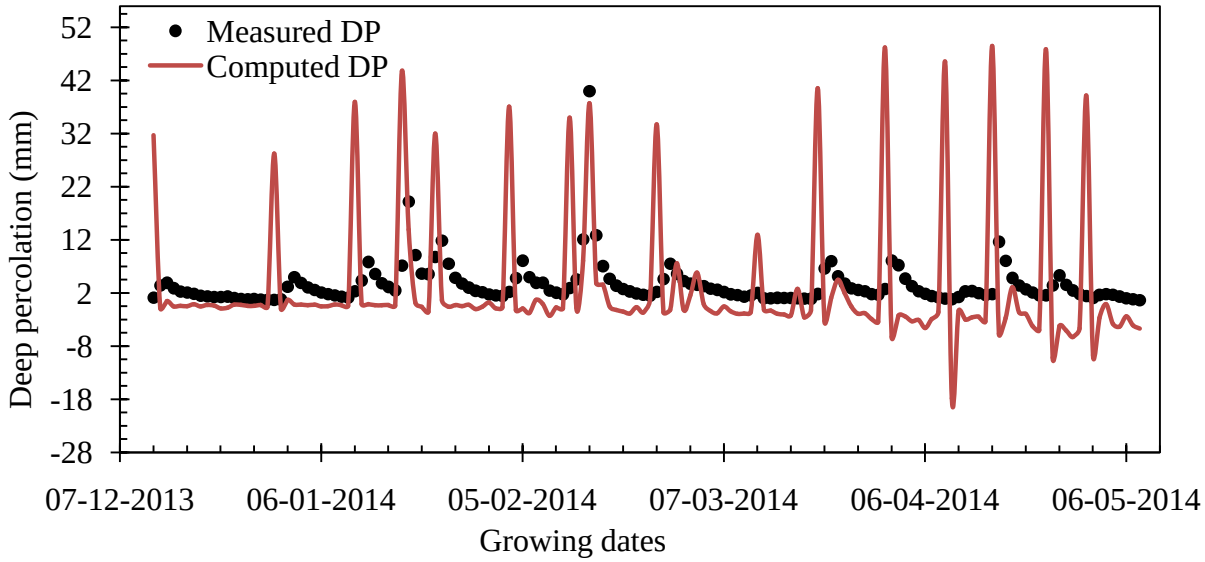

Fig. 4.27 Computed and measured deep percolation on daily time step in lysimeter 1 in berseem season 1

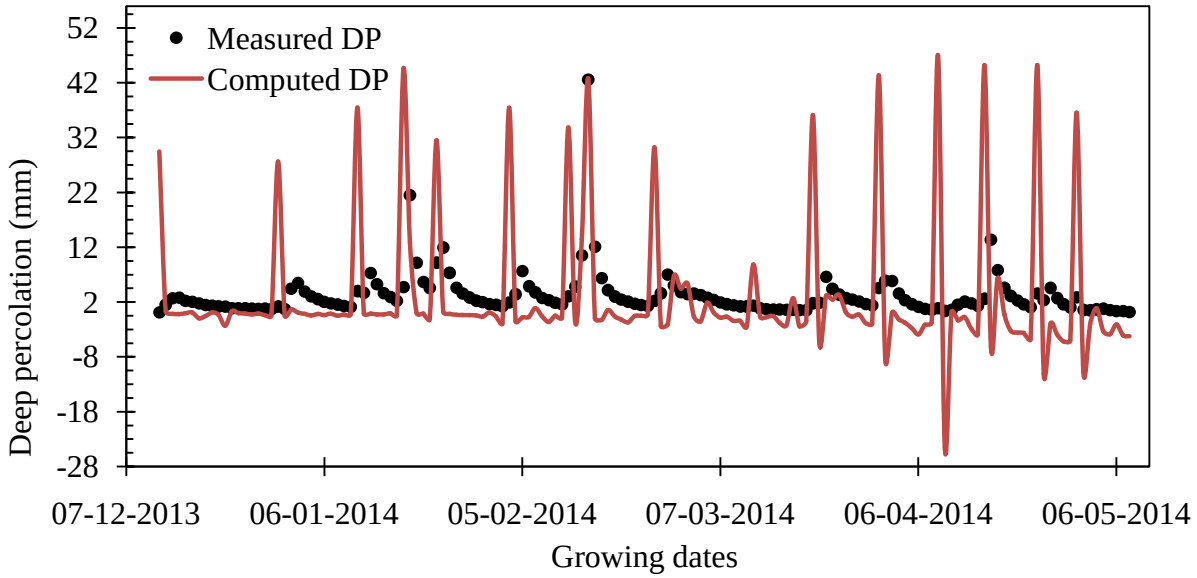

Fig. 4.28 Computed and measured deep percolation on daily time step in lysimeter 2 in berseem season 1

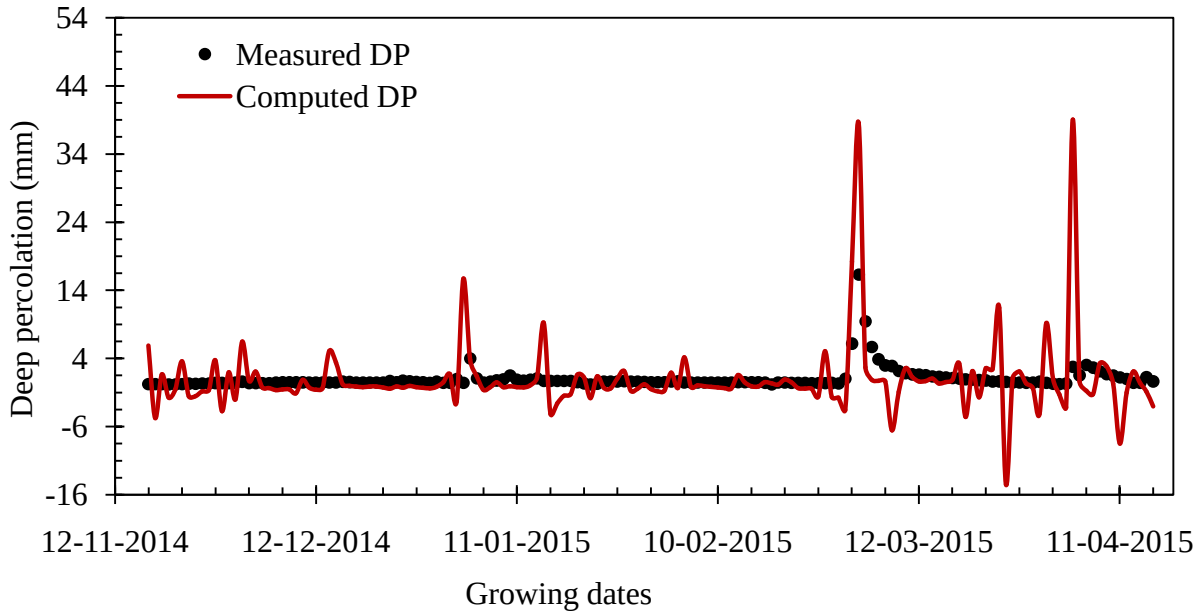

Fig. 4.29 Computed and measured deep percolation on daily time step in lysimeter 1 in berseem season 2

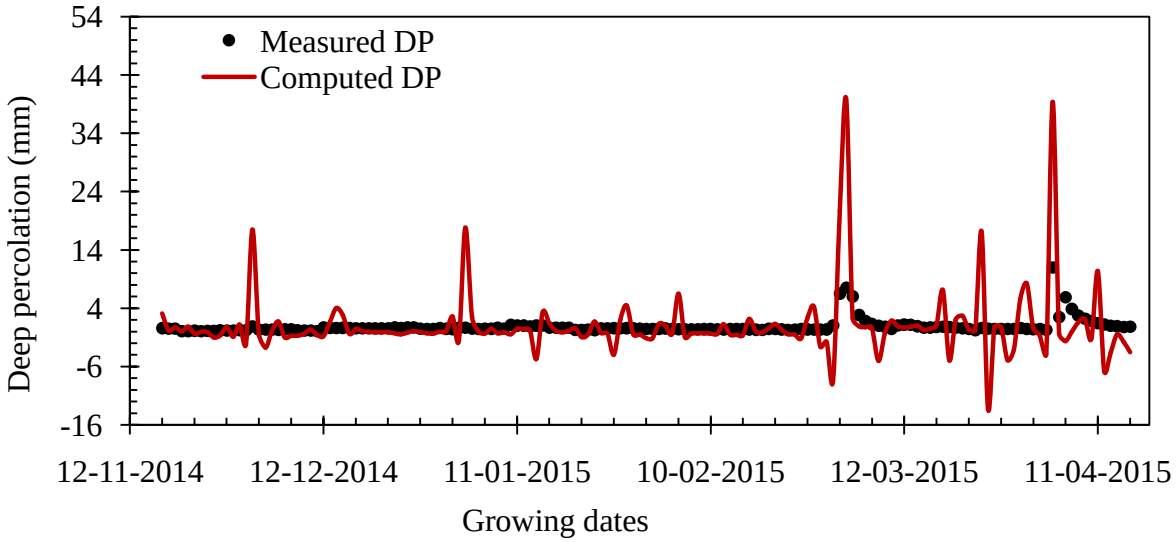

Fig. 4.30 Computed and measured deep percolation on daily time step in lysimeter 2 in berseem season 2

4.8.2.2 Estimation of deep percolation in berseem season with lumped time steps

As worked out for rice seasons, different cases of time lumping scenarios were considered to compute the deep percolation on lumped time steps in the berseem season. Unlike the rice seasons, deep percolation computed with lumped time steps (between the wetting intervals) showed good relation with the field observed deep percolation in both berseem seasons and lysimeter conditions. Figs. 2.31 to 2.34 provide the variations of computed and measured deep percolation values on lumped time steps.

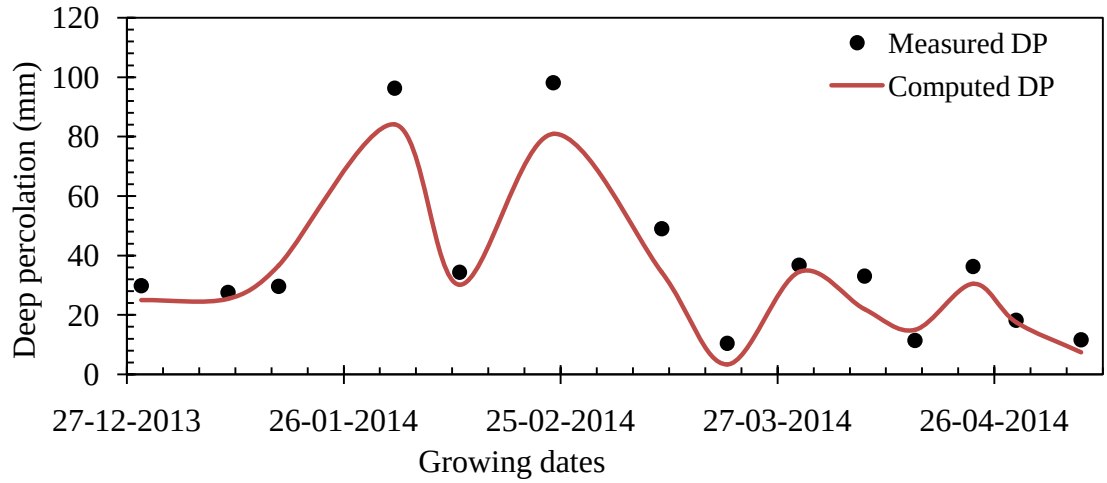

Fig. 4.31 Computed and measured deep percolation with lumped time steps in lysimeter 1 in berseem season 1

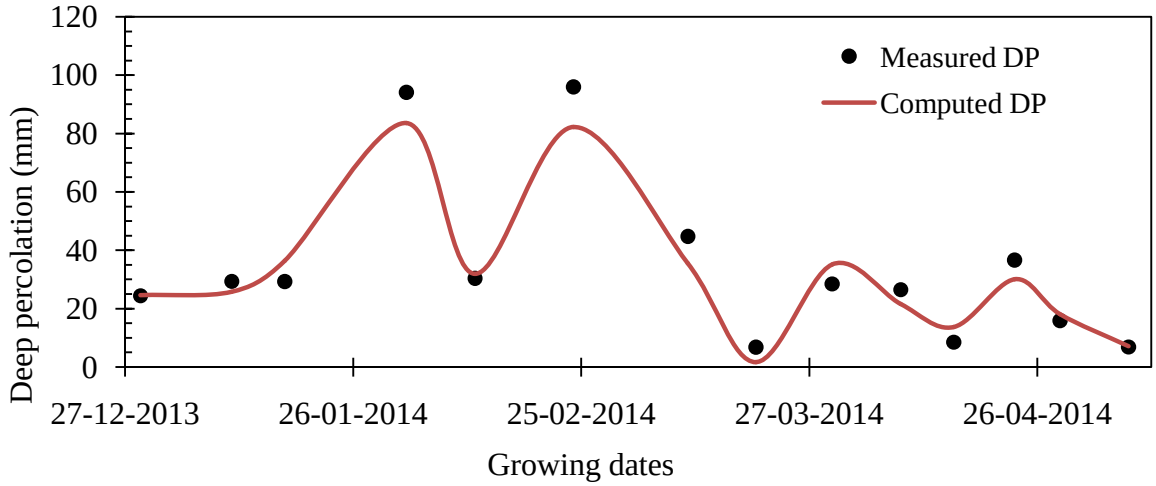

Fig. 4.32 Computed and measured deep percolation with lumped time steps in lysimeter 2 in berseem season 1

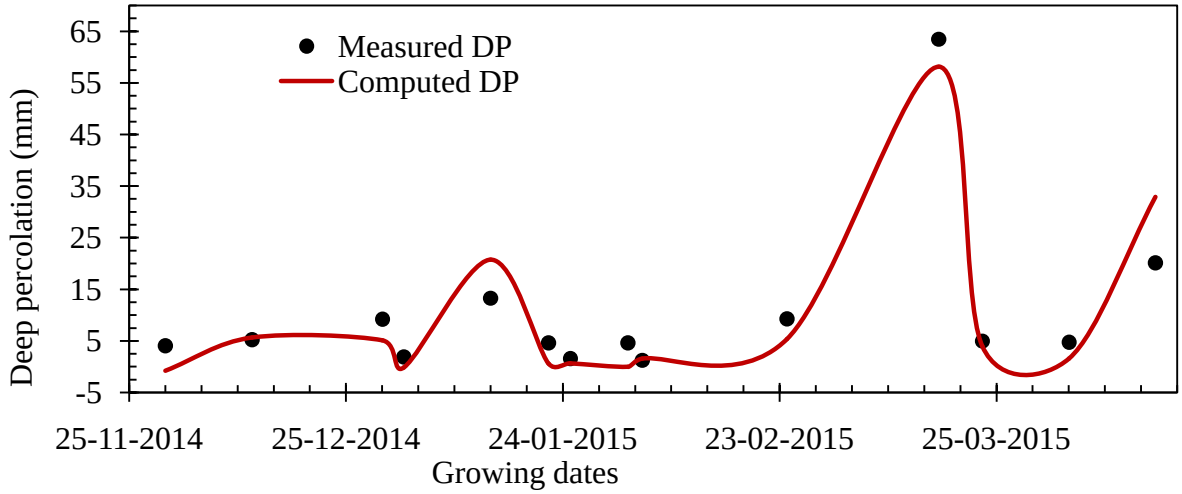

Fig. 4.33 Computed and measured deep percolation with lumped time steps in lysimeter 1 in berseem season 2

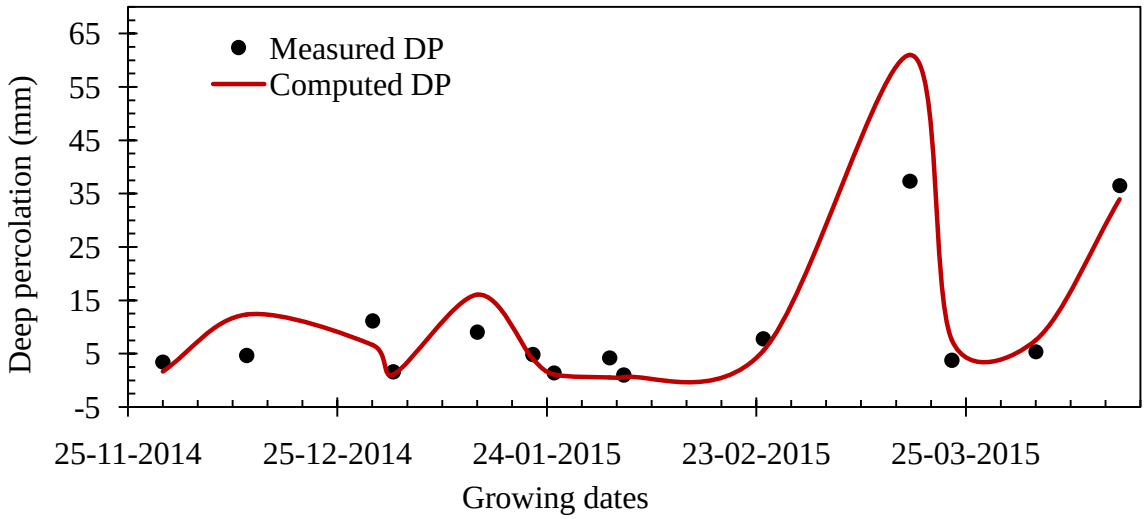

Fig. 4.34 Computed and measured deep percolation with lumped time steps in lysimeter 2 in berseem season 2

It is evident from the analysis that the performance of the water balance model is better when lumped time step is used than daily time step to compute the deep percolation. This would be attributable to different factors such as subsurface flow condition, observation point, model structure and limitations in the lysimeter facilities. The effect of these factors is discussed in section 4.8.3.

4.8.3 Discussion on Deep Percolation

The deep percolation computed using the water balance model on daily time step poorly agrees with the field measured daily deep percolation. This is partly due to the inherent nature of the model in which it assumes the deep percolation to occur on the day of event irrigation or rainfall. However, deep percolation may occur from soil moisture storage even after rainfall or irrigation. Flow may also occur in reverse direction (upwards) from saturated bottom layers in response to evapotranspiration. This may be taken as negative percolation (Watanbe et al. 2004). Flury et al. (1999) have investigated that the soil moisture content near the bottom of lysimeters is nearly saturated. This condition favours upward flow from lower layers in response to evapotranspiration on specific non wetting dry days. Watanabe et al. (2004) also have observed the upward water flow from deeper layers in the dry season in actual field conditions in Northern Thailand. On the other hand, measured deep percolation in drainage type lysimeters is always positive and hence a discrepancy arises between the measured and computed deep percolation based on daily time step. The computed deep percolation on lumped time step showed a good agreement with the measured deep percolation.

The discrepancy between the measured and computed percolation, on daily time step may also be attributed to limitations in the lysimeter water balance, disregarding of the variability in soil hydraulic property, and non consideration of lysimeter edge flow effects. The limitations in the lysimeter water balance can be expressed in terms of the spatial domain under consideration for the water balance. While the water balance equation computes deep percolation right at the bottom of the dynamic crop root zone, observations of deep percolation in lysimeters were made at lysimeter outlets well below the bottom of crop root zones. The crop root depths in both crop seasons were observed to be shallow (Fig. 3.24). The assumption is that the water that leaves the bottom of the root zone reaches the lysimeter outlets. Recently, Ochoa et al. (2013) have made similar assumption to estimate ground water recharge from irrigated fields using the water balance method. Had the observation of water fluxes been made at the bottom of the crop root zones, the performance of the model on daily time step would have been more accurate; however, such an observation is practically very difficult. The subsurface flow dynamics in the crop root zone is also affected by soil retention and hydraulic characteristics which are not considered in the water balance approach. Particularly, the temporal and spatial variability in hydraulic conductivity arising due to variability in water content or pressure head was not taken into account. Physically based modelling approach might be employed to capture the subsurface flow processes but this demands huge amount of input data. In addition, edge effects in drainage type lysimeters might have also contributed to the poor performance of water balance model with daily time step. Edge effects in lysimeters favour more preferential transport than natural flow condition under normal field conditions which may affect the soil moisture storage condition in the root zone (Abdulkareem et al. 2015). However, these effects may get diminished due to time lumping because individual errors in the water balance components may possibly cancel each other (Hatiye et al. 2016).

Deep percolation could take place starting from the day of triggered irrigation or rainfall occurrence to the next consecutive days (Wang et al. 2012; Liu et al. 2006). Wang et al. (2012) illustrated the temporal variation of deep percolation from root zones of irrigated summer corn and winter wheat on silt loam soil employing both water and isotope mass balance methods. They showed that for event irrigation, deep percolation was the maximum on the first day after irrigation and decreases quickly until it ceases on the eighth day after irrigation. This result agrees with our lysimeter experiments particularly for berseem growing season. Deep percolation becomes maximum on the first or second day after irrigation/ rainfall and then decreases until it becomes negligibly small as illustrated in the field lysimeter experiments in this study. However, this condition did not regularly reproduce during the rice growing season

when irrigation was frequently applied. In rice season, deep percolation becomes maximum on the day of irrigation/rainfall owing to the wetter antecedent moisture conditions except in few cases (when it becomes at pick on the first day after irrigation or rainfall). Liu et al. (2006) also showed that deep percolation follows a characteristic decay curve after a wetting event.

An insight into daytime and nocturnal percolation also shows some characteristic difference. Typically, deep percolation occurred on day time was less than that occurred during night time in both crop seasons which is attributable to the effect of evapotranspiration during day time. For example, the measured seasonal deep percolation in lysimeter 2 in the morning (night time deep percolation) in rice 1 and berseem 1 seasons were, respectively, 1527.05 mm and 258.43 mm while it was 998.81 mm and 220.06 mm in the evening (day time deep percolation). Similar trends were also observed during the growing seasons and lysimeter 1 conditions. Figs. 4.35 and 4.36 show, as a typical example, the measured deep percolation in the two lysimeters in berseem 1 and rice 2 crop seasons due to specific irrigation and rainfall events.

During the crop periods, the deep percolation event was observed to strictly follow the input water pattern. Occurrence of intense storms caused high deep percolation than event irrigations (Figs. 4.9 and 4.10). For example, during rice growing season 1, an intense downpour of magnitude 126.5 mm on 06 August, 2013 caused 113 mm percolation on that day. Similarly, a heavy rainfall event of 43.5 mm in berseem one season caused a deep percolation depth of 42.6 mm on February 15, 2014. Such storm events were often observed to be accompanied by showers of an earlier date satisfying soil moisture storage to its field capacity and above. Therefore, almost all the rainfall which occurs after such consecutive wetting occurrences were evolved as deep percolation. Kendy et al. (2004), for example, have indicated that long-term pattern of groundwater recharge has closely followed that of irrigation while short-term perturbations in the recharge pattern are responses to precipitation, which fluctuates greatly from year to year, and periodically generates significant pulses of groundwater recharge. Since, the wetting events during the rice seasons were frequent (Fig. 4.9); the soil was remained above field capacity for most of the growing period and hence large deep percolation values were observed. Generally, deep percolation showed a decreasing trend from the monsoon season (July-September) to late season stage of the crop season (October-November) in the rice period. The decreasing trend would be due to the coupled effects of reduced irrigation size, irrigation frequency and the receding of monsoon season. In particular case of berseem crop seasons, deep percolation was fairly modified by soil moisture deficit.

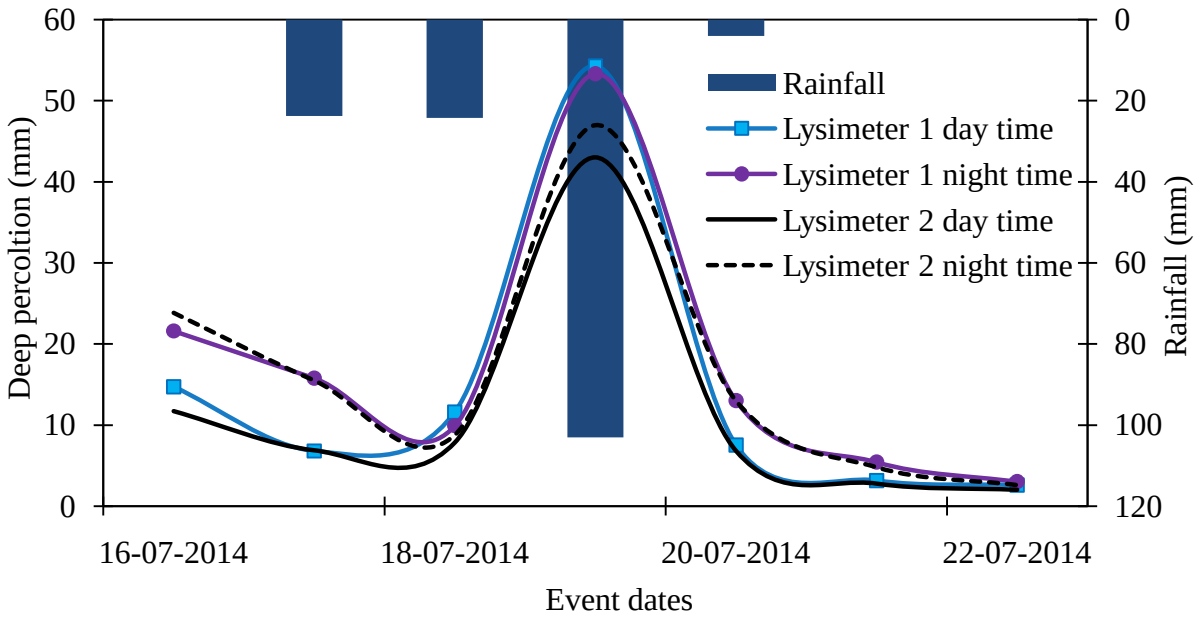

Fig. 4.35 Typical rainfall events and deep percolation measured during day and night times in the two lysimeters during rice 2 growing season.

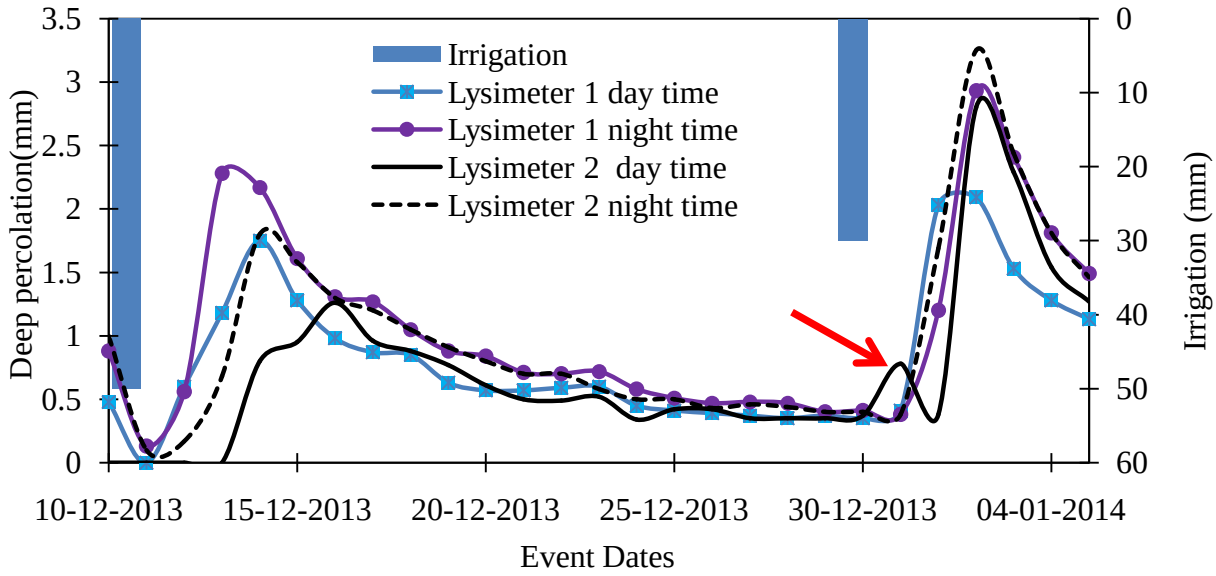

Fig.4.36 Typical event irrigation and deep percolation measured during day and night times in the two lysimeters during berseem 1 growing season: arrow shows preferential flow shock after irrigation application in the lysimeter 2 measured in the evening.

4.8.4 Statistical Parameters

Statistical parameters have been employed to test the performance of the water balance model in evaluating the deep percolation both on daily and lumped time steps. Three parameters including coefficient of determination (R^2), root mean square error (*RMSE*) and

coefficient of variation (*COV*) as used in (Liu et al. 1998; Cholpankulov et al. 2008; Shankar et al. 2012) have been employed in this study. A value of R^2 close to unity indicates a high degree of association between the observed and simulated values or shows that most of the total variance of the observed values is explained by the model. The *COV* quantifies the amount of random scatter of the simulated and measured values about 1:1 line and *RMSE* characterises the variance of the estimation errors. As errors are squared before they are averaged, the *RMSE* gives a relatively high weightage to large errors. The respective statistical parameters are defined below.

$$R^2 = \left\{ \frac{\sum_{i=1}^{n} \left(DP_{oi} - \overline{DP_o}\right)\left(DP_{ci} - \overline{DP_c}\right)}{\left[\sum_{i=1}^{n} \left(DP_{oi} - \overline{DP_o}\right)^2\right]^{0.5} \left[\sum_{i=1}^{n} \left(DP_{ci} - \overline{DP_c}\right)^2\right]^{0.5}} \right\}^2 \tag{4.13}$$

$$RMSE = \left[\frac{\sum_{i=1}^{n} \left(DP_{ci} - DP_{oi}\right)^2}{n} \right]^{0.5} \tag{4.14}$$

$$COV = \frac{1}{\overline{DP_o}} \left[\sum_{i=1}^{n} \frac{\left(DP_{oi} - DP_{ci}\right)^2}{n} \right]^{0.5} \tag{4.15}$$

where DP_{oi} and DP_{ci} are, respectively, observed and model computed values of deep percolation with the respective means $\overline{DP_o}$ and $\overline{DP_c}$; n refers to the number of sample data points. Statistical parameters for the model during the crop seasons for both lysimeters are shown in Table 4.3.

Table 4.3 Statistical parameters for the crop periods and lysimeters for daily and lumped time steps

Crop season	Location	Seasonal percolation(mm)		Daily deep percolation			Deep percolation based on lumped time step		
		Measured	Computed	R^2	*RMSE* (mm)	*COV*	R^2	*RMSE* (mm)	*COV*
Rice season1	L1	2668.83	2681.30	0.22	24.20	0.94	0.87	43.30	0.24
	L2	2525.86	2674.30	0.18	24.70	1.00	0.90	38.00	0.23
Rice season 2	L1	937.19	952.73	0.44	12.80	1.40	0.77	27.60	0.37
	L2	1064.16	980.06	0.62	10.30	0.98	0.89	19.40	0.23
Berseem season 1	L1	522.79	447.20	0.03	12.61	3.57	0.96	8.41	0.60
	L2	478.49	447.77	0.08	11.94	3.69	0.96	6.64	0.47
Berseem season 2	L1	148.15	135.14	0.30	4.79	4.90	0.91	5.05	0.48
	L2	132.27	159.70	0.42	5.13	5.86	0.86	7.24	0.77

As can be seen from the error statistics from Table 4.3 that the performance of the model on daily time step is poor owing to the model structure in which it assumes deep percolation occurs only on the day of irrigation or rainfall. In fact, deep percolation takes place whenever the soil water content is above the field capacity. On the other hand, deep percolation computed on lumped time steps, weekly for rice season and between two consecutive wetting intervals in the berseem season, yields better estimation of deep percolation when compared to measured deep percolation. The other reason that could be mentioned is that, the point of measurement for drainage in the lysimeters is located well below the rooting depths in which there is some time needed for the draining water to reach to the outlet point. Therefore, the measured and computed percolation on daily time step, for the considered model domain of lysimeter monolith, yields poor agreement. But the measured and computed percolations agree well on lumped time step since the percolating water gets adequate time to arrive at lysimeter outlets.

Similar water balance computations making use of independently measured soil moisture data, outside the lysimeters, were also made for each field plot (A11–A14) particularly for rice season 1 and berseem season 1 periods during which time similar water applications were maintained in the lysimeters and in all the field plots (A11-A14) in each crop

season. The time step considered for accumulating percolation in rice season was seven days and between wetting intervals in the berseem season. There is good agreement between the observed DP in the lysimeters and computed DP in the field plots. Tables 4.4 to 4.7 show error statistics between the observed and computed deep percolation for rice season 1 and berseem season 1 periods. R^2 values ranging between 0.87 to 0.89 in rice season 1 and 0.96 to 0.98 in berseem season 1 period were observed. It is evident that the quantity of deep percolation in the field plots estimated using the model approximately reproduces the measured deep percolation in the lysimeters. Percolation near field boundaries and tail ends of irrigated fields is not the case in this study which has been dealt elsewhere. Field conditions in central and head ends of an irrigated plot could emulate our experimental field condition.

Table 4.4 Statistical parameters for computed deep percolation in field plots when compared with lysimeter 1 deep percolation in rice season 1

Location	Seasonal percolation		Statistical parameters		
	Measured	Computed DP	R^2	*RMSE* (mm)	*COV*
L1	2668.83	2681.30	0.87	43.30	0.24
A11	-	2667.50	0.89	37.70	0.21
A12	-	2664.30	0.89	39.30	0.22
A13	-	2668.70	0.88	40.10	0.23
A14	-	2668.40	0.88	39.70	0.22

Table 4.5 Statistical parameters for computed deep percolation in field plots when compared with lysimeter 2 deep percolation in rice season 1

Location	Seasonal percolation (mm)		Statistical parameters		
	Measured	Computed	R^2	*RMSE* (mm)	*COV*
L2	2525.86	2674.30	0.90	38.00	0.23
A11	-	2667.50	0.90	37.10	0.22
A12	-	2664.30	0.90	38.50	0.23
A13	-	2688.70	0.89	39.20	0.23
A14	-	2668.40	0.89	39.00	0.23

Table 4.6 Statistical parameters for computed deep percolation in field plots when compared with lysimeter 1 deep percolation in berseem season 1

Location	Seasonal percolation (mm)		Statistical parameters		
	Measured	Computed	R^2	*RMSE* (mm)	*COV*
L1	522.79	447.20	0.96	8.41	0.60
A11	-	455.08	0.97	7.56	0.54
A12	-	456.21	0.96	7.79	0.56
A13	-	449.16	0.97	7.72	0.55
A14	-	455.15	0.95	8.47	0.61

Table 4.7 Statistical parameters for computed deep percolation in field plots when compared with lysimeter 2 deep percolation in berseem season 1

Location	Seasonal percolation (mm)		Statistical parameters		
	Measured	Computed	R^2	*RMSE* (mm)	*COV*
L2	478.49	448.00	0.96	6.64	0.47
A11	-	455.08	0.97	5.88	0.42
A12	-	456.21	0.97	6.19	0.44
A13	-	449.16	0.98	5.84	0.42
A14	-	455.15	0.96	7.00	0.50

4.8.5 Stage wise Deep Percolation

Deep percolation in different crop development stages during the rice season and between individual cutting intervals for berseem crop have also been computed using the water balance model as shown in Table 4.8. In the initial and crop development stages of rice season, the largest volume of deep percolation was observed while the lowest volume of percolation occurred in the late season. This might be mainly due to the occurrence of intense storms in the initial and development seasons and the receding of monsoon in the late season of the crop besides the reduced size of irrigation application. During the berseem season 1, the largest volume of deep percolation was recorded before the first cutting period. The period from sowing up to the first cutting was characterized by high humidity and low temperatures resulting in low evapotranspiration rates, besides relatively sporadic heavy rainfall events, favoured more deep percolation in the period. In contrast, the interval between the first and

second cut season was characterised by low deep percolation and large green forage production which would be attributed to relatively larger root water uptake in the interval. Contrarily, in berseem season 2, heavy rain events were shifted to the end of the crop season and hence more rate of percolation occurred in the interval between third and fourth cutting periods. In general, consideration of irrigation schedules which limit water application in the initial and development periods of the rice field could reduce deep percolation. Since berseem is sown on or before the cold winter in the area, application of water before the first cut produces more percolation loss. Hence, limiting water application depth and its rate until first cut would benefit in reducing deep percolation.

Table 4.8 Comparison of field observed and model computed deep percolation in crop growth stages and individual cutting intervals

Crop season	Crop growth stage/ cutting intervals	Lysimeter 1		Lysimeter 2	
		Measured	Computed	Measured	Computed
Rice season 1	Initial	512.11	585.11	497.07	607.41
	Development	1050.67	1066.52	1029.10	1039.15
	Mid season	828.05	811.22	759.53	813.80
	Late season	278.00	218.45	240.16	213.94
Rice season 2	Initial	351.91	294.85	339.90	301.21
	Development	171.84	228.27	242.33	222.36
	Mid season	342.88	392.06	406.86	406.75
	Late season	70.56	37.56	75.07	49.73
Berseem 1	sowing to cutting No 1	310.54	283.93	299.01	285.77
	cutting No 1 to cutting No 2	63.77	37.37	55.57	37.52
	cutting No 2 to cutting No 3	71.85	100.82	56.71	102.21
	cutting No 3 to cutting No 4	76.63	25.09	67.20	22.26
Berseem 2	sowing to cutting No 1	46.08	37.32	41.86	50.60
	cutting No 1 to cutting No 2	60.57	51.59	37.71	52.87
	cutting No 2 to cutting No 3	18.79	11.83	12.88	20.10
	cutting No 3 to cutting No 4	22.71	34.40	39.82	36.13

4.9 PERFORMANCE OF THE LYSIMETERS

The performance of the two lysimeters in metering deep percolation has also been investigated. Figs. 4.37 and 4.38 present the relation between the measured deep percolation in the two lysimeters during rice season 1 and berseem season 1 growing periods. The same amount of input water was applied or occurred in both lysimeters in these growing seasons. It has been seen that the amount of deep percolation from both lysimeters is fairly similar

showing the repacked soil monolith exhibits fairly same property in both lysimeters particularly during the non-storm periods. During storm periods, however, the lysimeters were observed to demonstrate variations in allowing percolation. This may be due to the fact that the lysimeters portray differences in preferential flow which is significant during the rainy seasons. Specific events of preferential flow (Fig. 36) were observed in the lysimeters which could not be avoided from field as well as lysimeter monoliths (Tournebize et al. 2006; Garg et al. 2009). Thus we deduce from these results that locally constructed drainage type lysimeters could owe better understanding of deep percolation phenomena in an irrigated farm.

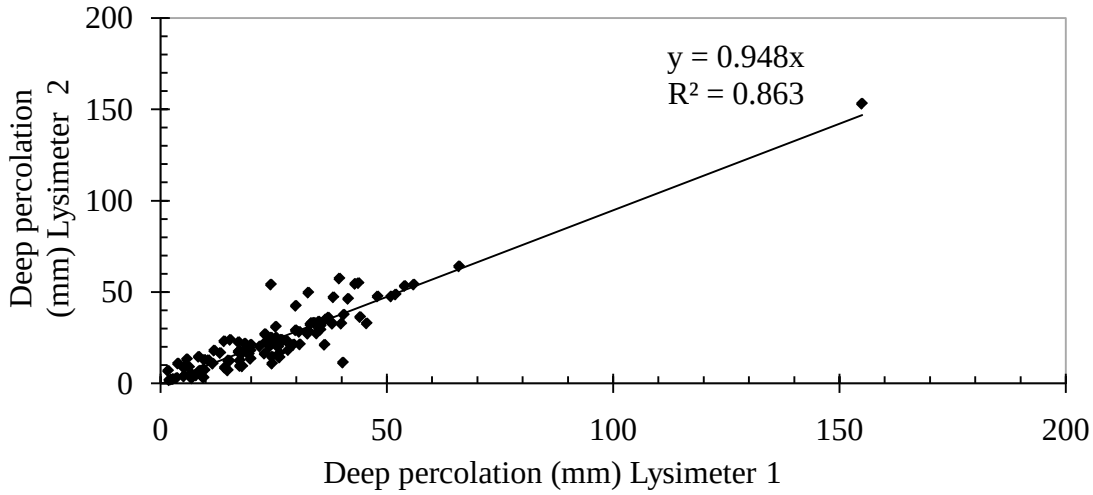

Fig. 4. 37 Correlation between measured deep percolations in the lysimeters in rice season 1

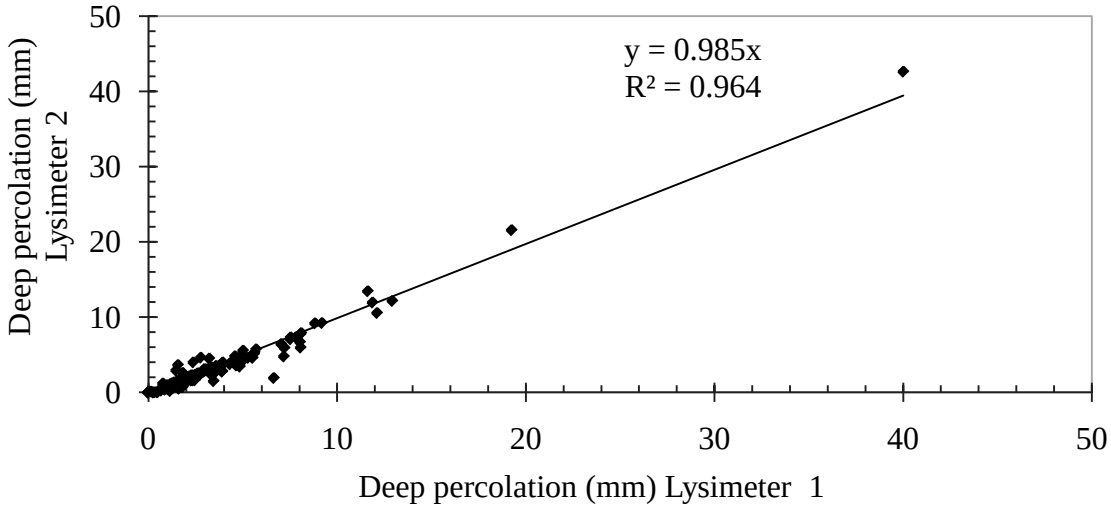

Fig. 4.38 Correlation between measured deep percolations in the lysimeters in berseem season 1

4.10 SEASONAL WATER BALANCE

The total amount of water balance components in each crop periods is provided in Tables 4.10 and 4.11. The computed actual evapotranspiration is fairly similar in the two rice

seasons, despite the large differences in the seasonal water input. During berseem seasons, however, there is large variation of evapotranspiration owing to large gap in dates of sowing. It can be inferred from the seasonal water balance that the seasonal soil moisture storage is dependent on input water and crop season. In rice season 1, only slight change in seasonal soil moisture storage is observed while in rice season 2, large changes in soil moisture storage are attributed to reduced irrigation application indicating accumulated soil moisture deficits. Similarly, in berseem season 1 relatively large change in seasonal soil moisture is attributed to comparatively increased evaporative demand of the growing season than berseem season 2.

The overall share of deep percolation in the water balance is quite large. Table 4.10 and 4.11 present the computed and measured deep percolation values along with other water balance components of the two crop seasons. During the continuous irrigation season of rice, nearly 82-87 % of input water has been returned as deep percolation while in the intermittent irrigation season; approximately 77-80% of the overall input water has been lost through deep percolation. For coarse textured soils, nearly similar value of percolation has been reported (Sudhir-Yadav et al. 2011; Bouman et al. 2007a). In coarse textured soils with deep groundwater table (more than 1.5 m) deep percolation can account for 50 - 85% of input water (Bouman et al. 2007a). Bouman et al. (2007b) reported that around 70% of input water could go for percolation loss when groundwater depth is equal to or more than 2 m in rice fields in Northern China. Sudhir-Yadav et al. (2011) observed that about 81% of water added was drained beyond the root zone (0–60 cm) with continuously flooded rice in clay loam soil. Dewandel et al. (2008), on the other hand, explained that the flooded type irrigation of rice fields can contribute more than 50% of applied irrigation water as deep percolation return flow in sandy clay loam soils. However, almost all these cases of research outputs were obtained considering the presence of a puddled layer below the root zone of rice crop. In fact, the efficacy of puddling in reducing percolation depends greatly on soil properties and the operation itself also requires additional water. Puddling practice may not be effective in coarse textured soils (Bouman et al. 2007a) while it is very efficient in clay soils (Tuong et al. 1994). Unfortunately, studies on deep percolation involving berseem fodder are not available.

While deep percolation is large during frequent irrigation of the rice season, it is comparatively less during berseem season owing to the intermittent irrigation application and reduced rainfall. Respectively, 67.4% and 61.8% of input water was lost through deep percolation during berseem season 1 in lysimeters 1 and 2. Due to the imposed irrigation schedule, deep percolation was reduced to 52.2% and 42.3% of input water in lysimeters 1 and 2, respectively, during berseem season 2.

Tables 4.9 and 4.10 show the seasonal water balance in both crop seasons in the experimental field.

Table 4.9 Seasonal water balance for rice seasons

Crop season	Location	Irrigation (mm)	Rainfall (mm)	Deep Percolation (mm)		Actual ET(mm)	Soil moisture storage (mm)
				computed	measured		
Rice season 1	L1	2418.8	659.3	2681.30	2668.83	410.99	-14.29
	L2	2418.8	659.3	2674.30	2525.86	410.91	-7.11
	A11	2418.8	659.3	2667.50	-	408.64	1.96
	A12	2418.8	659.3	2664.30	-	411.72	2.08
	A13	2418.8	659.3	2668.70	-	411.72	-2.32
	A14	2418.8	659.3	2668.40	-	411.62	-1.92
Rice season 2	L1	630	532.9	952.73	937.19	431.5	-221.33
	L2	851	532.9	980.06	1064.16	414.04	-10.20
	A11	643.1	532.9	952.06	-	430.87	-206.93
	A12	639	532.9	962.29	-	430.91	-221.30
	A13	855	532.9	952.98	-	431.05	3.87
	A14	644	532.9	958.24	-	430.62	-211.96

Table 4.10 Seasonal water balance for berseem

Crop season	Location	Irrigation (mm)	Rainfall (mm)	Deep Percolation (mm)		Actual ET (mm)	Soil moisture storage (mm)
				Computed	Measured		
Berseem season 1	L1	550	225.8	447.20	522.79	342.36	-13.76
	L2	550	225.8	448.00	478.49	341.38	-13.58
	A11	550	225.8	455.08	-	341.38	-20.66
	A12	550	225.8	456.21	-	342.36	-22.77
	A13	550	225.8	449.16	-	342.36	-15.72
	A14	550	225.8	455.15	-	342.36	-21.71
Berseem season 2	L1	63.1	220.8	135.14	148.15	162.81	-14.05
	L2	91.9	220.8	159.7	132.27	162.62	-9.62
	A11	175.1	220.8	243.96	-	162.81	-5.87
	A12	164.5	220.8	229.32	-	162.81	-1.83
	A13	127	220.8	194.83	-	162.81	-4.84
	A14	127	220.8	199.15	-	162.81	-9.16

4.11 CLOSURE

The water balance model has been modified to consider soil moisture change based on crop root growth in the respective crop growing periods. The deep percolation computed on daily time step using the measured input data on irrigation, rainfall and root zone soil moisture in both crop periods did not agree well with the daily measured deep percolation using drainage type lysimeters. However, the cumulative deep percolation calculated in a lumped time step (weekly basis) during the rice and between the wetting intervals during the berseem seasons agrees well with the measured cumulative deep percolation in the lysimeters. This would be partly due to the fact that more time is needed for water flow to arrive at lysimeter bottom which is well below the crop root zones. On the other hand, the model is structured in such a way that deep percolation occurs on the day of irrigation or rainfall, which produces an error when the model is applied to drainage type lysimeters having depths in the range of more than 1 meter. Further, disregarding of the variability in soil hydraulic property and non consideration of lysimeter edge flow effects in water balance model also contributed for the poor performance of the model on daily time step. Therefore, it can be concluded that computations

of deep percolation using the water balance model can accurately be made on weekly time steps for frequently watered fields and between wetting intervals for intermittently wetted crop fields.

Large deep percolation from rice and berseem crop fields has been investigated in this study due to the soil texture and frequency of water application. Similar results were also reported in earlier studies although they were mainly dealing with the puddled rice field conditions. The deep percolation varies primarily in response to the input water depth and frequency of application/occurrence. Intense and continuous storms particularly caused high percolation rate and depth than applied irrigation in most of the observation periods owing to the saturated antecedent moisture conditions during and after these incidences. The deep percolation on day time was less than night time as can be verified from lysimeter measurements. This shows that evapotranspiration poses some influence on deep percolation.

Observed cumulative deep percolation in the lysimeters and computed deep percolation (on weekly and between wetting intervals for rice and berseem, respectively) using independent soil moisture content data from different field plots also show very good agreement. Percolation is characterized by a sort of decaying curve after certain peak value is achieved in response to input water. Such behaviour was also described by earlier researchers. It is concluded that locally constructed drainage type lysimeters are robust enough in monitoring deep percolation phenomena from crop root zones.

CHAPTER 5
ESTIMATING DEEP PERCOLATION USING PHYSICALLY BASED MODEL

5.1 PREAMBLE

In chapter four, the performance of water balance model in estimating deep percolation has been discussed in detail. It has been observed that the prediction of deep percolation on daily basis was not accurate owing to the simplification of root zone soil moisture dynamics.

In the present chapter, the performance of physically based numerical model in estimation of deep percolation is discussed. The root zone soil moisture is commonly analysed by solving the Richards (1931) equation governing water flow in the root zone (which is unsaturated in nature) and accounting the water uptake by roots as a sink term. For this purpose, HYDRUS-1D software package (Šimůnek et al. 2008) is employed. Recently, HYDRUS-1D has got wide acceptance in simulating the flow processes in the unsaturated zone including infiltration, percolation, root water uptake, soil moisture storage, evaporation, surface runoff etc. due to its versatility and adaptation to various conditions of the subsurface environment (Li et al. 2014). In the following sections, an overview of HYDRUS-1D software and its application in estimating deep percolation is discussed in detail.

5.2 WATER FLOW IN THE ROOT ZONE

Richards equation (1931) is commonly used to analyse soil moisture dynamics in the crop root zone with a sink term accounting for the uptake of water by the plant roots. The equation is basically derived from the concepts of conservation of mass and momentum. HYDRUS-1D uses the mixed form of Richards equation as (Šimůnek et al. 2008):

$$\frac{\partial \theta}{\partial t} = \frac{\partial}{\partial t}\left[K\left(\frac{\partial \psi}{\partial z} + \cos\beta \right) \right] - S \qquad (5.1)$$

where ψ is the pressure head [L], θ is the volumetric moisture content [L^3L^{-3}], t is time [T], z is the vertical coordinate [L] (positive upwards), S is the sink term [$L^3L^{-3}T^{-1}$], β is the angle between the flow direction and the vertical axis (i.e., β = 0° for vertical flow, β = 90° for horizontal flow and 0° < β < 90° for inclined flow), and K is the unsaturated hydraulic conductivity function [LT^{-1}] given by:

$$K(\psi, z) = K_{sat}(z) K_r(\psi, z) \qquad (5.2)$$

where $K_r(\psi,z)$ is the relative hydraulic conductivity [-] and $K_{sat}(\psi,z)$ is the saturated hydraulic conductivity [LT^{-1}].

Equation (5.1) describes a uniform water flow considering only the liquid phase in partially saturated rigid porous medium using the assumptions that the air phase plays an insignificant role in the liquid flow process and that water flow due to thermal gradients is neglected. The equation is highly non-linear since the independent variable (soil moisture content) and the hydraulic conductivity are functions of the dependent variable (pressure head). In order to solve equation (5.1), constitutive relationships between the dependent variable, θ, and non linear terms (ψ and K) have to be specified. In HYDRUS-1D, Brooks and Corey (1964), van Genuchten (1980), and Kosugi (1996) relationships are given. In the present study, van Genuchten (1980) constitutive relationships are used. The van Genuchten (1980) relationships are given as:

$$\theta(\psi) = \theta_r + \frac{\theta_s - \theta_r}{\left[1 + \left|\alpha_v \psi\right|^{n_v}\right]^m} \qquad \psi \le 0 \tag{5.3a}$$

$$\theta(\psi) = \theta_s \qquad \psi > 0 \tag{5.3b}$$

$$K(\psi) = K_{sat}\Theta^{0.5}\left[1 - \left(1 - \Theta^{1/m}\right)^m\right]^2 \tag{5.4}$$

where θ_s is the saturated moisture content [L^3L^{-3}]; θ_r is the residual moisture content [L^3L^{-3}]; m, α_v [L^{-1}] and n_v are empirical shape factors in the water retention function with $m = 1-1/n_v$. m and n_v are dimensionless parameters. Θ (dimensionless) is the effective saturation which is defined as follows:

$$\Theta = \frac{\theta - \theta_r}{\theta_s - \theta_r} \tag{5.5}$$

5.3 HYDRUS-1D SOFTWARE

The one-dimensional HYDRUS-1D computer program (Šimůnek et al. 2008) has been used to simulate water movement in this study. Since the flow in the soil profile is predominantly in the vertical direction for coarse textured soils (Ji et al. 2007), the one dimensional vertical flow solution by HYDRUS-1D is taken as adequate for simulating flow in the soil root zone of the experimental field. HYDRUS-1D program numerically solves the Richards equation for variably saturated water flow, the convection-dispersion equations for heat and solute transport (Li et al. 2014). It solves the equation using standard Galerkin-type linear finite element scheme. The flow equation also incorporates a sink term to account for root water uptake by plants. A number of modifications were made to this particular software package since its first release (HYDRUS-1D version 1). In this study, HYDRUS-1D version 4.16.0110 (Šimůnek et al. 2008) has been employed. Comprehensive discussions on model

development, calibration and validation procedures using HYDRUS-1D is provided in Šimůnek et al. (2012).

HYDRUS-1D owes interactive graphics-based user-friendly interface for the Microsoft windows environment and its interface is directly connected to the HYDRUS-1D computational programs. Problems with regard to large input data preparation, grid design and graphical presentation of the output results have been greatly simplified (Šimůnek et al., 2013). Various program units/modules are included in the package. HYDRUS-1D is the main program unit defining the overall computational environment of the system which controls the execution of the program and determines other optional modules required for a particular application. It contains a project manager and both the pre-processing and post-processing units. The pre-processing unit includes specification of all the necessary parameters to successfully run the HYDRUS FORTRAN codes, a catalogue of soil hydraulic properties, and plant salt tolerance database. The post-processing unit, alternatively, consists of simple x-y graphics for graphical presentation of soil hydraulic properties and transient output values of a particular variable (such as pressure head and water content) at selected observation points in the domain, and actual or cumulative water and solute fluxes across the boundaries (Šimůnek et al. 2013).

5.4 APPLICATIONS OF THE HYDRUS-1D PACKAGE

Few list of applications of HYDRUS-1D package for actual field and laboratory conditions has been presented in this section referring to recent publications. Garg et al. (2009) have employed the HYDRUS-1D package on puddled transplanted rice fields to study soil water regime considering preferential transport. They used Marquardt-Levenberg algorithm built in the HYDRUS-1D simulation environment to inversely estimate soil hydraulic parameters. Jiang et al. (2010) studied water flow and bacterial transport in undisturbed lysimeters under irrigations of dairy shed effluent and water using HYDRUS-1D. Soylu et al. (2011) compared different models to quantify the impact of groundwater depth on evapotranspiration in semi arid grassland including HYDRUS-1D, Integrated Biosphere Simulator (IBIS) and two forms of a steady-state capillary flux model coupled with a single-bucket soil moisture model. In general, they found out that all the models were compared reasonably well with the observations, particularly when the effect of groundwater is included. Ramos et al. (2011) evaluated a multi-component solute transport water flow in soils irrigated with saline waters in Portugal using HYDRUS-1D package. Here also the authors reported the success story of the model to simulate root water and nutrient uptake reductions due to osmotic

stress proving it to be a powerful tool for analyzing solute concentrations related to overall soil salinity and nitrogen species.

Sutanto et al. (2012) have utilized the HYDRUS-1D model for partitioning of evaporation into transpiration, soil evaporation and interception. They have obtained comparable results of the component processes investigated with that of the isotope mass balance method. Tafteh and Sepaskhah (2012) applied HYDRUS-1D model for simulating water and nitrate leaching from continuous and alternate furrow irrigated rapeseed and maize fields in Fars province, Iran. Again, in this particular case it has been shown that HYDRUS-1D model can simulate deep percolation water and NO_3-N leaching with a very good accuracy. Mavimbela and van Rensburg (2013) used analytical models and inverse application in the HYDRUS-1D and internal drainage experiments to estimate in situ hydraulic conductivity in Bloemfontein (South Africa) and found out adequate results.

Li et al. (2014) used HYDRUS-1D package to evaluate water movement and water losses in a direct-seeded rice field experiment. Tan et al. (2014) simulated soil water regime in lowland rice fields under different water managements (continuous flooding and alternate wetting and drying (AWD) irrigation application) using HYDRUS-1D in China. They showed that HYDRUS-1D model can properly simulate the water flow in multi-layer rice field by employing the inverse simulation approach embedded in the HYDRUS-1D. Tan et al. (2015) further extended their study to analyse the fate of water flow and nitrogen transport in lowland rice fields under different water management conditions using HYDRUS-1D. The model successfully enabled to figure out the effect of alternate wetting and drying (AWD) and continuous irrigation practices on water flux and nitrogen movement. Han et al. (2015) have coupled HYDRUS-1D with a crop growth model to evaluate the impact of groundwater on cotton growth and root zone water balance. They have also showed that HYDRUS-1D is a powerful modelling tool for evaluating the effects of groundwater table on local land management.

Recently, Gonzalez et al. (2015) have used HYDRUS-1D model to simulate soil water dynamics of full and deficit irrigated (drip systems) maize crop grown under a rainout shelter during two crop seasons in Brazilian conditions. The HYDRUS-1D model successfully simulated the temporal variability of soil water dynamics in the treatments irrigated with full and deficit irrigation as demonstrated in the study. A number of applications of HYDRUS-1D package for various problems ranging from controlled laboratory studies to complex field conditions from various parts of the world, different soil, climate, water management and solute transport conditions can be listed. The software package also consists of single porosity, dual

porosity as well as dual permeability modelling approaches. Single porosity approach has been utilized in this study.

5.5 THE NUMERICAL MODEL

HYDRUS-1D solves the Richards equation numerically by employing finite element approach. To solve the flow problem in the root zone, required input parameters, space and time descritization, initial and boundary conditions are required to be defined.

5.5.1 Model Inputs and Parameters

Depending on a specific model, model inputs are required to run the model. In this study, model inputs and parameters required to compute the flow flux at the bottom of lysimeters are discussed in the following sessions.

5.5.1.1 Spatial and temporal descritization

For numerical solution of the problem, the flow domain consisting layered soil configuration as described using soil hydraulic parameters has been considered. In fact, the United States Department of Agriculture (USDA) textural classification of the experimental field soil shows uniform sandy loam texture fairly distributed to a depth up to 1.4 m (section 3.9.3). However, this does not mean that the soil hydraulic characteristics are equally similar. It can be noted that the same soil texture may have different soil hydraulic and retention characteristics given that the textural classification is determined based on a range of values than specific magnitudes of soil properties. Earlier studies in the experimental field assumed homogeneous soil material in the root zone (Shankar et al. 2012; Ram et al. 2012) based on textural classification. However, no extensive experiments on soil hydraulic and retention parameters in the crop root zone were carried out in the earlier studies to distinguish soil heterogeneity.

The whole flow domain is divided into layers, based on the soil hydraulic parameters and has been provided as geometry information in the model environment. The 135 cm soil monolith in the lysimeters is divided into 1 cm nodal points using the soil profile-graphic editor module in the HYDRUS-1D package. Observation points were assigned for specific depths where percolation and moisture content values were observed in the field. Fig. 5.1 presents the soil profile with mesh points and material configuration used during preliminary model run for lysimeters in this study.

A temporal descritization of 0.001 day (1.44 minutes) for initial time step has been considered for each crop season. However, output values for pressure, water content and

percolation were computed on daily time basis for the total length of growing periods. The total length of growth periods for each crop season was provided in chapter three and Table 3.12.

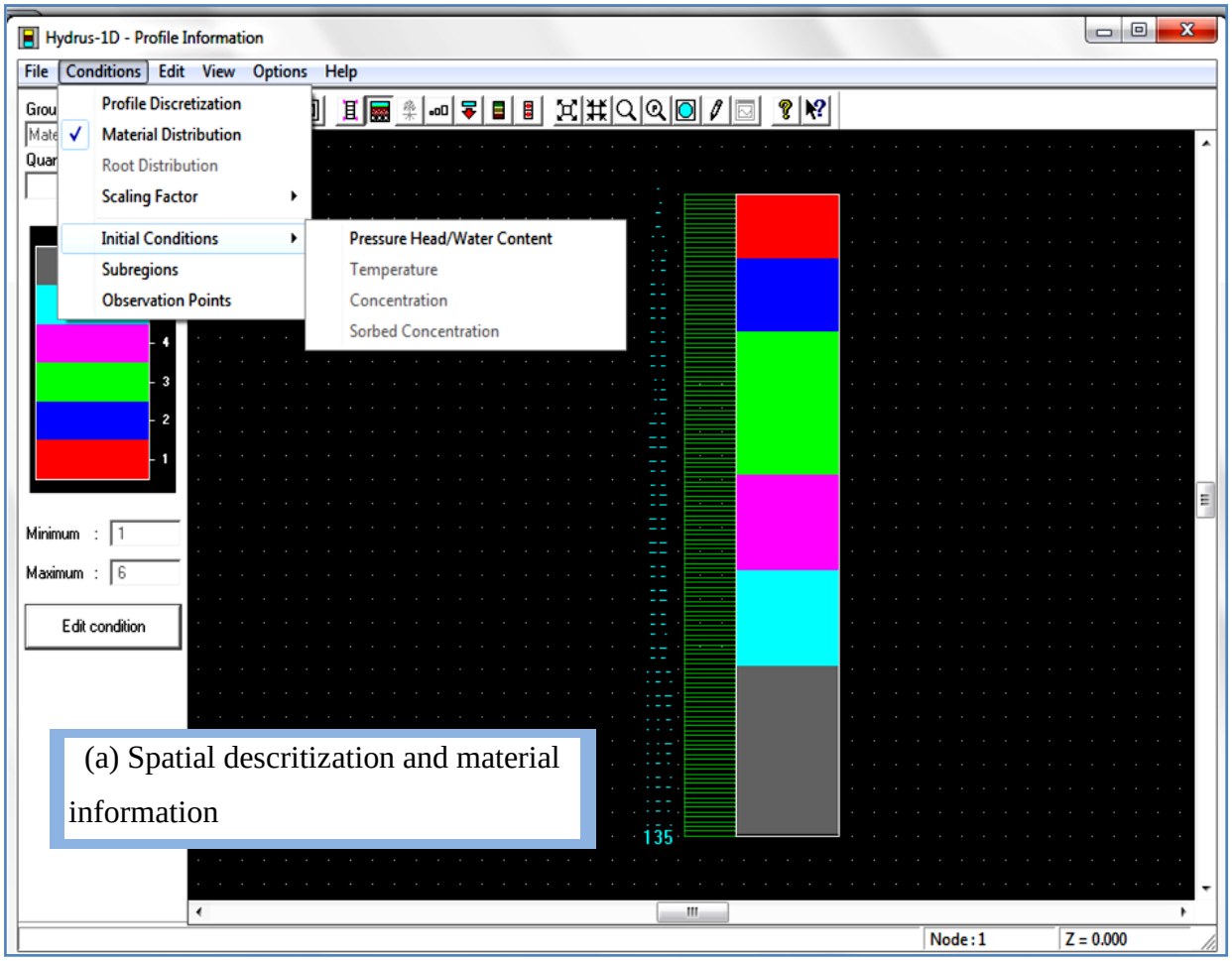

(a) Spatial descritization and material information

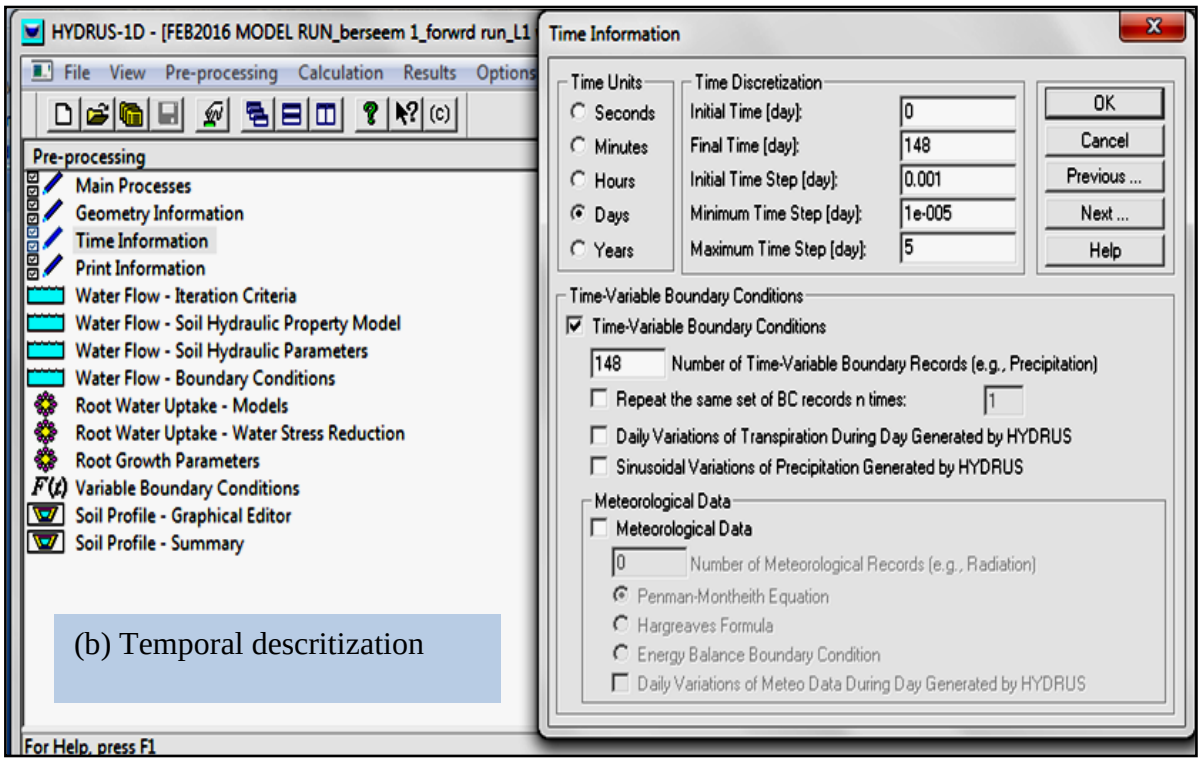

Fig. 5.1 (a) Model profile descritization and material distribution (b) time descritization and HYDRUS-1D model environment

5.5.1.2 Soil hydraulic parameters

The van Genuchten soil hydraulic parameters, θ_r, θ_s, n_v, and α_v(1/cm) required by the model were estimated using the RETC code by fitting the retention data and saturated hydraulic conductivity obtained from field observations were used for preliminary model run. The preliminary model simulation was conducted using measured data. Table 5.1 provides the data used in preliminary model simulations.

Table 5.1 Soil hydraulic parameters used in preliminary model runs

Soil depth (cm)	θ_r	θ_s	α_v (1/cm)	n_v	K_{sat} (cm/day)
0-15	0.049	0.357	0.016	1.493	209.0
15-30	0.046	0.399	0.006	1.741	118.0
30-60	0.043	0.381	0.006	1.741	118.0
60-80	0.034	0.390	0.013	1.545	106.10
80-100	0.046	0.399	0.022	1.366	106.10
100-135	0.046	0.391	0.018	1.473	106.10

5.5.2 Initial Condition

Initial conditions characterising the initial state of the soil root zone can be specified either in terms the water content or pressure head. Initial conditions are required to be defined before model simulation or the start of crop season to run the HYDRUS-1D model. In this study, measured water content values were used as initial condition.

$$\theta(z,t) = \theta_i(z,0) \qquad for \;\; 0 \le z \le L \qquad (5.6)$$

where θ_i (cm^3cm^{-3}) is the initial soil moisture content measured at the start of model simulation (before transplanting rice or sowing berseem crops), z (cm) is the root zone depth and L(cm) the length of flow domain. Moisture content values were observed at specific depths below the ground at observation points. The moisture content values for the other nodal points were determined by interpolation.

5.5.3 Boundary Conditions

5.5.3.1 Top boundary condition

The processes such as rainfall, irrigation and evaporation occurring at the ground surface have to be specified as top boundary conditions. In the present study, during the days of rainfall or irrigation, an infiltration boundary condition is specified. When there is no rainfall/irrigation, evaporation from ground surface is specified as top boundary condition. Therefore, the top boundary condition is given as:

$$-K(\psi)\left(\frac{\partial \psi}{\partial z}+1\right) = \pm q_z(z,t) \qquad for\; t \ge 0; z = L \qquad (5.7)$$

where q_z refers to either infiltration (negative) from rainfall/irrigation or evaporation (positive) from soil surface.

Evaporation from the surface changes with crop growth stage and is computed depending on plant transpiration from evapotranspiration.

5.5.3.1.1 Potential evapotranspiration

Reference crop evapotranspiration was computed using the Penman Monteith approach and potential evapotranspiration was determined using the crop coefficients in the respective crop growth seasons. Further, the potential evapotranspiration has been partitioned into crop transpiration and soil evaporation using Beer's law that partitions the solar radiation component of the energy budget (Ritchie 1972) as follows:

$$E_s = ET_c e^{-\lambda.LAI} \quad (5.8a)$$

$$T_p = ET_c - E_s \quad (5.8b)$$

where ET_c is the potential evapotranspiration, E_s and T_p respectively are the evaporation and transpiration components, *LAI* is the leaf area index of the crop measured at regular intervals during the growing seasons using LP-80 Ceptometer and λ is an extinction coefficient for global solar radiation. The value of extinction coefficient equal to 0.32 and 0.3 for rice and berseem crops, respectively, has been used in the present study (Li et al. 2014). Estimated values of E_s and T_p were then used as time variable input boundary conditions in the HYDRUS-1D simulations. Figs. 5.2 and 5.3 present the ET_c, E_s and T_p values for each crop season in this study.

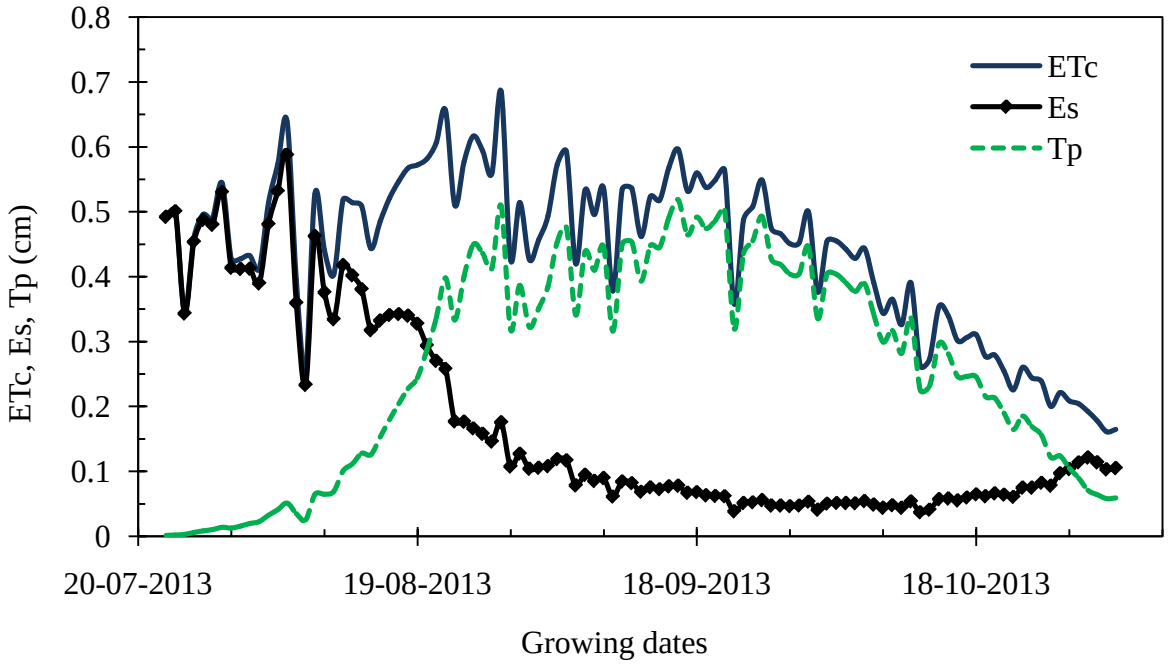

Fig. 5.2(a) Daily potential evaporation, E_s, transpiration, T_p, and evapotranspiration, ET_c during rice season 1

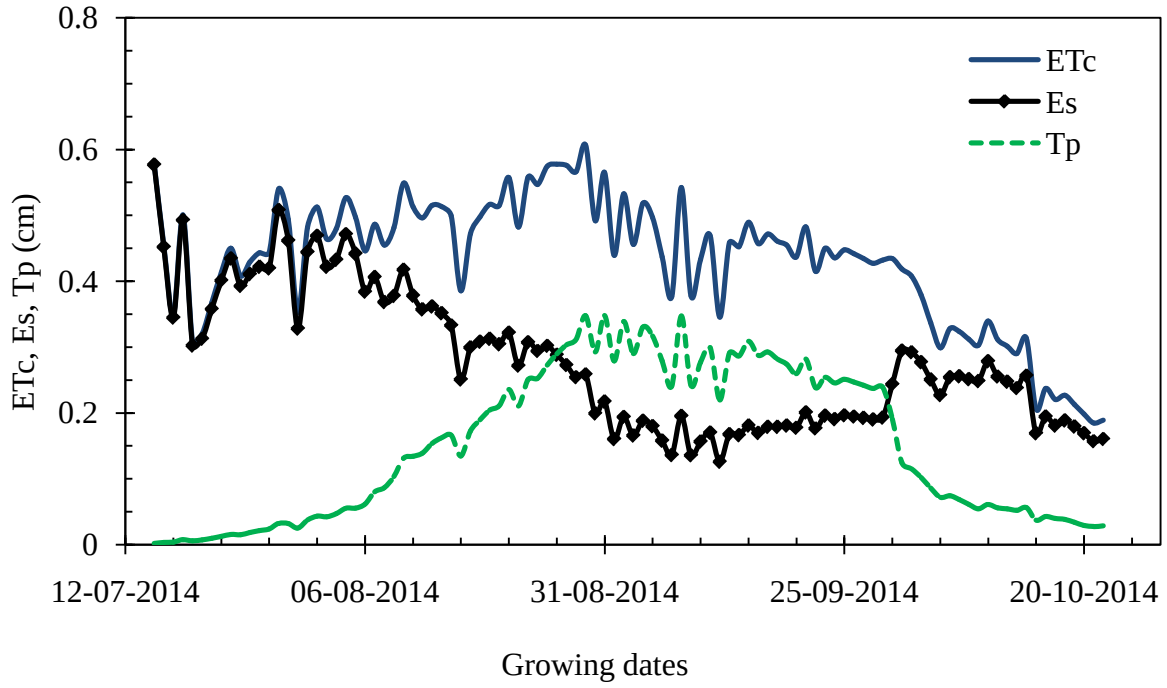

Fig. 5.2(b) Daily potential evaporation, E_s, transpiration, T_p, and evapotranspiration, ET_c during rice season 2

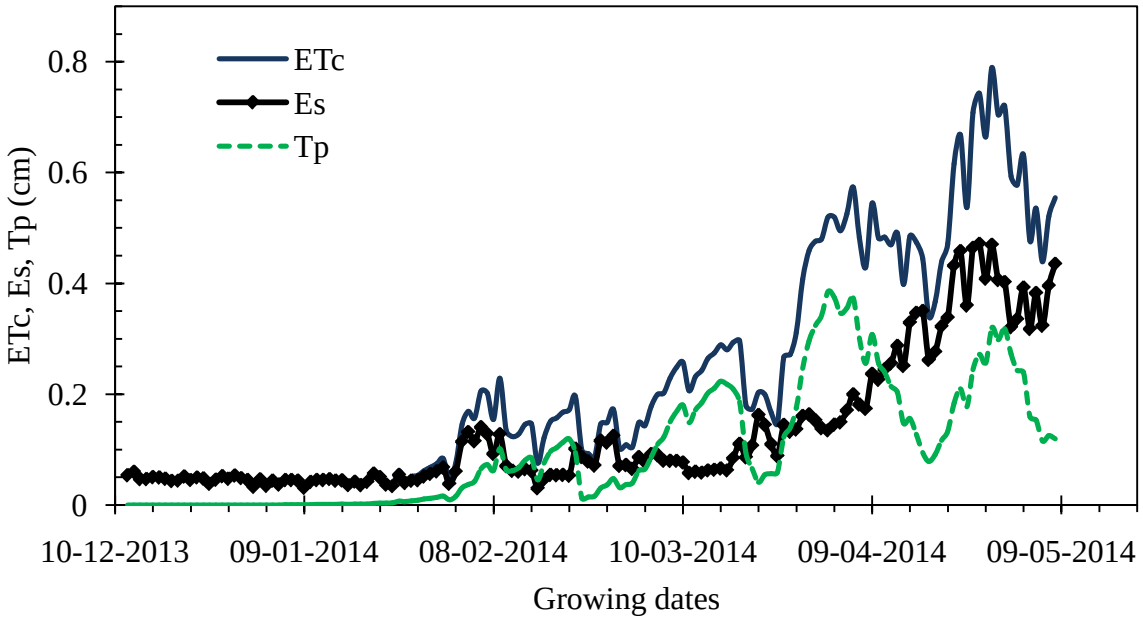

Fig. 5.3(a) Daily potential evaporation, E_s, transpiration, T_p, and evapotranspiration, ET_c during berseem season 1

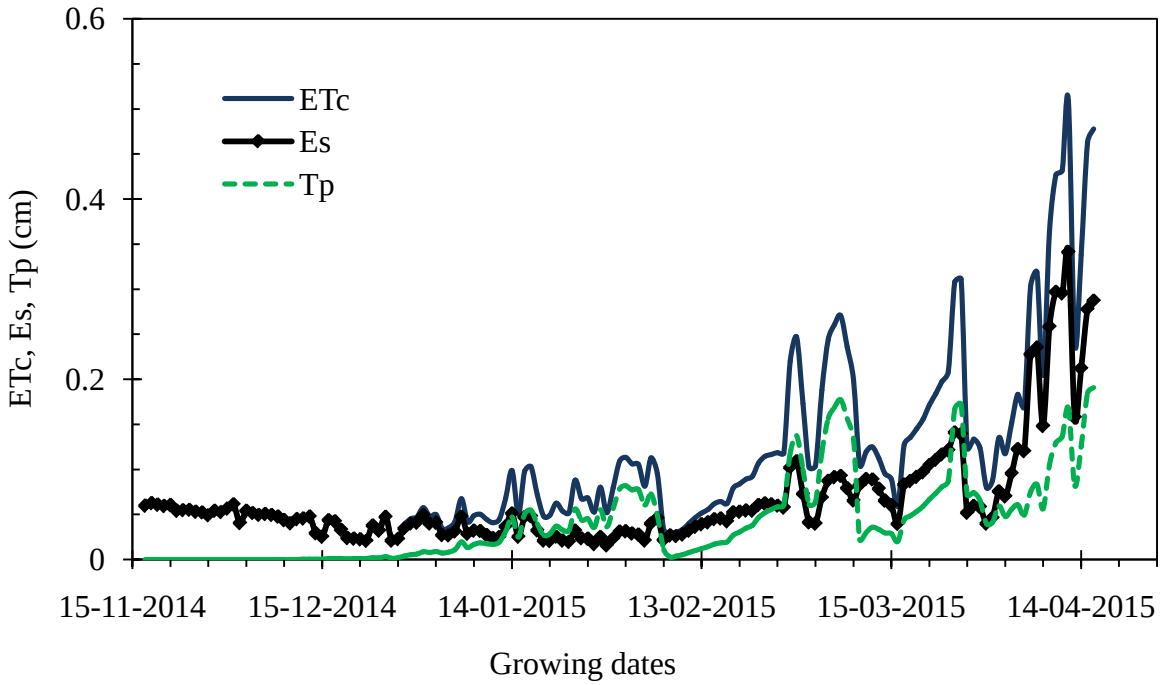

Fig. 5.3(b) Daily potential evaporation, E_s, transpiration, T_p, and evapotranspiration, ET_c during berseem season 2

5.5.3.1.2 The critical pressure head

In actual field conditions, the soil evaporation is limited by available soil moisture. When the soil moisture is sufficient at soil surface, evaporation can take place at potential rate. But when the potential evaporation exceeds the capability of the soil to deliver enough water toward the soil surface, evaporation rate can be significantly reduced to an actual evaporation rate. To account for these conditions, critical pressure head (h_{crt}) at soil surface is considered in HYDRUS-1D package. The critical pressure head is the minimum allowed pressure head at soil surface provided along with the time dependent boundary condition. The value of critical surface pressure head can be activated only by evaporation. As long as the pressure head at the soil surface is higher than h_{crit}, actual evaporation rate is equal to the potential evaporation rate. Once the h_{crit} value is reached, the actual evaporation rate is decreased from the potential value since the soil is too dry to deliver the potential rate.

The critical surface pressure head is computed using the following equation (Šimůnek et al. 2013).

$$h_{crit} = \ln(H_r) \times \frac{RT}{Mg} \qquad (5.9)$$

where H_r is the relative humidity, g is the gravitational acceleration [LT^{-2}] (= 9.81 ms^{-2}), M is the molecular weight of water [M/ mol] (=0.018015 kg mol^{-1}), R is the universal gas constant [J

$mol^{-1}K^{-1}$, $ML^2T^{-2}mol^{-1}K^{-1}$] (= 8.314 J/ mol/K), T is the absolute temperature [K], and h_{crit} is the pressure head [L].

5.5.3.2 Bottom boundary condition

Since the water table in the study area is located at considerably deeper depths, gravity drainage is considered as the bottom boundary condition, i.e., at the bottom boundary:

$$-K(\psi)\left(\frac{\partial\psi}{\partial z}+1\right)=-K(\psi) \qquad for\ t\geq 0, z=0 \qquad (5.10)$$

5.5.4 Root water uptake term

Different models were developed so far for simulating root water uptake (RWU). Exhaustive list of such models have been provided by Shankar (2007). In the HYDRUS-1D, two root water uptake models are given: the Feddes (1976) linear root water uptake and the van Genuchten (1987) (S-curve) root water uptake models. In this particular study, the van Genuchten (1987) root water uptake model has been used. The van Genuchten (1987) (S-curve) root water uptake model considers the non-linear nature of root water uptake which is close to the natural field conditions. The van Genuchten (1987) root water uptake, S, is given as:

$$S(\psi)=\alpha(\psi,\psi_\phi)S_p \qquad (5.11)$$

where S_p is the potential root water uptake rate [T^{-1}], ψ_ϕ is the osmotic head (L) and $\alpha(\psi, \psi_\phi)$ is the root-water uptake water stress response function, the dimensionless function of the soil water pressure head. The value of the response function falls between 0 and 1 and is given as:

$$\alpha(\psi,\psi_\phi)=\frac{1}{1+\left(\frac{\psi+\psi_\phi}{\psi_{50}}\right)^p} \qquad (5.12)$$

where p is an experimental parameter and ψ_{50} represents the pressure head at which the water extraction rate is reduced by 50% during conditions of negligible osmotic stress.

Root growth or rooting depth information is also required for determination of root water uptake for a given crop season. Different alternatives are provided in the HYDRUS-1D package to supply root growth information. The root depth may be provided with the time variable boundary conditions or a table of root growth data could be supplied from measured data from which the program determines rooting depths for each time interval using linear interpolation. In this study, observed rooting depths have been used. The observed rooting

depths at different days after transplanting (DAT) or days after sowing (DAS) are shown in Tables 5.2 to 5.5 for each crop season.

Table 5.2 Variation of root depth for rice season 1

DAT	4	12	19	31	37	43	49	57	64	69	76	85	97	103
Root depth (cm)	4	7	11	20	23	23	25	26	27	27.5	27.5	27.5	27.5	27.5

Table 5.3 Variation of root depth for rice season 2

DAT	1	9	22	25	28	35	42	60	66	72	78	84	90	96
Root depth (cm)	5.3	6	15	18	19	21	23	24.5	26	31	31	31	31	31

Table 5.4 Variation of root depth for berseem season 1

DAS	0	17	23	39	46	54	59	65	70	79	83	86
Root depth (cm)	0	1.5	2	2.6	8	10	12.3	13.6	16.1	21.5	24.4	19.4
DAS	91	95	100	103	111	126	134	140	144	148		
Root depth (cm)	21	20	24	24	37.5	38	40	42	40	40		

Table 5.5 Variation of root depth for berseem season 2

DAS	0	31	59	71	80	85	93	100	106	108	115	120
Root depth (cm)	0	3	13	18	26	30	38	47	47	47	47	47
DAS	124	128	132	137	145	149						
Root depth (cm)	47	47	47	47	47	47						

The two parameters, p and ψ_{50}, used in the van Genuchten (1987) root water uptake model need calibration. The value of p equal to 3 is used which is also adopted in many other studies (Šimůnek et al. 2013). The calibrated values for ψ_{50} parameter equal to -420 cm during

rice and -500 cm during the berseem seasons, respectively, has been used in the present study for negligible osmotic stress.

5.5.5 Preliminary estimation of deep percolation using measured parameters

In the preliminary investigation, HYDRUS-1D was used to estimate the deep percolation on daily time step using field measured hydraulic parameters given in Table 5.1. Model simulations were carried out for both lysimeters and each spot described in chapter three. For brevity, results are provided in case of lysimeters, where deep percolation measurements were possible. The HYDRUS-1D model computed deep percolation values at the bottom of each lysimeter are compared with measured data and are shown in Figs. 5.4 to 5.7. Table 5.6 also presents the error statistics between field observed and model computed deep percolation values in each crop season.

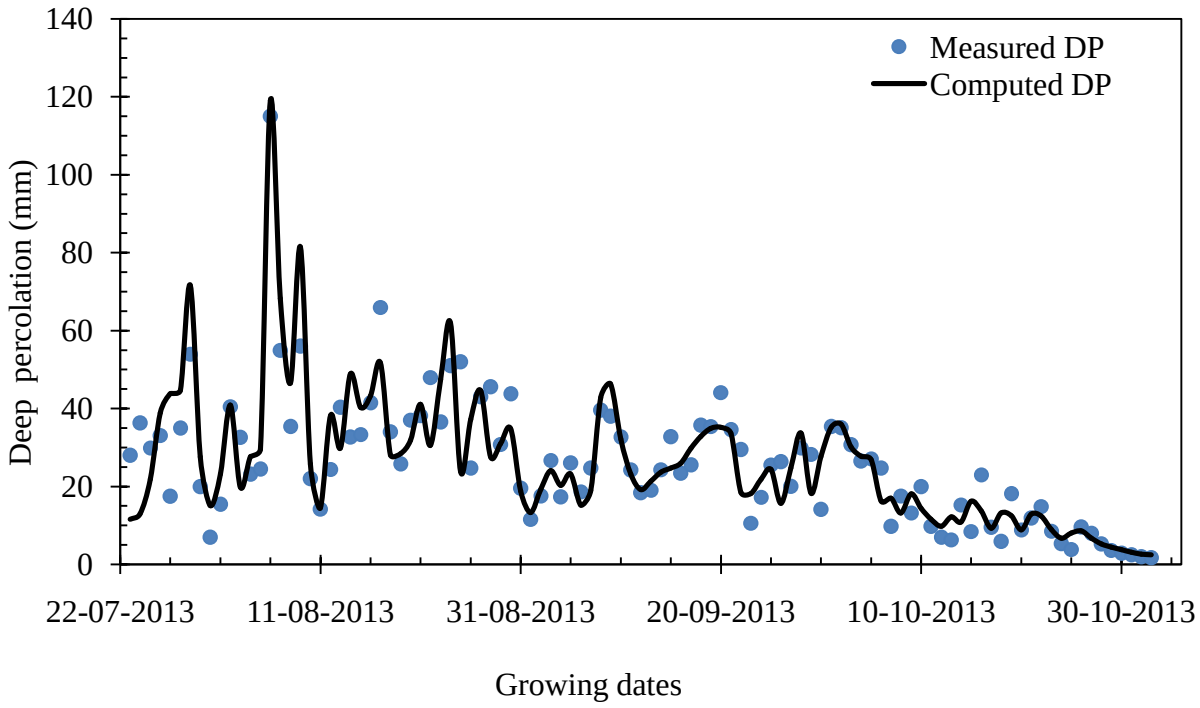

Fig. 5.4(a) Measured and model predicted deep percolation in lysimeter 1 for rice season 1

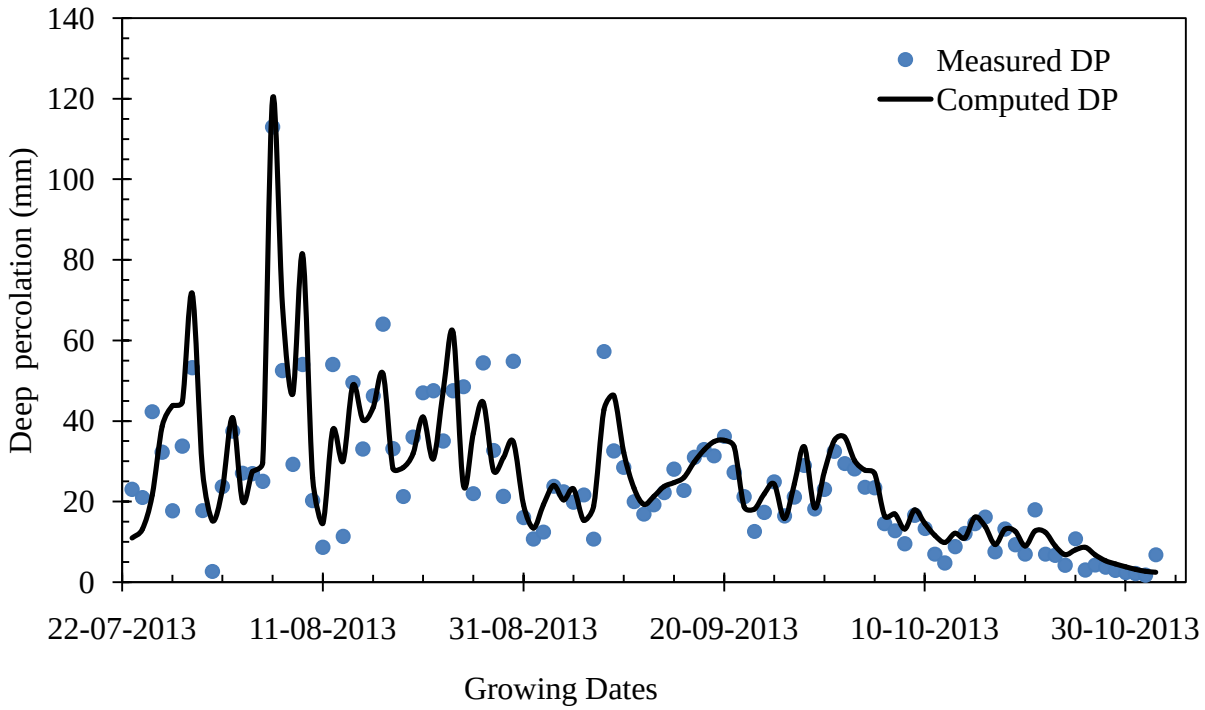

Fig.5.4 (b) Measured and model predicted deep percolation in lysimeter 2 for rice season 1

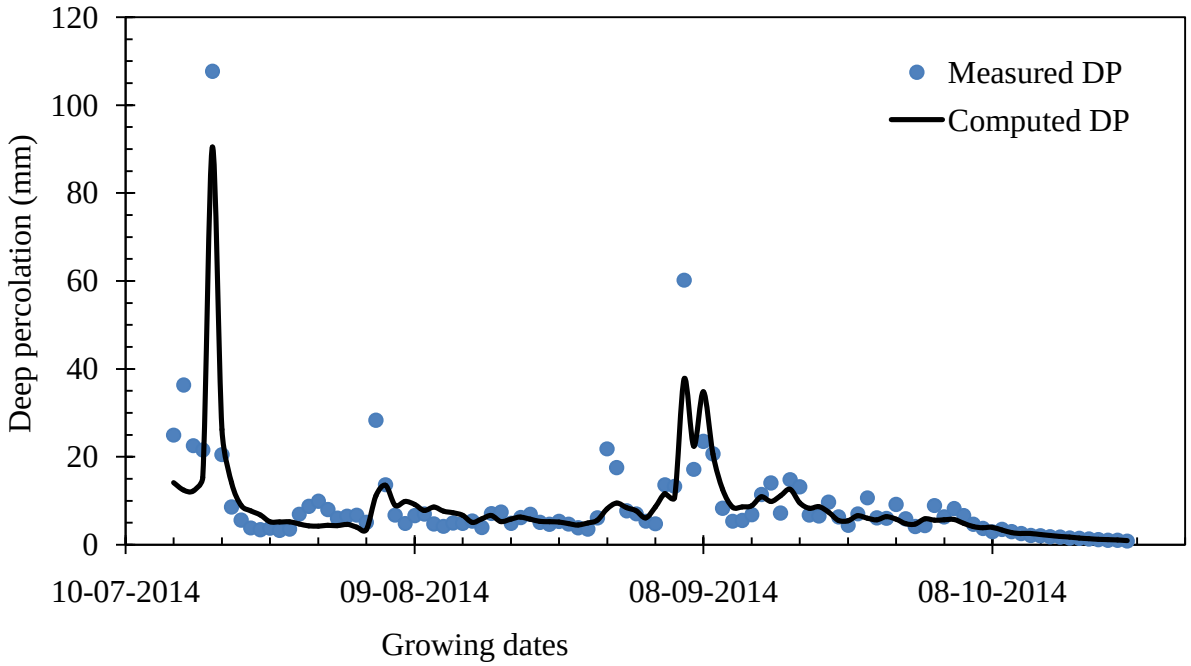

Fig.5.5 (a) Measured and model predicted deep percolation in lysimeter 1 for rice season 2

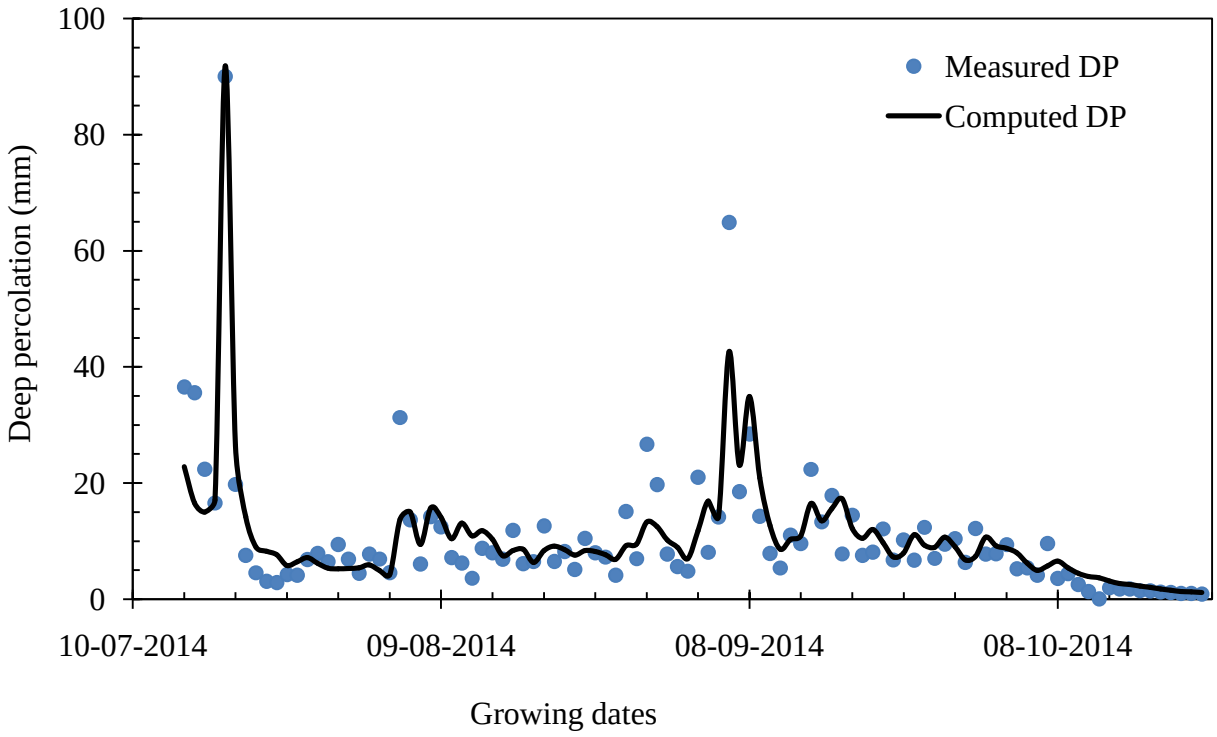

Fig.5.5 (b) Measured and model predicted deep percolation in lysimeter 2 for rice season 2

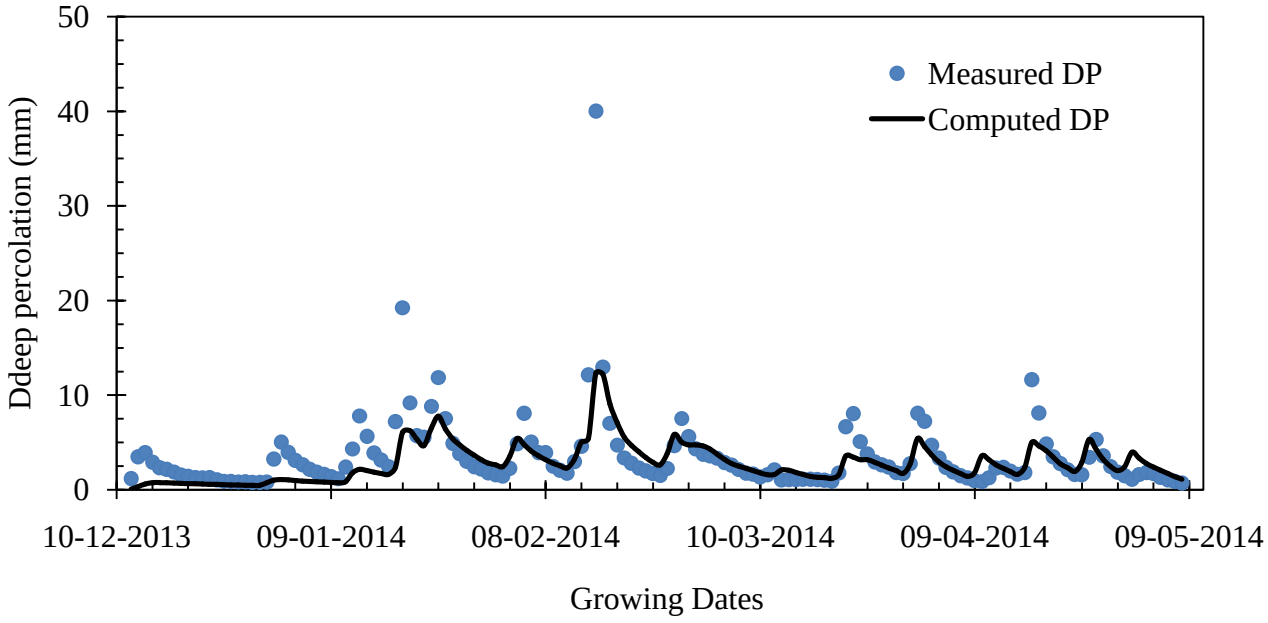

Fig.5.6 (a) Measured and model predicted deep percolation in lysimeter 1 for berseem season 1

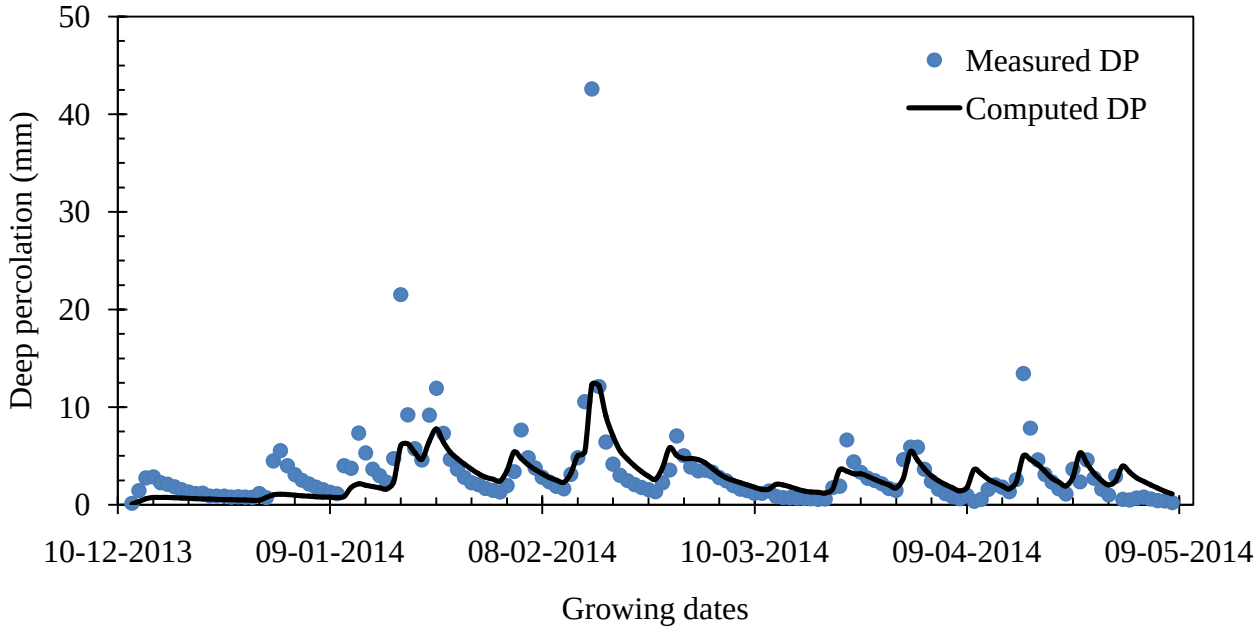

Fig.5.6 (b) Measured and model predicted deep percolation in lysimeter 2 for berseem season 1

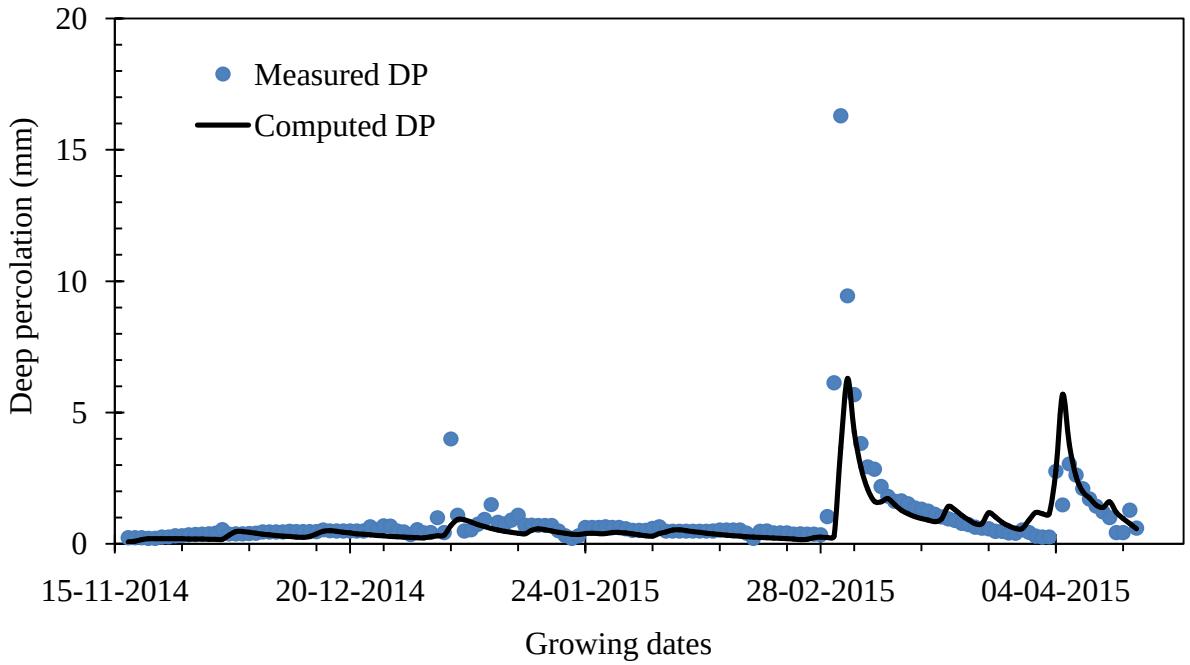

Fig. 5.7(a) Measured and model predicted deep percolation in lysimeter 1 for berseem season 2

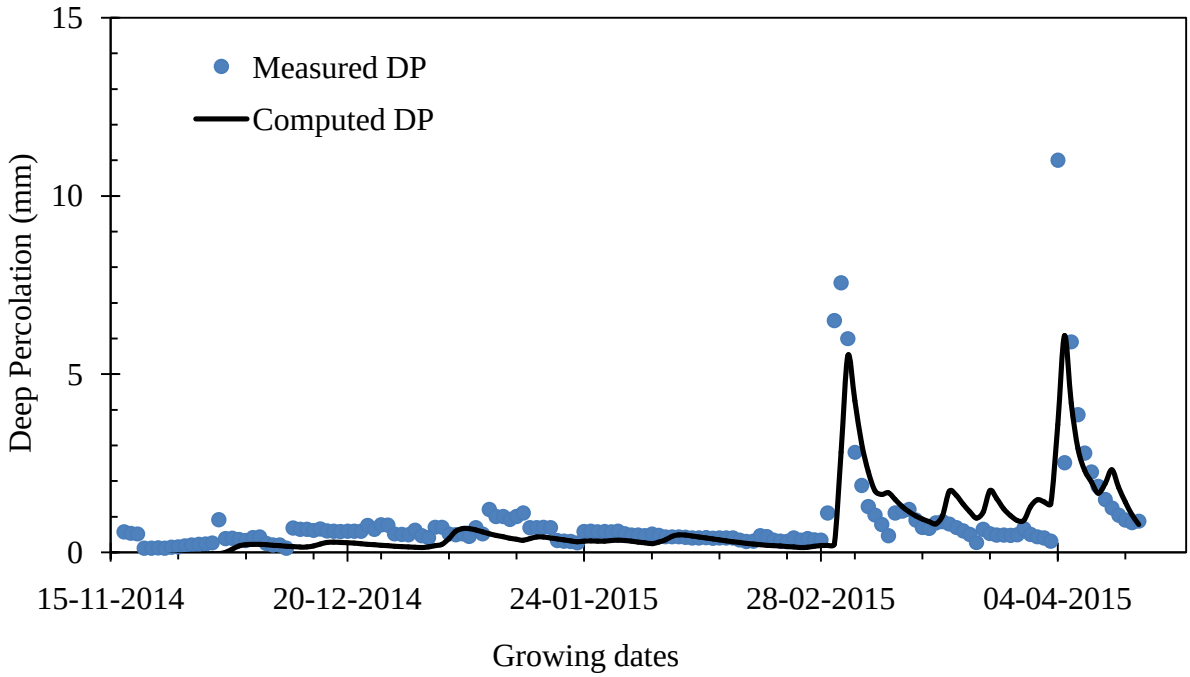

Fig. 5.7(b) Measured and model predicted deep percolation in lysimeter 2 for berseem season 2

Table 5.6 Statistical parameters for model run using spot 2 soil hydraulic data

Crop Season	Lysimeter	R^2	*RMSE* (mm)	*COV*	Total Deep Percolation (mm)	
					Measured	Computed
Rice season 1	L1	0.75	8.92	0.34	2668.83	2692.31
	L2	0.77	8.86	0.36	2525.86	2692.31
Rice season 2	L1	0.82	5.93	0.63	937.19	888.95
	L2	0.77	5.81	0.55	1064.16	1063.93
Berseem season 1	L1	0.52	3.06	0.86	522.79	421.40
	L2	0.50	3.29	1.00	478.49	421.40
Berseem season 1	L1	0.44	1.31	1.34	148.15	107.72
	L2	0.42	1.05	1.20	132.27	98.22

It is evident from Figs. 5.4 to 5.5 that the measured and model predicted deep percolation values on daily time step agree fairly well during the rice crop seasons. The correlation between model predicted and measured deep percolations during the berseem season, on the other hand, is relatively poor (Figs. 5.6 to 5.7). While the model predicts percolation acceptably well during the rice season, it does not sufficiently predict percolation during the berseem season. This would be attributable to the preferential flow phenomena in

the berseem crop season in which flow of water through soil cracks, seems, openings and macrospores during the season is prevalent.

The phenomena of preferential flow in lysimeters could not be avoided even under strict laboratory and experimental conditions (Bethune et al. 2008; Sutanto et al. 2012). Preferential flow can take place through macropores, root stretches, soil cracking, earthworm burrows, structural boundaries of such facilities as lysimeters etc. Specifically, as lysimeters do not account for lateral flow, the vertical boundaries may cause fringe effects and preferential transport (Abdulkareem et al. 2015). Preferential flow phenomena are also significant under normal field conditions and often received the attention of many researchers (Baram et al. 2012; Garg et al. 2009; Sander and Gerke 2009). In Figs. 5.4 to 5.7 above, measured deep percolations often show early and higher peaks than model simulated peak deep percolation values. In actual field conditions the response of deep percolation is faster and reaches its maximum (peak) value quicker than the model simulated maximum deep percolation. The model could not able to capture the peak percolation value accurately in all growing seasons. Field observed *DP* is higher than model simulated *DP* in many incidences. This is essentially attributable to preferential transport which is clearly observed in all the experimental periods. Such a flow phenomena have also been reported by Baram et al. (2012), who have observed that preferential flow caused quick rises in sediment water content following rain events even at deeper layers of clayey vadose zone through a desiccation-crack network. It is also interesting that such condition becomes more significant during the less frequent irrigation seasons (berseem periods) due to the possible effect of soil cracking and shrinkage which would form comparatively large openings during the long intervals of irrigation or rainfall. For example, during the second berseem season both irrigation and rainfall were so erratic that a sudden rise in measured percolation after heavy rainfall events confirm the presence of large openings formed in the lysimeters. On the other hand, the model simulated percolation was slowly responded to the particular input rainfall.

The model predicts the peak deep percolation on slightly later time step might be based on the response of flow processes in the subsurface environment which are consecutive in nature: viz infiltration followed by redistribution which is again followed by drainage. After the pore storage is satisfied, drainage out of the considered zone starts either laterally or vertically. Therefore, it gives rise to certain time lapse for drainage water to appear at specified boundary. Despite the variations between the predicted and measured percolation on the daily time step, the general performance of the model can be taken as good for such field conditions.

In most instances of deep percolation estimation, the estimation is either limited to temporal or spatial lumping which could deprive through understanding of the particular process.

The performance of the two lysimeters can also be described using the statistical parameters shown in Table 5.6. In general, lysimeter 1 is performing better than lysimeter 2. Evidently, variations due to formation of macropores, influence of subsurface biota, soil heterogeneity and agronomic practices would be responsible for this. In the next session, the performance of the model using calibrated soil hydraulic parameters has been presented.

5.5.6 Model Calibration

From the preliminary investigations, it is observed that the model predictions are not in very good agreement with field observations, specifically in the case of berseem season. Hence to achieve better results, the soil hydraulic parameters are calibrated by altering their respective measured values to minimize the deviation between measured and model predicted deep percolations. The calibration is done by using deep percolation of season 1 for both rice and berseem and its accuracy is validated using field observed data of season 2.

During model calibration, some of the soil retention parameters were made fixed, i.e., measured values of the parameters were maintained. The saturated moisture content, θ_s, was determined using both bulk density-soil porosity relationship and RETC code (van Genuchten, 1980). Almost similar values of the saturated moisture content have been obtained by the two methods. Therefore, the measured value of θ_s has been maintained. Deep percolation is reported to be less sensitive to variations in the residual moisture content, θ_r, and hence the value of θ_r obtained from the field has been maintained. Šimůnek and Nimmo (2005), for example, have shown that the standard error of the residual moisture content is in the order of 10^{-4} which is optimized using the multistep centrifuge experiment. Thus, the calibration of the model was conducted by changing three of the remaining soil hydraulic (K_{sat}, α_v and n_v) parameters. The material distribution in the soil monolith has also been slightly modified during model calibration considering possible changes under field conditions due to cultivation process. Manual calibration process was undertaken. Table 5.7 presents soil hydraulic parameters estimated from model calibration.

As can be observed from Table 5.7, large values of saturated hydraulic conductivity near the soil surface depict the relative importance of root proliferation, the activities of soil micro organisms, soil cracking which favour more porous upper zone than the bottom layers.

Table 5.7 Calibrated soil hydraulic parameters for various layers

Soil depth (cm)	θ_r	θ_s	$^{\dagger}\alpha_v$ (1/cm)	n_v	K_{sat} (cm/day)
0-15	0.049	0.357	0.06(0.016)	1.52(1.49)	204(209)
15-30	0.046	0.399	0.02(0.006)	1.52(1.74)	177(118)
30-60	0.043	0.381	0.01(0.006)	1.79(1.74)	115(118)
60-80	0.034	0.390	0.02(0.013)	2.00(1.54)	115(106.10)
80-100	0.046	0.399	0.02(0.022)	1.52(1.37)	177(106.10)
100-135	0.046	0.391	0.06(0.018)	2.00(1.47)	106(106.10)

† *Values outside the bracket show calibrated values*

Figs. 5.8 to 5.9 provide the comparison of measured and model predicted deep percolations at the bottom of the lysimeters during model calibration for rice season 1 and berseem season 1 periods. Table 5.8 also presents the error statics for model calibration season.

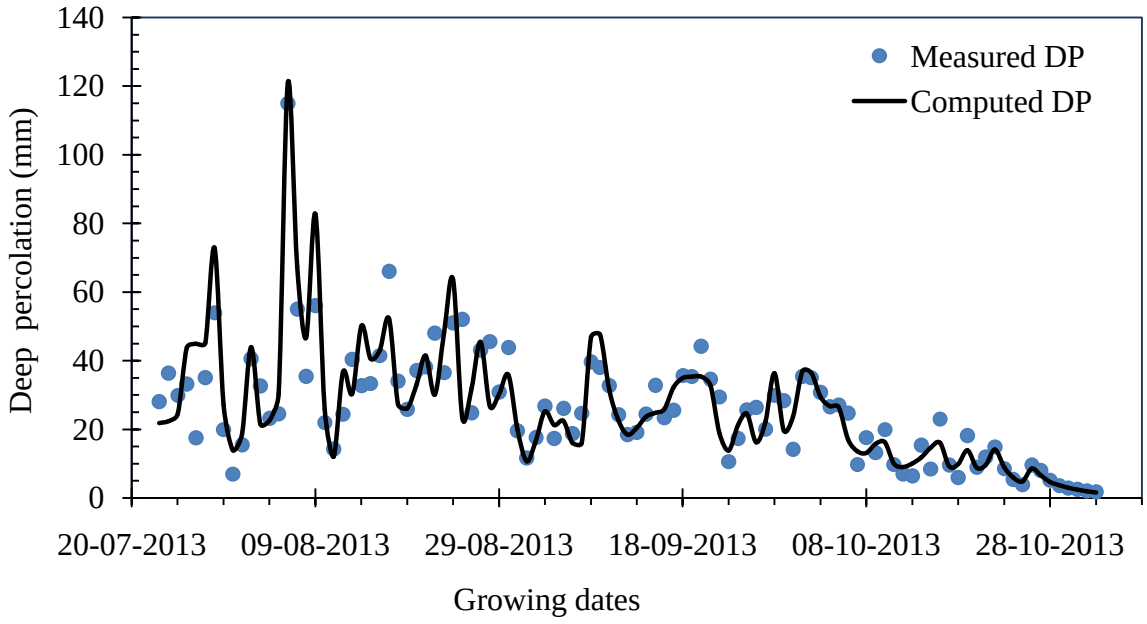

Fig. 5.8(a) Measured and model predicted deep percolation in lysimeter 1 for rice season 1

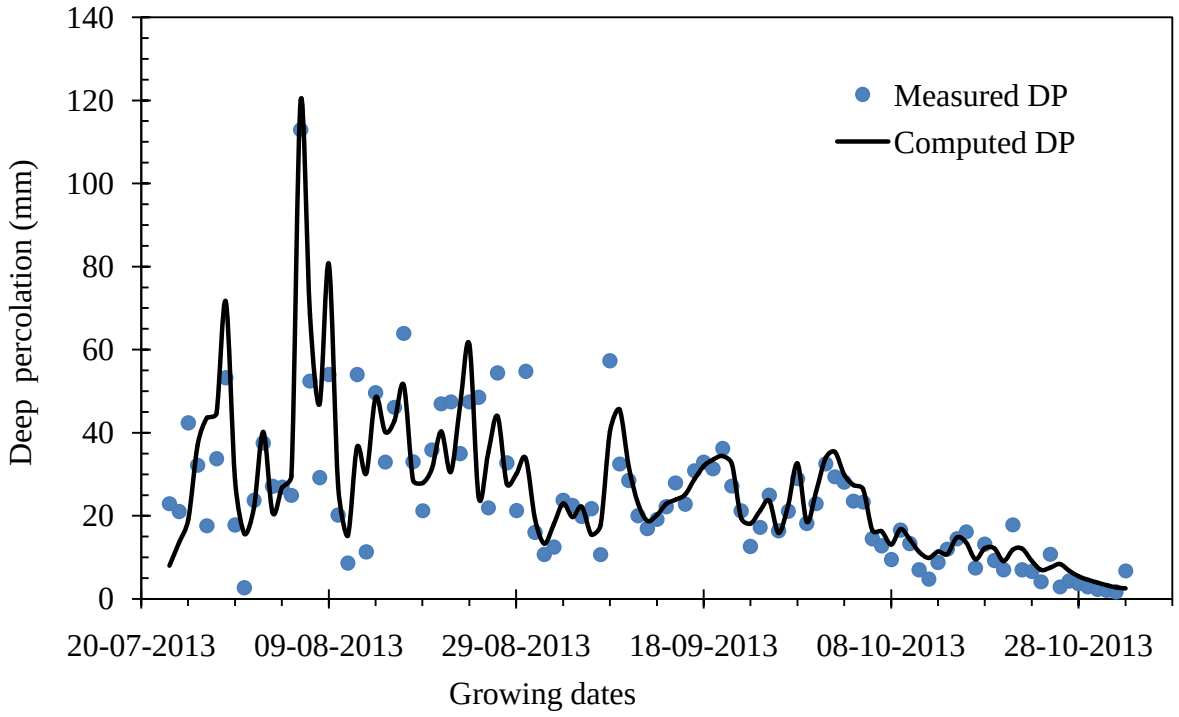

Fig. 5.8(b) Measured and model predicted deep percolation in lysimeter 2 for rice season 1

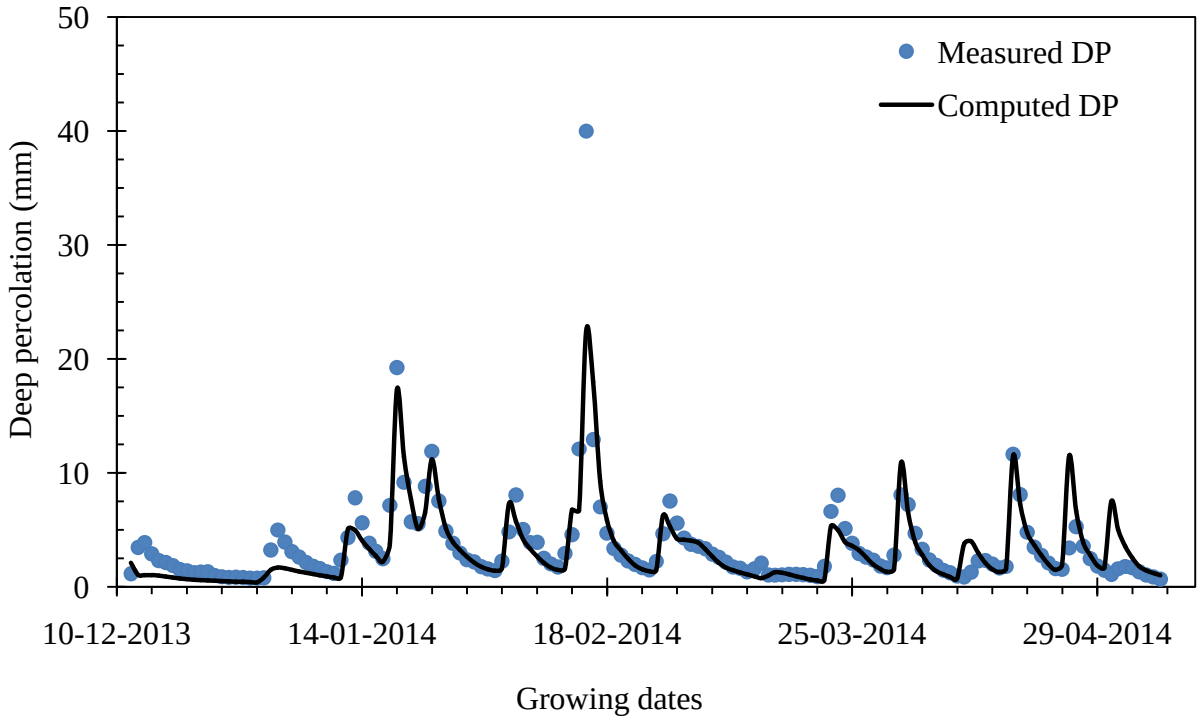

Fig. 5.9(a) Measured and model predicted deep percolation in lysimeter 1 for berseem season 1

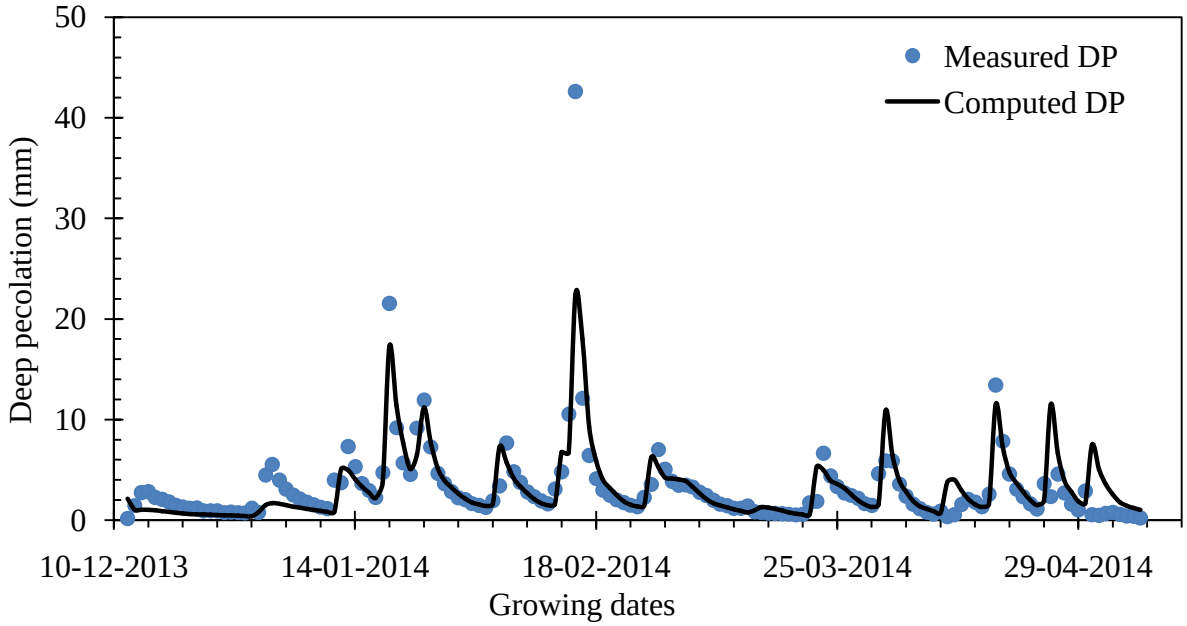

Fig. 5.9(b) Measured and model predicted deep percolation in lysimeter 2 for berseem season 1

Table 5.8 Statistical parameters for model run using calibrated parameters

Crop season	Lysimeter	R^2	*RMSE* (mm)	*COV*	Total Deep Percolation (mm)	
					Measured	Computed
Rice season 1	L1	0.80	8.18	0.32	2668.83	2698.10
	L2	0.79	8.56	0.35	2525.86	2698.10
Berseem season 1	L1	0.74	2.13	0.60	522.79	478.28
	L2	0.68	2.44	0.75	478.49	478.28

The performance of the model has been improved after model calibration. Comparisons of Figs. 5.4 with 5.8 and Figs. 5.5 with 5.9, for the respective crop and lysimeters, show that there is an improvement of model fit when calibrated parameters are employed. Comparison of Tables 5.6 and 5.8 also show that, in both crop seasons, the coefficient of determination (R^2) has been increased while both root mean square error (*RMSE*) and coefficient of variation (*COV*) have been decreased. Significant, improvement in model performance with the calibrated parameters has been achieved during berseem season than the rice season. However, in general, the performance of the model is better during the wetter seasons (rice season) than the drier seasons (berseem season). The prevalence of macropores in the crop root zone may impose errors to the solution of Richards equation which is mainly based on the matrix flow. Despite the effect of such flow conditions, the model strongly predicts the deep percolation flow in the wetter season due to the fact that (i) the large openings are occupied by pre-existing

water (due to saturation) or/filled by migratory particles taken by gravity drainage. Nevertheless, at the initial dates, i.e., at the start of model simulation, the soil pores might not have been occupied by such pre-existing soil water as far as there is no earlier irrigation or rainfall and thus large deviations between measured and computed percolation values could prevail. ii) Long periods of saturation are not conducive to macropore development except during eluviations and piping (Beven and Germann, 1982). iii) Saturation inhibits the activity of soil micro organisms and roots besides its tendency to lead a breakdown of soil structure. Thus the role of macropores in increasing the hydraulic conductivity of the saturated soil may be largely limited to depths where saturation is a temporary phenomenon.

5.5.7 Model Validation

Model validation was carried out by comparing the model predicted deep percolation with the field observed deep percolation in rice season 2 and berseem season 2 periods. During these periods, the parameters used for model calibration (Table 5.7) were used for computing deep percolation in both lysimeters. Figs. 5.10 and 5.11 present the measured and computed deep percolations for rice and berseem season 2 crop periods in both the lysimeters.

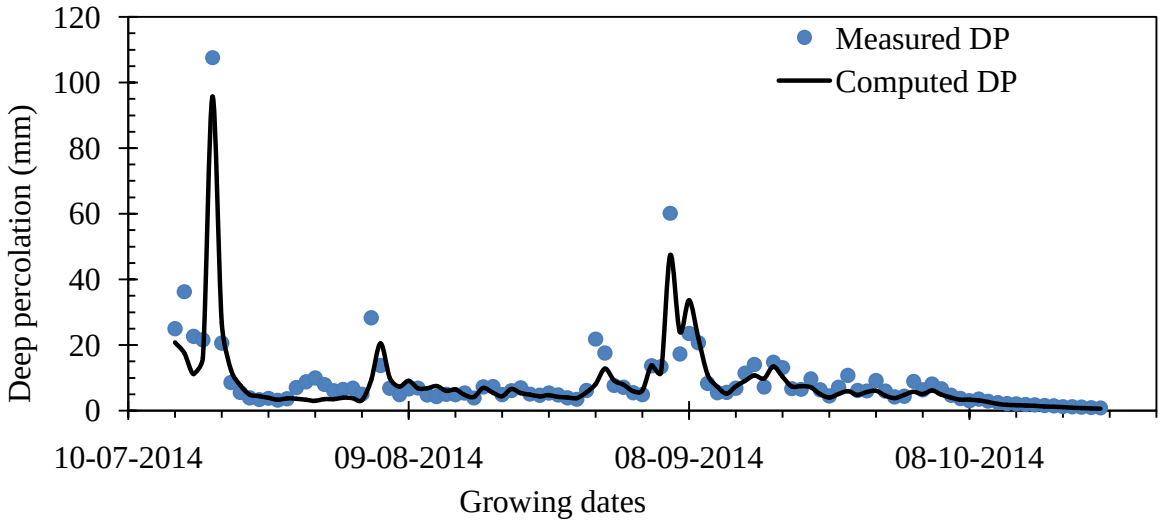

Fig. 5.10(a) Measured and model predicted deep percolation in lysimeter 1 for rice season 2

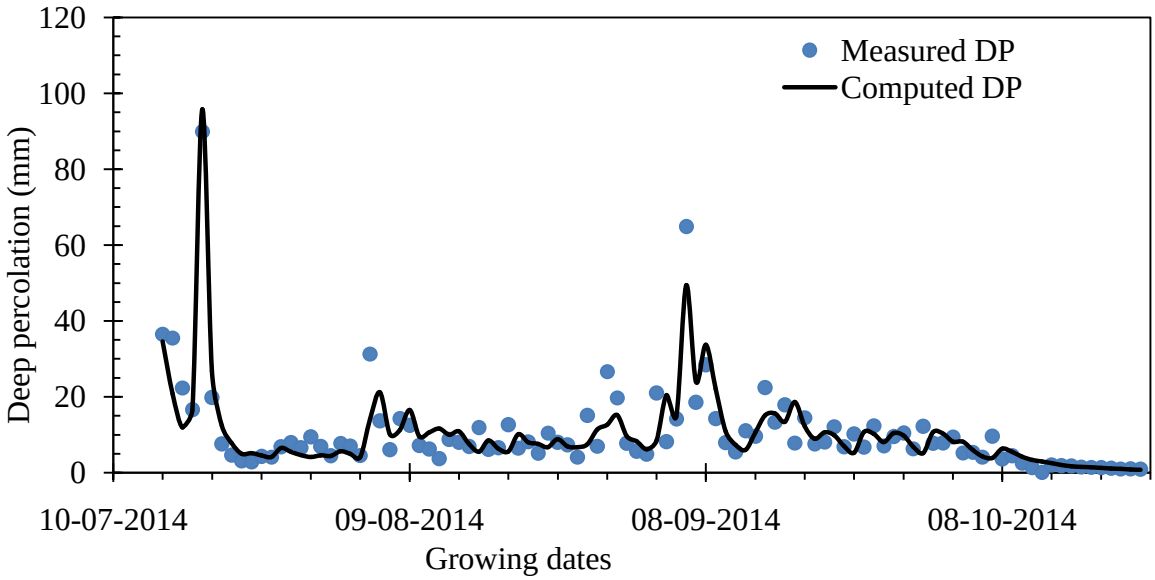

Fig. 5.10(b) Measured and model predicted deep percolation in lysimeter 2 for rice season 2

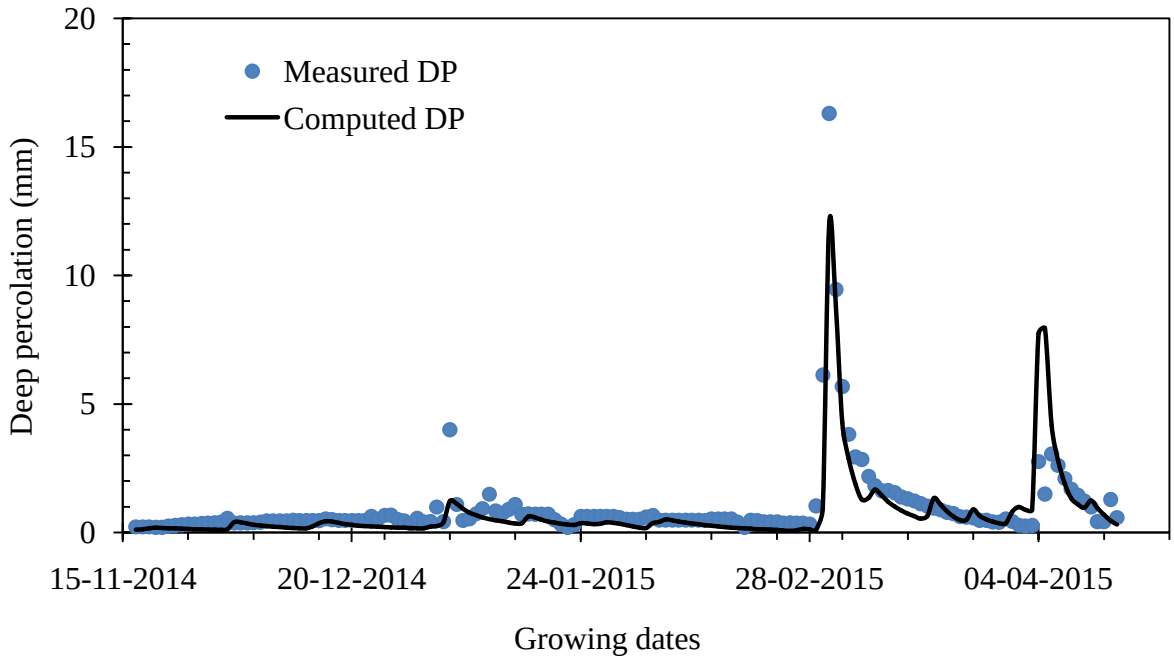

Fig. 5.11(a) Measured and model predicted deep percolation in lysimeter 1 for berseem season 2

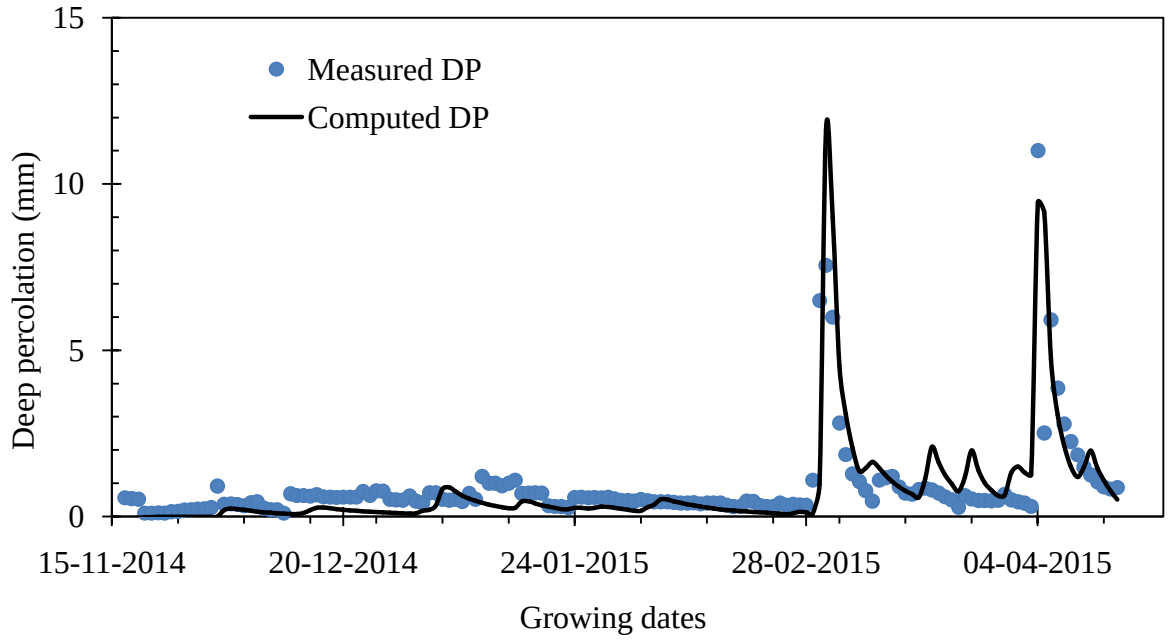

Fig. 5.11(b) Measured and model predicted deep percolation in lysimeter 2 for berseem season 2

Table 5.9 provides statistical indices computed using the observed and computed deep percolation during model validation periods.

Table 5.9 Statistical parameters for model validation

Crop Season	Lysimeter	R^2	*RMSE* (mm)	*COV*	Total Deep percolation (mm)	
					Measured (mm)	Computed (mm)
Rice season 2	L1	0.89	4.45	0.47	937.19	924.93
	L2	0.83	5.04	0.47	1064.16	1047.05
Berseem season 2	L1	0.69	0.97	0.99	148.15	116.88
	L2	0.67	0.96	1.1	132.27	124.10

As can be depicted from comparison of Figs. 5.5 with 5.10 and Figs. 5.7 with 5.11, for the respective crops and lysimeters, the performance of the model has been significantly improved. Similarly, comparisons of the error statistics in Tables 5.6 and 5.9, for the respective crop seasons and lysimeters, show that there is a good prediction of deep percolation by employing calibrated parameters.

As can be seen, the performance of the model is better in rice season 2 (validation season) than rice season 1 (calibration season). This would be attributed to deviations in measured deep percolation in rice season 1 than rice season 2. More intense rainfall events

were occurred in rice season 1 than rice season 2 in addition to continuous and large irrigation depths which contributed for exaggerated percolation rates in the lysimeters. However, this is not the case for berseem season. The performance of the model in berseem season 1 (calibration season) is better than berseem season 2 (validation season). This suggests the dominance of macropore flow during berseem season 2 (when there was very limited water input) than berseem season 1 (when there was better water input).

Again, it is interesting to observe that the performance of the model is comparatively low in the winter season (dry season) than the monsoon season (wet season). Both coefficient of determination (R^2) and coefficient of variation (*COV*) suggest that the performance of the model is comparatively better during the rice season than the berseem season. Higher values of R^2 and lower values of the *COV* in rice season indicate good model fit in the rice season than berseem season. The root mean square error (*RMSE*), on the other hand, shows larger values of magnitude in the rice season than berseem. This would be attributable to the nature of *RMSE* that it offers relatively high weightage to large errors in a given pool of data set. During rice seasons the input water and consequently the response of deep percolation was large. Therefore, large values of *RMSE* were computed in the rice seasons than the berseem seasons when the input water as well as deep percolation magnitudes were less. The *RMSE* value is rather better for comparison of the model performance against individual crop season and lysimeters.

In Tables 5.8 and 5.9, seasonal values of observed and computed deep percolation values are also given. There is a good agreement between the field observed and model computed DP values for all crop periods. In general, model predicted seasonal deep percolation in the crop seasons was lower than the measured deep percolation except the first rice crop season. In this particular study, all the largest peak percolation magnitudes are in relation to the intense rainfall events which are often succeeded by substantial periods of non-wetting days. Hence, it is imperative to conclude that occurrences of large rainfall events following long periods of dry season could majorly contribute to spontaneous deep percolation. This shows that deep percolation estimated on longer time intervals may not provide an insight into the fate of water transport through macropores or large pulses taken place in short time intervals. Ries et al. (2015) observed from a basin scale study that deep percolation occurs mainly from intense rainfall events within a short period of time (5-10 days) for long periods of simulation in Israel. Eilers et al. (2007) also described that annual rainfall totals are not the main predictor of annual recharge and thus temporal distribution of daily rainfall and the magnitude of the

antecedent soil moisture condition are the key determinants of deep drainage at a particular location, in a particular year.

5.5.8 Soil Moisture Profiles

5.5.8.1 Soil moisture profile in rice season

Apart from deep percolation, comparison of model simulated and field observed soil moisture profiles was also made to investigate the performance of the HYDRUS-1D model. For this purpose, few days were selected at random in the crop seasons. Soil moisture observations were made at specific depths in the lysimeters during the growth periods of each crop season. Figs. 5.12 to 5.19 present the comparison of model predicted and field observed soil moisture profiles in different growth stages for the selected dates after transplanting (DAT) in both rice crop seasons.

Statistical terms such as R^2, *RMSE* and *COV* were again used to assess the performance of the model using these set of data. The range of statistical terms is R^2: 0.57-0.90, *RMSE*: 0.013-0.051 and *COV*: 0.04-0.20 for rice season 1, R^2: 0.63-0.77, *RMSE*: 0.034-0.047 and *COV*: 0.14-0.0.19 for rice season 2. The values of error statics for the crop periods show that there exists a visible association between the observed and model simulated soil moisture content in the soil profile.

The deviations between the field observed and model computed soil moisture content values are attributed to prevalence of soil macropores in the field soil, variation in temporal resolution for moisture data record and computation, inherent errors in measurement due to the moisture profile probe and its operation and flow characteristics in the lysimeters.

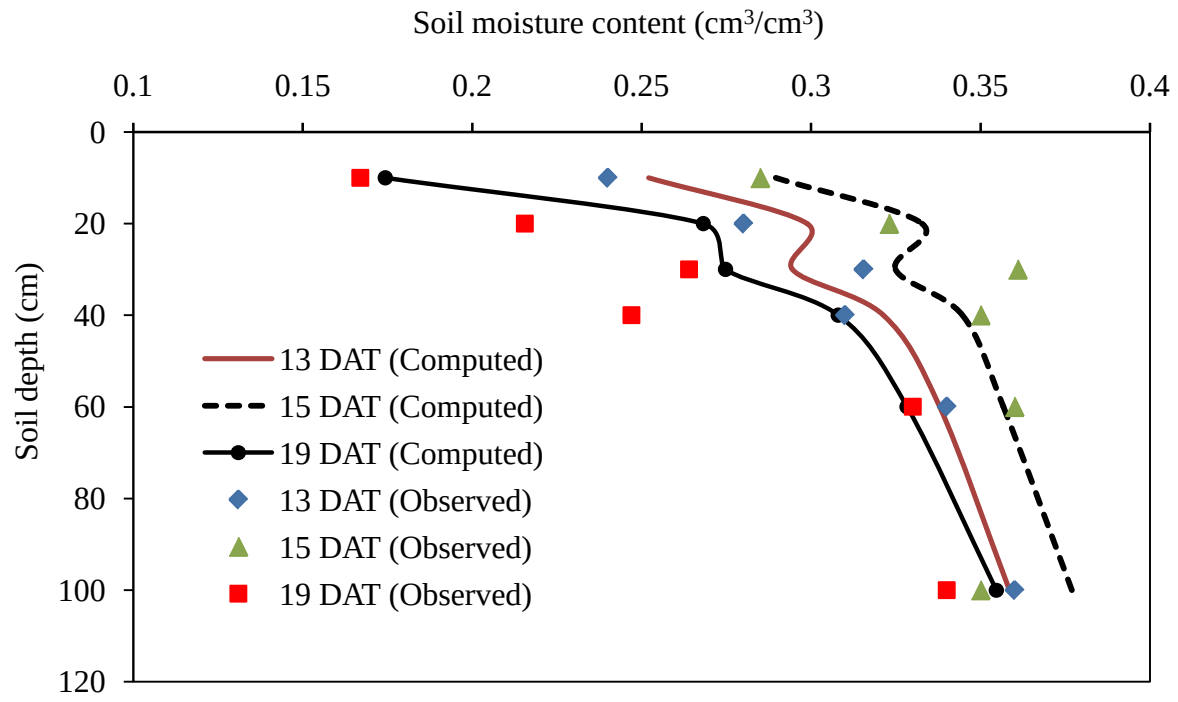

Fig. 5.12 Comparison of model predicted and field observed soil moisture profiles on 13, 15 and 19 DAT for rice season 1(initial season stage)

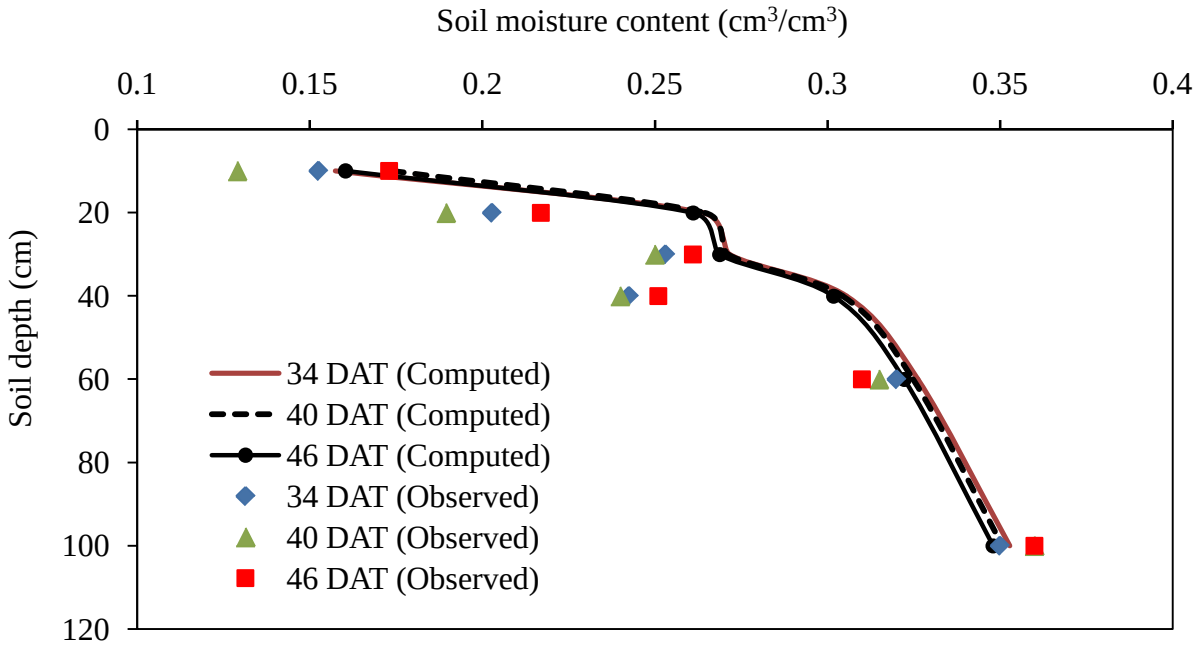

Fig. 5.13 Comparison of model predicted and field observed soil moisture profiles on 34, 40 and 46 DAT for rice season 1(development season stage)

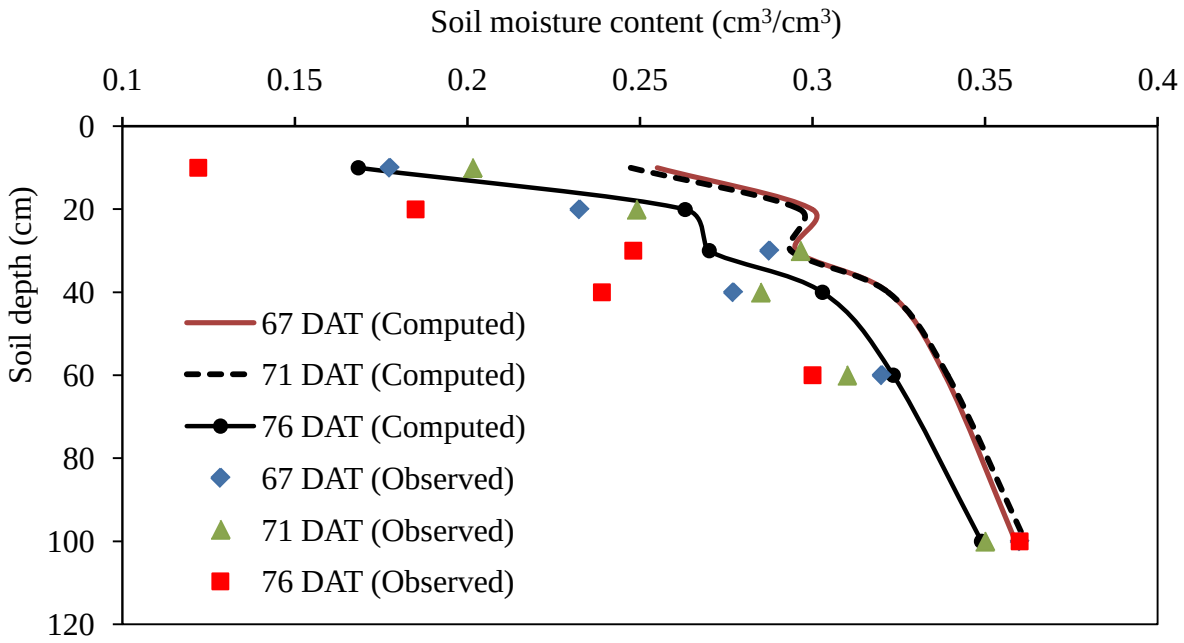

Fig. 5.14 Comparison of model predicted and field observed soil moisture profiles on 67, 71 and 76 DAT for rice season 1(mid season stage)

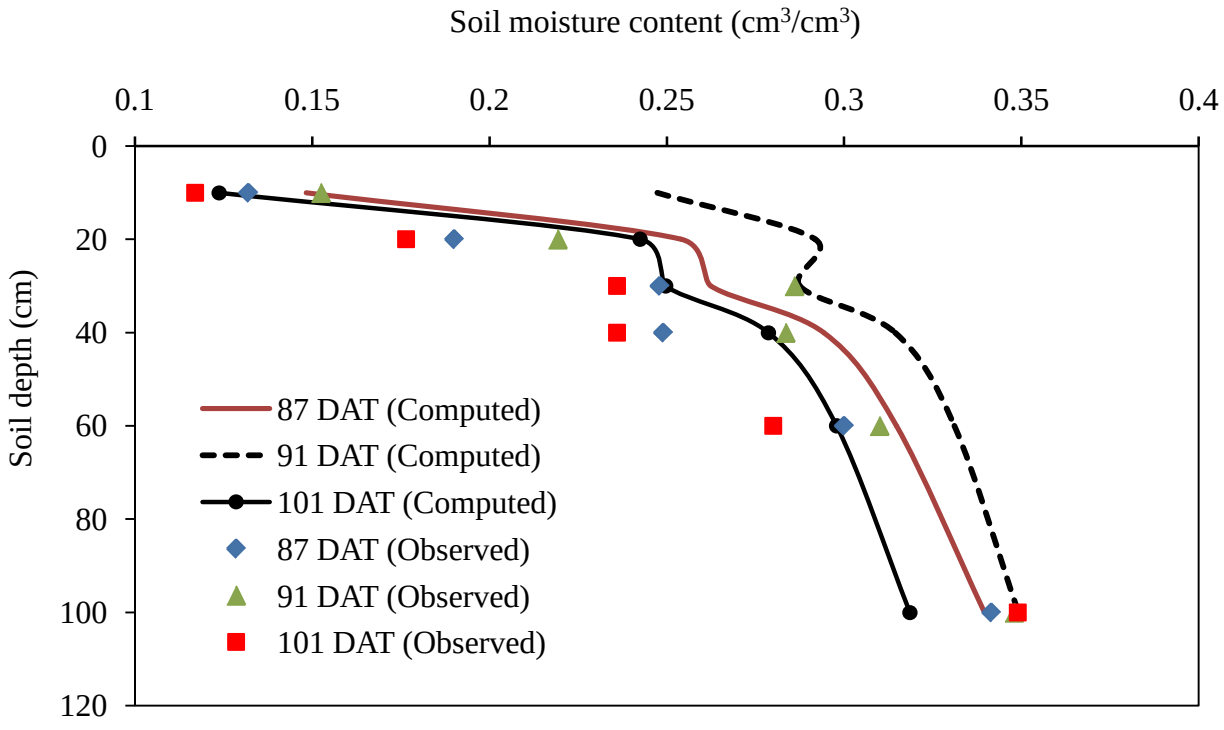

Fig. 5.15 Comparison of model predicted and field observed soil moisture profiles on 87, 91 and 101 DAT for rice season 1 (late season stage)

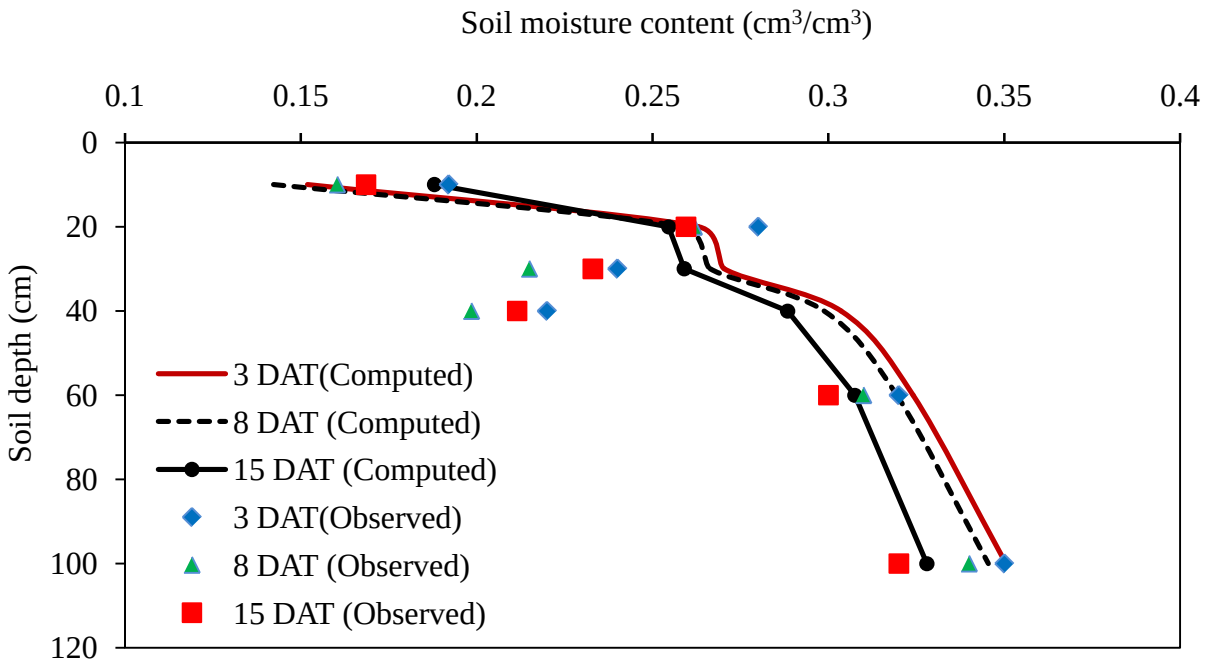

Fig. 5.16 Comparison of model predicted and field observed soil moisture profiles on 3, 8 and 15 DAT for rice season 2 (initial season stage)

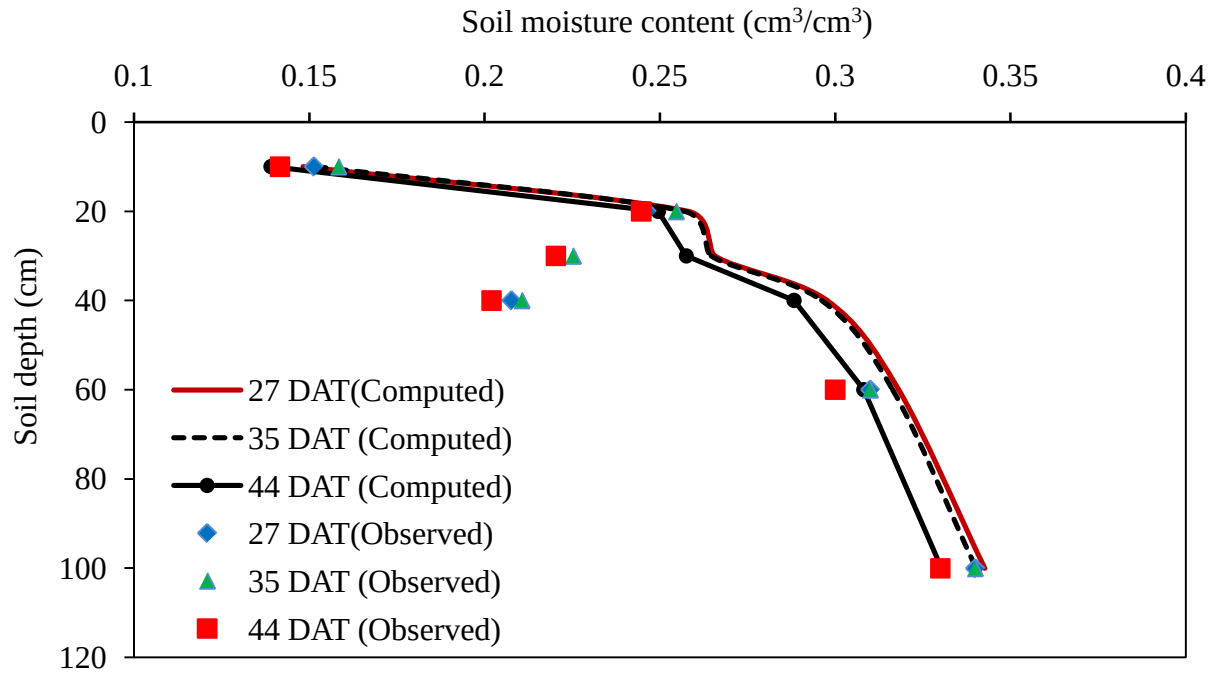

Fig. 5.17 Comparison of model predicted and field observed soil moisture profiles on 27, 35 and 44 DAT for rice season 2 (development season stage)

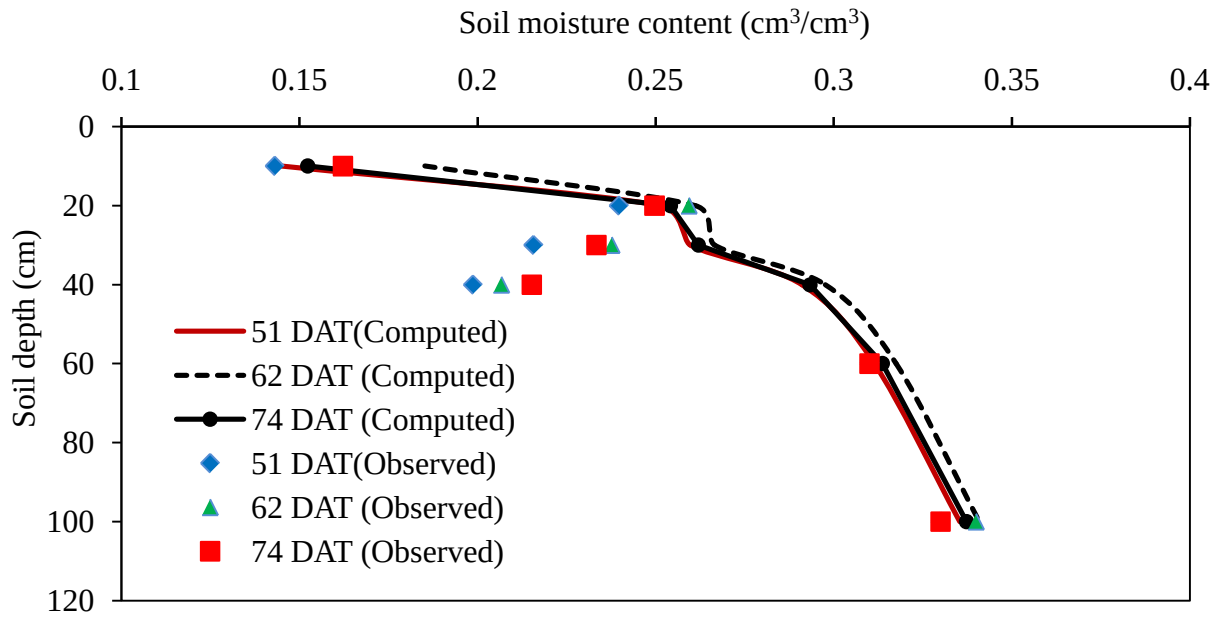

Fig. 5.18 Comparison of model predicted and field observed soil moisture profiles on 51, 62 and 74 DAT for rice season 2 (mid season stage)

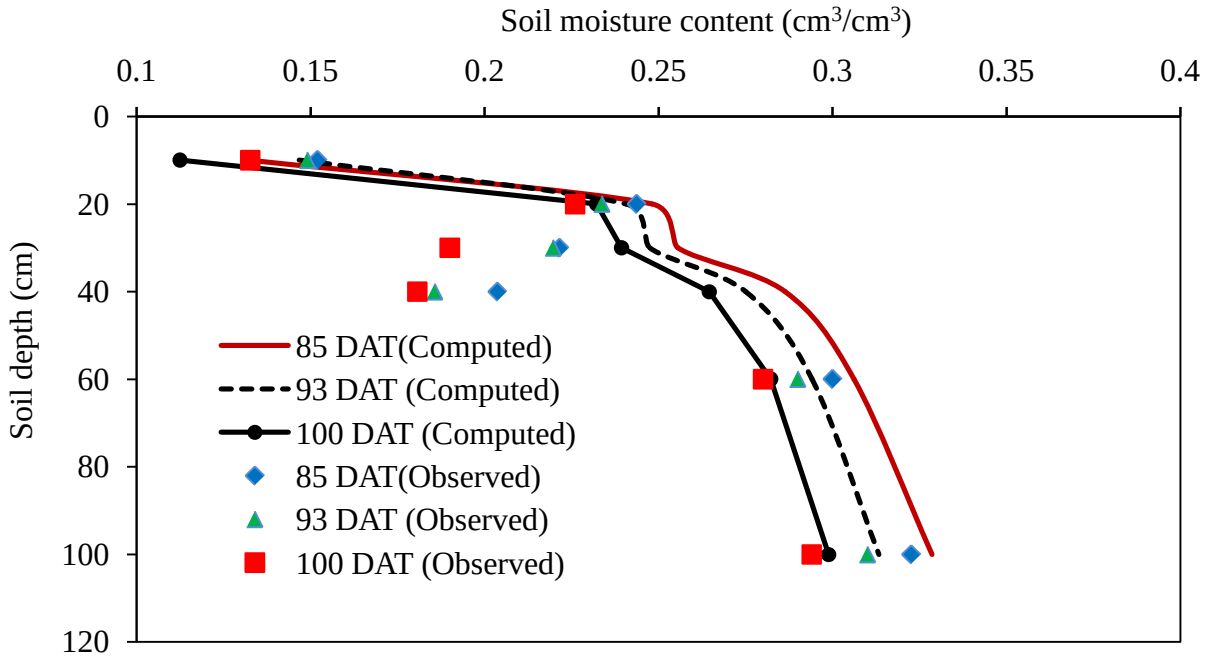

Fig. 5.19 Comparison of model predicted and field observed soil moisture profiles on 85, 93 and 100 DAT for rice season 2 (late season stage)

5.5.8.2 Soil moisture profile in berseem season

Comparison of soil moisture profile for berseem seasons also has been made by selecting specific days after sowing (DAS). The dates are selected between sowing dates and individual cutting intervals in the crop season. Error statistics values ranging from R^2: 0.68-

0.83, *RMSE*: 0.034-0.051 and *COV*: 0.15-0.26 for berseem season 1 and R^2: 0.56-0.87, *RMSE*: 0.024-0.047 and *COV*: 0.10-0.24 for berseem season 2 were observed.

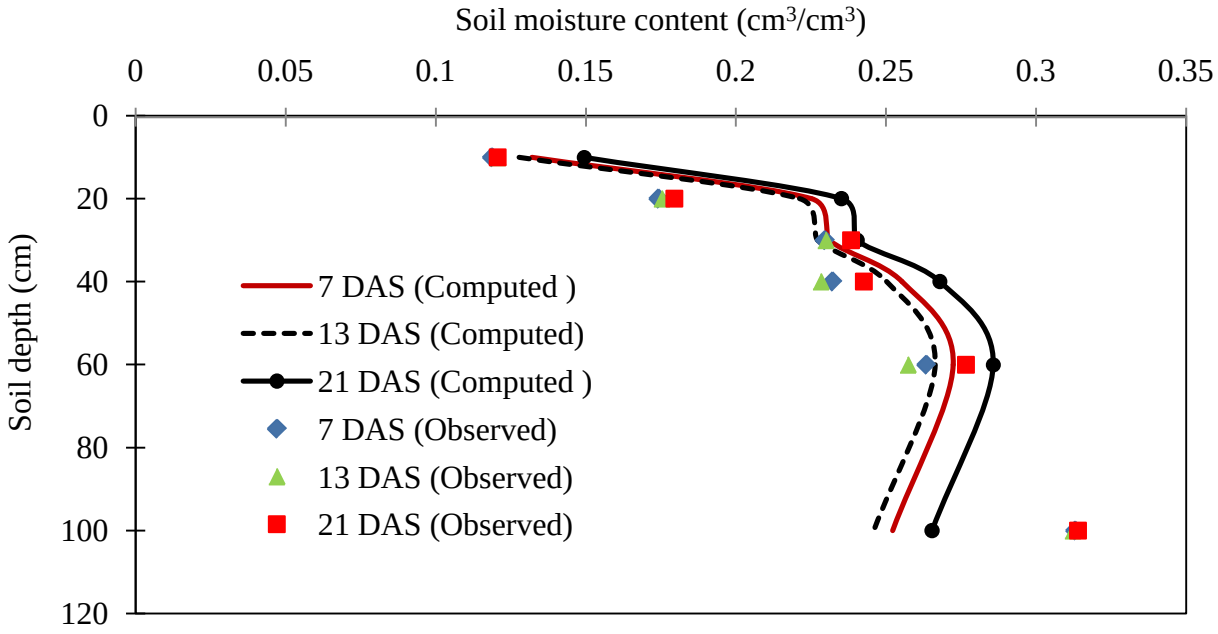

Fig. 5.20 Comparison of model predicted and field observed soil moisture profiles on 7, 13 and 21 DAS for berseem season 1

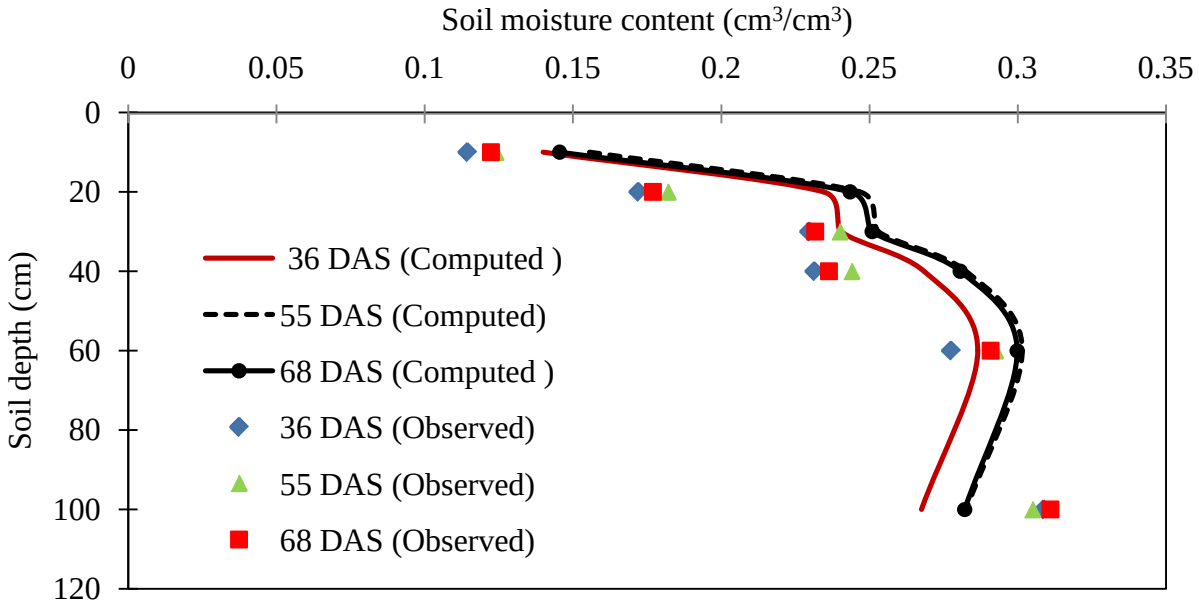

Fig. 5.21 Comparison of model predicted and field observed soil moisture profiles on 36, 55 and 68 DAS for berseem season 1

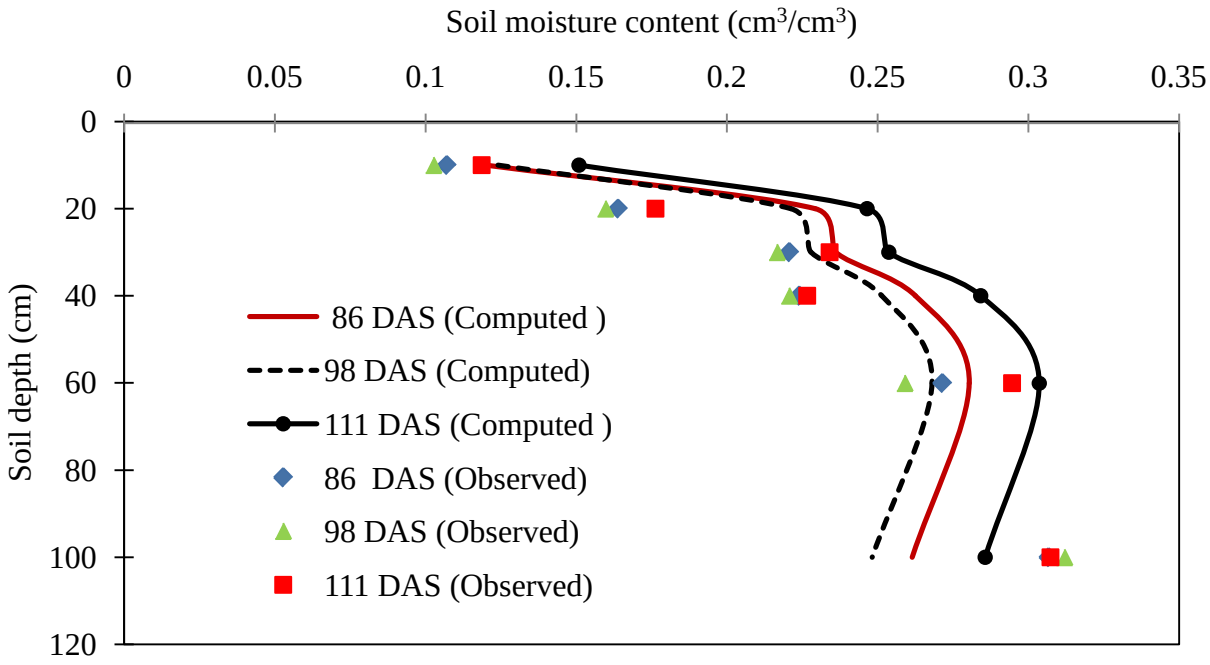

Fig. 5.22 Comparison of model predicted and field observed soil moisture profiles on 86, 98 and 111 DAS for berseem season 1

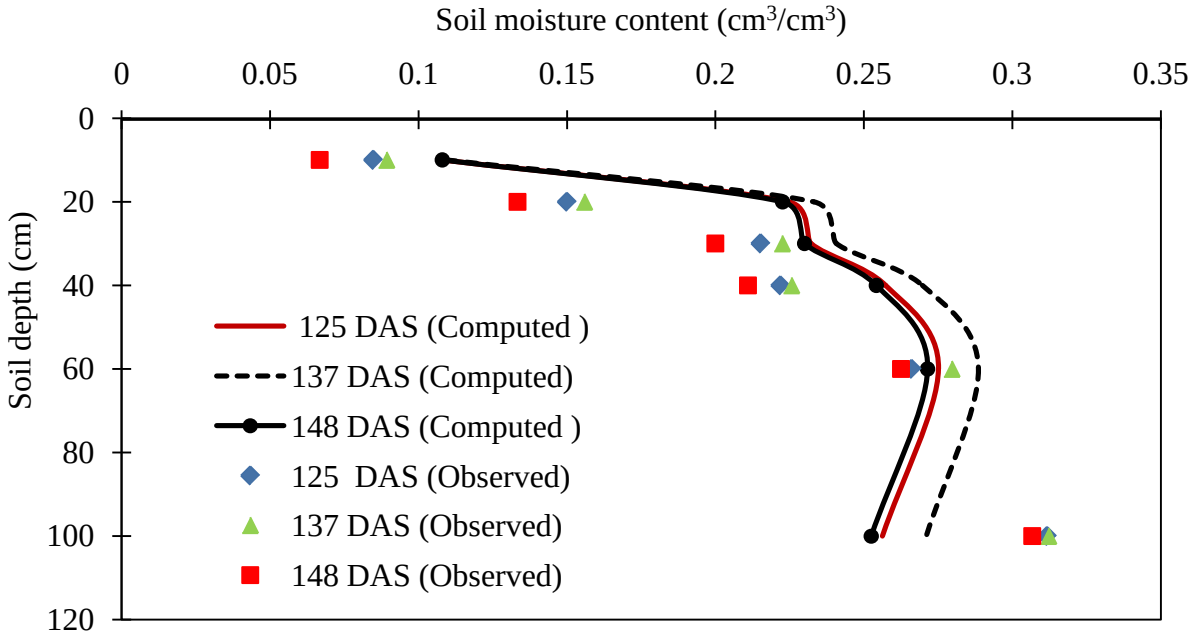

Fig. 5.23 Comparison of model predicted and field observed soil moisture profiles on 125, 137 and 148 DAS for berseem season 1

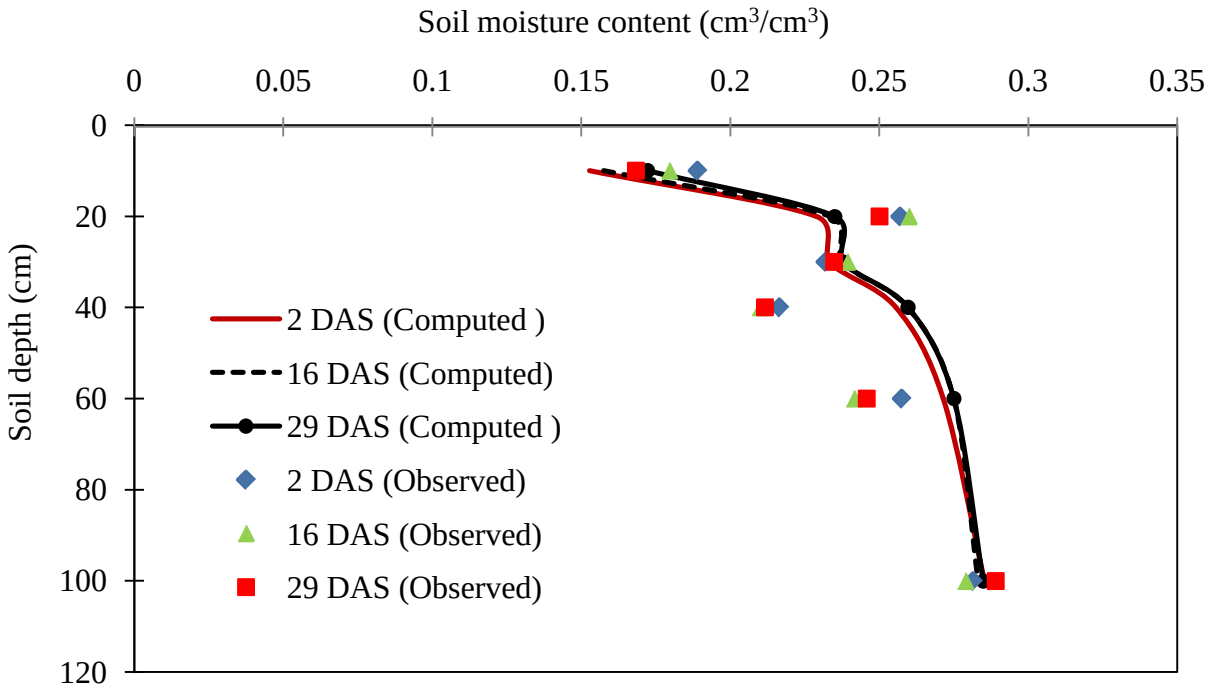

Fig. 5.24 Comparison of model predicted and field observed soil moisture profiles on 2, 16 and 29 DAS for berseem season 2

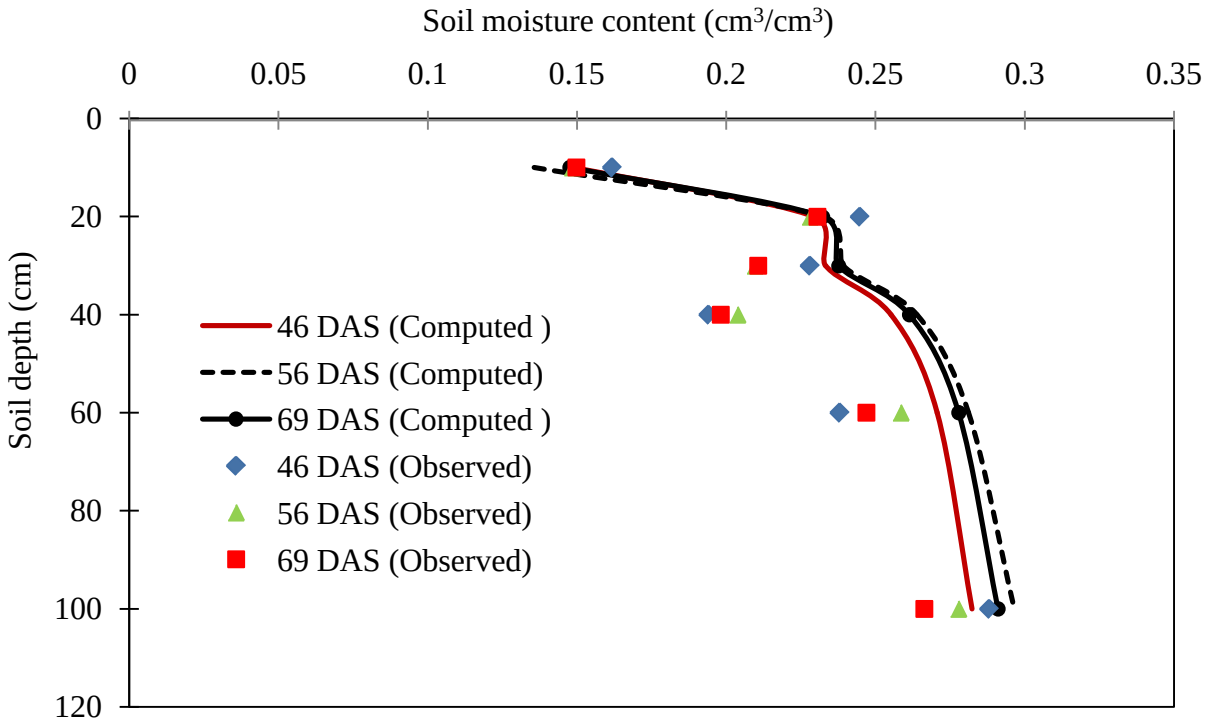

Fig. 5.25 Comparison of model predicted and field observed soil moisture profiles on 46, 56 and 69 DAS for berseem season 2

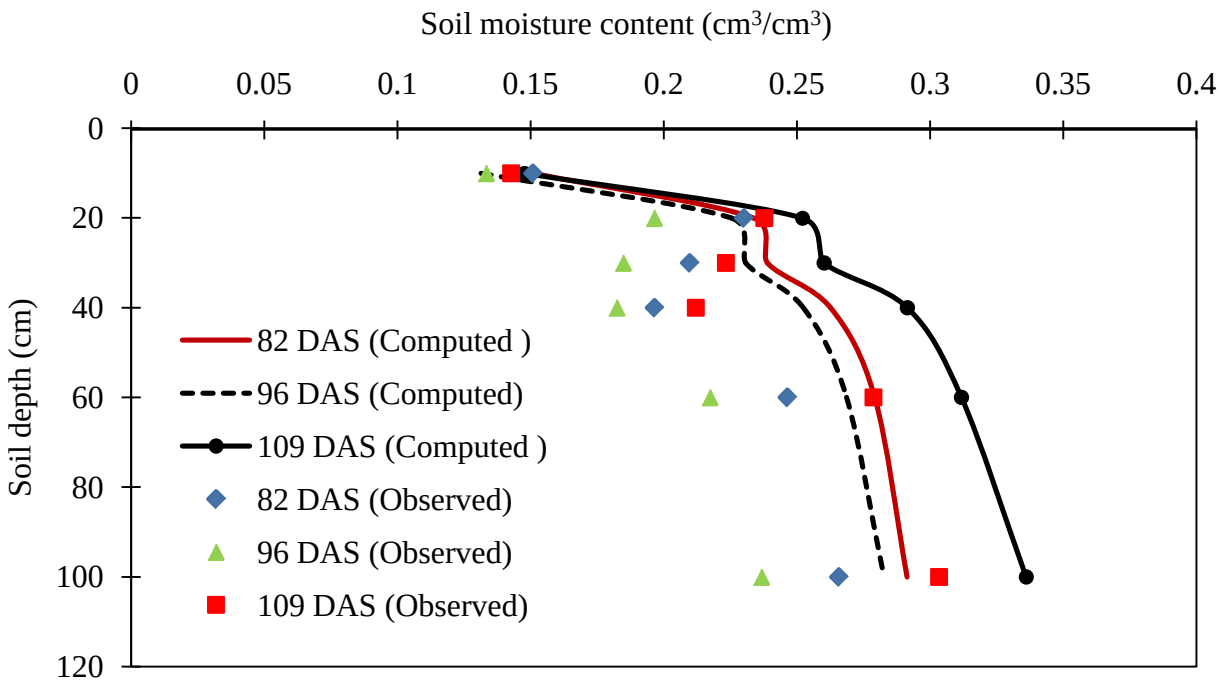

Fig. 5.26 Comparison of model predicted and field observed soil moisture profiles on 82, 96 and 109 DAS for berseem season 2

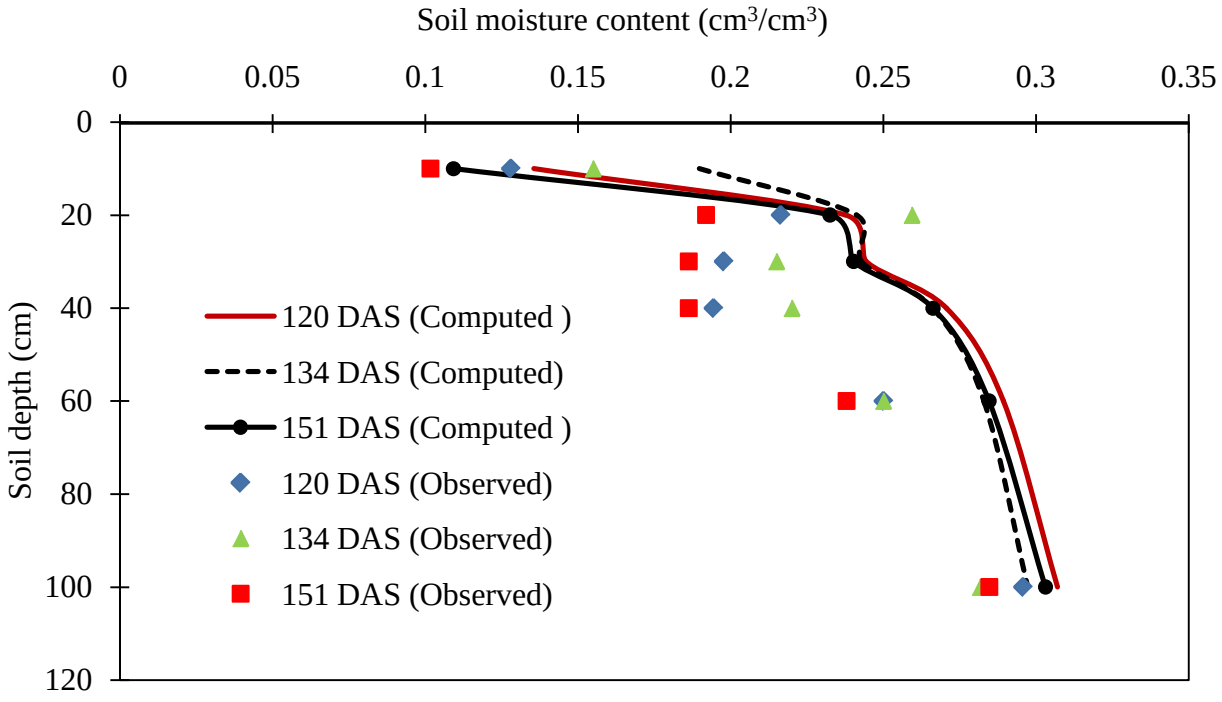

Fig. 5.27 Comparison of model predicted and field observed soil moisture profiles on 120, 134 and 151 DAS for berseem season 2

Generally, it has been observed that the measured soil moisture content values were less than the model computed soil moisture content values. This may be attributed to the soil

moisture measurement errors by the particular probe. The probe is reported to be extremely sensitive to large pore spaces (air gaps) near the access tubes (Whally et al. 2004). Air gaps (large pores) near the access tubes could not be avoided due to soil heterogeneity and soil cracking. In the first instance, the experimental field soil exhibits coarse textured soil with prevalence of large macropores which would cause an error in water content reading by the probe. Wetting and drying processes during the growing periods can create cracked zones which leave open spaces in the root zone (Zhang et al. 2014; Tournebize et al. 2006). It has also been anticipated that continuous manual operation of the probe might have also formed annular spaces between the access tube and soil column.

It has been observed that the soil moisture content variation in the field was so rapid, after rainfall or irrigation, that an instantaneous record of soil moisture content may not provide good correlation with average simulated water content (Liu and Shao 2015). More precise measurement of soil moisture content with high temporal resolution may be necessary to capture the soil moisture variation aiming for calibration in physically based models. On the other hand, soil moisture content values measured in drainage type lysimeters depict a slightly different condition than that of the actual field conditions as described by Flury et al. (1999) and Abdulkareem et al. (2015). Particularly at the bottom of drainage type lysimeters, evolution of saturated zone persists before free drainage takes place (Abdo and Flury 2004). Hence, an excellent agreement between the measured and computed water content values is unexpected. However, it should be noted that the change in measured soil moisture content is useful, in irrigation decisions, than the absolute water content as it provides relative soil moisture variation in soil column (Whally et al. 2004). It is being suggested that soil moisture monitoring instruments should exhibit high accuracy in acquiring moisture content data (Mittelbach et al. 2012). Moreover, operation of the soil moisture probe using data loggers is advisable which limits frequent movements of the access tube and may provide a representative data set.

5.6 COMPARISON OF PHYSICALLY BASED MODEL WITH WATER BALANCE MODEL

In the preceding and current chapters, deep percolation has been estimated using both simple water balance and physically based models. In this section, a comparison between the two approaches is made. As indicated earlier, the simple water balance model is easy to apply since the input data requirement is less when compared to the physically based model. On the

other hand, physically based approach requires more complete description of soil hydraulic properties and crop characteristics which limits their use under most field conditions.

From the preceding discussions it can be inferred that the performance of the physically based model is significantly better for the case of estimation of deep percolation on daily basis. However, there are certain merits and drawbacks in both approaches. If seasonal volume of percolation is of interest, both approaches can provide good estimation of the flow flux below the crop root zone. Table 5.10 provides the seasonal percolation values estimated using both approaches. As can be seen from Table 5.10, the seasonal deep percolation in both crop seasons and lysimeters is in close agreement with the field observed deep percolation.

Detailed information of flow flux for short time interval at specified depth below the ground can be obtained accurately by employing physically based model than the water balance approach. As can be inferred from the earlier sections that physically based model predicts deep percolation far better than the simple water balance on daily time step. In addition, other water balance components such as soil moisture storage, root water uptake as well as evaporation can be estimated well using the physically based approach for any specified time step. The simple water balance mainly works well for longer time steps.

Table 5.10 Comparison of measured and computed seasonal deep percolations

Crop season	Lysimeter	Deep percolation (mm)		
		Measured	Computed	
			physically based model	water balance model
Rice season 1	L1	2668.83	2698.10	2681.30
	L2	2525.86	2698.10	2674.30
Rice season 2	L1	937.19	924.93	952.73
	L2	1064.16	1047.05	980.06
Berseem season 1	L1	522.79	478.28	447.20
	L2	478.49	478.28	447.77
Berseem season 2	L1	148.15	116.88	135.14
	L2	132.27	124.10	159.70

Deep percolation was computed on weekly time basis for rice and between wetting intervals for berseem season using both physically based and simple water balance models to investigate the performance of the models. Figs. 5.28 to 5.35 depict model computed deep

percolation on weekly and between wetting intervals from both modelling approaches. The performance of both models is well when compared to field observations. However, the performance of the physically based model is again superior to the simple water balance model. Hence, detailed behaviour of flow phenomena in the root zone can be studied using the physically based modelling approach than the simple water balance model. Table 5.11 presents the error statistics for the two models in the crop seasons for both lysimeters. The performance of both models is good. The value of R^2 using the water balance model is ranging between 0.77-0.96 while it is falling between 0.84 and 0.98 using the physically based model. The *COV* value using the water balance model is 0.23-0.77 while it is ranging between 0.09-0.66 employing the physically based model in the crop seasons showing better performance of the models when they are used on lumped time basis.

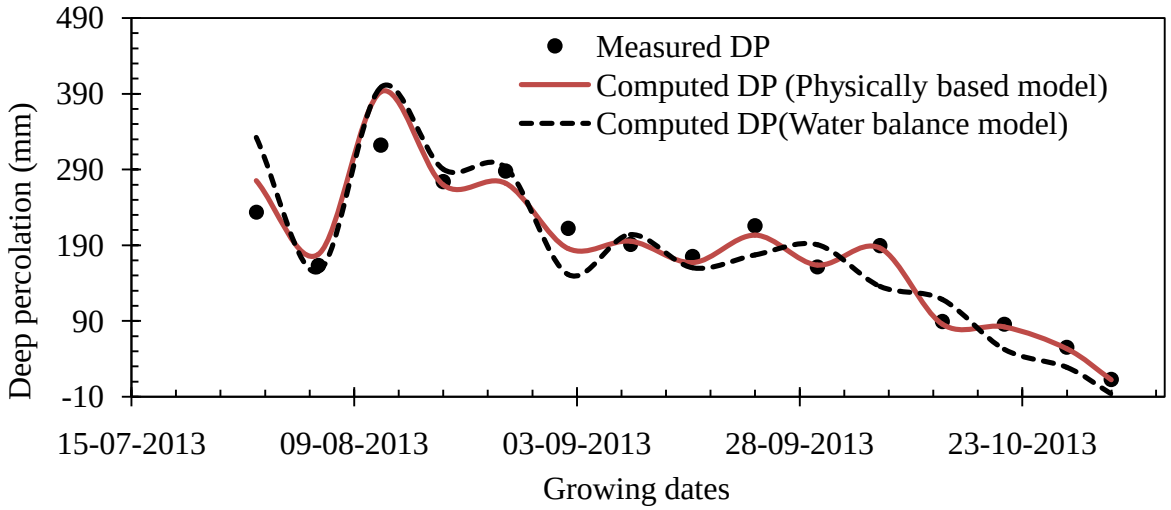

Fig. 5.28 Model computed and measured deep percolation for rice season 1 from lysimeter 1 with weekly time step

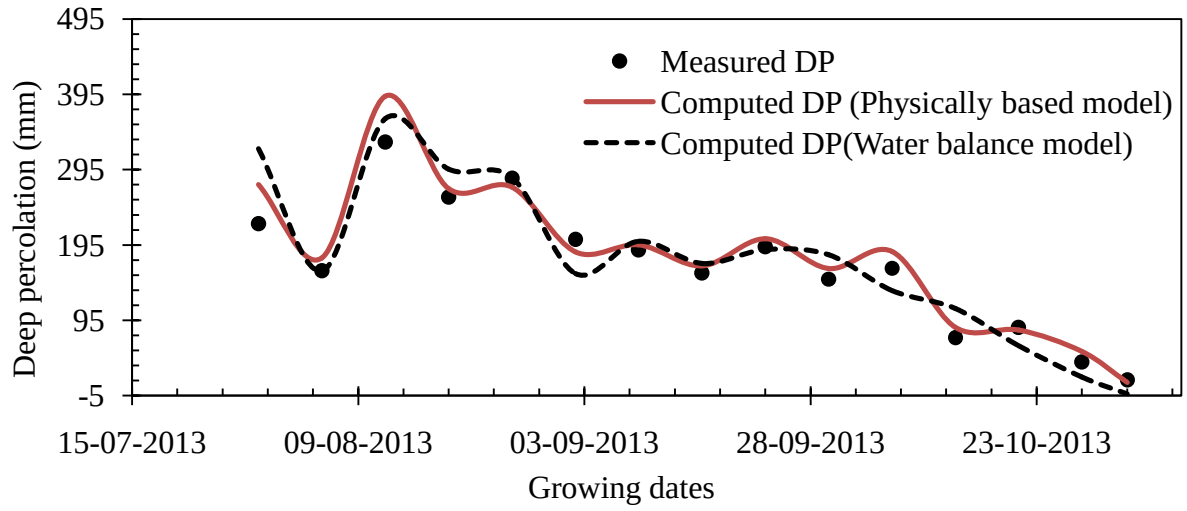

Fig. 5.29 Model computed and measured deep percolation for rice season 1 from lysimeter 2 with weekly time step

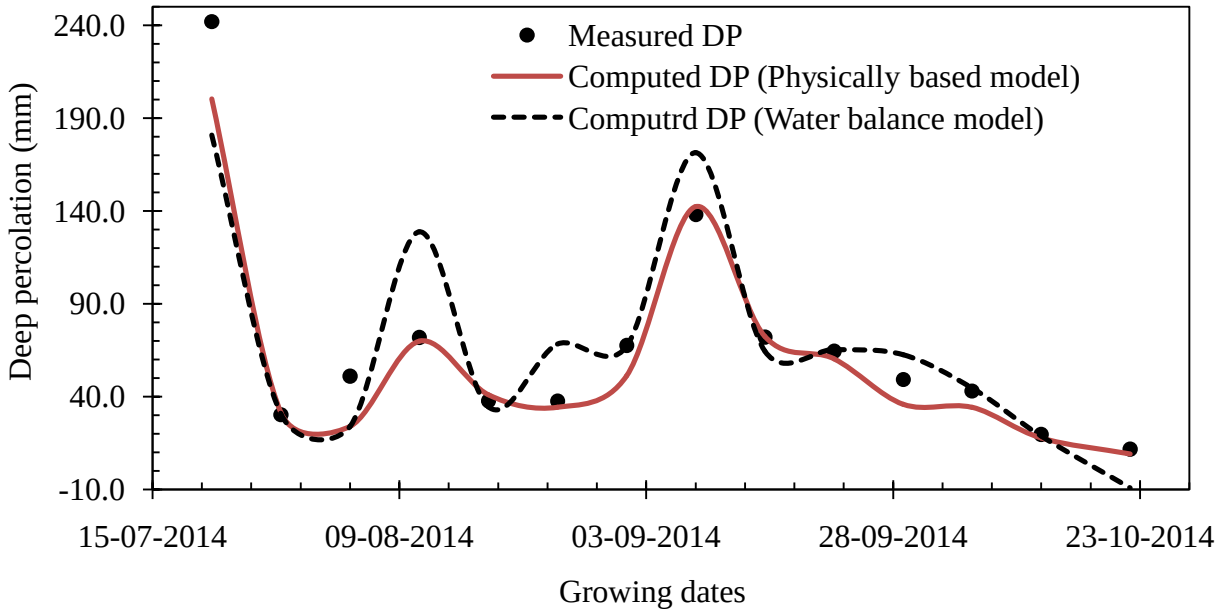

Fig. 5.30 Model computed and measured deep percolation for rice season 2 from lysimeter 1 with weekly time step

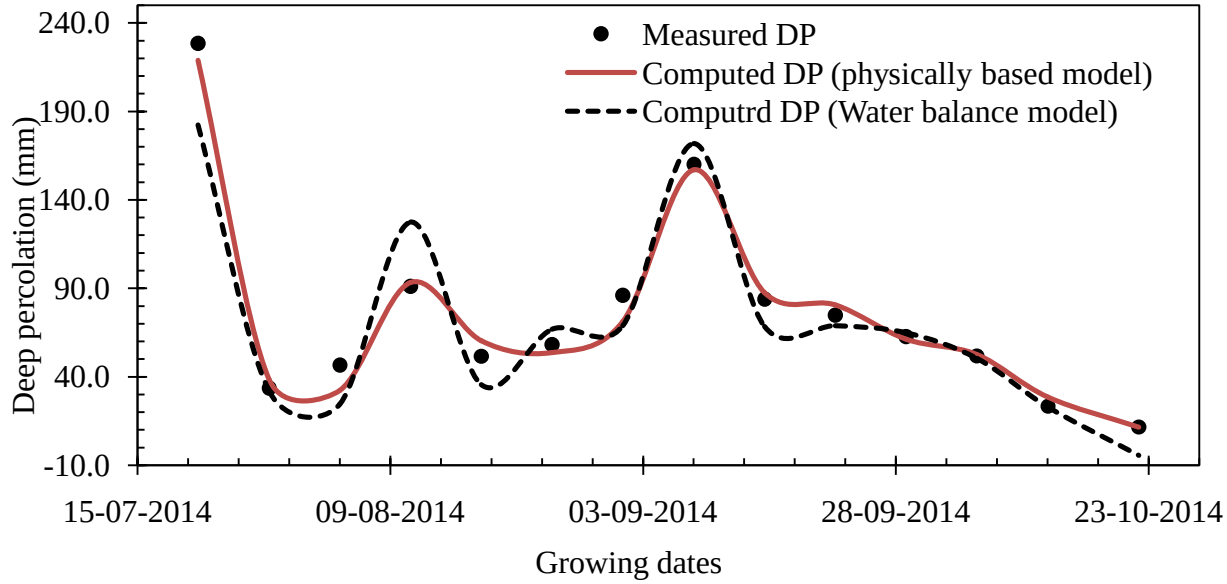

Fig. 5.31 Model computed and measured deep percolation for rice season 2 from lysimeter 2 with weekly time step

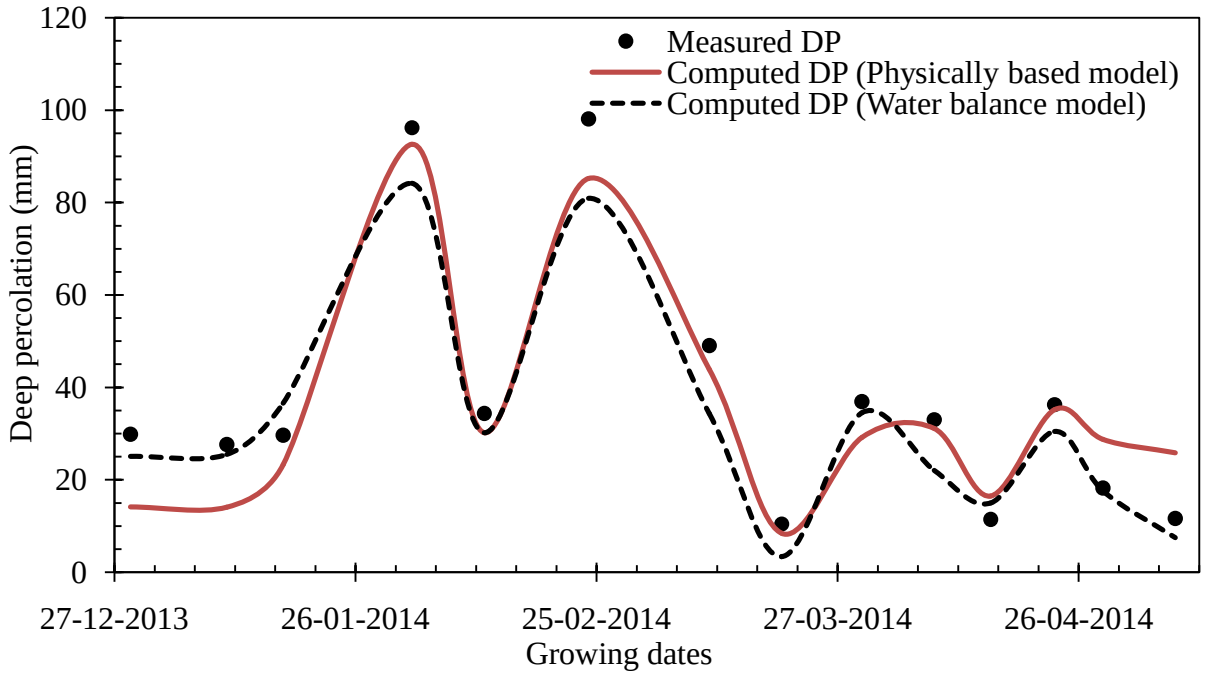

Fig. 5.32 Model computed and measured deep percolation for berseem season 1 from lysimeter 1 for time step between wetting intervals

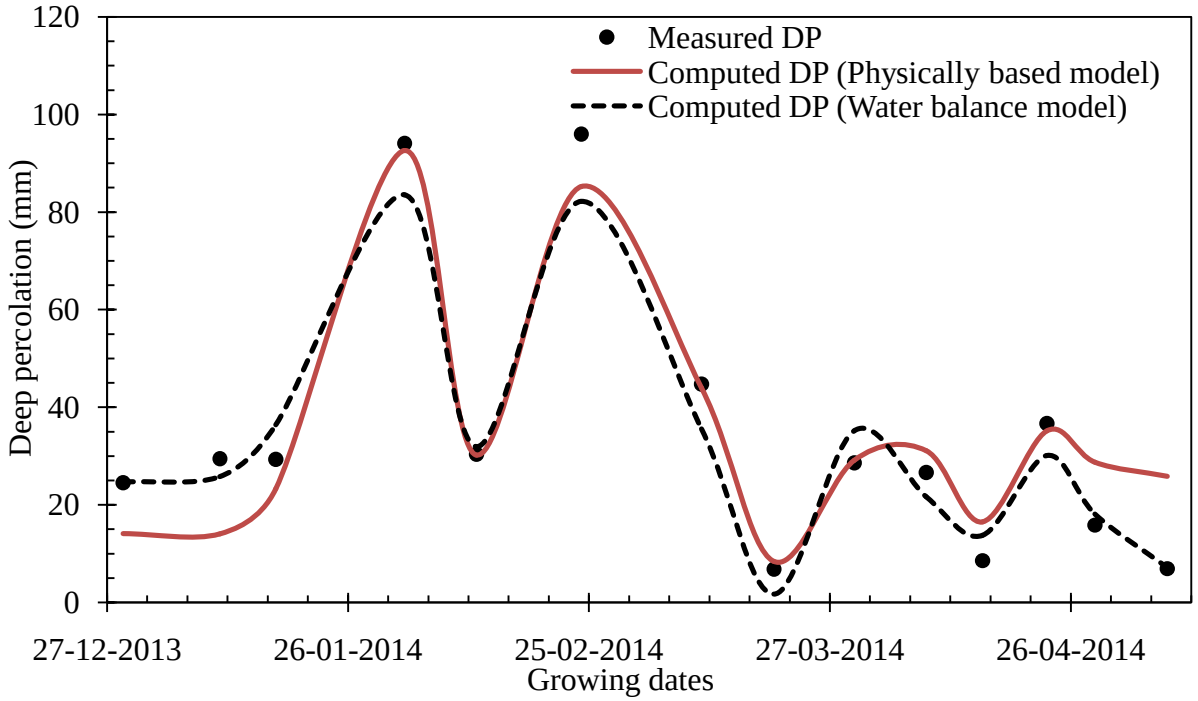

Fig. 5.33 Model computed and measured deep percolation for berseem season 1 from lysimeter 2 for time step between wetting intervals

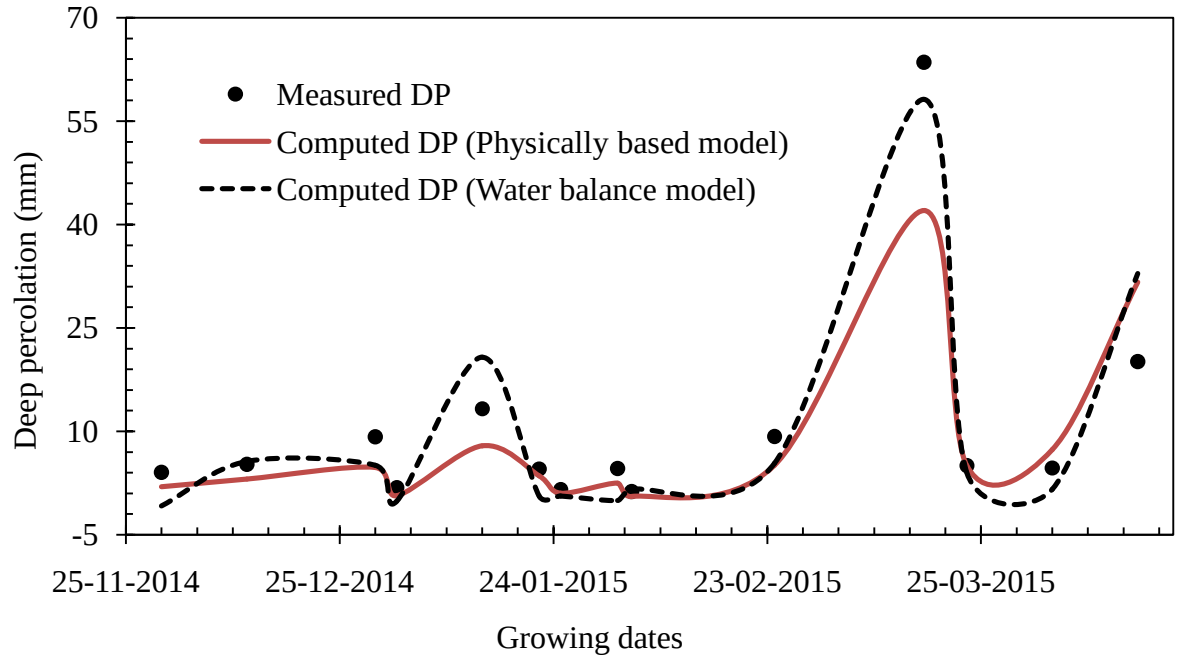

Fig. 5.34 Model computed and measured deep percolation for berseem season 2 from lysimeter 1 for the time step between wetting intervals

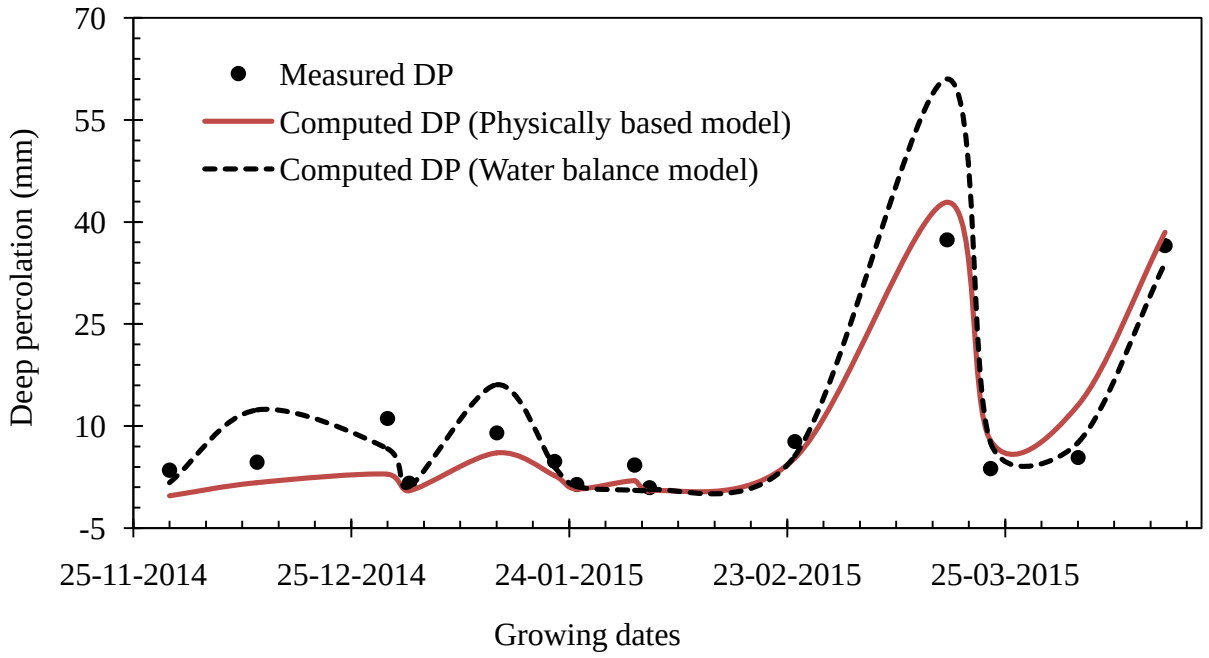

Fig. 5.35 Model computed and measured deep percolation for berseem season 2 from lysimeter 2 for the time step between wetting intervals

Table 5.11 Statistical performance of the employed models in estimating deep percolation on weekly (rice) and between wetting intervals (berseem season) using both models

Crop season	Lysimeter	Physically based model			Water balance model		
		R^2	*RMSE* (mm)	*COV*	R^2	*RMSE* (mm)	*COV*
Rice season 1	L1	0.95	23.20	0.13	0.87	43.30	0.24
	L2	0.96	23.90	0.14	0.90	38.00	0.23
Rice season 2	L1	0.96	14.8	0.21	0.77	27.60	0.37
	L2	0.98	7.2	0.09	0.89	19.40	0.23
Berseem season 1	L1	0.91	8.87	0.63	0.96	8.41	0.60
	L2	0.90	8.90	0.64	0.96	6.64	0.47
Berseem season 2	L1	0.84	6.99	0.66	0.91	5.05	0.48
	L2	0.92	4.03	0.43	0.86	7.24	0.77

5.7 CLOSURE

In this chapter, physically based model employing the HYDRUS-1D package has been used to compute deep percolation below the crop zone in the lysimeters. After preliminary model simulations using the observed soil retention and hydraulic parameters, model calibration has been made using the deep percolation data of the first season of each crop. Model validation was then conducted for the second season of each crop period. Fairly better results were obtained after model calibration. It has been observed that large values of saturated hydraulic conductivity prevail near the soil surface. This would be attributed to root proliferation, the activities of soil micro organisms and soil cracking near soil surface which favour more porous upper zone than the bottom layers.

The computed deep percolation has been compared with the field observed deep percolation on different temporal scales using physically based model. The percolation computed on daily time basis fairly agrees with the field observed deep percolation in both lysimeters and crop periods. Deep percolation was also computed on lumped time steps and compared with the field observed and deep percolation computed using the simple water balance model. The performance of the physically based model is again better than the water balance model when the lumped time step is used to compute deep percolation. In general, the two models perform better when a lumped time step is considered. However, for small

temporal resolution, the performance of physically based model is superior to the simple water balance model.

The HYDRUS-1D model has been calibrated for the soil hydraulic and crop parameters and performs well in predicting deep percolation during the crop seasons. It has been observed that the performance of the model is well in the wetter season of rice than the drier season of berseem. This would be attributed to comparatively large macropore development in the dry season than in the wetter season. This is a clear indication that physically based models which are based on the Richards equation perform well in wetter condition of the soil than the drier conditions.

CHAPTER 6
WATER SAVING AND WATER PRODUCTIVITY

6.1 PREAMBLE

In this chapter, water saving and water productivity in each crop season for the experimental field condition is presented. Water saving refers to the reduction in water input and/or irrigation size for a particular crop period without an appreciable decrease in crop yield. It is a relative term in which the difference between typical water input/irrigation schedules is compared. Water productivity, on the other hand, is generally defined as crop yield per cubic metre of water consumption (Cai et al. 2003). It also refers to the amount of water stored in the root zone to meet the evapotranspiration needs to water delivered at field head (Michael 2005). These terms indirectly refer to irrigation efficiency which can be expressed based on crop water use efficiency, irrigation water use efficiency or field water use efficiency. In the current chapter, water saving and water productivity are being discussed.

6.2 WATER SAVING

In this study, the role of imposed irrigation scheduling option of the two field crops grown in unpuddled sandy loam soil has been evaluated. During the first season of each crop, typical irrigation schedules as practiced in the farmers' field in the study area was followed while in the second season of each crop, a reduced irrigation schedule was imposed aiming for water saving and to study response of deep percolation. Taking the first season of each crop as reference, comparative water saving has been studied for the experimental field conditions. The water saving can be expressed in terms of either input water (irrigation + rainfall) saving or irrigation water saving. However, rainfall cannot be controlled as irrigation and hence irrigation water saving has been presented in this section. Tables 6.1 and 6.2 show comparative irrigation water saving in both crop seasons.

In rice season 1, irrigation water size amounting 30 to 80 mm was applied frequently as practiced in the study area. Overall there were 59 irrigation applications conducted in rice season 1. In rice season 2, 31 irrigations with depths ranging between 10-50 mm have been applied intermittently. In berseem season 1, irrigation sizes ranging between 30-60 mm were applied following the soil moisture status of the field. Irrigation was applied when nearly 40 percent of moisture depletion took place in the root zone. Overall 11 irrigations were conducted. In berseem season 2, irrigation was applied when nearly 50-60 % percent of moisture depletion took place in the root zone. In this season, irrigation sizes were also reduced to 7-19 mm. Overall, 6 irrigations were applied in the second berseem season.

Table 6.1 Seasonal irrigation depths and irrigation water saving in rice crop season

Crop season	Lysimeter/Plot	Irrigation (mm)	Rainfall (mm)	Measured *DP* (mm)	Irrigation water saving (%)
Rice season 1	L1	2418.80	659.30	2668.83	—
	L2	2418.80	659.30	2525.86	
	A11	2418.80	659.30	-	
	A12	2418.80	659.30	-	
	A13	2418.80	659.30	-	
	A14	2418.80	659.30	-	
Rice season 2	L1	630.00	532.90	937.19	73.95
	L2	851.00	532.90	1064.16	64.82
	A11	643.10	532.90	-	73.41
	A12	639.0	532.90	-	73.58
	A13	855.0	532.90	-	64.65
	A14	644.0	532.90	-	73.38

Table 6.2 Seasonal irrigation depth and irrigation water saving in berseem crop season

Crop season	Lysimeter/Plot	Irrigation (mm)	Rainfall (mm)	Measured *DP* (mm)	Irrigation water saving (%)
Berseem season 1	L1	550.00	225.80	522.79	—
	L2	550.00	225.80	478.49	
	A11	550.00	225.80	-	
	A12	550.00	225.80	-	
	A13	550.00	225.80	-	
	A14	550.00	225.80	-	
Berseem season 2	L1	63.10	220.80	148.15	88.53
	L2	91.90	220.80	132.27	83.29
	A11	175.10	220.80	-	68.16
	A12	164.50	220.80	-	70.09
	A13	127.00	220.80	-	76.91
	A14	127.00	220.80	-	76.91

Irrigation water saving ranging from nearly 65% to 74% of the reference season has been achieved by imposing an alternative irrigation schedule to the rice crop in the experimental field. On the other hand, in berseem season 2 irrigation water saving ranging from 68% to 88% was achieved when compared to the first season. Evidently, due to reduction in irrigation water application, input water saving was also attained. In fact, rainfall was also reduced in the second seasons of both crop periods. During rice season 2 there was significant reduction in rainfall when compared to rice season 1. On the other hand, the reduction in rainfall depth was not so large in berseem season 2 when compared to berseem season 1.

6.3 CROP YIELD AND WATER PRODUCTIVITY

Crop yield refers to the weight of a crop that is harvested per unit of land area. Crop yield is the measurement often used for a cereal, grain or legume and is normally measured in kilograms per hectare (metric tons per hectare). In each of the rice crop seasons, grain yield has been adjusted to have 14% grain moisture content (Chahal et al. 2007). Yield responses of different water applications of the two seasons were compared to investigate the effect of

reduced water application on yield for the particular experimental condition. The yield of berseem crop refers to harvested and measured green forage. There were four cuts made during the first and second growing seasons of the berseem crop. Sunil et al. (2012) pointed out that 5 to 6 cuts of berseem can be made if the first cut is made 55 days after sowing. However, in the current study, in both seasons of berseem the first cut was made after 72 days of sowing which resulted in reduced number of cuts.

Further, the water productivity (water use efficiency) of the crops is determined to evaluate the effect of water saving on crop yield in these experimental conditions. Several definitions exist for water productivity (Li et al. 2014; Singh et al. 2014; Mahajan et al. 2009; Zwart and Bastiaanssen 2004). Water productivity may be defined as the ratio of crop yield per unit of actual evapotranspiration (WP_{ETa}); or the ratio of crop yield per unit of irrigation water utilized (W_I) or both irrigation and rainfall input (WP_{I+P}). These particular cases mainly apply at field level assessment. In broader context, at basin level, regional or global assessment, the water productivity term may be applied in a different form and context. In this study, field level applications are referred as applicable to experimental field condition.

The water productivity can be expressed using the following equations (Li et al. 2014; Sudhir-Yadav et al. 2011; Michael 2005):

$$WP_{ETa} = \frac{Y}{ET_a} \tag{6.1}$$

where WP_{ETa} = water productivity based on evapotranspiration (Kg.m^{-3}); Y= actual crop yield (Kg); ET_a = actual evapotranspiration (m^3).

$$WP_I = \frac{Y}{I} \tag{6.2}$$

where WP_I (Kg.m^{-3}) is water productivity based on irrigation input; I(m^3) is irrigation input

$$WP_{I+P} = \frac{Y}{I+P} \tag{6.3}$$

where WP_{I+P} = water productivity based on total water input or field water productivity (Kg.m^{-3}). Tables 6.3 and 6.4 present the water productivity indices of the crop seasons based on measured yield, evapotranspiration, irrigation and total water input.

Table 6.3 Crop yield and water productivity indices for rice (grain yield)

Rice season 1						
Plot ID	A11	A12	A13	A14	L2	L1
Average Yield (kg/ha)	4140.00	4140.00	4030.00	4860.00	3250.00	3540.00
ET_a (mm)	408.64	411.72	411.72	411.72	410.91	410.99
I (mm)	2418.80	2418.80	2418.80	2418.80	2418.80	2418.80
I+P(mm)	3087.10	3087.10	3087.10	3087.10	3087.10	3087.10
WP_{ETa} (Kg/m^3)	1.01	1.01	0.98	1.18	0.79	0.86
WP_I (Kg/m^3)	0.17	0.17	0.17	0.20	0.13	0.15
$WP_{(I+P)}$ (Kg/m^3)	0.13	0.13	0.13	0.16	0.11	0.11
Rice season 2						
Yield (kg/ha)	3036.44	2666.67	2603.00	4700.00	2695.00	2688.17
ET_a (mm)	430.87	430.91	431.05	430.62	414.04	431.05
I (mm)	643.1	639	855	644	851.00	630.00
I+P(mm)	1176	1171.9	1387.9	1176.9	1383.9	1162.9
WP_{ETa} (Kg/m^3)	0.70	0.62	0.60	1.09	0.65	0.62
WP_I (Kg/m^3)	0.47	0.42	0.30	0.73	0.32	0.43
$WP_{(I+P)}$ (Kg/m^3)	0.26	0.23	0.19	0.40	0.19	0.23
Yield decrease (%)	26.66	35.59	35.41	3.29	17.08	24.06

Table 6.4 Crop yield and water productivity indices for berseem (green forage)

Berseem season 1						
Plot ID/Lysimeter	A11	A12	A13	A14	L2	L1
Average Yield (kg/ha)	48900	53800	55500	51700	41200	37200
ET_a (mm)	341.38	342.36	342.36	342.36	341.38	342.36
I (mm)	520.00	520.00	520.00	520.00	520.00	520.00
$I+P$(mm)	745.8	745.8	745.8	745.8	745.8	745.8
WP_{ETa} (Kg/m^3)	14.32	15.71	16.21	15.10	12.07	10.87
WP_I (Kg/m^3)	9.40	10.35	10.67	9.94	7.92	7.15
$WP_{(I+P)}$ (Kg/m^3)	6.56	7.21	7.44	6.93	5.52	4.99
Berseem season 2						
Yield (kg/ha)	40641.21	49660.29	35944.24	40904.00	27333.00	27893.00
ET_a (mm)	162.81	162.81	162.81	162.81	162.81	162.81
I (mm)	175.10	164.50	127.00	127.00	91.90	63.10
$I+P$(mm)	395.90	385.30	347.80	347.8	312.70	283.90
WP_{ETa} (Kg/m^3)	24.96	30.50	22.08	25.12	16.79	17.13
WP_I (Kg/m^3)	23.21	30.19	28.30	32.21	29.74	44.20
$WP_{(I+P)}$ (Kg/m^3)	10.27	12.89	10.33	11.76	8.74	9.82
Yield decrease (%)	16.89	7.69	35.24	20.88	33.66	25.02

Evidently, reducing the amount of water input, mainly through irrigation application increased the water productivity in terms of irrigation and overall water input. In rice season 1, irrigation water productivity was between 0.13-0.20 kg.m^{-3} which was increased to 0.3-0.73 kg.m^{-3} in rice season 2. The respective figures of overall input water productivity were ranging between 0.11-0.16 kg.m^{-3} and 0.19-0.40 kg.m^{-3} in rice season 1 and rice season 2, respectively. Yield responses as well as water productivity based on evapotranspiration in these experimental conditions agree with earlier studies for rice crop (Zwart and Bastiaanssen 2004). In fact, yield response of rice can vary widely depending on rice variety, environmental factors, climatic conditions, soil characteristics and agronomic practices applied in an area (Ladha et al. 2000; de Vries et al. 2010; Zwart and Bastiaanssen 2004). Yields ranging from 2-3.5 tonnes/ha are common as reported by Ladha et al. (2000). de Vries et al. (2010) also investigated rice yield

responses ranging 2-11.8 tonnes/ha in their water saving and continuous flooded rice field in the Sahelian environment. Zwart and Bastiaanssen (2004) have made an extensive review on water productivity based on four crops; wheat, rice, cotton and maize based on the evaporative demand. They realized that the water productivity of rice exceed the FAO values as reported by many research studies ranging between 0.6–1.6 kgm^{-3}. The FAO report of water productivity for rice is ranging between 0.7-1.16 kgm^{-3} which is in an agreement with the present study.

Yield values ranging between nearly 37-58 tonnes/ha in berseem season 1 and 27-50 tonnes/ha in berseem season 2 were observed. Sunil et al. (2012) have shown indicative values of berseem green fodder yield for the different varieties of berseem in India. JB-1 is a commonly grown variety in the central and North-Western India which was also grown in the experimental field. An average green fodder yield of 85 tonnes/ha was indicated by Sunil et al. (2012) which is significantly different from the yield obtained in this study. The number of cuts, agronomic conditions, sowing dates and other unaccounted factors may be responsible for the variation in yield. In this particular study, water stress is not the major factor for berseem crop yield reduction since during berseem season 2, no significant moisture stress was observed due to the low evaporative demand of the climate in the season. The seasonal evapotranspiration in berseem season 2 period was almost half of that of berseem season 1 as shown in chapter four. Similar agronomic conditions for both crop seasons were maintained except varying irrigation input. Hence, variation in sowing date and consequently reduced number of cuts is believed to be responsible for yield reduction for berseem crop in the particular experimental field. Further research may be required to investigate the effect of sowing dates on yield for berseem fodder crop. On the other hand, yield reduction for rice season was majorly attributed to water stress since the seasonal evapotranspiration was slightly increased while water input was reduced in rice season 2 compared to rice season 1. All the water productivity indices were increased during the berseem season 2 when compared with the berseem season 1.

In general, large saving in input water has been attained in both crop seasons which has resulted in nominal yield reduction. Additionally, crop yield can be improved by employing improved agronomic practices, shifting of sowing/planting dates and adoption of appropriate technologies (Humphreys and Gaydon, 2015b).

6.4 REDUCTION IN DEEP PERCOLATION

Besides large reduction in irrigation and input water, the percentage reduction in deep percolation was also investigated. Percentage reduction refers to the comparative reduction in

percolation between two growing seasons of rice and berseem crops. The computed seasonal deep percolation from water balance model has been used to calculate the percentage reduction.

The percentage amount of deep percolation was computed as a percentage of the total amounts of input water. For example, during rice season 1 in lysimeter 1, the computed percentage of deep percolation is 87.1% of total input water. In rice season 2, for the same lysimeter, the computed deep percolation is 81.9% showing a percentage reduction of 5.2% due to the imposed irrigation schedule. The reduction in *DP* ranges from 4.4 to 18 % in rice season while in the berseem season it ranges from -0.60 to 12.4%. In general, this study shows that reduction in percolation could also be achieved by changing irrigation scheduling strategy in the crop periods. Tables 6.5 and 6.6 show reduction in deep percolation in the corresponding crop seasons along with input water and computed *DP*.

Table 6.5 Reduction in deep percolation in rice season

Crop season	Lysimeter/Plot	Irrigation (mm)	Rainfall (mm)	Computed *DP* (mm)	*DP* (%)	Percentage reduction in *DP* (%)
Rice season 1	L1	2418.8	659.3	2681.3	87.1	—
	L2	2418.8	659.3	2674.3	86.9	
	A11	2418.8	659.3	2667.5	86.7	
	A12	2418.8	659.3	2664.3	86.6	
	A13	2418.8	659.3	2668.7	86.7	
	A14	2418.8	659.3	2668.4	86.7	
Rice season 2	L1	630.0	532.9	952.73	81.9	5.2
	L2	851.0	532.9	980.06	70.8	16.1
	A11	643.1	532.9	952.06	81.0	5.7
	A12	639.0	532.9	962.29	82.1	4.4
	A13	855.0	532.9	952.98	68.7	18.0
	A14	644.0	532.9	958.24	81.4	5.3

Table 6.6 Reduction in deep percolation in berseem season

Crop season	Lysimeter/Plot	Irrigation (mm)	Rainfall (mm)	Computed *DP* (mm)	*DP* (%)	Percentage reduction in *DP* (%)
Berseem season 1	L1	520.0	225.80	447.2	59.96	—
	L2	520.0	225.80	448.0	60.07	
	A11	520.0	225.80	455.1	61.02	
	A12	520.0	225.80	456.2	61.17	
	A13	520.0	225.80	449.2	60.23	
	A14	520.0	225.80	455.2	61.03	
Berseem season 2	L1	63.1	220.80	135.1	47.60	12.36
	L2	91.9	220.80	159.7	51.07	9.00
	A11	175.1	220.80	244.0	61.62	-0.60
	A12	164.5	220.80	229.3	59.52	1.65
	A13	127.0	220.80	194.8	56.02	4.21
	A14	127.0	220.80	199.2	57.26	3.77

6.5 CLOSURE

This chapter has provided an insight about crop yield and crop water productivity, based on measured crop yields under different irrigation regimes. Large saving in irrigation water can be achieved by practicing alternative irrigation schedules when compared with the conventional irrigation application in both rice and berseem seasons in an unpuddled coarse textured soil. Nominal yield reduction has been observed in both crops due to large reduction in irrigation water. Further, percentage reduction in deep percolation has also been observed in both crop seasons due to the shifting from conventional ways of irrigation application to reduced irrigation application strategy. In this study, only the impact of irrigation scheduling on crop yield has been investigated. However, yield can be affected by many other input variables such as crop variety, fertilizer application, planting date etc. which can be investigated in future for the unpuddled rice and berseem field conditions.

CHAPTER 7
CONCLUSIONS AND SCOPE OF FUTURE WORK

7.1 GENERAL

The present study is concerned with the analysis of deep percolation from the bottom of crop root zones. For this purpose the conventional water balance and physically based models were used for simulating one dimensional vertical flow in the unsaturated zone. The water balance model has been modified to take into account soil moisture change in the root zone and applied to the model domain. The model domain is the depth profile from ground surface to the bottom of lysimeters where observations of deep percolation were made. The physically based model is established to simulate the vertical flow in the unsaturated soil with the inclusion of root water uptake component. The physically based model is essentially based on the solution of Richards equation using finite element approach in HYDRUS-1D package. The model simulates the moisture flow in the model domain by assigning appropriate initial and boundary conditions. The top boundary conditions considered consist of irrigation, rainfall and evaporation. The bottom boundary condition is taken as free draining.

Two water intensive field crops which are commonly grown in the region at different seasons have been considered to evaluate the models and to study the deep percolation from the root zones of these crops. Rice has been grown in the summer (kharif) season while berseem fodder crop has been grown in the winter (rabi) season. Each crop was grown for two seasons in such a way that in the first crop season conventional irrigation was applied as practiced in a typical farmer's field while in the second season a reduced application was implemented. In all the cases, the unpuddled field condition was maintained.

To investigate the applicability of the aforementioned models laboratory and field experiments were conducted. The laboratory and field experiments consisted of determination of various soil and crop parameters which are used in the models. Lysimeter experiments were undertaken for monitoring deep percolation at the bottom of drainage type lysimeters which were installed in the experimental field. Model computed deep percolation have been compared with the field measured deep percolation both on daily and lumped time steps to investigate the applicability of the models for study of deep percolation in a cropped area.

7.2 CONCLUSIONS

The following conclusions can be drawn from the present study.

1. Deep percolation computed using the water balance model on daily time basis do not agree with the daily field observed deep percolation for both crop seasons and

lysimeters. Small values of coefficient of determination (R^2) (0.03-0.62) and large values of coefficient of variation (COV) (0.94-5.86) describe the weak performance of water balance model when used on daily time basis. However, the model predicts deep percolation very well on lumped time steps. The values of R^2 and COV, respectively, were ranging between 0.77-0.96 and 0.21-0.77 when lumped time step is considered. Therefore, accurate estimation of deep percolation can be made on lumped time steps using simple water balance model which do not require large number of input data.

2. Physically based model, unlike the water balance model, predicts deep percolation well below crop root zone in irrigated areas on daily time step. R^2 values ranging between 0.67-0.89 and COV in the range of 0.32-1.1 in the crop periods signify the better performance of the model when compared with the simple water balance model. The model also performs very well when lumped time step is considered to compute deep percolation when compared with the water balance model. R^2 values were 0.84-0.98 and COV values were 0.09-0.66 when deep percolation was computed on lumped time basis using the physically based model. Therefore, depending on the requirement of input data and the requirement of temporal resolution, one can use either water balance or physically based approach to predict deep percolation. When deep percolation is needed on coarser time resolution, one can use the water balance approach since it demands less input data. If estimation of deep percolation is needed on shorter time interval, in order of daily or less time steps, physically based model could provide a better result.
3. Although the physically based model captures deep percolation well, it could not attain the peak deep percolation values which usually occur during the heavy rainfall events in both crop seasons and lysimeters.
4. Large losses of deep percolation during both crop periods have been observed. Field experiments have showed that deep percolation value ranging 82-87% of input water has been lost through deep percolation during the continuous irrigation season in rice field. However, the amount of deep percolation was observed to decrease in response of reduced input water during the intermittent application of irrigation. In rice season 2, deep percolation was 77-80% of the overall input water. Similarly, in berseem season 1 the field measured deep percolation was 62-67% while it has reduced to 42-52% in berseem season 2. Nearly similar ranges of seasonal deep percolation have been predicted by the models. Deep percolation varies primarily in response to the input water depth and frequency of irrigation application/occurrence. Intense and continuous

storms particularly caused high percolation rate and depth than applied irrigation in most of the observation periods. During the summer seasons, saturated antecedent moisture conditions usually favour more deep percolation as consecutive daily rains prevail in the season. On the other hand, few intensive storms in winter season which occur after long periods of time in the season contribute to large deep percolation owing to the subsurface condition which facilitates pronounced preferential transport in the season.

5. Locally constructed drainage type lysimeters are robust enough in capturing deep percolation from the bottom of crop root zones. The lysimeters were responding well to the imposed irrigation and rainfall events during the growing seasons of rice and berseem crop fields subjected to varying regimes of water application. The lysimeters were also depicted the phenomena of preferential flow transport, distinguished the difference between daily and nocturnal deep percolation values. Deep percolation on day time was less than night time as verified from lysimeter measurements which show that evapotranspiration poses some influence on deep percolation. These types of lysimeters are easy to construct, maintain, monitor and affordable for field implementation in a given area.
6. Simulations using physically based model also showed a visible association between the observed and model simulated soil moisture content in the soil profile although there are discrepancies. The discrepancies between observed and model simulated soil moisture content are attributed to various factors including measurement error by the moisture probe, soil heterogeneity and the behaviour of water flow in lysimeters. Measurement errors using the probe due to large pores and soil heterogeneity under field conditions are unavoidable. Soil moisture content values measured in drainage type lysimeters depict a slightly different condition than that of the actual field condition; particularly at the bottom of drainage type lysimeters, evolution of saturated zone persists before free drainage takes place (Abdo and Flury 2004) which could not agree with the computed soil moisture content. Moreover, the model computes soil moisture content as daily cumulative value while field measurements were conducted on a given instant of time on a particular day.
7. Close investigation of the performance of the physically based model shows that the physically based model performs better in wet season than the dry season. An error statistics during the growing periods shows this fact. R^2 values of 0.79 to 0.89 have been computed during the rice seasons (wet summer) while R^2 values ranging between

0.67- 0.74 have been calculated in the berseem season (dry winter). The coefficient of variation was also low (below 0.5) in rice season when compared to the berseem season (above 0.5). The better performance of physically based model in wet seasons is attributed to the fact that (i) large openings are occupied by pre-existing water due to saturation or filled by migratory particles taken by gravity drainage, (ii) long periods of saturation are not conducive to macropore development and (iii) restriction of the activity of soil micro organisms and root penetration during the wet season.

8. Large values of the hydraulic conductivity parameter near the soil surface indicate the effect of crop root penetration, the activities of soil fauna and surface soil cracking. The hydraulic conductivity near the soil surface is over 200 cm/day while it decreases along the soil profile.
9. In the present study, the possibility of reducing deep percolation has been shown without the implementation of puddling, a traditional practice to reduce deep percolation, particularly in rice fields. Large saving in input water has been achieved with nominal yield decrease by employing alternative irrigation scheduling strategy during both crop seasons. Input water saving ranging from nearly 55% to 62% compared to the conventional approach has been achieved by imposing an alternative irrigation schedule to the rice crop in the experimental field. Irrigation water saving on the other hand ranges from approximately 65% to 74% of the typical existing irrigation application for the rice crop in the region. On the other hand, in the berseem season input water saving ranging from 47% to 62% has been achieved. Irrigation water saving in the order of 66% to 88% of the conventional approach in berseem has been attained. The alternative irrigation schedule considered in rice crop consisted of 20-27 mm applied on average interval of 2 days while for berseem an irrigation depth of 8 -11.5 mm applied on an average interval of interval 12 days.
10. Due to the imposed irrigation (reduced water application); yield reduction has been investigated in both crop periods. Yield reduction ranging from 17 % to 36% has been observed for rice when compared with the conventional water application. In the berseem season, yield reduction in the order of nearly 8 to 35 % has been investigated. However, yield reduction in berseem season may also be attributed to difference in sowing date (early sowing). The alternative irrigation strategy can educate farmers, particularly farmers under volumetric water pricing obligations, for reducing irrigation input in unpuddled field conditions to increase the net return. The net return would be

the result of nominal yield decrease and reduced cost of water, labour and energy for unpuddled field condition.

7.3 SCOPE FOR FUTURE WORK

The present work is mainly focused on the estimation and analysis of deep percolation from the root zones of water intensive crops. There are certain issues which can be investigated further in future.

1. The trial experiments in our experimental fields are limited due to the shortage of experimental plots and time. Large trial experiments are needed to assess an optimum irrigation scheduling option which could reduce deep percolation and induce no yield reduction.
2. Field experiments and modelling work were carried out for the sandy loam textured soil in the present study. These works may be extended to other soil types for the rice, berseem and other cropping conditions to quantify and investigate deep percolation characteristics.
3. In this study, due consideration is given for single porosity model, assuming matrix flow conditions prevail in the field. However, the role of macropore flow (preferential transport under field conditions and lysimeters) on deep percolation may not be ignored. Further investigation is required to quantify the macropore flow component of the deep percolation.
4. Yield response of rice and berseem can vary widely depending on rice variety, environmental factors, climatic conditions, soil characteristics and agronomic practices apart from availability of water. In the current study, only the effect of altering irrigation schedule has been investigated. The effect of variations on other conditions is left for further investigation.
5. The locally constructed drainage type lysimeters play an important role in monitoring deep percolation in an irrigated area. These types of lysimeters can be constructed elsewhere at wider scale for study of groundwater recharge, solute transport etc.

BIBLIOGRAPHY

1. Abdou, H.M. and Flury M. (2004). "Simulation of water flow and solute transport in free-drainage lysimeters and field soils with heterogeneous structure. Eur. J. Soil Sci., 55, 229-241.
2. Abdulkareem, J. H., Abdulkadir, A., and Abdu, N. (2015). "A Review of Different Types of Lysimeter Used in Solute Transport Studies." International Journal of Plant & Soil Science, 8(3), 1-14.
3. Ahmad, A., Bastiaanssen, W.G.M., and Feddes, R.A. (2002). "Sustainable use of groundwater for irrigation: a numerical analysis of the subsoil water fluxes." Irrig. Drain. 51 (3), 227-241.
4. Ahmad, M.D., Masih, I., and Giordano, M. (2014). "Constraints and opportunities for water savings and improving productivity through Resource Conservation Technologies in Pakistan." Agric. Ecosyst. Environ., 187, 106–115.
5. Allen, R. G., Pereira, L. S., Raes, D., and Smith, M. (1998). "Crop evapotranspiration: guidelines for computing crop water requirements." Food and Agriculture Organization of the United Nations, Rome.
6. Allen, S.J. (1990). "Measurement and estimation of evaporation from soil under sparse barley crops in northern Syria." Agricultural and Forest Meteorology, 49(4), 291–309.
7. Angus, J.F., and Zandstra, H.G. (1980). "Climatic factors and the modelling of rice growth and yield." Proceedings of the WMO-IRRI Symposium on Agro meteorology of the Rice Crop. Los Banos, pp.189-190.
8. Ansley, R. J., Dugas, W. A, Heuer, M. L., and Trevino, B.A. (1994). "Stem flow and porometer measurements of transpiration from honey mesquite (*Prosopis glandulosa*)." Journal of Experimental Botany, 45(6), 847–856.
9. Antonopoulos, V. Z. (2010). "Modelling of water and nitrogen balances in the ponded water and soil profile of rice fields in Northern Greece." Agricultural Water Management, 98, 321–330.
10. Anuraga, T. S., Ruiz, L., Kumar, M. S. M., Sekhar, M., and Leijnse, A. (2006). "Estimating groundwater recharge using land use and soil data: A case study in South India." Agricultural Water Management, 84(1-2), 65–76.

11. Arnold, L.R. (2011). “Estimates of deep-percolation return flow beneath a flood- and a sprinkler-irrigated site in Weld County, Colorado, 2008–2009.” U.S. Geological Survey Scientific Investigations Report, 2011–5001, 225 p.
12. Asadi, M. E., and Clemente, R. S. (2003). “Evaluation of CERES-Maize of DSSAT model to simulate nitrate leaching, yield and soil moisture content under tropical conditions.” Environment, 1(December), 270–276.
13. Baram, S., Kurtzman, D., and Dahan, O. (2012). “Water percolation through a clayey vadose zone.” J. Hydrol., 424-425, 165-171.
14. Beamer, J. P., Huntington, J. L., Morton, C. G., and Pohll, G. M. (2013). “Estimating Annual Groundwater Evapotranspiration from Phreatophytes in the Great Basin Using Landsat and Flux Tower Measurements.” Journal of the American Water Resources Association, 49(3), 518–533.
15. Belmans, C., Wesseling, J.G., and Feddes, R.A. (1983). “Simulation model of the water balance of a cropped soil: SWATRE.” J. Hydrol. 63 (3), 271–286.
16. Benes, S.E., Adhikari, D.D., Grattan, S.R., and Snyder, R.L. (2012). “Evapotranspiration potential of forages irrigated with saline sodic drainage water.” Agricultural Water Management, 105, 1-7.
17. Bethune, M. G., Selle, B., and Wang, Q. J. (2008). “Understanding and predicting deep percolation under surface irrigation.” Water Resources Research, 44, W12430, doi: 10.1029/2007WR006380.
18. Bethune, M., Austin, N., and Maher, S. (2001). “Quantifying the water budget of irrigated rice in the Shepparton Irrigation Region, Australia.” Irrigation Science, 20, 99-105.
19. Beven, K., and Germann, P. (1982). “Macropores and water flow in soils.” Water Resources Research, 18 (5), 1311–1325.
20. Bhuiyan, S. I., Sattar, M. A., and Khan, M. A. K. (1995). “Improving water use efficiency in rice irrigation through wet seeding.” Irrigation Science, 16, 1-8.
21. Bittelli, M. (2010). “Measuring Soil Water Potential for Water Management in Agriculture: A Review.” Sustainability, 2, 1226-1251.
22. Blyth, E.M., and Harding, R.J. (1995). “Applications of aggregation models to surface heat flux from the sahelian tiger bush.” Agricultural and Forest Meteorology, 17, 213-235.

23. Blyth, E., and Harding, R.J. (2011). “Methods to separate observed global evapotranspiration into the interception, transpiration and soil surface evaporation components.” Hydrol. Process. 25, 4063–4068.
24. Böhm, W. (1979). “Ecological studies series, 33, Methods of studying root systems.” Eds: Billings, W.D., Goiley,F., Lange, G.L., Oslon, J.S., and Ridge, O.,188.
25. Boehm, W., Maduakor, H. and Taylor, H.M. (1977). “Comparison of five methods for characterizing soybeans rooting density and development.” Agronomy J., 69, 615-419.
26. Bohren, C.F. and Huffman. D.R. (1983). “Absorption and scattering of light by small particles.” John Wiley, New York.
27. Bolstad, P.V., and Gower, S.T. (1990). “Estimation of leaf area index in fourteen southern Wisconsin forest stands using a portable radiometer.” Tree Physiol., 7, 115–124.
28. Bolton, F.R., and Zandstra, H.G. (1981). “A soil moisture based yield model of wetland rain-fed rice.” IRRI Research Paper, 62. IRRI, Los Banos.
29. Bouman, B.A.M., Castañeda, A.R., and Bhuiyan, S.I. (2002). “Nitrate and pesticide contamination of groundwater under rice-based cropping systems: past and current evidence from the Philippines.” Agriculture, Ecosystems and Environment, 92 (2-3), 185-199.
30. Bouman, B.A.M., Feng, L., Tuong, T.P., Lu, G., Wang, H., and Feng, Y. (2007b). “Exploring options to grow rice using less water in northern China using a modelling approach II. Quantifying yield, water balance components, and water productivity.” Agricultural Water Management, 88 (1-3), 23-33.
31. Bouman, B.A.M., Kropff, M.J., Tuong, T.P., Wopereis, M.C.S., Ten Berge, H.F.M., and van Laar, H.H. (2001). “ORYZA2000: Modelling Lowland Rice.” International Rice Research Institute, Wageningen University and Research Centre, Los Banõs, Philippines, Wageningen, Netherlands, p. 235.
32. Bouman, B.A.M., Lampayan, R.M., and Tuong, T.P. (2007a). “Water management in irrigated rice: Coping with water scarcity.” International Rice Research Institute, Los Banos.
33. Bouwer, H. (1987). “Effect of Irrigated Agriculture on Groundwater.” Journal of Irrigation and Drainage Engineering, 113, 4-15.
34. Breda, N. (2003). “Ground-based measurements of leaf area index: A review of methods, instruments and current controversies.” Journal of Experimental Botany, 54, 2403–2417.

35. Brooks, R. H., and Corey, A. T. (1964). “Hydraulic properties of porous medium hydrology.” Hydrology Paper, 3, Dept. of Civil Engineering, Colorado State Univ., Fort Collins, CO.
36. Burdine, N.T. (1953). “Relative permeability calculations from size distribution data.” Trans., AIME, 198, 71-78.
37. Cai, X., Cai, X., Rosegrant, M. W., and Rosegrant, M. W. (2003). “World Water Productivity: Current Situation and Future Options.” World Water, 163–178.
38. Campbell, G.S. (1974). “A simple method for determining unsaturated conductivity from moisture retention data.” Soil Sci., 117, 311-314.
39. Celia, M.A., Bouloutas, B.T., and Zarba, R.L. (1990). “A general mass conservative solution for the unsaturated flow equation.” Water Resources Research, 26(7), 1483-1496.
40. Chahal, G.B.S., Sood. A., Jalota, S.K., Choudhury, B.U., and Sharma, P.K. (2007). “Yield, evapotranspiration and water productivity of rice (Oryza sativa L.)–wheat (Triticum aestivum L.) system in Punjab (India) as influenced by transplanting date of rice and weather parameters.” Agricultural Water Management, 88, 14-22.
41. Chen, C. (2003). “Evaluation of air oven moisture content determination methods for rough rice.” Biosystems Engineering, 86(4), 447–457.
42. Chen, J.M., and Black, T.A. (1992). “Defining leaf-area index for non-flat leaves. Plant Cell and Environ., 15, 421–429.
43. Chen, S., and Wuing, C. (2002). “Analysis of water movement in paddy rice fields (I) experimental studies.” J. Hydrol., 260, 206–215.
44. Chen, S.K., and Liu, C.W. (2002). “Analysis of water movement in the paddy rice fields. (I) Experimental studies.” J. Hydrol., 260, 206-215.
45. Chien, C.P., and Fang, W.T. (2012). “Modeling irrigation return flow for the return flow reuse system in paddy fields.” Paddy Water Environ., 10,187-196.
46. Childs, E.C. and Collis-George, N. (1950). “The permeability of porous materials.” Proc., Roy. Soc. Ser. A., 201, 392-405.
47. Cholpankulov, E.D., Inchenkova, O.P., Paredes, P., and Pereira, L.S. (2008). “Cotton irrigation scheduling in Central Asia: Model calibration and validation with consideration of groundwater contribution.” Irrig. and Drain., 57: 516-532.
48. Choudhury, B.U., Singh A. K., and Pradhan, S. (2013). “Estimation of crop coefficients of dry-seeded irrigated rice-wheat rotation on raised beds by field water balance method in the Indo-Gangetic plains, India.” Agricultural Water Management, 123, 20-31.

49. Chow, V.T., Maidment, D.R., and Mays, L.W. (1980). “Applied hydrology.” McGraw-Hill, New York.
50. Clement, T.P., William, R.W., and Fred J. M. (1994). “A physically based, two-dimensional, finite-difference algorithm for modeling variably saturated flow.” J. Hydrol., 161, 71-90.
51. Clemente, R.S., De Jong, R., Hayhoe, H.N., Reynolds, W.D., and Hares, M. (1994). “Testing and comparison of three unsaturated soil water flow models.” Agricultural Water Management, 25(2), 135-152.
52. Cuenca, B.H. (1989). “Irrigation system design: An engineering approach.” Prentice Hall, New Jersey.
53. Daamen, C.C., Simmonds, L.P., Wallace, J.S., Laryea, K.B., and Sivakumar, M.V.K. (1993). “Use of micro lysimeters to measure evaporation from sandy soils.” Agricultural and Forest Meteorology, 65, (3-4), 159-173.
54. Danuso, F., Gani, M., and Giovanardi, R. (1995). “Field water balance:BidriCo2.” In: Pereira, L.S., vandenBroek, B.J., Kabat, P.,Allen,R.G. (Eds.), Crop-Water-Simulation Models in Practice.Wageningen Pers,Wageningen, pp.49-73.
55. Dauer, J. M., Withington, J. M., Oleksyn, J., Chorover, J., Chadwick O. A., Reich P. B., and Eissenstat, D.M. (2009). “A scanner-based approach to soil profile-wall mapping of root distribution.” Dendrobiology, 62, 35–40.
56. Daughtry, C.S.T. (1990). “Direct measurements of canopy structure.” Remote Sens. Rev., 5, 45–60.
57. Davis, R.G., Wiese, A.F., and Pafford, J.L. (1965). “Root moisture extraction profiles of various weeds.” Weeds, 13, 98-100.
58. de Azevedo, M. C. B., Chopart, J. L., and de Medina, C. C., (2011). “Sugarcane root length density and distribution from root intersection counting on a trench-profile.” Sci. Agric., 1, 94–101.
59. de Vries, M. E., Rodenburg, J., Bado, B. V., Sow, A., Leffelaar, P. A., and Giller, K. E. (2010). “Rice production with less irrigation water is possible in a Sahelian environment.” Field Crops Res., 116, 154-164.
60. Dewandel, B., Gandolfi, J.-M., de Condappa, D., and Ahmed, S. (2008). “An efficient methodology for estimating irrigation return flow coefficients of irrigated crops at watershed and seasonal scale.” Hydrol. Process, 22, 1700-1712.
61. Doorenbos, J., and Kassam, A. H. (1979). “Crop yield response to irrigation.” Irrigation and drainage Div., FAO-Rome, paper No.33.

62. Doorenbos, J., and Pruitt, W.O. (1977). “Guidelines for Predicting Crop Water Requirements.” FAO Irrig. Drain. Paper 24 (revised) p. 144.
63. Dunn, W., and Gaydon, D.S. (2011). “Rice growth, yield and water productivity responses to irrigation scheduling prior to the delayed application of continuous flooding in south-east Australia.” Agricultural Water Management, 98, 1799-1807.
64. Eilers, V.H.M., Carter, R.C., and Rushton, K.R. (2007). “A single layer soil water balance model for estimating deep drainage (potential recharge): An application to cropped land in semi-arid North-east Nigeria.” Geoderma, 140, 119–131.
65. Evett, S. R., Schwartz, R. C., Howell, T. A., Louis Baumhardt, R., and Copeland, K. S. (2012). “Can weighing lysimeter ET represent surrounding field ET well enough to test flux station measurements of daily and sub-daily ET?” Advances in Water Resources, Elsevier Ltd, 50, 79–90.
66. Evett, S.R., Warrick, A.W., and Matthias, A.D. (1995). “Wall material and capping effects on micro lysimeter temperatures and evaporation.” Soil Science Society of America Journal, 59 (2), 329-336.
67. FAO, (2002). “Deficit Irrigation Practices.” Water Reports 22, Rome, Italy. http://www.superglossary.com/Definition/Agriculture/Return_Flow.html
68. FAO, (2004). “Economic valuation of water resources in agriculture.” Rome, Italy.http://www.superglossary.com/Definition/Agriculture/Return_Flow.html.
69. FAO, (2003). “Unlocking the Water Potential of Agriculture. Food and Agriculture Organization of the United Nations.” http://www.fao.org/DOCREP/006/Y4525S/Y4525S00.HTM>.
70. Feddes, R. A., E. Bresler, and S. P. Neuman (1974). “Field test of a modified numerical model for water uptake by root systems.” Water Resources Research, 10(6), 1199-1206.
71. Feddes, R. A., Kowalik, P.J., and Zaradny, H. (1978). “Simulation of field water use and crop yield.” John Wiley & Sons, New York, NY, 1978.
72. Feddes, R.A., de Rooij, G.H., and van Dam, J. C. (2004). “Unsaturated Zone Modelling: Progress, Challenges and Applications.” Kluwer Academic Publishers, Dordrecht.
73. Feltrin, R. M., de Paiva, J. B. D., de Paiva, E. M. C. D., and Beling, F. A. (2011). “Lysimeter soil water balance evaluation for an experiment developed in the Southern Brazilian Atlantic Forest region.” Hydrol. Processes, 25(15), 2321–2328.
74. Ferrra, G., and Flore, J.A (2003). “Comparison between different methods for measuring transpiration in potted apple trees.” Biologia Plantarum, 46(1), 41-47.

75. Flumignan, D. L., Faria, R. T. De, and Lena, B. P. (2012). “Test of a microlysimeter for measurement of soil evaporation.” Engenharia Agrícola, 32(1), 80–90.
76. Flury, M., Yates, M. V., and Jury, W. A. (1999). “Numerical analysis of the effect of the lower boundary condition on solute transport in lysimeters.” Soil Sci. Soc. Am. J. 63, 1493 1499.
77. Fredlund, D. G., and Xing, A. (1994). “Equations for the soil-water characteristic curve.” Can. Geotech. J., 31(4), 521–532.
78. García-Garizábal, I., and Causapé, J. (2010). “Influence of irrigation water management on the quantity and quality of irrigation return flows.” J. Hydrol., 385, 36-43.
79. Gardner W.R. (1992) in H. J. W. Verplancke et al. (eds.). “Water Saving Techniques for Plant Growth.” Kluwer Academic Publishers, 13-19.
80. Garg, K.K., Das, B.S., Safeeq, M., and Bhadoria, P.B.S. (2009). “Measurement and modelling of soil water regime in a lowland paddy field showing preferential transport.” Agricultural Water Management, 96, 1705-1714.
81. Gee, G.W., and Hillel, D. (1998). “Groundwater recharge in arid regions: Review and critique of estimation methods.” Hydrol. Processes, 2: 255-266.
82. Glass, R.J., Steenhuis, T.S., and Parlange, J.Y. (1988). “Wetting front instability as a rapid and far-reaching hydrologic process in the vadose zone.” Journal of Contaminant Hydrology, 3 (2–4), 207–226.
83. Gonzalez, G. G. , Ramos, T. B. , Carlesso, R. , Paredes, P. , Petry, M. T. , Martins, J. D. , Aires, N. P. , and Pereira, L. S. (2015). “Modelling soil water dynamics of full and deficit drip irrigated maize cultivated under a rain shelter.” Biosyst. Eng., 132, 1-18.
84. Ghosh, R. K. (1980). “Estimation of soil moisture characteristics from mechanical properties of soils.” Soil Science, 130, 60-63.
85. Govindaraju, R. S., Reddi, L. N., and Bhargava, S. K. (1995). “Characterization of Preferential Flow Paths in Compacted Sand-Clay Mixture.” Journal of Geotechnical Engineering, 121, 652–659.
86. Govindaraju, R.S., and Kavvas, M.L. (1993). “Development of an approximate model for unsaturated flow with root water uptake under rectangular water content profiles assumption.” J. Hydrol., 146,321-339.
87. Grelle, A., Lundberg, A., Lindroth, A., Moren, A.S., and Cienciala, E. (1997). “Evaporation components of a boreal forest: variations during the growing season.” J. Hydrol., 197, 70-87.

88. Gupta, S.C., and Larson, W.E. (1979). “Estimating soil water retention characteristics from particle size distribution, organic matter and bulk density.” Water Resources Research, 15(6), 1633-1635.
89. Guymon, G.L. (1994). “Unsaturated Zone Hydrology.” PTR PRENTICE HALL, New Jersey.
90. Ham, J.M., Heilman, J.L. and Lascano, R.J. (1990). “Determination of soil water evaporation and transpiration from energy balance and stem flow measurements.” Agricultural and Forest Meteorology, 52(3-4), 287-301.
91. Han, M., Zhao, C., Šimůnek, J., and Feng, G. (2015). “Evaluating the impact of groundwater on cotton growth and root zone water balance using Hydrus-1D coupled with a crop growth model.” Agricultural Water Management, 160, 64–75.
92. Hardie, M. A., Cotching, W. E., Doyle, R. B., Holz, G., Lisson, S., and Mattern, K. (2011). “Effect of antecedent soil moisture on preferential flow in a texture-contrast soil.” J. Hydrol., 398, 191-201.
93. Hatiye, S.D., Hari Prasad, K.S., Ojha, C.S.P., and Adeloye, A.J. (2016). “Estimation and characterization of deep percolation from rice and berseem fields using lysimeter experiments on sandy loam soil-case study.” J.Hydrol. Eng., 21(5), 05016006.
94. Hatiye, S.D., Hari Prasad, K.S., Ojha, C.S.P., and Kaushika, G.S. (2014). “Estimation of deep percolation from rice paddy field using lysimeter experiments on sandy loam soil.” International Conference on “Hydraulics, Water Resources, Coastal and Environmental Engineering (HYDRO-2014 International)”, December 18-20, 2014. National Institute of Technology, Bhopal, India.
95. Hendrickx, J.M.H., and Flury, M. (2001). “Uniform and preferential flow, mechanisms in the vadose zone. Conceptual Models of Flow and Transport in the Fractured Vadose Zone.” National Research Council, National Academy Press, Washington, pp. 149–187.
96. Hillel, D. (1977). “Computer simulation of soil water dynamics: a compendium of recent work.” Ottowa, IDRC, 214.
97. Hillel, D. (1980). “Environmental Soil Physics.” Elsevier Academic Press, Amsterdam.
98. Hillel, D. (2004). “Introduction to Environmental Soil Physics.” Elsevier Academic Press, Amsterdam.
99. Hillel, D., Van Beek, C.G.E.M., and Talpaz, H., (1975). “A microscopic model of soil water uptake and salt movement to plants.” Soil Sci., 120, 385–399.

100. Hills, R. G., Hudson, D. B., Porro, I., and Wierenga, P. J. (1989). “Modeling one-dimensional infiltration into very dry soils: 2. Estimation of the soil water parameters and model predictions.” Water Resources Research, 25(6), 1271–1282.
101. Holmes, J.W., (1984). “Measuring evapotranspiration by hydrological methods.” Agricultural Water Management, 8, 29–40.
102. Home, P.G., Panda, R.K., Kar,S., 2002. “Effect of method and scheduling of irrigation on water and nitrogen use efficiencies of Okra (Abelmoschus esculentus).” Agricultural Water Management, 55, 159-170.
103. Hopmans, J. W., and J. N. M. Stricker (1989). “Stochastic analysis of soil water regime in a watershed.” J. Hydrol., 105, 57-84.
104. Huang, P. M., Li, Y., and Sumner, M. E. (2012). “Handbook of Soil Sciences: Properties and Processes, Second Edition.” CRC press, Tailor and Francis Group, New York.
105. Humphreys, E. (1992). “Lockup bay test guidelines.” Farmers' Newsletter Large Area. 140: 45- 46.
106. Humphreys, E., and Gaydon, D. S. (2015a). “Options for increasing the productivity of the rice–wheat system of North West India while reducing groundwater depletion. Part 2. Is conservation agriculture the answer?” Field Crops Res., 173, 81–94.
107. Humphreys, E., and Gaydon, D. S. (2015b). “Options for increasing the productivity of the rice–wheat system of north-west India while reducing groundwater depletion. Part 1. Rice variety duration, sowing date and inclusion of mungbean.” Field Crops Res., 173, 68–80.
108. Huntington, J. L., and Allen, R. G. (2009). “Evapotranspiration and Net Irrigation Water Requirements for Nevada.” World Environmental and Water Resources Congress 2009: Great Rivers, 1–15.
109. IRRI (International Rice Research Institute) (2004). “Annual Report.” IRRI, Los Banõs, Philippines.
110. Jackson, N. A., and Wallace, J. S. (1999). “Soil evaporation measurements in an agro forestry system in Kenya.” Agricultural and Forest Meteorology, 94(3-4), 203–215.
111. Janssen, M., and Lennartz, B. (2009). “Water losses through paddy bunds: Methods, experimental data, and simulation studies.” J. Hydrol., 369, 142-153.
112. Jarvis, N.J. (1994). The MACRO model (version 3.1): “Technical descriptions and sample simulations, reports and dissertations 19.” Department of soil science, Swedish University of Agricultural Sciences, Uppsala, Sweden.

113. Ji, X. Bin, Kang, E. S., Chen, R. S., Zhao, W. Z., Zhang, Z. H., and Jin, B. W. (2007). "A mathematical model for simulating water balances in cropped sandy soil with conventional flood irrigation applied." Agricultural Water Management, 87(3), 337–346.

114. Jiang, S., Pang, L., Buchan, G. D., Šimůnek, J., Noonan, M. J., and Close, M. E. (2010). "Modelling water flow and bacterial transport in undisturbed lysimeters under irrigations of dairy shed effluent and water using HYDRUS-1D." Water research, 44, 1050-1061.

115. Jonckheere, I., Fleck, S., Nackaerts, K., Muys, B., Coppin P., Weiss M., and Baretet, F. (2004). "Review of methods for in situ leaf area index determination Part I. Theories, sensors and hemispherical photography." Agricultural and Forest Meteorology, 121, 19-35.

116. Jung, J. W., Yoon, K. S., Choi, D. H., Lim, S. S., Choi, W. J., Choi, S. M., and Lim, B. J. (2012). "Water management practices and SCS curve numbers of paddy fields equipped with surface drainage pipes." Agricultural Water Management, 110, 78–83.

117. Kabat, P., van den Broek, B.J., and Feddes, R.A. (1992). "SWACROP: a water management and crop production simulation model." ICID Bull., 41 (2), 61-84.

118. Kendy, E., Zhang, Y., Liu, C., Wang, J., and Steenhuis, T. (2004). "Groundwater recharge from irrigated cropland in the North China Plain: Case study of Luancheng County, Hebei Province, 1949-2000." Hydrol. Processes, 18(12), 2289–2302.

119. Kim, H.K., Jang, T.I., Im, S.J., and Park, S.W. (2009). "Estimation of irrigation return flow from paddy fields considering the soil moisture." Agricultural Water Management, 96, 875-882.

120. Kirkham, M.B. (2005). "Principles of soil and plant water relations." Academic press, pp 101-105.

121. Klocke, N. L., Heermann, D. F., and Duke, H. R. (1985). "Measurement of evaporation and transpiration with lysimeters." Transactions of the ASAE, 183–190.

122. Köhne, J. M., Köhne, S., and Šimůnek, J. (2009). "A review of model applications for structured soils: b) Pesticide transport." Journal of Contaminant Hydrology, 104(1-4), 36–60.

123. Kosugi, K. (1996). "Lognormal distribution model for unsaturated soil hydraulic properties." Water Resources Research, 32(9), 2697-2703.

124. Kottek, M., Grieser, J., Beck, C., Rudolf, B., and Rubel, F. (2006). “World map of the Köppen-Geiger climate classification updated.” Meteorologische Zeitschrift, 15(3), 259-263.
125. Kowalik, P. J. (2006). “Drainage and capillary rise components in water balance of alluvial soils.” Agricultural Water Management, 86, 206-211.
126. Kücke, M., Schmid, H., and Spiess, A. (1995). “A comparison of four methods for measuring roots of field crops in three contrasting soils.” Plant and Soil, 172, 63-71.
127. Kukal, S. S., and Aggarwal, G. C. (2003). “Puddling depth and intensity effects in rice-wheat system on a sandy loam soil. I. Development of subsurface compaction.” Soil and Tillage Res., 72(1), 1–8.
128. Kukal, S. S., Hira, G. S., and Sidhu, A. S. (2005). “Soil matric potential-based irrigation scheduling to rice (Oryza sativa).” Irrigation Science, 23(4), 153–159.
129. Kukal, S.S., and Aggarwal, G.C. (2002). “Percolation losses of water in relation to puddling intensity and depth in a sandy loam rice (Oryza sativa) field.” Agricultural Water Management, 57, 49-59.
130. Kukal, S.S., and Sidhu, A.S., (2004). “Percolation losses of water in relation to pre-puddling tillage and puddling intensity in a puddled sandy loam rice (Oryza sativa L.) field.” Soil and Tillage Res., 78, 1-8.
131. Kung, K.J.S. (1990). “Preferential flow in a sandy vadose zone: 2. Mechanism and implications.” Geoderma, 46 (1–3), 59–71.
132. Ladha, J.K., Fischer, K.S., Hossain, M., Hobbs, P.R., and Hardy, B. (Eds.). (2000). “Improving the productivity and sustainability of rice-wheat systems of the Indo-Gangetic Plains: a synthesis of NARS-IRRI partnership research.” IRRI Discussion Paper Series No. 40. Int. Rice Research Institute, Los Banos, Philippines, 31 pp.
133. Leuning, R., Condon, A.G., Dunin, F.X., Zegelin, S., and Denmead, O. T. (1994). “Rainfall interception and evaporation from soil below a wheat canopy.” Agricultural and Forest Meteorology, 67, 221-238.
134. Li, D., and Shao, M. (2014). “Temporal stability analysis for estimating spatial mean soil water storage and deep percolation in irrigated maize crops.” Agricultural Water Management, 144, 140–149.
135. Li, Y., Šimůnek, J., Jing, L., Zhang, Z., and Ni, L. (2014). “Evaluation of water movement and water losses in a direct-seeded-rice field experiment using Hydrus-1D.” Agricultural Water Management, 142, 38-46.

136. Lin, Y., and Garcia, L. A. (2012). “Assessing the Impact of Irrigation Return Flow on River Salinity for Colorado’s Arkansas River Valley.” Journal of Irrigation and Drainage Engineering, 138(5), 406–415.
137. Liu, B., and Shao, M. (2015). “Modelling soil-water dynamics and soil-water carrying capacity for vegetation on the Loess Plateau, China.” Agricultural Water Management, 159, 176-184.
138. Liu, C.W., Chen, S.K., Jang, C.S. (2004). “Modelling water infiltration in cracked paddy field soil.” Hydrol. Proces., 18, 2503–2513.
139. Liu, Y., Pereira, L.S., and Fernando, R.M. (2006). “Fluxes through the bottom boundary of the root zone in silty soils: Parametric approaches to estimate groundwater contribution and percolation.” Agricultural Water Management, 84, 27-40.
140. Liu, Y., Teixeira, J.L., Zhang, H.J., and Pereira, L.S. (1998). “Model validation and crop coefficients for irrigation scheduling in the North China Plain.” Agricultural Water Management, 36, 233-246.
141. Lo´pez-Urrea, R., Olalla F. M. S., Fabeiro, C., and Moratalla, A. (2006). “Testing evapotranspiration equations using lysimeter observations in a semiarid climate. Agricultural Water Management, 88, 141-146
142. Loos, C., Gayler, S., and Priesack, E. (2007). “Assessment of water balance simulations for large-scale weighing lysimeters.” J. Hydrol., 335, 259- 270.
143. Ma, Y., Feng, S., Song, X. (2013). “A root zone model for estimating soil water balance and crop yield responses to deficit irrigation in the North China Plain.” Agricultural Water Management, 127, 13–24.
144. Madramootoo, C.A., and Fyles, H. (2010). “Irrigation in the context of today's global food crisis.” Irrigation and Drainage, 59(1), 40-52.
145. Mahajan, G., Bharaj, T. S., and Timsina, J. (2009). “Yield and water productivity of rice as affected by time of transplanting in Punjab, India.” Agricultural Water Management, 96(3), 525–532.
146. Malaya, C., and Sreedeep, S. (2012). “Critical Review on the Parameters Influencing Soil-Water Characteristic Curve.” Journal of Irrigation and Drainage Engineering, 138(1), 55–63.
147. Mavimbela, S. S. W. and van Rensburg L. D. (2013). “Estimating hydraulic conductivity of internal drainage for layered soils in situ.” Hydrol. Earth Syst. Sci., 17, 4349–4366.

148. Meiβner, R., Prasad, M.N.V., Laing, G. Du. and Rinklebe, J. (2010). "Lysiemter application for measuring the water and solute fluxes with high precision." Current Science, 99 (5),601- 607
149. Merta, M., Seidler, C., and Fjodorowa, T. (2006). "Estimation of evaporation components in agricultural crops." Biologia, 61(S19), 280–283.
150. Michael, A.M. (2005). "Irrigation Theory and Practice." Vikas Publshing House LTD, New Delhi, pp. 546-549.
151. Mitchell, J., Cheth, K., Seng, V., Lor, B., Ouk, M., and Fukai, S. (2013). "Wet cultivation in lowland rice causing excess water problems for the subsequent non-rice crops in the Mekong region." Field Crops Res., 152, 57-64.
152. Mittelbach, H., Lehner, I., and Seneviratne, S. I. (2012). "Comparison of four soil moisture sensor types under field conditions in Switzerland." J. Hydrol., 430-431, 39–49.
153. Mohanasundaram, S., Suresh Kumar, G. and Narasimhan, B. (2013). "Numerical modelling of fluid flow through unsaturated zone using a dual-porosity approach." ISH Journal of Hydraulic Engineering, 19(2), 97-110.
154. Mualem, Y. (1976). "A new model for predicting the hydraulic conductivity of unsaturated porous media." Water Resources Research, 12(3), 513-522.
155. Muthayya, S., Sugimoto, J. D., Montgomery, S., and Maberly, G. F. (2014). "An overview of global rice production, supply, trade, and consumption." Annals of the New York Academy of Sciences, 1324(1), 7-14.
156. Myneni, R.B., Nemani, R.R., and Running, S.W. (1997). "Estimation of global leaf area index and absorbed par using radiative transfer models." IEEE T. Geosci. Remote, 35, 1380–1393.
157. Naftchali, A. D., Mirlatifi, S. M., Shahnazari, A., Ejlali F., and Mahdian M. H. (2013). "Effect of subsurface drainage on water balance and water table in poorly drained paddy fields." Agricultural Water Management, 130, 61-68.
158. Nandagiri, L., and Kovoor, G. M. (2006). "Performance evaluation of reference evapotranspiration equations across a range of Indian climates." Journal of Irrigation and Drainage Engineering, 132(3), 238-249.
159. Nandagiri, L., and Kovoor, G. M. (2004). "Sensitivity of FAO Penman– Monteith evapotranspiration estimates to alternative procedures for estimation of parameters." Journal of Irrigation and Drainage Engineering, 131(3), 238–248.

160. Nandagiri, L., and Prasad, R. (1997). “Relative performance of textural models in estimating soil moisture characteristic.” Journal of Irrigation and Drainage Engineering, 123(3), 211-214.

161. Narasimhan, B, Srinivasan, R., and Whittaker, A.D. (2003). “Estimation of potential evapotranspiration from NOAA-AVHRR satellite.” Applied engineering in agriculture, 19 (3), 309.

162. Nie, L, Peng, S, Chen, M, Shah, F, Huang, J. Cui, K., and Xiang, J. (2012). “Aerobic rice for water-saving agriculture. A review.” Agron. Sustain. Dev., 32, 411-418.

163. Nouri, H., Beecham S., Kazemi, F., and Hassanli, A. M. (2013). “A review of ET measurement techniques for estimating the water requirements of urban landscape vegetation.” Urban Water J., 10 (4), 247–259.

164. Oad, R., Lusk, K., and Podmore, T. (1997). “Consumptive use and return flows in urban lawn water use.” Journal of Irrigation and Drainage Engineering, 123, 62-69.

165. Ochoa, C. G., Fernald, A. G., Guldan, S. J., and Shukla, M. K. (2007). “Deep percolation and its effects on shallow groundwater level rise following flood irrigation.” Am. Soc. Agri. and Biol. Engineers, 50(1), 73-81

166. Ochoa,C. G., Fernald, A. G., Guldan, S. J., Tidwell, V. C., and Shukla, M. K. (2013). “Shallow Aquifer Recharge from Irrigation in a Semiarid Agricultural Valley in New Mexico.” J. Hydrol. Eng., 18(10), 1219-1230.

167. Ojha, R., and Govindaraju, R. S. (2015). “A physical scaling model for aggregation and disaggregation of field-scale surface soil moisture dynamics.” Chaos: An Interdisciplinary Journal of Nonlinear Science, 25(7), 075401.

168. Paltineanu, C., Septar, L., and Moale, C. (2013). “Dynamics of soil water content during depletion cycles in peach orchards in a semiarid region.” Chilean Journal of Agricultural Research, 73(4), 399–405.

169. Parkes, M., Bailey, R., Williams, D., and Li,Y. (1995). “An irrigation scheduling model combining slow mobile water changes.” In: Pereira, L.S., vandenBroek, B.J.,Kabat, P., Allen, R.G. (Eds.), Crop-Water-Simulation Models in Practice.Wageningen Pers,Wageningen, pp.75–103.

170. Patil, M. D., Das, B. S., and Bhadoria, P. B. S. (2011). “A simple bund plugging technique for improving water productivity in wetland rice.” Soil and Tillage Research, 112(1), 66–75.

171. Pearcy, R.W., Schulze, E.-D. and Zimmermann R. (2000). “Measurement of transpiration and leaf conductance.” In Plant Physiological Ecology: Field Methods and

Instrumentation (eds. R.W. Pearcy, J.R. Ehleringer, H.A. Mooney & P.W. Rundel), pp. 137– 160. Kluwer Academic, Dordrecht, The Netherlands.

172. Perry, C., Steduto, P., Allen, R. G., and Burt, C. M. (2009). "Increasing productivity in irrigated agriculture: Agronomic constraints and hydrological realities." Agricultural Water Management, 96(11), 1517–1524.

173. Pruitt, W.O., and Angus, D.E. (1960). "Large weighing lysimeter for measuring evapotranspiration." Trans. ASAE 3, 13–18.

174. Qin, D., Qian, Y., Han, L., Wang Z., Li, C., and Zhao, Z. (2011). "Assessing impact of irrigation water on groundwater recharge and quality in arid environment using CFCs, tritium and stable isotopes, in the Zhangye Basin, Northwest China." J. Hydrol., 405, 194-208.

175. Qureshi, S. A., and Madramootoo, C. A. (2001). "Modelling the soil water balance of a sugarcane crop in Sindh, Pakistan with SWAP93." Canadian Water Resource Journal, 26(1), 129–150.

176. Raats, P.A.C. (2007). "Uptake of water from soils by plant roots." Transp. Porous Med., 68, 5–28.

177. Raes, D., and Deproost, P. (2003). "Model to assess water movement from shallow water table to the root zone." Agricultural Water Management, 62(2), 79–91.

178. Rallo, G., Agnese, C., Minacapilli, M., and Provenzano, G. (2012). "Comparison of SWAP and FAO Agro-Hydrological Models to Schedule Irrigation of Wine Grapes." Journal of Irrigation and Drainage Engineering, 138(7), 581–591.

179. Ram, S., Prasad, K. S. H., Gairola, A., Jose, M. K., and Trivedi, M. K. (2012). "Estimation of Border-Strip Soil Hydraulic Parameters." Journal of Irrigation and Drainage Engineering, 138(6), 493–502.

180. Ramos, T.B., Šimůnek, J., Gonçalves, M.C., Martins, J.C., Prazeres, A., Castanheira, N.L., and Pereira, L.S. (2011). "Field evaluation of a multi-component solute transport model in soils irrigated with saline waters." J. Hydrol. 407, 129-144.

181. Rana, G. and Katerji, N. (2000). "Measurement and estimation of actual evapotranspiration in the field under Mediterranean climate: a review." European Journal of Agronomy, 13 (2–3), 125–153.

182. Rao, H. B., and Singh, D.N. (2012). "Establishing soil-water characteristic curve and determining unsaturated hydraulic conductivity of kaolin by ultracentrifugation and electrical measurements." Can. Geotech. J. 49: 1369 –1377.

183. Rashton, K.R. and Ward, C. (1979). “The Estimation of groundwater Recharge.” J. Hydrol., 41, 345-361.

184. Reynolds, W.D. and Elrick, D.E. (1986). “A method for simultaneous in-situ measurement in the vadose zone of field saturated hydraulic conductivity, sorptivity and the conductivity-pressure head relationship.” Groundwater Monitoring Review, winter, 84-95.

185. Richards, L.A., (1931). Capillary condition of liquids through porous medium. Physics, 1:318-333.

186. Ries, F., Lange, J., Schmidt, S., Puhlmann, H., and Sauter, M. (2015). “Recharge estimation and soil moisture dynamics in a Mediterranean, semi-arid karst region.” Hydrol. Earth Syst. Sci., 19, 1439–1456.

187. Ritchie, J. T. (1972). “Model for predicting evaporation from a row crop with incomplete cover.” Water Resources Research, 8(5), 1204-1213.

188. Rizzo, A., Boano, F., Revelli, R., and Ridolfi, L. (2015). “Groundwater impact on methane emissions from flooded paddy fields.” Advances in Water Resources, 83, 340–350.

189. Ruiz, L., Varma, M. R. R., Kumar, M. S. M., Sekhar, M., Maréchal, J. C., Descloitres, M., Riotte, J., Kumar, S., Kumar, C., and Braun, J. J. (2010). “Water balance modelling in a tropical watershed under deciduous forest (Mule Hole, India): Regolith matric storage buffers the groundwater recharge process.” J. Hydrol., 380(3-4), 460–472.

190. Sammis, T.W., Evans D. D., and Warrick, A. W. (1982). “Comparison of Methods to Estimate Deep Percolation Rates. Journal of the American Water Resources Association, 18(3), 465-470.

191. Sander, T., and Gerke, H.H. (2009). “Modelling field-data of preferential flow in paddy soil induced by earthworm burrows.” Journal of Contaminant Hydrology, 104, 126-136.

192. Sasaki, S. and Amano, T. (2010). “Transpiration rate measurement using miniature temperature/humidity sensors.” Analytical Sciences J., 6, 827-829.

193. Schaap, M. G., De Lange, L., and Heimovaara, T. J. (1997). “TDR calibration of organic forest floor media.” Soil Technology, 11(2), 205–217.

194. Selle, B., Minasny, B., Bethune, M., Thayalakumaran, T., and Chandra S. (2011). “Applicability of Richards' equation models to predict deep percolation under surface irrigation.” Geoderma, 160, 569–578.

195. Shahraiyni, H. T., and Ataie-Ashtiani, B. (2012). “Mathematical Forms and Numerical Schemes for the Solution of Unsaturated Flow Equations.” Journal of Irrigation and Drainage Engineering, 138(1), 63–72.

196. Shankar, V. (2007). “Modelling of moisture uptake by plants.” Ph.D., Thesis. IIT Roorkee, Department of Civil Engineering, Roorkee, India.

197. Shankar, V., Hari Prasad, K.S., Ojha, C.S.P., and Govindaraju, R.S. (2012). “Model for nonlinear root water uptake parameter.” Journal of Irrigation and Drainage Engineering, 138(10), 905-917.

198. Sharma, P.K., Bhushan Lav, Ladha, J.K., Naresh, R.K., Gupta, R.K., Balasubramanian, B.V., and Bouman, B.A.M. (2002). “Crop-water relations in rice-wheat cropping under different tillage systems and water-management practices in a marginally sodic, medium-textured soil.” In: Bouman, B.A.M, Hengsdijk. H., Hardy, B., Bindraban, P.S., Tuong, T.P., Ladha, J.K., editors. Water-wise rice production. International Rice Research Institute, Los Baños, Philippines. p 223-235.

199. Sharma, R. K., and Singh, H.R. (2009). “Deep percolation losses in irrigation border-checks.” Journal of soil and water conservation. 8(2), 65-74.

200. Shawcroft, R.W., and Gardner, W.H. (1983). “Direct evaporation from soil under a row crop canopy.” Agricultural Meteorology, 28, 229-238.

201. Shrestha, S., Kazama, F., Newham, L. T. H., Babel, M. S., Clemente, R. S., Ishidaira, H., Nishida, K., and Sakamoto, Y. (2008). “Catchment scale modelling of point source and non-point source pollution loads using pollutant export coefficients determined from long-term in-stream.” Journal of Hydro-Environment Research 2, 134-147.

202. Šimůnek, J., and Nimmo, J. R. (2005). “Estimating soil hydraulic parameters from transient flow experiments in a centrifuge using parameter optimization technique.” Water Resources Research, 41(4), 1-9.

203. Šimůnek, J., and van Genuchten, M.T. (2007). “Contaminant transport in the unsaturated zone: theory and modelling.” In: Delleur, J.W. (Ed.), The Handbook of Groundwater Engineering, second ed. CRC Press, Boca Raton, pp. 221– 2238.

204. Šimůnek, J., Šejna, M., Saito, H., Sakai, M., and van Genuchten M. Th. (2013). “The HYDRUS-1D Software Package for Simulating the Movement of Water, Heat, and Multiple Solutes in Variably Saturated Media, Version 4.17, HYDRUS Software Series 3.” Department of Environmental Sciences, University of California Riverside, Riverside, California, USA, pp. 343.

205. Šimůnek, J., Sejna, M., and van Genuchten, M. Th. (1998). "The HYDRUS-1D software package for simulating the one-dimensional movement of water, heat, and multiple solutes in variably-saturated media, version 2.0, IGWMC-TPS-70." International ground water modelling centre, Colorado school of mines, Golden Colorado, pp. 202.

206. Šimůnek, J., van Genuchten M. Th., and Šejna, M. (2008). "Development and applications of the HYDRUS and STANMOD software packages and related codes." Vadose Zone J., (2), 587-600.

207. Šimůnek, J., van Genuchten, M. Th., and Šejna, M.(2012). "HYDRUS: Model use, Calibration, and Validation." American Society of Agricultural and Biological Engineers 55(4): 1261-1274.

208. Singh, A. (2011). "Estimating long-term regional groundwater recharge for the evaluation of potential solution alternatives to water logging and salinisation." J. Hydrol., 406(3-4), 245–255.

209. Singh, A. K., Madramootoo, C. A., and Smith, D. L. (2014). "Impact of Different Water Management Scenarios on Corn Water Use Efficiency." Transactions of the ASABE, 57(5), 1319–1328.

210. Singh, A., Krause, P., Panda, S. N., and Flugel, W. A. (2010). "Rising water table: A threat to sustainable agriculture in an irrigated semi-arid region of Haryana, India." Agricultural Water Management, 97(10), 1443–1451.

211. Singh, A.K., Choudhury, B.U., and Bouman, B.A.M. (2002). "Effects of rice establishment methods on crop performance, water use, and mineral nitrogen." In: Bouman BAM, Hengsdijk H, Hardy B, Bindraban, P.S., Tuong, T.P., Ladha, J.K., editors. Water-wise rice production. Los Baños (Philippines): International Rice Research Institute. p 237-246.

212. Skaggs, T. H., van Genuchten, M. Th., Shouse, P. J., and Poss, J. A. (2006). "Macroscopic approaches to root water uptake as a function of water and salinity stress." Agricultural water management, 86, 140-149.

213. Smith, N.J. (1991). "Predicting radiation attenuation in stands of Douglas-Fir." Forest Science, 37(5), 1213–1223.

214. Smith, R.J., Raine, S.R., and Minkevich, J. (2005). "Irrigation application efficiency and deep drainage potential under surface irrigated cotton." Agricultural Water Management, 71, 117–130.

215. Sobowale, A., Ramalan, A. A., Mudiare, O. J., and Oyebode, M. A. (2015). "Groundwater recharge studies in irrigated lands in Nigeria: Implications for basin sustainability." Sustainability of Water Quality and Ecology, 4(2014), 124–132.

216. Soylu, M. E., Istanbulluoglu, E., Lenters, J. D., and Wang T. (2011). "Quantifying the impact of groundwater depth on evapotranspiration in a semi-arid grassland region." Hydrol. Earth Syst. Sci., 15, 787–806.

217. Stroppiana, D., Boschetti M., Confalonieri R., Bocchi S., Brivio, P. A. (2006). "Evaluation of LAI-2000 for leaf area index monitoring in paddy rice." Field Crops Res., 99, 167–170.

218. Sudhir-Yadav, S., Li, T., Humphreys, E., Gill, G., and Kukal, S.S. (2011). "Evaluation and application of ORYZA2000 for irrigation scheduling of puddled transplanted rice in North West India." Field Crops Res., 122, 104-117.

219. Sunil, K., Agrawal, R.K., Dixit, A. K., Rai, A. K., and Rai, S. K. (2012). "Forage crops and their management." Indian grassland and fodder research institute, Jhansi, Uttar Pradesh, India. pp 60.

220. Sutanto, S. J., Wenninger, J., Coenders-Gerrits, A. M. J., and Uhlenbrook, S. (2012). "Partitioning of evaporation into transpiration, soil evaporation and interception: A comparison between isotope measurements and a HYDRUS-1D model." Hydrol. Earth Syst. Sci., 16(8), 2605–2616.

221. Tafteh A., and Sepaskhah, A. R. (2012). "Application of HYDRUS-1D model for simulating water and nitrate leaching from continuous and alternate furrow irrigated rapeseed and maize fields." Agricultural Water Management, 113, 19–29.

222. Tan, X., Shao, D., Gu, W., and Liu, H. (2015). "Field analysis of water and nitrogen fate in lowland paddy fields under different water managements using HYDRUS-1D." Agricultural Water Management, 150, 67–80.

223. Tan, X., Shao, D.,and Liu, H. (2014). "Simulating soil water regime in lowland paddy fields under different water managements using HYDRUS-1D." Agricultural water management, 132, 69-78.

224. ten Berge, H.F.M., Jansen, D.M., Rappoldt, K., and Stol, W. (1992). "The soil water balance model SAWAH: User's guide and outline." CABO-TPE Simulation Reports Series 22, CABO, Wageningen, Netherlands.

225. Thornthwaite, C.W. (1948). "An approach towards rational classification of climate." Geographical Rev., 38: 55-94.

226. Todd, D.K. (1980). “Ground Water Hydrology.” second Edition, John Wiley and Sons, California.

227. Tournebize, J., Watanabe, H., Takagi, K., and Nishimura, T. (2006). “The development of a coupled model (PCPF-SWMS) to simulate water flow and pollutant transport in Japanese paddy fields.” Paddy Water Environment, 4(1), 39–51.

228. Trout, T.J., Garcia-Castillas, I.G., and Hart, W.E. (1982). “Soil water engineering: Field and laboratory manual.” Academic Publishers, Jaipur, India.

229. Tuong, T.P., Bouman, B.A.M., Mortimer, M. (2005). “More rice, less water-integrated approaches for increasing water productivity in irrigated rice-based systems in Asia.” Plant Prod. Sci., 8, 231-241.

230. Tuong, T.P., Wopereis, M.C.S., Marquez, J.A., and Kropff, M.J. (1994). “Mechanisms and control of percolation losses in irrigated puddle rice fields.” Soil Sci. Soc. Am. J., 58, 1794-1803.

231. Tyagi, N. K., Sharma, D. K., and Luthra, S. K. (2003). “Determination of evapotranspiration for maize and berseem clover.” Irrigation Science, 21, 173-181.

232. Tyagi, N.K., Sharma, D.K., and Luthra, S.K. (2000). “Determination of evapotranspiration and crop coefficients of rice and sunflower with lysimeter.” Agricultural Water Management, 45, 41-54.

233. Vaccaro, J.J. (2007). “A deep percolation model for estimating ground-water recharge: Documentation of modules for the modular modeling system of the U.S. Geological Survey.” U.S. Geological Survey Scientific Investigations Report, 2006-5318, 30 p.

234. Vadez, V., Kholova, J., Medina, S., Kakkera, A., and Anderberg, H. (2014). “Transpiration efficiency: new insights into an old story.” Journal of Experimental Botany, 65(21), 6141–6153.

235. van Genuchten, M. T. (1980). “A closed form equation for predicting the hydraulic conductivity of unsaturated soils.” Soil Sci. Soc. Am. J., 44(5), 892–898.

236. van Genuchten, M. Th. (1987). “A numerical model for water and solute movement in and below the root zone.” Research Report No 121, U.S. Salinity laboratory, USDA, ARS, Riverside, California.

237. Vanclooster, M., Viaene, P., Diels, J., and Christiansen, K. (1994). “WAVE, a deterministic model for simulating water and agrochemicals in the soil and vadose environment.” Inst. Land and Water Management, K.U. Leuven.

238. Vanclooster, M., Viaene, P., Diels, J., and Feyen, J. (1995). “A deterministic evaluation analysis applied to an integrated soil-crop model.” Ecological Modelling, 81(1-3), 183–195.

239. Vanderborght, J., Tiktak, A, Boesten, J. J., and Vereecken H. (2011). “Effect of pesticide fate parameters and their uncertainty on the selection of 'worst-case' scenarios of pesticide leaching to groundwater.” Pest Manag Sci., 67(3):294-306.

240. Vaughan, P.J., Trout, T.J., and Ayars J.E. (2007). “A processing method for weighing lysimeter data and comparison to micrometeorological ETo predictions.” Agricultural Water Management, 88, 141-146.

241. Vereecken, H. (2005). “Mobility and leaching of glyphosate: A review.” Pest Management Science, 61(12), 1139–1151.

242. Vereecken, H., Huisman, J. A., Bogena, H., Vanderborght, J., Vrugt, J.A., Hopmans, J. W. (2008). “On the value of soil moisture measurements in vadose zone hydrology: a review.” Water Resour. Res., 44, W00D06.

243. Villalobos, F.J., and Fereres. E. (1990). “Evaporation measurements beneath corn, cotton, and sunflower canopies.” Agronomy Journal, 82, 1153–1159.

244. Walker, S.H. (1999). “Causes of high water losses from irrigated rice fields: Field measurements and results from analogue and digital models.” Agricultural water management, 40(1), 123-127.

245. Walker, W.R., Prajamwong, S., Allen, R.G., and Merkley, G.P. (1995). “USU command area decision support model CADSM.” In: Pereira, L.S., vandenBroek, B.J., Kabat, P., Allen, R.G.(Eds.), Crop-Water-Simulation Models in Practice. Wageningen Pers, Wageningen, pp. 231–271.

246. Wallis, K.J., Candela, L., Mateos, R.M., and Tamoh, K. (2011). “Simulation of nitrate leaching under potato crops in a Mediterranean area. Influence of frost prevention irrigation on nitrogen transport.” Agricultural Water Management, 98, 1629-1640.

247. Wang, P., Song, X., Han, D., Zhang, Y., and Zhang, B. (2012). “Determination of evaporation, transpiration and deep percolation of summer corn and winter wheat after irrigation.” Agricultural Water Management, 105, 32-37.

248. Watanabe, K., Yamamoto, T., Yamda, T., Sakuratani, T., Nawata, E., Noichana, C., Sributta, A., and Higuchi, H. (2004). “Changes in seasonal evapotranspiration, soil water content, and crop coefficients in sugarcane, cassava, and maize fields in north-east Thailand.” Agricultural Water Management, 67, 133-143.

249. Watson, D.J. (1947). “Comparative physiological studies in the growth of field crops. I. Variation in net assimilation rate and leaf area between species and varieties, and within and between and years.” Annals of Botany, 11, 41-76.

250. Weaver, T. B., Hulugalle, N. R., and Ghadiri, H. (2005). “Comparing deep drainage estimated with transient and steady state assumptions in irrigated vertisols.” Irrigation Science, 23(4), 183–191.

251. Weiss M., Baretet F., Smith, G.J., Jonckheere, I., and Coppin, P. (2004). “Review of methods for in situ leaf area index (LAI) determination Part II. Estimation of LAI, errors and sampling.” Agricultural and Forest Meteorology, 121, 37-53.

252. Wessolek, G., Schwärzel, K., Greiffenhagen, A., and Stoffregen, H. (2008). “Percolation characteristics of a water-repellent sandy forest soil.” European Journal of Soil Sci., 59, 14–23.

253. Whalley, W. R., Cope, R. E., Nicholl, C. J., and Whitmore, A. P. (2004). “In-field calibration of a dielectric soil moisture meter designed for use in an access tube.” Soil Use and Management, 20(2), 203–206.

254. White, R. (2006). “Principles and practice of soil science: The soil as a natural resource.” Fourth edition, Blackwell publishing, USA.

255. Willis, T. M. Black, A. S. · Meyer, W. S. (1997). “Estimates of deep percolation beneath cotton in the Macquarie Valley.” Irrigation Science, 17: 141-150.

256. Witkowska-Walczak, B. (2006). “Hysteresis between wetting and drying processes as affected by soil aggregate size.” Int. Agrophysics, 20, 359-365.

257. Xu, X. U., Sun, C., Qu, Z., Huang, Q., Ramos, T. B., and Huang, G. (2015). “Groundwater Recharge and Capillary Rise in Irrigated Areas of the Upper Yellow River Basin Assessed by an Agro-Hydrological Model.” Irrigation and Drainage, 64(5), 587–599.

258. Young, M.H., Wierenga, P.J., and Mancino, C.F. (1996). “Large weighing lysimeters for water use and deep percolation studies.” Soil Sci., 161, 491–501.

259. Yu, G.-R., Zhuang, J., Nakayama, K., Jin, Y. (2007). “Root water uptake and profile soil water as affected by vertical root distribution.” Plant Ecol., 189, 15-30.

260. Zhang, Z.B., Zhou, H., Zhao, Q.G., Lin, H., and Peng, X. (2014). “Characteristics of cracks in two paddy soils and their impacts on preferential flow.” Geoderma, 118, 22–31.

261. Zhang, Z.F., Groenevelt, P.H. and Parkin, G.W. (1998). “The well shape-factor for the measurement of soil hydraulic properties using the Guelph Permeameter.” Soil Tillage Res., 49:219-221.

262. Zhu, Y., Fox, R. H., and Toth, J. D. (2002). “Leachate Collection Efficiency of Zero-tension Pan and Passive Capillary Fibreglass Wick Lysimeters.” Soil Science Society of America Journal, 66(1), 37.

263. Zwart, S. J., and Bastiaanssen, W. G. M. (2004). “Review of measured crop water productivity values for irrigated wheat, rice, cotton and maize.” Agricultural Water Management, 69(2), 115–133.

PUBLICATIONS

In Journals

I. Hatiye, S.D., Hari Prasad, K.S., Ojha, C.S.P., and Adeloye, A.J. (2016). "Estimation and Characterization of Deep Percolation from Rice and Berseem Fields Using Lysimeter Experiments on Sandy Loam Soil-Case Study." ASCE J. Hydrol. Eng., 21(5), 05016006. doi.org/10.1061/ (ASCE) HE.1943-5584.0001365.

II. Hatiye, S.D., Hari Prasad K.S., Ojha, C.S.P., Kaushika, G.S., and Adeloye, A.J. (2015). "Evaluating Irrigation Scheduling Efficiency of Paddy Rice and Berseem Fodder Crops in Sandy Loam Soil." Irrigat Drainage Sys Eng., 4:147. doi:10.4172/2168-9768.1000147.

III. Hatiye, S.D., Hari Prasad, K.S., and Ojha, C.S.P. "Water Balance and Water Productivity of Rice Paddy in unpuddled Sandy Loam Soil." Sustain. Water Resour. Manag. (Minor corrections sent).

IV. Hatiye, S.D., Hari Prasad, K.S. and Ojha, C.S.P. "Study of deep percolation in paddy fields using drainage-type lysimeters under varying regimes of water application." ISH Journal of Hydraulic Engineering, doi:10.1080/09715010.2016.1228086 (in press).

In international Conferences

I. Hatiye, S.D., Hari Prasad, K.S., Ojha, C.S.P., and Kaushika, G.S. (2014). "Estimation of deep percolation from rice paddy field using lysimeter experiments on sandy loam soil." International Conference on "Hydraulics, Water Resources, Coastal and Environmental Engineering (HYDRO-2014 International)", December 18-20, 2014. National Institute of Technology, Bhopal, India.

II. Hatiye, S.D., Hari Prasad, K.S. and Ojha, C.S.P (2015). "Estimation of Deep Percolation Return Flow from Paddy Fields Using Hydrus-1D Flux Based Model " 20th International Conference on "Hydraulics, Water Resources, River Engineering (HYDRO-2015 International)", December 17-19, 2015. Indian Institute of Technology, Roorkee, India.

III. Hatiye, S.D. and Hari Prasad, K.S. and C.S.P. Ojha (2016). "Investigation of Deep Percolation Using Process Based and Simple Water Balance Models", fourth International Conference on "Advancements in Science and Technology in Civil and Water Resources Engineering", June 17-18, 2016. Bahir Dar Univeristy, Bahir Dar, Ethiopia.

APPENDIX (A)

Table A1 Grain size analysis data for spot 1 at different depths

Sample No 1		**Sample No 2**		**Sample No 3**		**Sample No 4**		**Sample No 5**		**Sample No 6**	
Particle Size(mm)	*% age Passing*	*Particle Size(mm)*	*% age Passing*	*Particle Size(mm)*	*% age Passing*	*Particle Size(mm)*	*% age Passing*	*Particle Size(mm)*	*% age Passing*	*Particle Size(mm)*	*% age Passing*
4.750	99.8	4.750	100.0	4.750	100.0	4.750	100.0	4.750	100.0	4.750	100.0
2.000	99.5	2.000	99.7	2.000	100.0	2.000	100.0	2.000	100.0	2.000	100.0
0.850	99.0	0.850	99.1	0.850	99.7	0.850	99.0	0.850	99.5	0.850	99.7
0.425	97.4	0.425	98.3	0.425	98.7	0.425	98.0	0.425	98.7	0.425	98.7
0.250	53.9	0.250	83.4	0.250	69.9	0.250	71.2	0.250	68.9	0.250	66.3
0.106	28.0	0.106	39.5	0.106	32.0	0.106	34.8	0.106	31.3	0.106	35.6
0.075	27.9	0.075	39.1	0.075	31.8	0.075	34.4	0.075	30.9	0.075	35.3
0.043	21.02	0.0460	21.02	0.0454	22.00	0.0599	25.40	0.056	27.028	0.057	32.683
0.033	15.94	0.0343	15.94	0.0336	17.79	0.0444	21.58	0.042	23.935	0.044	27.223
0.028	13.68	0.0285	13.68	0.0285	14.22	0.0332	16.71	0.032	17.751	0.033	21.036
0.024	12.55	0.0251	12.55	0.0253	11.94	0.0279	13.58	0.027	15.277	0.028	18.125
0.018	10.29	0.0183	10.29	0.0184	9.02	0.0246	11.85	0.024	13.730	0.024	16.305
0.013	7.74	0.0135	7.74	0.0137	6.75	0.0177	9.76	0.018	9.710	0.018	10.846
0.009	6.33	0.0097	6.33	0.0098	5.13	0.0133	6.29	0.013	7.236	0.014	8.662
0.007	5.20	0.0069	5.20	0.0070	3.83	0.0096	4.90	0.009	5.443	0.010	5.023
0.005	4.63	0.0049	4.63	0.0050	3.60	0.0068	3.81	0.007	2.969	0.007	3.931
0.001	2.15	0.0014	2.15	0.0014	1.75	0.0053	2.92	0.005	1.113	0.005	2.620
						0.0014	1.53	0.001	0.124	0.001	0.000

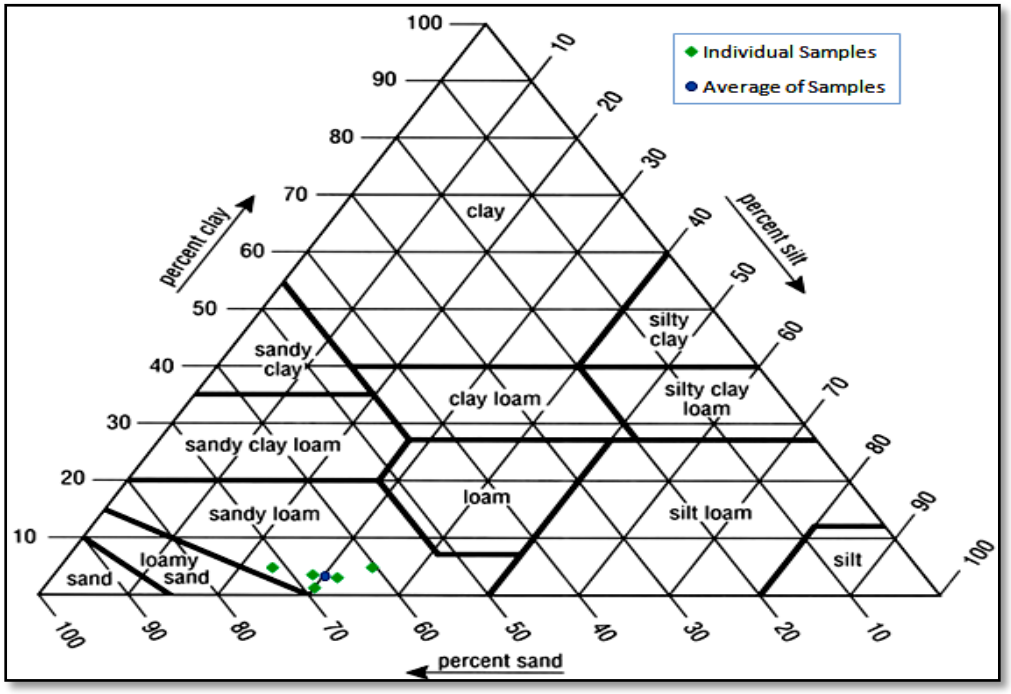

Fig. A1 Textural classification for soil samples (spot 1) (Cuenca, 1989)

Table A2 Summary of soil physical characteristics and textural class of spot 1

Sample No	Soil Depth (Below GL),cm	Sand (%)	Silt (%)	Clay (%)	Bulk Density (g/cm^3)	Particle Density (g/cm^3)	Soil Class (USDA)
1	0-30	72.0	23.23	4.63	1.65	2.57	Sandy Loam
2	30-60	60.9	34.50	4.63	1.57	2.62	Sandy Loam
3	60-80	68.2	28.22	3.60	1.58	2.55	Sandy Loam
4	80-100	65.6	31.48	2.92	1.59	2.61	Sandy Loam
5	100-120	69.1	29.81	1.113	1.61	2.64	Sandy Loam
6	120-140	64.7	32.65	2.620	1.54	2.52	Sandy Loam
Average	0-140	66.74	29.98	3.25	1.59	2.59	Sandy Loam

Table A3 Grain size analysis data for spot 2 at different depths

Sample No 1		**Sample No 2**		**Sample No 3**		**Sample No 4**		**Sample No 5**		**Average Size**	
Particle Size(mm)	*%age Passing*	*Particle Size(mm)*	*%age Passing*	*Particle Size(mm)*	*%age Passing*	*Particle Size(mm)*	*%age Passing*	*Particle Size(mm)*	*%age Passing*	*Particle Size(mm)*	*%age Passing*
4.750	99.8	4.750	100.0	4.750	100.0	4.750	100.0	4.750	100.0	4.750	99.97
2.000	99.7	2.000	99.9	2.000	100.0	2.000	100.0	2.000	100.0	2.000	99.91
0.850	99.3	0.850	99.5	0.850	99.7	0.850	99.9	0.850	100.0	0.850	99.66
0.425	98.1	0.425	98.2	0.425	98.5	0.425	98.8	0.425	98.8	0.425	98.49
0.250	71.0	0.250	64.4	0.250	64.1	0.250	56.8	0.250	60.5	0.250	63.35
0.106	31.2	0.106	31.2	0.106	32.1	0.106	26.5	0.106	34.7	0.106	31.13
0.075	30.8	0.075	30.8	0.075	31.9	0.075	26.4	0.075	34.6	0.075	30.90
0.058	26.75	0.0596	25.01	0.0591	27.66	0.0596	22.30	0.055	33.258	0.058	27.00
0.045	21.10	0.0441	21.58	0.0434	24.75	0.0449	18.29	0.041	28.745	0.044	22.89
0.033	16.07	0.0327	17.53	0.0332	18.27	0.0333	14.82	0.031	24.579	0.033	18.25
0.028	13.56	0.0274	15.34	0.0279	15.68	0.0280	12.68	0.026	21.802	0.027	15.81
0.025	12.31	0.0242	13.47	0.0246	13.73	0.0247	11.07	0.023	19.719	0.024	14.06
0.018	9.79	0.0176	10.98	0.0179	11.14	0.0181	8.13	0.017	16.942	0.018	11.40
0.013	7.91	0.0131	9.11	0.0133	8.88	0.0134	7.06	0.013	13.470	0.013	9.28
0.009	6.66	0.0095	6.92	0.0096	7.58	0.0096	5.99	0.009	11.040	0.009	7.64
0.007	5.40	0.0068	5.86	0.0068	6.28	0.0068	5.03	0.007	9.304	0.007	6.38
0.005	3.83	0.0048	5.30	0.0048	5.77	0.0053	4.23	0.005	7.707	0.005	5.37
0.001	2.57	0.0014	3.49	0.0014	3.56	0.0014	2.67	0.001	4.687	0.001	3.40

Table A4 Summary of soil physical characteristics and textural class of spot 2

Sample No	Soil Depth (Below GL),cm	Sand (%)	Silt (%)	Clay (%)	Bulk Density (g/cm^3)	Particle Density (g/cm^3)	Soil Class (USDA)
1	0-30	69.1	26.95	3.83	1.63	2.55	Sandy Loam
2	30-60	69.2	25.52	5.30	1.54	2.56	Sandy Loam
3	60-80	68.1	26.18	5.77	1.54	2.58	Sandy Loam
4	80-100	73.6	22.15	4.23	1.54	2.58	Sandy Loam
5	100-140	65.4	26.87	7.707	1.63	2.63	Sandy Loam
Average	0-140cm	69.1	25.53	5.366	1.58	2.58	Sandy Loam

Table A5 Grain size analysis data for spot 3 at different depths

Sample No 1		**Sample No 2**		**Sample No 3**		**Sample No 4**		**Sample No 5**	
Particle Size(mm)	*% age Passing*	*Particle Size(mm)*	*% age Passing*	*Particle Size(mm)*	*% age Passing*	*Particle Size(mm)*	*% age Passing*	*Particle Size(mm)*	*% age Passing*
4.75	99.63	4.75	100.00	4.75	100.00	4.75	100.00	4.75	100.00
2.00	99.26	2.00	99.81	2.00	99.81	2.00	99.83	2.00	100.00
0.85	98.51	0.85	99.44	0.85	99.42	0.85	99.13	0.85	99.64
0.43	97.39	0.43	98.32	0.43	98.27	0.43	97.92	0.43	98.55
0.25	60.89	0.25	68.47	0.25	66.54	0.25	61.70	0.25	52.72
0.11	20.86	0.11	29.76	0.11	30.96	0.11	31.89	0.11	28.62
0.08	20.48	0.08	29.38	0.08	30.58	0.08	31.89	0.08	28.26
0.07	11.75	0.06	23.59	0.06	23.33	0.06	26.68	0.06	23.35
0.05	8.81	0.05	18.44	0.05	19.59	0.04	21.82	0.04	19.35
0.04	6.71	0.03	14.19	0.03	14.60	0.03	16.62	0.03	14.21
0.03	5.24	0.03	12.37	0.03	12.10	0.03	13.37	0.03	11.93
0.03	4.20	0.03	9.95	0.03	10.85	0.02	12.08	0.02	10.22
0.02	3.57	0.02	6.91	0.02	8.36	0.02	9.48	0.02	7.94
0.01	3.36	0.01	5.70	0.01	6.49	0.01	7.86	0.01	6.22
0.01	2.98	0.01	4.79	0.01	5.93	0.01	6.88	0.01	5.08
0.01	2.56	0.01	4.25	0.01	5.36	0.01	5.91	0.01	4.22
0.00	1.99	0.00	3.70	0.00	4.43	0.01	5.36	0.00	3.37
0.00	1.64	0.00	2.58	0.00	2.65	0.00	3.41	0.00	2.51

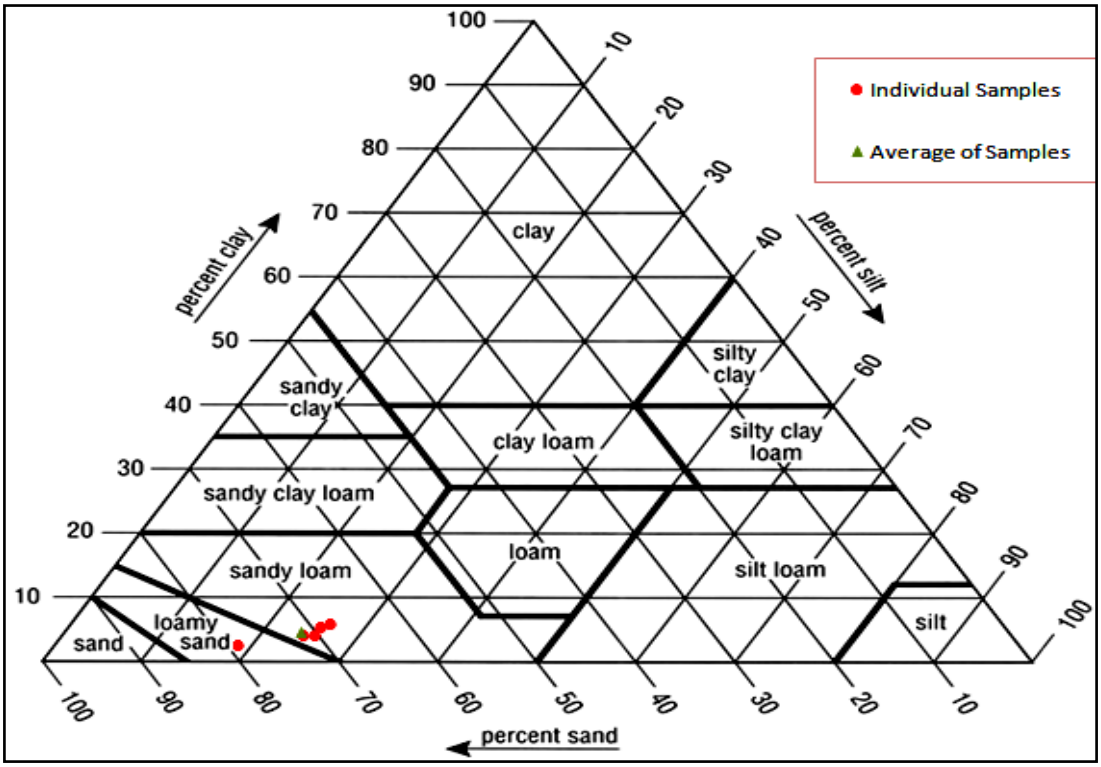

Fig. A2 Textural classification for soil samples (spot 3) (Cuenca, 1989)

Table A6 Summary of soil physical characteristics and textural class of spot 3

Sample No	Soil Depth (Below GL),cm	Sand (%)	Silt (%)	Clay (%)	Bulk Density (g/cm^3)	Particle Density (g/cm^3)	Soil Class (USDA)
1	0-30	79.11	17.93	2.56	1.47	2.54	Loamy Sand
2	30-60	70.61	25.14	4.25	1.55	2.52	Sandy Loam
3	60-80	69.4	25.21	5.36	1.50	2.55	Sandy Loam
4	80-100	68.1	25.98	5.91	1.49	2.56	Sandy Loam
5	100-120	71.7	24.04	4.22	1.53	2.60	Sandy Loam
Average	0-140	71.8	23.66	4.46	1.51	2.55	Sandy Loam

APPENDIX (B)

Table B1 GP data for saturated hydraulic conductivity determination at location A11 (Bore hall depth =30 cm)

Well head	Time (min)	Time interval (min)	Water level in the reservoir (cm)	Water level change (cm)	Rate of water level change (cm/min), R
H_1= 5 cm	0	-	9.0	-	-
	2	2	15.5	6.5	3.25
	4	2	21.0	5.5	2.75
	6	2	26.20	5.2	2.6
	8	2	31.30	5.1	2.55
	10	2	36.20	4.9	2.45
	12	2	41.20	5	2.5
	14	2	46.0	4.8	2.4
	16	2	50.8	4.8	2.4
	18	2	55.60	4.8	2.4
	20	2	60.40	4.8	2.4
	22	2	65.20	4.8	2.4
	R_1=				2.40 cm/min
H_2= 10 cm	0	-	6.50	-	-
	2	2	12.30	5.8	2.9
	4	2	18.50	6.2	3.1
	6	2	24.50	6	3.0
	8	2	30.50	6	3.0
	10	2	36.40	5.9	2.95
	12	2	42.20	5.8	2.90
	14	2	47.90	5.7	2.85
	16	2	53.60	5.7	2.85
	18	2	59.30	5.9	2.95
	R_2=				2.95 cm/min

Table B2 GP data for saturated hydraulic conductivity determination at location A11 (Bore hall depth = 60 cm)

Well head	Time (min)	Time interval (min)	Water level in the reservoir (cm)	Water level change (cm)	Rate of water level change (cm/min), R
H_1= 5 cm	0	-	5	-	-
	1	1	8.3	3.3	3.3
	2	1	11.3	3.0	3.0
	3	1	14.3	3.0	3.0
	4	1	17.2	2.9	2.9
	5	1	19.8	2.6	2.6
	6	1	22.6	2.8	2.8
	7	1	25.2	2.6	2.6
	8	1	27.8	2.6	2.6
	R_1=				2.6
H_2= 10 cm	0	-	9.00	-	-
	1	1	15.20	6.2	6.2
	2	1	21.10	5.9	5.9
	3	1	26.60	5.5	5.5
	4	1	31.90	5.3	5.3
	5	1	37.40	5.5	5.5
	6	1	42.60	5.2	5.2
	7	1	48.00	5.4	5.4
	8	1	53.00	5.0	5.0
	9	1	58.00	5.0	5.0
	10	1	63.00	5.0	5.0
	R_2=				5.0

Table B3 GP data for saturated hydraulic conductivity determination at location A12 (Bore hall depth =30 cm)

Well head	Time (min)	Time interval (min)	Water level in the reservoir (cm)	Water level change (cm)	Rate of water level change (cm/min), R
H_1= 5 cm	0	-	23.0	-	-
	2	2	27.20	4.2	2.1
	4	2	31.10	3.9	1.95
	6	2	34.80	3.7	1.85
	8	2	38.30	3.5	1.75
	10	2	41.80	3.5	1.75
	12	2	45.30	3.5	1.75
	14	2	49.0	3.7	1.85
	16	2	52.50	3.5	1.75
	18	2	55.80	3.3	1.65
	20	2	59.40	3.6	1.8
	22	2	63.0	3.6	1.8
	24	2	66.60	3.6	1.8
	R_1=				1.80
H_2= 10 cm	0	-	8.0	-	-
	2	2	12.5	4.5	2.25
	4	2	16.9	4.4	2.2
	6	2	21.1	4.2	2.1
	8	2	25.2	4.1	2.05
	10	2	29.3	4.1	2.05
	12	2	33.4	4.1	2.05
	14	2	37.5	4.1	2.05
	R_2=				2.05

Table B4 GP data for saturated hydraulic conductivity determination at location A12 (Bore hall depth = 60 cm)

Well head	Time (min)	Time interval (min)	Water level in the reservoir (cm)	Water level change (cm)	Rate of water level change (cm/min), R
H_1= 5 cm	0	-	5.0	-	-
	2	2	7.90	2.9	1.45
	4	2	10.80	2.9	1.45
	6	2	13.70	2.9	1.45
	8	2	16.60	2.9	1.45
	10	2	19.50	2.9	1.45
	12	2	22.40	2.9	1.45
	R_1=				1.45
H_2= 10 cm	0	-	7.0	-	-
	2	2	10.40	3.4	1.7
	4	2	13.40	3.0	1.5
	6	2	16.60	3.2	1.6
	8	2	19.60	3.0	1.5
	10	2	22.60	3.0	1.5
	12	2	25.60	3.0	1.5
	14	2	28.60	3.0	1.5
	R_2=				1.50

Table B5 GP data for saturated hydraulic conductivity determination at location A13 (Bore hall depth =30 cm)

Well head	Time (min)	Time interval (min)	Water level in the reservoir (cm)	Water level change (cm)	Rate of water level change (cm/min), R
H_1= 5 cm	0	-	7.00		
	2	2	13.40	6.4	3.2
	4	2	19.40	6.0	3.0
	6	2	25.20	5.8	2.9
	8	2	31.00	5.8	2.9
	10	2	36.80	5.8	2.9
	12	2	42.30	5.8	2.9
	R_1=				2.90
H_2= 10 cm	0	-	8.00		
	2	2	16.30	8.3	4.15
	4	2	24.00	7.7	3.85
	6	2	31.60	7.6	3.8
	8	2	39.20	7.6	3.8
	10	2	46.80	7.6	3.8
	12	2	54.40	7.6	3.8
	R_2=				3.80

Table B6 GP data for saturated hydraulic conductivity determination at location A13 (Bore hall depth =60 cm)

Well head	Time (min)	Time interval (min)	Water level in the reservoir (cm)	Water level change (cm)	Rate of water level change (cm/min), R
H_1= 5 cm	0	-	6.00	-	-
	2	2	9.00	3.0	1.5
	3	1	10.30	1.3	1.3
	4	1	11.90	1.6	1.6
	6	2	14.40	2.5	1.25
	8	2	17.10	2.7	1.35
	10	2	19.90	2.8	1.4
	12	2	22.40	2.5	1.25
	14	2	25.00	2.6	1.3
	16	2	27.70	2.7	1.35
	18	2	30.40	2.7	1.35
	20	2	33.10	2.7	1.35
	22	2	35.80	2.7	1.35
	R_1=				1.35
H_2= 10 cm	0	-	6.50	-	-
	2	2	10.00	3.5	1.75
	4	2	13.00	3.0	1.5
	6	2	16.00	3.0	1.5
	8	2	19.00	3.0	1.5
	10	2	22.00	3.0	1.5
	R_2=				1.5

Table B7 GP data for saturated hydraulic conductivity determination at location A14 (Bore hall depth =30 cm)

Well head	Time (min)	Time interval (min)	Water level in the reservoir (cm)	Water level change (cm)	Rate of water level change (cm/min), R
H_1= 5 cm	0	-	15.50	-	-
	2	2	19.30	3.8	1.9
	4	2	22.90	3.6	1.8
	6	2	26.80	3.9	1.95
	8	2	30.50	3.7	1.85
	10	2	34.30	3.8	1.9
	12	2	38.10	3.8	1.9
	14	2	41.90	3.8	1.9
	16	2	45.50	3.6	1.8
	18	2	49.40	3.9	1.95
	20	2	53.20	3.8	1.9
	22	2	57.00	3.8	1.9
	24	2	60.80	3.8	1.9
	26	2	64.60	3.8	1.9
	R_1=				1.90
H_2= 10 cm	0	-	10.00	-	-
	2	2	16.20	6.2	3.10
	4	2	21.70	5.5	2.75
	6	2	27.20	5.5	2.75
	8	2	32.70	5.5	2.75
	10	2	38.20	5.5	2.75
	R_2=				2.75

Table B8 GP data for saturated hydraulic conductivity determination at location A14 (Bore hall depth = 60 cm)

Well head	Time (min)	Time interval (min)	Water level in the reservoir (cm)	Water level change (cm)	Rate of water level change (cm/min), R
H_1= 5 cm	0	-	9.00	-	-
	2	2	13.80	4.8	2.4
	4	2	18.00	4.2	2.1
	6	2	21.80	3.8	1.9
	8	2	25.70	3.9	1.95
	10	2	29.40	3.7	1.85
	12	2	32.50	3.1	1.55
	14	2	36.70	4.2	2.1
	16	2	40.30	3.6	1.8
	18	2	43.90	3.6	1.8
	20	2	47.50	3.6	1.8
	22	2	51.10	3.6	1.8
	R_1=				1.80
H_2= 10 cm	0	-	7.00	-	-
	2	2	12.70	5.7	2.85
	4	2	17.90	5.2	2.6
	6	2	23.10	5.2	2.6
	8	2	28.30	5.2	2.6
	10	2	33.50	5.20	2.6
	R_2=				2.60

Table B9 GP data for saturated hydraulic conductivity determination at location A21 (Bore hall depth = 60 cm)

Well head	Time (min)	Time interval (min)	Water level in the reservoir (cm)	Water level change (cm)	Rate of water level change (cm/min), R
H_1= 5 cm	0	-	5.00	-	-
	2	2	8.20	3.2	1.6
	4	2	11.40	3.2	1.6
	6	2	1450	3.1	1.55
	8	2	17.40	2.9	1.45
	10	2	20.40	3	1.5
	12	2	23.40	3	1.5
	14	2	26.40	3	1.5
	16	2	29.40	3	1.5
	18	2	30.50	3	1.5
	20	2	35.50	3.1	1.55
	22	2	38.50	3	1.5
	24	2	41.50	3	1.5
	R_1=				1.50
H_2= 10 cm	0	-	7.00	-	-
	2	2	10.70	3.7	1.85
	4	2	14.30	3.6	1.8
	6	2	17.80	3.5	1.75
	8	2	21.40	3.6	1.8
	10	2	25.00	3.6	1.8
	12	2	28.50	3.5	1.75
	14	2	32.00	3.5	1.75
	16	2	35.50	3.5	1.75
	18	2	39.00	3.5	1.75
	20	2	42.50	3.5	1.75
	R_2=				1.75

Table B10 GP data for saturated hydraulic conductivity determination at location A22 (Bore hall depth = 30 cm)

Well head	Time (min)	Time interval (min)	Water level in the reservoir (cm)	Water level change (cm)	Rate of water level change (cm/min), R
H_1= 5 cm	0	-	8.00	-	-
	2	2	15.10	7.1	3.55
	4	2	21.80	6.7	3.35
	6	2	28.30	6.5	3.25
	8	2	34.80	6.5	3.25
	10	2	41.30	6.5	3.25
	12	2	48.50	7.2	3.6
	14	2	55.40	6.9	3.45
	16	2	62.60	7.2	3.6
	18	2	69.80	7.2	3.6
	20		77.00	7.2	3.6
	R_1=				3.60
H_2= 10 cm	0	-	9.00	-	-
	1	1	17.80	8.8	8.8
	2	1	25.80	8.0	8.0
	3	1	33.80	8.0	8.0
	4	1	41.50	7.7	7.7
	5	1	49.50	8.0	8.0
	6	1	57.50	8.0	8.0
	7	1	65.50	8.0	8.0
	8	1	73.50	8.0	8.0
	R_2=				8.0

Table B11 GP data for saturated hydraulic conductivity determination at location A22 (Bore hall depth = 60 cm)

Well head	Time (min)	Time interval (min)	Water level in the reservoir (cm)	Water level change (cm)	Rate of water level change (cm/min), R
H_1= 5 cm	0	-	15.00	-	-
	2	2	18.60	3.6	1.8
	4	2	21.90	3.3	1.65
	6	2	25.10	3.2	1.6
	8	2	28.30	3.2	1.6
	10	2	31.50	3.2	1.6
	12	2	34.70	3.2	1.6
	14	2	37.90	3.2	1.6
	16	2	41.10	3.2	1.6
	R_1=				1.60
H_2= 10 cm	0	-	10.50	-	-
	2	2	16.30	5.8	2.9
	4	2	21.70	5.4	2.7
	6	2	27.10	5.4	2.7
	8	2	32.30	5.2	2.6
	10	2	37.50	5.2	2.6
	12	2	42.70	5.2	2.6
	14	2	48.00	5.3	2.65
	16	2	53.30	5.3	2.65
	18	2	58.60	5.3	2.65
	20	2	63.90	5.3	2.65
	R_2=				2.65